Lancaster University

Investigating the Innate Immune Systems of Bats and Their Roles as Zoonotic Viral Reservoirs

By

Emily Clayton

PhD Thesis in Biomedical and Life Sciences

Lancaster University
Faculty of Health and Medicine
Biomedical Life Sciences

July 2023

Declaration

I declare that the content of this thesis is my own work and has not been submitted by myself in substantially the same form for the award of a higher degree elsewhere. Where information has been derived from other sources, I confirm this has been indicated in the thesis.

Emily Clayton

Experimental Contributions

Some of the data collection and experimental contributions for sections of this Thesis were completed by the individuals stated below:

Dr Waqas Kokhar collated the RNA-seq data used in Chapters 3 and 4 using specialised bioinformatic techniques to generate all figures used within these chapters.

Dr Ana Cláudia Franco generated the data shown in Figure 5.8.

Dr Mohammad Rohaim generated the data shown in Figure 5.7 and also contributed to the generation of Figures 5.5, Figure 6.9 and Figure 6.15.

Dr Mustafa Atasoy contributed to the generation of data in Figure 6.4.

Acknowledgements

Firstly, I would like to thank my supervisor Professor Muhammad Munir for presenting me with the opportunity to complete this research and for the guidance and support he has provided me throughout. I would also like to thank my secondary supervisor Dr Leonie Unterholzner for providing a valued immunological perspective towards my research. I would also like to express a collective thank you to members of the Molecular Virology lab at Lancaster who have supported me throughout my studies, with a special thanks to Mahmoud Bayoumi, Dr Mustafa Atasoy and Manar Khalifa.

I wish to extend my thanks to my life-long friends Jordan Mundy, Alex Mclaughlin and Emily Halsall, I am forever grateful for your support and the endless volumes of joy and laughter you provide. I would like to express a special thank you to Lauryn Buckley-Benbow for never failing to cheer me up, for always supporting me both in and out of the lab and for being an all-round amazing friend. I would also like to thank the girls at Grad Netball for making so many fun memories whilst I was a postgrad student at Lancaster (including getting to compete in Roses!) and for making my evenings so entertaining.

Lastly, I would like to thank all my family. To Mum and Dad, without your continuous love and endless support, both financially and emotionally, I would not have been able to pursue and accomplish this venture and I am forever thankful for this. My sister Leah, thank you for your continued support and I am so happy that you decided to study at Lancaster. Living in the same city as you again made my final years in Lancaster all the more enjoyable.

List of Figures

List of Tables

List of Abbreviations

5'pp	5'diphosphate group
5'ppp	5'triphosphate group
a.a	Amino acid
A3	Alternative 3' splice-site
A5	Alternative 5' splice-site
ACE2	Angiotensin converting enzyme 2
AIM2	Absent in melanoma 2
AP-1	Activator protein 1
APS	Ammonium persulfate
AS	Alternative splicing
ATP	Adenosine triphosphate
ATSS	Alternative transcription start site
ATTS	Alternative transcription termination site
BFV	Bovine foamy virus
BP	Biological process
BSA	Bovine serum albumin
BSL	Biosafety level
CAD	Consitutive-activation domain
CC	Cellular component
CCHF	Crimean-Congo haemorrhagic fever
CDS	Coding sequence
CedPV	Cedar virus
cGAMP	Cyclic guanosine monophosphate-adenosine monophosphate
cGAS	Cyclic-GMP-AMP synthase
CMC	Carboxymethyl cellulose
DAMP	Damage-associated molecular patterns
DAPI	4′,6-diamidino-2-phenylindole
DBatVir	Database of Bat-associated viruses
DBD	DNA-binding domain
DEG	Differentially expressed genes
DGE	Differential gene expression
DMSO	Dimethylsulfoxide
DNA	Deoxyribonucleic acid
dsRNA	Double-stranded ribonucleic acid
EBV	Epstein-Barr virus
ECL	Enhanced chemiluminescence
EDTA	Ethylenediaminetetraacetic acid
ER	Endoplasmic reticulum
ES	Exon skipping
EV	Empty vector
FDR	False discovery rate

GFP	Green fluorescent protein
GO	Gene ontology
HeV	Hendra virus
HIV	Human immunodeficiency virus
HRP	Horseradish peroxidase
HSV	Herpes simplex virus
IAV	Influenza A virus
ID	Inhibitory domain
IDR	Intrinsically disordered regions
IF	Immunofluorescence
IFI16	Interferon gamma-inducible protein 16
IFI35	Interferon induced protein 35
IFI6	Interferon-alpha inducible protein 6
IFIT	Interferon-induced proteins with tetratricopeptide repeats
IFN	Interferon
IFNAR	Type I interferon receptor
IFNLR	Type III interferon receptor
IR	Intron retention
IRF	Interferon regulatory factor
ISG	Interferon stimulated gene
ISGF3	Interferon-stimulated gene factor 3
ISRE	Interferon-stimulated response element
JAK	Janus kinase
JE	Japenese encephalitis virus
kb	Kilobase
LASV	Lassa virus
LGP2	Laboratory of genetics and physiology 2
LPS	Lipopolysaccharides
MAVS	Mitochondrial antiviral-signalling protein
MDA5	Melanoma differentiation-assocaited protein 5
MEE	Mutually exclusive exon
MERS-CoV	Middle East respiratory syndrome Coronavirus
MES	Multiple exon skipping
MF	Molecular function
MOI	Multiplicity of infection
mRNA	Messenger ribonucleic acid
MSA	Multiple sequence alignment
MW	Molecular weight
Mx1	Myxovirus resistance protein 1
NDV	Newcastle disease virus
NES	Nuclear export signal
NF-κB	Nuclear factor kappa B
NID	N-myc-interacting domains

NiV	Nipah virus
NK	Natural killer
NLR	NOD-like receptors
NLRP3	NOD-, LRR- and pyrin domain-containing protein 3
NMD	Non-sense mediated decay
NMI	N-myc interacting protein
NOD	Nucleotide-binding oligomerization domain
OAS1	Oligoadenylate synthetase 1
OAS2	Oligoadenylate synthetase 2
OH	Hydroxyl group
ORF	Open reading frame
PaBr	*Pteropus alecto* brain cells
PAMP	Pattern-associated molecular pattern
PBS	Phosphate-buffered saline
PC1	Principal component 1
PC2	Principal component 2
PCA	Principal component analysis
PCR	Polymerase chain reaction
PFU	Plaque-forming units
PKR	Protein kinase RNA-activated
poly(I:C)	Polyinosinic-polycytidylic acid
PRR	Pattern recognition receptor
PRV	Pteropine orthoreovirus
PSI	Percent spliced in
PVDF	Polyvinylidene fluoride
PYHIN	Pyrin and HIN domain
RBD	Receptor-binding domain
RFP	Red fluorescent protein
RIG-I	Retenoic acid-inducible gene I
RLR	RIG-I-like recpeptors
RLU	Relative light units
RNA	Ribonucleic acid
RNA-seq	RNA sequencing
RNase L	Ribonuclease L
rRNA	Ribosomal RNA
RT-qPCR	Reverse transcription quantitative real-time PCR
RVFV	Rift Valley fever virus
SARS-CoV	Severe acute respiratory syndrome Coronavirus
SARS-CoV-2	Severe acute respiratory syndrome Coronavirus 2
SDS-PAGE	Sodium dodecyl-sulfate polyacrylamide gel electrophoresis
SDT	Sequence demarcation tool
ssRNA	Single-stranded ribonucleic acid
STAT	Signal transucer and activator of transcription

STING	Stimulator of interferon genes
TAE	Tris-acetate-EDTA
TBK1	TANK-binding kinase 1
TEMED	Tetramethylethylenediamine
TLR	Toll-like receptor
Tpm	Transcripts per million
TPR	Tetratricopeptide repeats
TRAF	Tumour necrosis factor receptor-associated factor
TRIF	TIR-domain-containing adapter-inducing interferon-β
tRNA	Transfer RNA
TYK2	Tyrosine kinase 2
VAD	Virus-activated domain
VLPs	Virus-like particles
VSV	Vesicular stomatitis virus
WB	Western blotting
WHO	World Health Organisation
WT	Wild-type

Abstract

The zoonotic spillover of viral pathogens from wild animal reservoirs into human populations remains the leading cause of emerging and re-emerging infectious diseases globally. Bats represent important viral reservoirs, notorious for the diversity and richness of the viruses they host, several of which are highly pathogenic when transmitted to humans. Remarkably, bats appear to host an abundance of these viruses without exhibiting any clinical signs of disease. A dominant hypothesis for this ability suggests that bats can control viral replication early in the innate immune response, which acts as the first line of defence against infection. However, bat immunology remains fundamentally understudied, largely due to their high species diversity and the lack of accessible reagents required for bat research. Therefore, in this work we explored and characterised key components of bat innate immunity to gain a better understanding of bats as viral reservoirs and contribute to the currently limited literature.

Here, we demonstrated the *in vitro* transcriptomic response of the bat model species, *Pteropus alecto* (*P.alecto*) upon stimulation with the bat henipavirus Cedar virus and also with a type III bat interferon (paIFNλ). These investigations highlighted key transcripts, some of which were immune-related, in the response of bats to the separate stimuli and presents a foundation for further research into significant genes concerned in bat viral infection. Building from genome-wide transcriptomics, three distinctive bat innate immune genes representative of different stages of interferon signalling were selected for comparative genomics and functional characterisation. Our work demonstrated the conservation of genes between bats and humans, including IRF7, IFIT5 and IFI35. Specific findings for IRF7 included its successful translocation to the cell nucleus upon stimulation. IFIT5 and IFI35 were specifically selected for exploration due to previous research demonstrating the respective

antiviral and conflicting anti- or pro-viral roles of these genes in humans. Significantly, our research demonstrated the direct antiviral action of *P.alecto* IFIT5 against negative-sense RNA viruses. Collectively, our findings offer valuable contributions to the field of bat antiviral immunity and provide the framework for future investigative studies into the role and function of the bat innate immune system and bat viral tolerance mechanisms.

Table of Contents

Chapter 1. General Introduction

1.1 The Importance of Emerging and Re-emerging Zoonotic Viruses

A zoonotic disease is defined by the World Health Organisation (WHO) as an infectious disease that has been transmitted from a vertebrate animal to humans (Birhan et al., 2015, WHO, 2023). Zoonotic pathogens can be of viral, bacterial or parasitic origin and pose major threats globally to public health (Hayman et al., 2013, Daszak et al., 2000). An emerging infectious disease can be defined as a newly recognised disease which has appeared in a population for the first time, a known disease that has reappeared (re-emerged) following a previous decline in incidences, or alternatively an extension of the geographical range of a previously recognised disease (Howard and Fletcher, 2012, Feldmann et al., 2002). Many emerging and re-emerging diseases are zoonotic in origin, in which they are transmitted from animal reservoirs into human populations in spillover events, either directly or indirectly via vectors and intermediate animals (Feldmann et al., 2002). A spillover event occurs when a virus overcomes the several barriers necessary to become viable in another species (Power and Mitchell, 2004, Becker et al., 2019).

Amongst all emerging infectious diseases, viral agents, specifically zoonotic, remain the most severe threat to human populations worldwide (Schwartz, 2021). Emerging viral diseases posing a risk for human infection encompass viruses that had previously remained undetected or had roles in disease that had not been formerly identified. They may also consist of new genetic strains that have evolved from established viral agents or viruses that have spread to new ecological niches and geographical locations (Schwartz, 2021). High death and morbidity rates caused by emerging viruses have been observed within the last few decades, such as Ebola virus, human immunodeficiency virus (HIV), West Nile virus, Zika virus and most recently, severe acute respiratory syndrome virus 2 (SARS-CoV-2), the causative agent of the COVID-19 pandemic (Schwartz, 2021). Re-emerging viruses have also

demonstrated significant impact on global health, with viruses such as dengue, yellow fever and influenza producing high mortality rates. Over 1,400 total human pathogens have now been identified, 61% of which are of zoonotic origin (Taylor et al., 2001, Jones et al., 2008, Woolhouse and Gowtage-Sequeria, 2005). Notably, of all emerging infectious disease outbreaks, approximately 75% of these are zoonotic, conveying that zoonotic pathogens are twice as likely to be associated with emerging disease outbreaks than non-zoonotic pathogens (Taylor et al., 2001).

Throughout the course of history, emerging infections from animal reservoirs have proceeded to infect human populations, causing devastating consequences to public health and economies globally. Figure 1.1 highlights a timeline representing newly identified emerging infections and outbreaks of diseases in humans in new areas between 2003 and 2022. Recent emerging pathogens have included a select few bacterial and parasitic diseases but are majorly comprised of zoonotic viruses, as highlighted on the timeline. The overwhelming predominance of viruses as significant recent emerging pathogens highlights their importance and why they require attention. Notable recent zoonotic emerging viruses posing threats to human health worldwide include; HIV, avian influenza, Ebola and Marburg filoviruses, Lassa virus (LASV), Rift Valley fever virus (RVFV), Hendra (HeV) and Nipah (NiV) viruses, Crimean-Congo haemorrhagic fever (CCHF) and the coronaviruses such as severe acute respiratory syndrome (SARS-CoV), Middle East respiratory syndrome (MERS-CoV) and severe acute respiratory syndrome 2 (SARS-CoV-2) (Afrough et al., 2019). Remarkably, bats are the source reservoir host species for several of these highly pathogenic zoonotic viruses, including the filoviruses; Ebola, whereby bats have been identified as putative hosts and Marburg virus, whose reservoir are fruit bats (Koch et al., 2020, Towner et al., 2007). Bats are also the reservoir species for the henipaviruses (NiV and HeV) hosted by fruit bats (Halpin et al., 2011, Halpin et al., 2000, Middleton et al., 2007). The coronaviruses (SARS, MERS and potentially

SARS-CoV-2) are all understood to have originated from natural reservoir bat hosts, before spilling over into intermediate hosts for subsequent transmission to humans (Shi and Hu, 2008, Lau et al., 2005, Li et al., 2005, De Benedictis et al., 2014, Wacharapluesadee et al., 2013, Zhang and Holmes, 2020). A large range of animals act as reservoir species for viruses. Other noteworthy examples include small mammals such as rats, which are reservoirs for LASV (Kouadio et al., 2015) and primates which are the reservoir hosts for HIV (Sharp and Hahn, 2010, Lemey et al., 2003). The initial host reservoir for RVFV remains unknown but is hosted and transmitted by mosquitoes, with bats and rodents implicated as potential hosts (Chevalier et al., 2010, Oelofsen and Van der Ryst, 1999). Ticks present as reservoirs and vectors for CCHF (Bente et al., 2013), whilst wild aquatic birds such as geese, swans and ducks are the primary source hosts of avian influenza (Long et al., 2019).

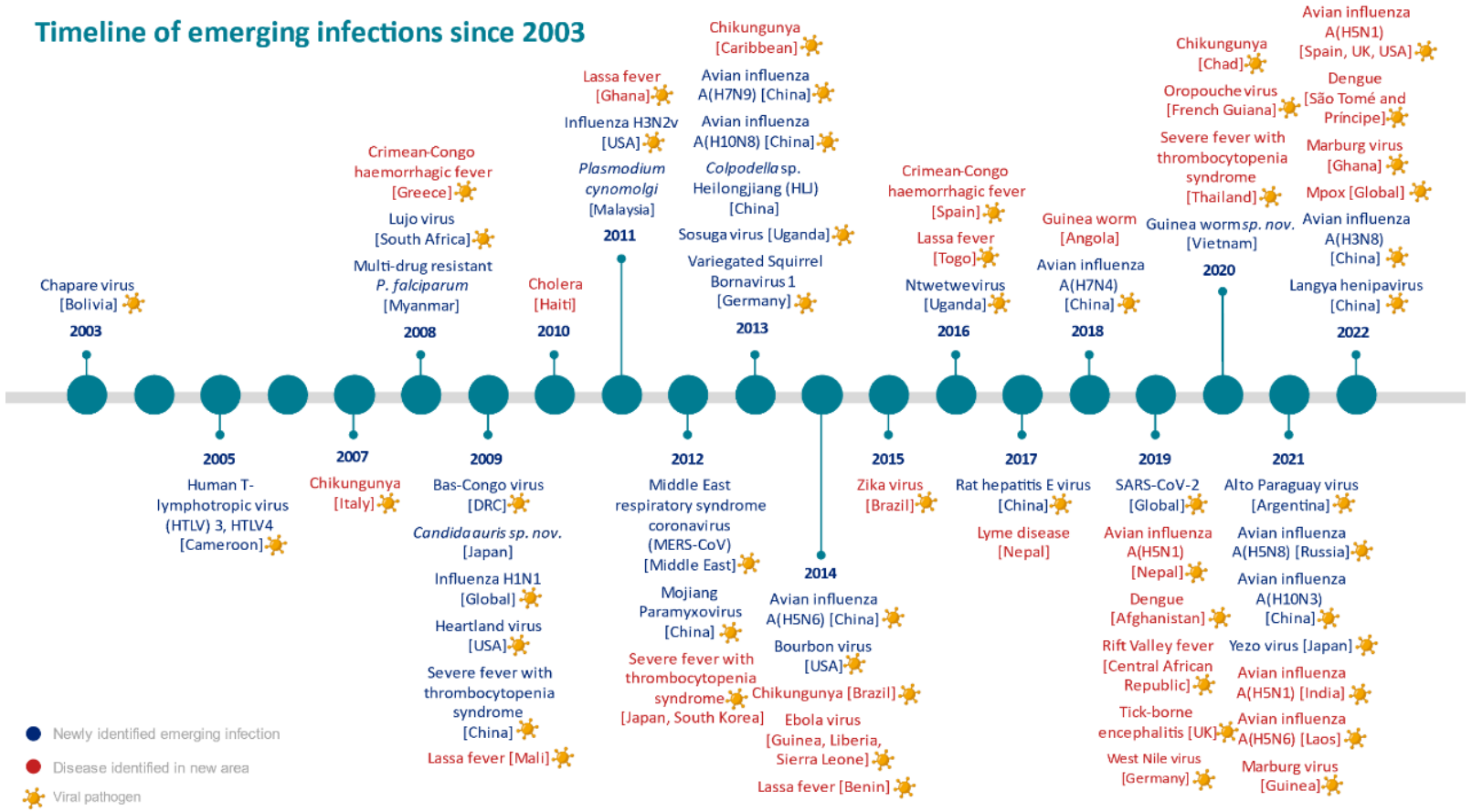

Figure 1.1- Timeline showing emerging infections between 2003 and 2022. *Newly identified emerging infections are written in blue and notable outbreaks of diseases in humans in new areas are in red. Emerging diseases caused by viral pathogens are highlighted alongside the disease name as symbolised by a yellow-coloured virus. Adapted from UK Health Security Agency (2023).*

Spillover of zoonotic viruses from reservoir hosts occurs via successive processes that must spatially and temporally align in order to facilitate the capacity of a pathogen to be transmitted from a reservoir host into a recipient host of a different species, such as human (Plowright et al., 2017, Becker et al., 2019). Generally, a reservoir source host species firstly sheds the viral pathogen, which in turn infects a susceptible recipient host. Transmission is often, but not always, facilitated by an intermediate host, which is an invertebrate or vertebrate vector that acts as a bridge between the reservoir host and the human recipient (Borremans et al., 2019, Ellwanger and Chies, 2021). In order for spillover to happen, several factors encouraging spillover from the reservoir animal host and the susceptibility of humans to infection must align with one another (Plowright et al., 2017). Such factors facilitating viral spillover include the distribution and abundance of the reservoir host, pathogen prevalence and shedding, pathogen survival in the intermediate host or environment, recipient host contact and susceptibility to the infectious agent and lastly, the sustained viability of the pathogen within the recipient host (Becker et al., 2019, Ellwanger and Chies, 2021). Several pathogens possess the ability to survive and remain viable outside of their hosts, whereby a pathogen surviving in the environment can be transmitted via indirect contact to susceptible recipients. Exposure of humans to zoonotic viruses can consequently occur either via direct

transmission from the reservoir host, or indirectly via the environment or an intermediate vector (Borremans et al., 2019) (Figure 1.2).

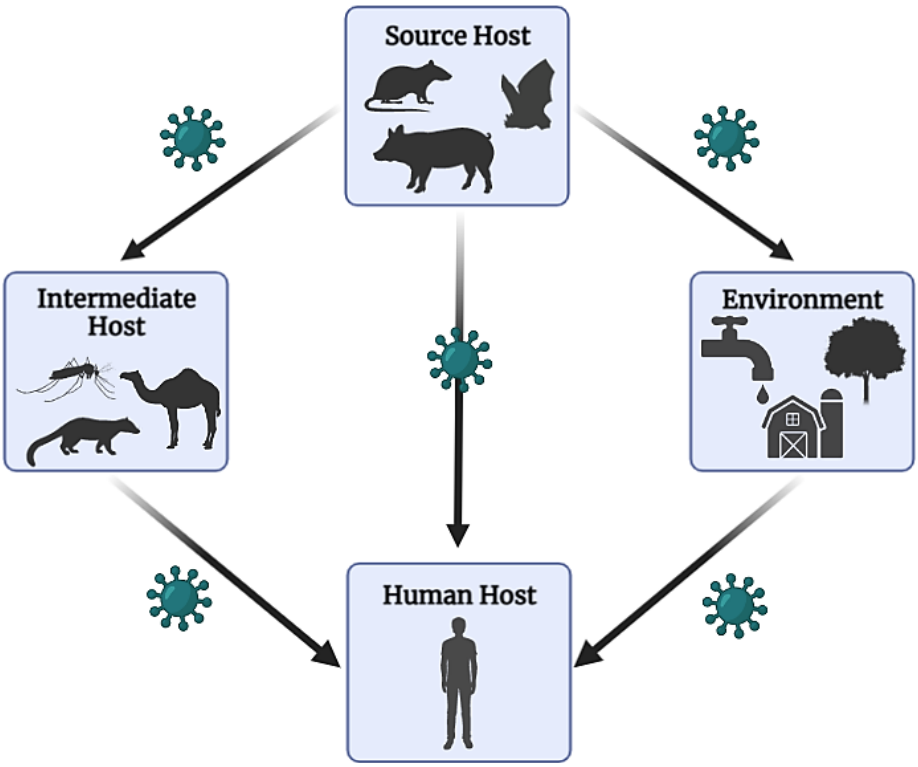

***Figure 1.2 - Alternative modes of transmission for viral spillover from source hosts into humans**. Viral spillover can occur via direct transmission into human host or indirectly via intermediate host vectors or the environment. Figure created with Biorender.com.*

Common routes of zoonotic viral spillover into human populations include direct and indirect contact with the infected animal and via contamination of food or water sources. Viral transmission via direct contact can occur when an individual comes into connection with fluids from the infected animal, such as saliva, blood, urine and faeces, and can also occur through touching animals or from animal bites or scratches (Prevention, 2023). Furthermore, bushmeat is considered a viral vector, whereby legal or illegal trade and consumption of infected animals can result in the direct transmission of viral species to humans (Milbank and Vira, 2022, Kurpiers et al., 2016). The ability of several viruses to survive outside of the host, results in the ease of indirect environmental transmission. Humans may encounter the virus when infiltrating areas where animals naturally reside, or from touching contaminated

surfaces or objects such as plants, habitats, soil and barns. Alternatively, consumption and contact with contaminated food or water sources also permits viral spillover. For example, consumption or contact with substances such as water and raw fruit and vegetables, that have been contaminated with faeces or other bodily fluids from an infected animal can result in viral transmission.

Emerging zoonotic viruses remain a constant and imminent threat to public health worldwide, due to the occurrence of spillover events and the highly pathogenic human infectious diseases they often give rise to. Several environmental and socioeconomic factors encourage and permit the spillover of zoonotic pathogens into human populations. Activities that increase the interaction of humans with wild animal species such as poaching, illegal trade, bushmeat consumption and cultural practices, can all result in the direct transfer of viral pathogens into human populations (Ellwanger et al., 2018, Kurpiers et al., 2016, Murray et al., 2016). For example, the spillover of HIV from non-human primates occurred via the hunting and handling of bushmeat, likely sourced for human consumption (Hahn et al., 2000). The distribution and selling of bushmeat is a common practice in several countries taking place in animal markets, also known as wet markets, whereby wild animals and their products are traded for consumption or for cultural and medicinal purposes. Wet markets are hence major centres for viral transmission, not only directly between wild animals and humans, but also cross-species transmission, due to the crowding of numerous and diverse species all within one place, encouraging the spillover of pathogens with pandemic potential (Keatts et al., 2021, Haider et al., 2020, Huong et al., 2020, Johnson et al., 2020). Crowded wet markets facilitate the ease of transmission of viruses between species, which can occur via direct contact with the infected animal meat or bodily fluids and also via the contamination of surfaces or aerosol spread within these markets, whereby sufficient hygiene and safety practices are often lacking (Brown, 2004, Lo et al., 2019, Aguirre et al., 2020, Wassenaar and

Zou, 2020, Nadimpalli and Pickering, 2020). Agriculture and farming are also practices commonly associated with disease emergence and spillover into human populations, due to the trade and consumption of potentially infected livestock and animal products, often resultant from high concentrations of farm animals interacting with wild animals and with one another (Kingsley, 2018). For example, spillover can occur from bad animal husbandry practices, such as raising swine in close proximity to chickens, feeding dead chickens to swine, or selling live chickens at open bird markets, can collectively result in the spread of influenza strains in poultry and swine farming (Kingsley, 2018). Laws and regulations are enforced within the farming industry to prevent disease spillover into humans, but occasionally pathogens remain undiscovered when food or water sources become contaminated. In farming for example, animal skin, fur or milk may often become polluted by faeces and environmental pathogens. Contamination of meat can occur during food processing via incorrect handling or from pathogens in other agricultural products, occasionally resulting in potential human infections such as Norovirus for example, which is often implicated in deli meat transmission (Kingsley, 2018, Velebit et al., 2015).

Trade, consumption and handling of animals and animal products are not the only factors responsible for the continuous emergence of zoonotic viruses worldwide. The growth and expansion of the human population and associated activities are also central to the anthropogenic global emergence of pathogens (Wolfe et al., 2005, Wolfe et al., 2007, Johnson et al., 2020). Human encroachment into habitats rich in wildlife biodiversity has been proposed as a key element in the emergence of zoonotic infectious diseases (Gibb et al., 2020). Human land use change has been deemed a globally significant driver of pandemics and has caused the emergence of over 30% of new diseases reported since 1960 (Daszak et al., 2020, Mendoza et al., 2020). Land use-induced spillover has been well described by Plowright et al. (2021) who stated that land use change drives an “infect-shed-spill-spread cascade”. In this

manner, land use change induces new environmental stressors on wildlife distribution and abundance, and shapes pathogen infection dynamics within wildlife, whilst driving pathogen shedding and facilitating novel contact opportunities between species to allow spillover, ultimately leading to human infections (Patz et al., 2004, Faust et al., 2018, Plowright et al., 2021). Land use change encompasses both deforestation and urbanisation, which collectively provide new pathways for pathogens to spill over into human populations. For example, destruction of habitats via deforestation increases the concentration of several species within a much smaller space, and the construction of human settlements in close proximity to natural habitats drives further interactions between humans and their livestock with wild animal species, promoting viral spillover into human populations (Ellwanger et al., 2018, Ellwanger and Chies, 2021).

In conjunction to increased human land use, global warming has also demonstrated a significant influence on pathogenic spillover, specifically on the ecology and distribution of arthropod vector-borne diseases. Increases in temperatures influence the population and disease transmission dynamics of arthropod vectors, resulting in a decrease in the incubation period in vector species such as mosquitoes and ticks (Chan and Johansson, 2012, Gloria-Soria et al., 2017, Wilke et al., 2019). Furthermore, viral emergence from arthropod vectors is influenced by warmer winters, which enable vectors to survive almost all-year round, whilst travelling and colonizing more extensive regions globally, thereby facilitating a wider distribution of potential viral spillover opportunities (Wilke et al., 2019).

Further factors influencing global viral emergence include global travel and natural disasters. The flow of people and tourism fuelled by global travel plays a vital role in the epidemiology of zoonotic diseases. Yearly, billions of people travel around the globe to and from endemic countries, inadvertently spreading pathogens between locations (Grubaugh et al., 2017, Semenza et al., 2014, Chen and Wilson, 2008,

Wilke et al., 2019). Additionally, natural disasters often result in outbreaks of infectious diseases (Suk et al., 2020). Disease often arises following disasters such as hurricanes, earthquakes, tropical storms, drought, and famine due to the impact on infrastructure and major population displacement commonly caused. Availability of sanitation and healthcare services alongside local disease ecology, result in disease emergence and also death in affected populations (Watson et al., 2007, Wilke et al., 2019). Following natural disasters, diseases can spread not only via large-scale relocation of human populations, but also the relocation of wildlife from these areas. Vector-borne diseases are often commonly spread following natural disasters whereby they are dispersed to new areas and create new breeding grounds, often increasing the vector populations and thereby capacity for disease transmission (Patricola and Wehner, 2018, O'Leary et al., 2002, Caillouët et al., 2008). Weakened infrastructures and crowding of susceptible or infected individuals are all risk factors for the transmission of vector-borne viruses and other pathogens (Lifson, 1996). In summary, the emergence of viral pathogens is facilitated by several biological, social, and environmental factors, from increased human-animal interaction to urbanisation and climate change. To prevent future spillover events and outbreaks of zoonotic viruses, barriers must be implemented against factors encouraging spillover, to reduce and prevent the emergence and re-emergence of zoonotic viruses.

Following the recent COVID-19 pandemic, zoonotic spillover events remain prominent and are projected to continue to persist for the foreseeable future. Both emerging and re-emerging viruses will consequently continue to pose a threat on human populations globally unless substantial actions are taken. In order to prepare for the next emerging virus outbreak, institutions and governments worldwide must assign their attention and resources to the scientific, medical and public health sectors, so that future zoonotic outbreaks can be detected and prevented (Schwartz, 2021).

1.2 Bats as Viral Reservoirs

Bats belong to the order Chiroptera and are one of the most abundant and geographically widespread vertebrates worldwide, present on every continent except for Antarctica (Calisher et al., 2006, Fenton and Simmons, 2020). Bats are also the second most diverse mammalian group following rodents, and represent over 20% of all mammals on Earth (Afelt et al., 2018). Chiroptera consists of over 1,300 species, which fall into one of two suborders that diverged 63 million years ago; Yinpterochiroptera, consisting of all megabat families and several microbat families, and Yangochiroptera which contains all remaining microbat species (Lei and Dong, 2016). This suborder classification has recently been accepted as correct, following conflicting studies on the earlier classification system of bats, which was invalidated via key phylogenomic findings (Nishihara et al., 2009, Zhang et al., 2013b, Zhou et al., 2012, Tsagkogeorga et al., 2013). The previous classification system, subdivided Chiroptera into; Microchiroptera, containing microbats which utilised 'true' laryngeal echolocation systems, and Megachiroptera, containing old world megabats which employed enhanced visual activity. It is now generally accepted that bat echolocation systems either evolved independently in Rhinolophoid and other microbat species, or were alternatively lost during megabat evolution (Teeling et al., 2000). Bats are rich in species diversity and also exhibit variations in their morphology, size, geographical locations, ecological niches, physiological range of body temperatures and behaviours such as diet, social interaction, migration and sensory perception (Banerjee et al., 2020, Wang and Anderson, 2019, Luis et al., 2013). Bats play important roles in ecosystems, assisting in fertilisation, pollination, and seed dispersion alongside control of insect populations across a vast range of regions and habitats (Voigt and Kingston, 2016, Irving et al., 2021, Fenton and Simmons, 2020). However, bats are receiving increased attention due to their role as natural host reservoirs of high-impact zoonotic viruses, which studies have shown are increasing

in diversity (Luis et al., 2013, Olival et al., 2017). Intriguingly, bats have been identified to host more zoonotic viruses per species than rodents, perhaps due to influencing ecological factors such as the commonality of species overlap in bats, encouraging viral richness (Luis et al., 2013).

Bats host a diverse range of viruses and to date, thousands of viral species have been identified in bats, from numerous different viral families (Figure 1.3). Over the past few decades, a huge international effort was undertaken in order to identify viruses recovered from, or present in a range of bat species (Afelt et al., 2018). Chen et al. (2014) have provided a valuable database (DBatVir) that collates this data and provides an extensive list of all known bat viruses which is readily accessible and updated often. Notably, bats host several zoonotic viruses which are highly pathogenic and can induce severe disease when transmitted to humans, including filoviruses, lyssaviruses, henipaviruses and coronaviruses (Moratelli and Calisher, 2015, Fisher et al., 2018, Calisher et al., 2006, Zhou et al., 2018). These viruses are of a particular concern to public health due to their rapid evolutionary rate, their previous known ability to emerge and spillover into human populations and ability to cause severe pathogenicity in humans and other hosts (Letko et al., 2020). RNA viruses such as Marburg virus, HeV and NiV have been directly isolated from bats which were thus confirmed as natural reservoirs for these viruses (Letko et al., 2020, Halpin et al., 2011). Increasing evidence suggests that bats are also the natural source reservoir species for countless other emerging viruses including; SARS-CoV, MERS-CoV, SARS-CoV-2 and Ebola virus, despite these pathogens entering human populations via other intermediate animals, such as civet cats in SARS-CoV infection (Olival and Hayman, 2014, Memish et al., 2013, Leroy et al., 2005).

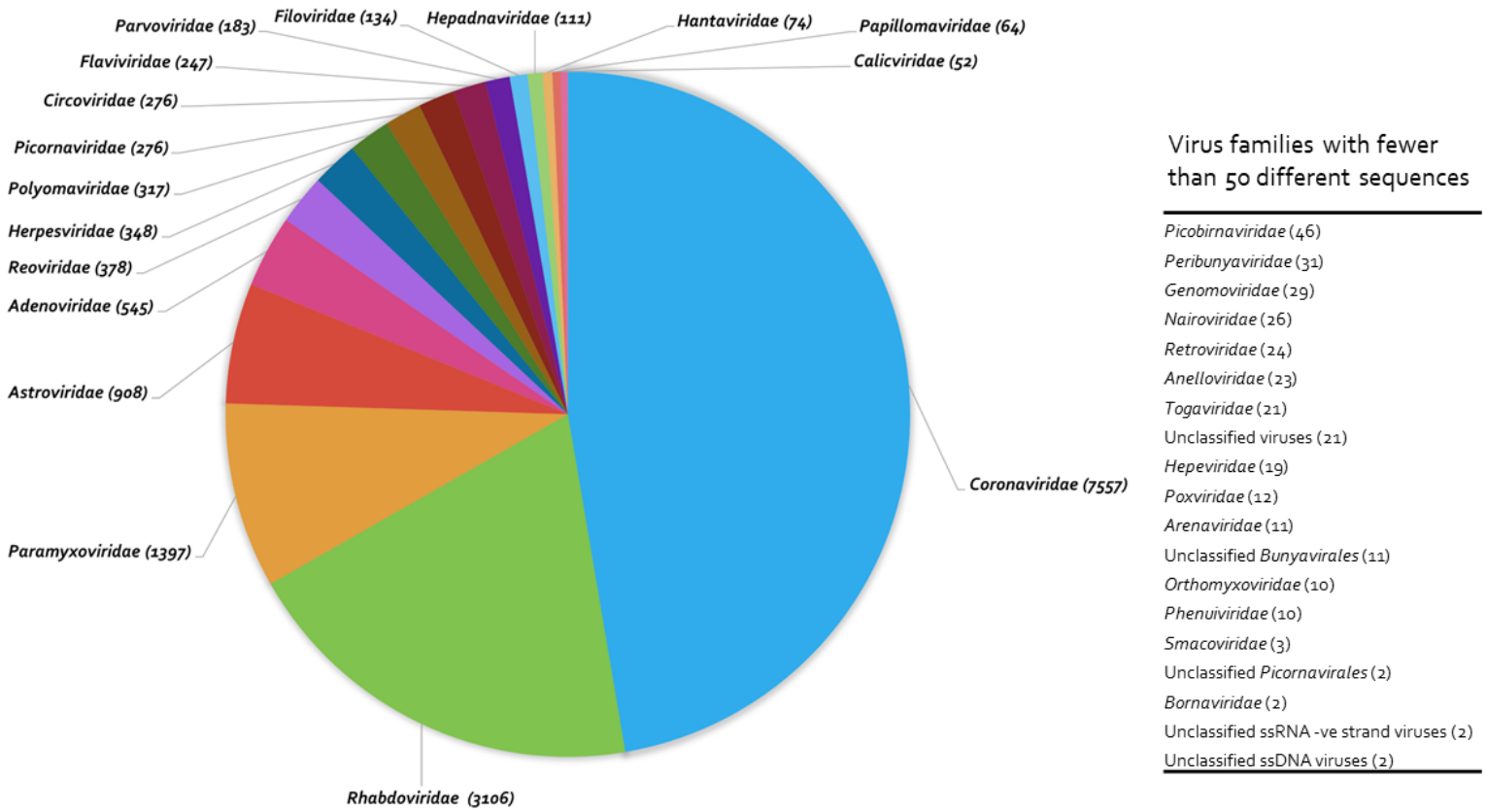

Figure 1.3 - Currently described viral diversity in bats. *Genetic sequence data was retrieved for bat-derived viruses from the public DBatVir database (Chen, Liu et al. 2014), recently updated in March 2023. Sequence data was collated and categorized by viral family. Viral families containing over 50 different sequences were selected and presented via pie chart, with remaining families containing less than 50 different sequences listed on the side. It is worth noting that several bat viruses remain uncharacterised. Adapted from Letko et al. (2020).*

Despite the persistent infection of bats with many viruses, evidence from naturally and experimentally infected bats has demonstrated that they rarely display any clinical symptoms of illness (Sulkin et al., 1970, Swanepoel et al., 1996, Williamson et al., 1998, Williamson et al., 2000, Leroy et al., 2005, Leroy et al., 2009, Middleton et al., 2007, Towner et al., 2009). This ability to host viruses without displaying signs of illness, alongside the extensive plethora of viruses they host, continues to gain a lot of interest within scientific research and the public eye, particularly succeeding the recent COVID-19 pandemic. Despite their recognised ability to host several viruses without overt disease, virus-related bat mortality events do occur but appear to be infrequent in comparison. A select few known or suspected viruses that can cause pathology and sometimes kill bat species include; rabies virus and the closely related Australian bat lyssavirus, Tacaribe arenavirus and also the Lloviu virus, which is closely related to Ebola and Marburg (Field et al., 1999, McColl et al., 2002, Cogswell-Hawkinson et al., 2012, Negredo et al., 2011). However, it is generally understood that bats can harbour zoonotic viruses without exhibiting any clinical signs of disease via establishing a host-virus co-existence. Research suggests that the underlying ability of bats to co-exist with viruses is due to their immune systems and mechanisms that they have evolved to control viral replication. Despite the defence mechanisms of bats allowing them to be persistently or latently infected with viruses without displaying disease, they are still capable of shedding the virus, resulting in the transmission and spillover of bat viruses into other animals and humans (Figure 1.4) (Subudhi et al., 2019). The risk of cross-species transmission of

zoonotic pathogens from bats continues to pose a threat on the health of human and animal populations globally (Allen et al., 2017).

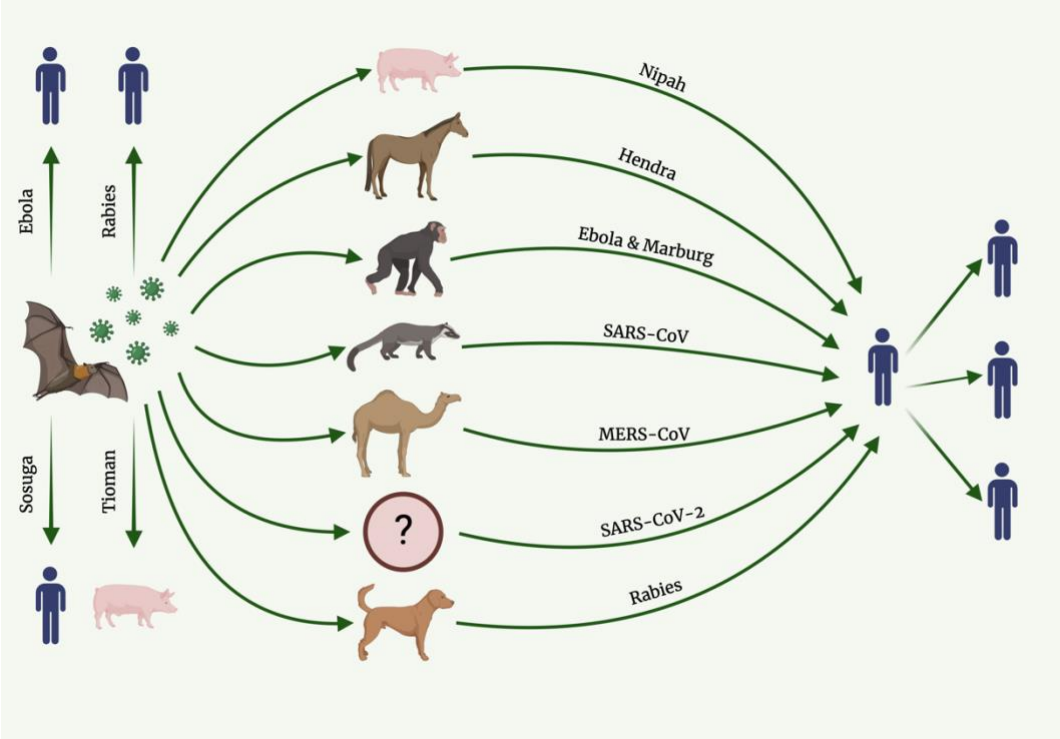

Figure 1.4 - Common routes of transmission in viral spillover events from bat reservoirs into humans. *Bats rich in viral diversity can transmit viruses directly to humans or animals. Spillover of viruses from bats into human often occurs via intermediate animal reservoirs that act as amplifying hosts in successively transmitting the virus to humans. Following infection of a susceptible individual with a zoonotic virus, the virus is then easily further spread throughout human populations. Figure adapted from Gupta et al. (2021) and created with Biorender.com..*

Transmission of emerging zoonotic viruses from bats has increased by a substantial amount over the past few decades, largely due to the growing encroachment of humans into the natural habitats of bats, especially within tropical regions (Ruiz-Aravena et al., 2022). Extrinsic factors driving viral spillover from bats include environmental stressors and climatic events causing the destruction of bat habitats and food sources, which have been conjectured to impact the health of bats (Field, 2009, Wood et al., 2012, Mathews, 2009, Daszak et al., 2001, Streicker et al., 2012). Human activities resulting in land use change are causing the increased contact between humans, livestock and bats, with domesticated animals commonly acting as

intermediate, amplifying hosts in bat virus spillover, such as HeV, NiV and Menangle viruses for example (Plowright et al., 2011, Chua et al., 2000, Philbey et al., 1998, Murray et al., 1995). Additionally, the change and loss of bat habitats caused by deforestation and urbanisation alter the population density and migratory patterns of bats, which alongside population growth and the increasing consumption of meat, substantially contribute to the spillover of viruses from bats into humans and other animals (Rulli et al., 2021). Such anthropogenic factors are likely causing spillover of viruses from bats due to disrupting their natural host-viral equilibrium status (Field et al., 2007, Morse, 2004, Wolfe et al., 2005, Smith and Wang, 2013). Key investigations by Brierley et al. (2016) mapped the global distribution of viruses commonly shared between bats and humans, emphasizing their governing presence worldwide, whilst highlighting hotspot regions such as sub-Saharan Africa and Southeast Asia (Figure 1.5). Annotations added to the graph display the geographical origins of major zoonotic viral outbreaks that have caused devastation in human history, the locations of the first recorded outbreaks of these viruses largely support the projected zoonosis risk as predicted by Brierley et al. (2016). Analyses also determined global risk patterns of human drivers governing spillover of viruses from bats, indicating that if human populations continue to encroach into the virus-rich territories of bats, the threat of zoonoses is projected to increase (Brierley et al., 2016). It is consequently imperative that measures are undertaken to decrease any opportunities for viral spillover, including reducing habitat intrusion and hunting of bat populations, in order to mitigate the risk of future zoonotic spillover (Brierley et al., 2016).

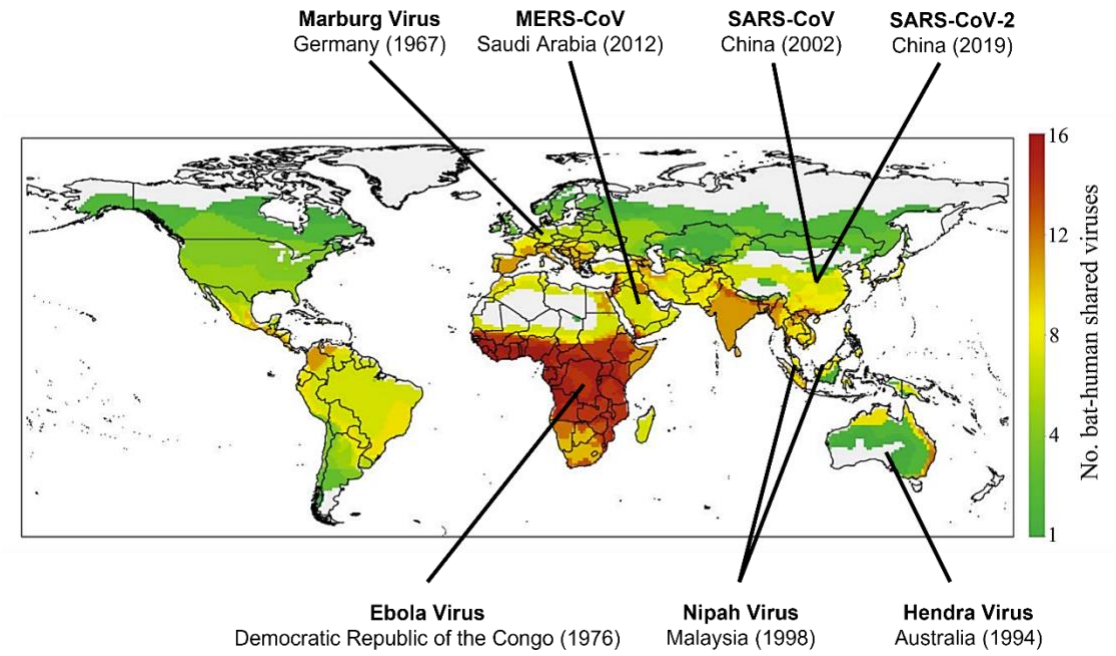

Figure 1.5 - Global distribution of viruses shared between bats and humans and annotated origins of major zoonotic viruses of the past few decades. *Colour represents a linear scale of the number of bat-human shared viruses from 1 (green) to 16 (red). Mapping of shared human-bat viruses represented here is dated until 2016. Origins of previous major zoonotic outbreaks have also been displayed to further observe specific regions at risk of future zoonotic outbreaks from bats. Shared bat-human virus data obtained and adapted from Brierley et al. (2016).*

1.3 Bat Characteristics

1.3.1 Bat Evolution

Although bats belong to the mammalian order and share selected traits with other mammals such as rodents, bats are incredibly unique in the host of characteristics and attributes that they possess (Calisher et al., 2006). Bats evolved early and remained comparatively unchanged, in comparison to other mammals (Hill and Smith, 1984). However, the evolutionary history of bats remains largely unidentified due to limited fossil records, alongside the contradictory phylogenetic hypotheses of the two Chiroptera suborders; whether laryngeal echolocation and flight in bats arose from a single origin, or from multiple origins with subsequent loss in megabats (Wang et al., 2017, Hutcheon et al., 1998, Teeling et al., 2000, Teeling et al., 2003, Baker et al., 1997). Therefore, the subordinal classifications within bats remain largely

conflicting due to contrasting molecular and morphological data and thus warrant further investigations (Baker et al., 1997, Teeling et al., 2005). In order to gain a better understanding of bat evolutionary history, a notable study by Teeling et al. (2005) analysed 17 nuclear genes, representative of all bat families. Results dated the Chiroptera origin to the early Eocene, which was 52 to 50 million years ago, parallel to significant increases in global temperatures, alongside rises in plant and insect diversity and abundance. Calisher et al. (2006) have discussed how the ancient origins of zoonotic viruses hosted by bats, such as lyssaviruses, align with the Chiropteran origin, suggesting a long history of cospeciation (Badrane and Tordo, 2001). Calisher et al. (2006) have subsequently proposed that co-evolution of viruses in bats may have resulted in certain viruses utilising biochemical pathways and receptors common in mammals, instigating the potentially increased capacity for transmission of bat viruses into other susceptible mammalian species. However, further analyses into the coevolution of bat-borne viruses with their bat hosts are required to better understand potential cospeciation events and opportunities.

1.3.2 Long Life Span

Bats have been documented to have exceedingly long lifespans, a longevity seldom observed in other mammals that share a similar body mass to metabolic-rate ratio (Austad, 2005, Austad and Fischer, 1991). On average, bats live 3.5 times as long as non-flying mammals of the same size, with some species even exceeding this, such as the Brandt's bat for example, whereby an 8g male was documented to live for at least 38 years, which was nine times as long as an average mammal of similar size (Wilkinson and South, 2002). Accounts have identified six different bat species living to over 30 years of age, five of which were observed in the wild; the long-eared bat (*Plecotus auratus*), little brown bat (*Myotis lucifugus*), Blyth's bat (*Myotis blythii*), greater horseshoe bat (*Rhinolophus ferrumequinum*) and the previously mentioned Brandt's bat (*Myotis brandti*) (Wilkinson and South, 2002). The remaining species,

the giant flying fox (*Pteropus giganteus*), was also observed, but this instance was in captivity (Wilkinson and South, 2002). Therefore, bats display an extreme longevity for small mammals and do not fit into the principle that mammalian life expectancy is directly related to body size and metabolic weight (Austad, 2005, Eisenberg, 1980, Calisher et al., 2006). A long-life expectancy is a significant influencing factor for virulence in bats, as persistent infection of bat hosts for long periods of months and possibly years, may significantly impact on the reproductive number of infection (R_0). The R_0 represents the number of newly infected secondary hosts arising from a single infectious individual host during its time of being infectious, occurring within a large population of susceptible individuals (Halloran, 1998). Therefore, assuming a persistent viral infection in bats and their capacity to transmit the virus to susceptible hosts, the increased duration of infectiveness in long-lived bats may dramatically contribute to the heightened potential for secondary infections, occurring not only within bat populations but also encouraging viral transmission into other susceptible species.

1.3.3 Bat Population Dynamics

Bats typically reside in crowded population densities and aggregate in even larger numbers for roosting events. Such circumstances greatly influence the potential for intra- and interspecies transmission of viruses from bats (Calisher et al., 2006). The dense population of bat species, often encompassing several million individuals, heightens the ease of viral spillover. For example, the dense population of Mexican free-tailed bats residing in the southwestern caves of the United States, displayed the sole, fascinating case of airborne rabies, occurring via droplet or aerosol transmission (Constantine, 1967, Constantine, 1968, Winkler, 1968). Furthermore, the ability of bats to fly, allows several bat species to travel over diverse geographical distances during seasonal migrations and in pursuit of food, whereby bat populations can mix, providing additional opportunities for viral spillover (Griflin, 2012, Holland, 2007).

Large distances are covered by a variety of migratory bat species, including *Myotis* bats which can travel up to 400 miles from their winter hibernation sites (Griflin, 2012). The Mexican free-tailed bat (*Tadarida brasiliensis Mexicana*) can migrate even further, covering 800 miles between their summer and winter roosting sites (Villa and Cockrum, 1962). Interestingly, sometimes bats of the same species may also display different migratory patterns to one another, such as the silver-haired bat (*Lasionycteris noctivagans*) which are recognized hosts of Rabies virus and largely contribute to its spread across several locations (Mondul et al., 2003, Rohde et al., 2004). The varying migration patterns within one species of the same bat, encourages the exchange of novel viruses or variants between migrating and nonmigrating populations and additionally with other bat species, increasing the prevalence and transmissibility of zoonotic viruses within the same species and to others (Calisher et al., 2006). Fluctuations in population density of bats during migration and their coloniality behaviours thereby heavily impact contact rates occurring between infected and susceptible individuals and hence influence disease dynamics and risk of zoonotic viral spillover (Altizer et al., 2011, Hayman et al., 2013).

1.3.4 Powered Flight

As previously mentioned, bats are unique in remaining the only mammal known to be capable of powered flight (Anderson and Ruxton, 2020). During flight, bats exhibit an increase in their metabolic rate, at an estimated 15-16 fold in comparison to the resting metabolic rate of normothermic, otherwise active, bats (Speakman et al., 2003, O'shea et al., 2014). The high metabolic demands required for powered flight result in an increase of the core body temperatures of bats up to 38°C- 41°C, which has been demonstrated in multiple bat species (O'shea et al., 2014). High body temperatures such as these are known to increase the rate of several immune responses in mammals and lie within the temperature range commonly observed in

the presence of a typical mammalian fever (Blatteis, 2003, O'shea et al., 2014). Consequently, the metabolic demands of flight produce by-products known to cause DNA damage, resulting in the release of self-DNA into the cell cytoplasm (Barzilai et al., 2002). Nonetheless, bats appear to have undergone positive selection of their oxidative phosphorylation pathway as a result of this increased metabolic capacity, allowing bats to adapt to the huge demand in energy required during flight and remain unaffected by the consequences caused by the release of self-DNA (Shen et al., 2010). Furthermore, bats are known to harbour a variety of DNA viruses, and the further infection of RNA viruses can also result in the production of cytosolic DNA due to intracellular damage (Brook and Dobson, 2015). Both self-DNA and viral DNA (from DNA viruses or by-products of RNA viruses) trigger the immune response in the bat host, leading to activation of the inflammasome and constitutive interferon (IFN) production (Schlee and Hartmann, 2016). Overactivation of the inflammasome or IFN system is usually detrimental to hosts, however, research suggests that the evolution of flight in bats has resulted in the positive selection of an important set of antiviral immune responses that regulate virus propagation, whilst controlling the self-detrimental inflammatory responses induced during flight (Banerjee et al., 2020). A speculative "flight-as-fever" hypothesis by O'shea et al. (2014), theorises that the increased metabolic rates and high body temperatures observed in bats during flight may facilitate the activation of the immune system on a regular basis, whereby bats are able to balance the oxidative stressors of flight, whilst maintaining a high burden of viruses and regulating the sensing of self and viral cytosolic DNA, all to avoid the overactivation of pro-inflammatory pathways (Xie et al., 2018, Peckham et al., 2017). Therefore, flight could potentially underpin the evolution of bat immunity in enabling bats to remain unaffected by the metabolic stress induced by flight, proving highly advantageous in their ability to host viruses without showing signs of disease.

1.3.5 Torpor and Hibernation

Several bat species, including temperate bats belonging to the Rhinolophidae and Vespertilionidae families, are capable of using daily torpor, or seasonal torpor during hibernation (Calisher et al., 2006). Through torpor, bats decrease their physiological activity by reducing their body temperatures and metabolic rate in order to conserve energy in periods of physiological stress such as cold nights and winter months, when prey is scarce and when food requirements outweigh available resources (Humphries et al., 2002, Lyman, 1970, Geiser and Körtner, 2010, Geiser and Stawski, 2011, Fumagalli et al., 2021). Remarkably, hibernating temperate bats have been recorded to lower their body heat to just above freezing and tropical bats have also been identified to largely lower their heart rates from over 1,000 to just 200 beats per minute (O'Mara et al., 2017, Hayman, 2019, Geiser and Stawski, 2011). During hibernation, some pathogens such as the fungus that causes white-nose syndrome (*Pseudogymnoascus destructans*) which thrives in extremely cold temperatures, are able to infect bats with decreased physiological responses and replicate efficiently (Blehert et al., 2009). Notably, this fungus also tends to cause harmful immunopathology once hibernating bats resume flight (Meteyer et al., 2012). Although this pathogen is not a virus and actually exhibits the opposite temperature pattern of infection to RNA viruses, it highlights the potential importance of torpor on infection dynamics in bats (O'shea et al., 2014). The impact that torpor and hibernation impose on the role of bats as viral reservoirs remains largely unknown, however, studies have evidenced that cold temperatures maintained in bats during hibernation and torpor contribute to the maintenance of viraemia and persistent viral infection at low levels, perhaps due to the suppression of immune responses induced by cold body temperatures (Kuno, 2001, Sulkin and Allen, 1974, Fumagalli et al., 2021). Further studies concluded that the presence of daily torpor contributed to a reduction of immune responses, thereby preventing the pathology associated with sustained inflammation, which could be directly associated with their ability to fly

(Fumagalli et al., 2021). Investigations have also demonstrated that viral replication could rise with temperature without affecting the body temperature of bats, which could suggest that the total viral load bats can carry is somewhat limited by torpor, rather than by variations in temperature, contrasting to the aforementioned “flight-as-fever” hypothesis (Munster et al., 2016, Miller et al., 2016, O’shea et al., 2014). In summary, further investigations into the influence of both daily torpor fluctuations and winter hibernations in bats are necessary to better understand the molecular mechanisms underlying the ability of bats to maintain viral infection without exhibiting signs of disease.

1.3.6 Echolocation

Bats are the only land mammals capable of utilising echolocation (the emission of sounds that detect and characterise time delay and signal properties of returning echoes) and magnetoreception (the ability to differentiate between north and south poles), which are utilised by microbats and a few megabat species for navigation (Hill and Smith, 1984, Holland et al., 2004, Jones and Holderied, 2007, Springer et al., 2001, Wang et al., 2007). Echolocation signals are produced by the larynx which occurs via contraction of the muscles in the bats abdominal wall and are emitted through their mouth or nostrils (Neuweiler, 2000). Calisher et al. (2006) have suggested that the generation of a loud sound could result in the emission of mucus and saliva in the form of droplets or aerosols from the bats during echolocation, allowing the transmission of viruses from the bat host into susceptible nearby individuals (Neuweiler, 2000). This theory is supported by reports of the successful isolation of Rabies virus from the nostrils and mucus obtained from naturally infected Mexican-free tailed bats (Constantine et al., 1972). The extent to which bats are capable of producing echolocation signals whilst protecting them from their own potentially deafening emissions is unique and warrants future studies observing the

muscular and neural systems that bats have evolved to enable this ability (Calisher et al., 2006).

1.4 Bat Innate Immunity

1.4.1 Why Investigate Bat Antiviral Immunity?

Little is currently known about the immune systems of bats in comparison with immunity in other mammals, partly due the large species diversity observed in bats and the lack of prior investigations into their immune response to viral infection due to difficulties encountered with bat research. However recently, increasing research efforts have been directed towards studying bats as key viral reservoirs, due to their competence in hosting a multitude of viruses without exhibiting any clinical symptoms of disease. The ability of bats to host highly pathogenic viruses such as henipaviruses, filoviruses and coronaviruses without displaying signs of illness, has raised increasing interest into potential adaptations of their antiviral immune responses. Immunological responses to viral infection in bats remains largely uncharacterised, but are believed to be heavily influenced by several factors and characteristics as mentioned prior, such as their ability to fly, population dynamics and their co-evolution with viruses (Zhang et al., 2013b, Hawkins et al., 2019, Calisher et al., 2006). Bat research is now advancing at an increasing rate due to the recent availability and accessibility of bat data and reagents. For example, researchers utilise the existing understanding of other mammalian reservoir-virus relationships to investigate viral maintenance in bats and employ next-generation sequencing methods (Garg et al., 2023). Furthermore, genome sequences are now available for over 50 bat species and whole genome and transcriptome sequences of at least 18 bat species are also accessible (Hawkins et al., 2019, Jebb et al., 2019). Ongoing efforts by the Bat1K consortium aim to generate reference-quality genomes for all known bat species to provide a useful foundation for the immunological investigations of bats (Jebb et al., 2019). Although limited, the availability of bat-

derived cell lines has also enabled *in vitro* investigations into the immune systems of bats and how they respond to viral infection, in addition to the usage of bat primary tissue and organoids for research (Banerjee et al., 2018, Zhou et al., 2020).

Prospective investigations into the bat immune system may enable researchers to understand immune mechanisms utilised by bats in managing virus-mediated pathogenesis and could also potentially provide novel treatments and therapeutic targets against pathogenic zoonotic viruses (Banerjee et al., 2020). Bats possess both innate and adaptive immunity, but the innate arm of the immune response, which acts as the first line of defence against infection, is hypothesised to underlie the novel antiviral potential of bat hosts (Diamond and Kanneganti, 2022, Banerjee et al., 2020). A dominant hypothesis for the ability of bats to host pathogenic viruses without exhibiting any clinical signs of disease, is their facility to control viral replication early on in the immune response via innate immune antiviral mechanisms (Baker et al., 2013). Recent research describing several bat innate immune genes provides the foundation for the understanding the fundamental role of bat innate system and their potentially novel antiviral immunity (Baker et al., 2013). Research has shown that the IFN induction pathway in response to viral infection in bats appears highly conserved with that of humans, which proves useful for the direct comparison of antiviral immune mechanisms in bats to what is known in other mammalian species (Randall and Goodbourn, 2008, Banerjee et al., 2020, Baker et al., 2013).

1.4.2 Bat Pattern Recognition Receptors

Pattern recognition receptors (PRRs) are a class of conserved mammalian receptors that can directly recognise pathogen associated molecular patterns (PAMPs) derived from pathogens such as viruses, which are markers and molecular signatures distinguishable from ‘self’ (Collins and Mossman, 2014, Koyama et al., 2008, Janeway Jr and Medzhitov, 2002). PAMPS are pathogenic features that are not

usually present within the host, but are often essential for the survival and replication of the pathogen, such as double-stranded RNA (dsRNA), or the presence of 5' diphosphate (5'pp) and 5' triphosphate (5'ppp) groups, often present in RNA viruses (Killip et al., 2015). DNA viruses are also recognised by PRRs when viral DNA is released into the cell cytoplasm whereby it acts as a PAMP. DNA of eukaryotic cells is located within nuclei or mitochondria and consequently the presence of the viral DNA within the cytoplasm is detected by host PRRs as non-self (Ma et al., 2018). PRRs present in the host are hence able to directly recognise PAMPs as non-self via discrimination between host and foreign molecular species and successfully bind PAMPs within infected cells. As bats are important reservoirs of several zoonotic RNA viruses, it is central to investigate the intracellular PRRs in bats that may induce antiviral signalling pathways during viral infection (Banerjee et al., 2016, Banerjee et al., 2020).

IFNs are essential immune modulators produced by the body's cells in response to viral infection. In order for IFNs to be produced, the invading virus must first be recognised by the host via PRR recognition of viral PAMPs. There are different classes of PRR involved in IFN activation pathways in humans which have also been identified as conserved in bats including Toll-like receptors (TLRs), retinoic acid inducible gene-I (RIG-I)-like receptors (RLRs), nucleotide oligomerization domain (NOD)-like receptors (NLRs) and cytosolic DNA sensors (La Cruz-Rivera et al., 2018). The roles of different PRRs are largely dependent on the viral stimuli and their cellular location. For example, TLRs are located at the cell surface or inside endosomes of phagocytic cells, whereby they are able to detect viruses that have been taken up from the extracellular space (Kawasaki and Kawai, 2014). Other PRRs such as RLRs, NLRs and DNA sensors reside in the cell cytoplasm and membranes, whereby they detect viral PAMPS within infected host cells (Li and Wu, 2021). Furthermore, TLRs and RLRs mainly respond to RNA viruses, whereas cytosolic

DNA sensors such as cyclic GMP-AMP synthase (cGAS), interferon gamma inducible protein 16 (IFI16) and absent in melanoma 2 (AIM2) respond to DNA viruses (Lee et al., 2019). Upon recognition of PAMPS on an invading viral pathogen, PRRs activate a network of downstream intracellular signalling cascades which mediate type I IFN signalling that ultimately leads to the expression of antiviral and proinflammatory molecules (Mogensen, 2009). These processes immediately initiate host defence against the invading pathogen whilst also priming the adaptive immune response which is antigen-specific (Janeway Jr and Medzhitov, 2002, Kawasaki and Kawai, 2014).

TLRs are considered the first line of defence against viral infection due to their extracellular or endosomal location (Cowled et al., 2011). TLRs have been successfully described in two species of fruits bats; *Pteropus alecto* (*P.alecto*) and *Rousettus leschenaultia*, whereby studies demonstrated that the TLRs of bats are highly conserved with other mammals (Iha et al., 2010, Cowled et al., 2011). Full-length transcripts for TLRs 1-10 have been sequenced in *P. alecto*, providing key evidence that bats can recognise a range of pathogens including viruses. In addition to the conserved TLRs present in bats, an almost intact TLR13 pseudogene has also been identified in *P.alecto*, which is markedly lacking in humans but has been previously identified in the endosome of mice whereby it recognises bacterial RNA, yet its function remains poorly understood (Cowled et al., 2011, Signorino et al., 2014). The observation of the upregulation of type I IFNs in response to viral infection and poly I:C treatment in several bat species, supports the notion that dsRNA sensing via TLRs is highly conserved between humans and bats (Banerjee et al., 2016, Cowled et al., 2012, Omatsu et al., 2008, Banerjee et al., 2017). Further experiments confirming the presence and action of TLRs in bats include the study of dsRNA sensing by TLR3 in big brown bats (*Eptesicus fuscus*) and the computational analysis of TLR8 in twenty-one bat species, identifying sequence differences

between bat TLR8 in different bat species and with its human counterpart (Banerjee et al., 2017, Schad and Voigt, 2016).

Cytoplasmic PRRs including RIG-I, laboratory of genetics and physiology 2 (LGP2) and melanoma differentiation-associated protein 5 (MDA5) which detect exogenous RNA have also been characterised in *P. alecto* and described in several bat genome and transcriptome investigations (Papenfuss et al., 2012, Banerjee et al., 2017). In *P. alecto*, both RIG-I and MDA5 are shown to possess similar structures and cellular distribution to their human equivalents and an additional study in *E. fuscus* observed the role of bat RIG-I and MDA5 in poly(I:C) sensing. Overall, the presence of several characterised PRRs provides strong evidence for the conservation and functionality of extracellular, endosomal and cytosolic viral RNA sensors in bats, consistent with that of humans and other mammals (Cowled et al., 2012, Baker et al., 2013).

1.4.3 Bat Interferons

1.4.3.1 Background on Interferons and their Role in Immunity

The IFN response plays a crucial part in innate immunity, acting as the first line of defence against viral infection, facilitating the induction of an antiviral state in infected host cells and the prevention of further spread of viral infection (Randall and Goodbourn, 2008). IFNs are cytokines, which fall into one of three classes; type I IFNs, type II IFNs and type III IFNs, differing in their sequence and receptor signalling (Pestka et al., 2004, Schroder et al., 2004). Type I and type III IFNs are produced in most cell types and are induced directly in response to viral infection whereby they bind to their cognate receptors ultimately inducing interferon stimulated genes (ISGs). Despite both type I and type III IFNs activating similar genes via shared pathways, they act via different receptors resulting in distinct responses. Type I IFNs bind to the IFNAR IFN receptor, which is expressed ubiquitously, whereas type III IFNs bind IFNLR which is largely restricted to expression in epithelial cells and neutrophils (Lazear et al., 2019). Type II IFNs, refers to a single IFNγ species, a cytokine specific

to immune cells such as natural killer and T cells, which is hence commonly associated with the adaptive immune response (Stanifer et al., 2019, Baker et al., 2013, Corrales-Aguilar and Schwemmle, 2020). Both type I and type III IFNs activate the transcription of hundreds of ISGs, which commonly have valuable roles in antiviral immunity and the capacity to target almost every step of viral replication (Sadler and Williams, 2008, Schoggins and Rice, 2011). Despite both type I and type III IFNs inducing similar sets of ISGs, signalling by type I IFN notably causes a more rapid ISG induction and subsequent decline in expression (Lazear et al., 2019, Park and Iwasaki, 2020). Ultimately, an early IFN response is therefore essential in limiting viral replication and further spread (Schoggins and Rice, 2011, Grandvaux et al., 2002a, Goodbourn et al., 2000).

1.4.3.2 Characterisation of Interferons and Interferon Induction in Bats

The number of type I IFNs differs between mammalian species, but notably humans possess 14 IFNα species and a single species of IFNβ, IFNκ, IFNω and IFNε respectively (Capobianchi et al., 2015, Pestka et al., 2004). Type I IFNs have been described in five species of bat; *Rousettus aegyptiacus*, *P.alecto*, *Pteropus vampyrus*, *Dobsonia viridis* and *Myotis lucifugus* (Kepler et al., 2010, He et al., 2010, Omatsu et al., 2008). IFNs in bats were first investigated in 2010 using partial genome sequences isolated from *P. vampyrus* and *M. lucifugus*, whereby a single type II IFN gene was identified in both species, similar to humans (Kepler et al., 2010, Van Pesch et al., 2004). Interesting findings showed that both bats differed in their type I IFN genes in comparison to human, exhibiting a larger number of genes encoding IFNδ and IFNω. Both humans and mice possess only one IFNω, whereas *P.vampyrus* was identified to possess 28 assemblies, 18 intact ORFs and 8 pseudogenes and *M.lucifugus* possessing up to a dozen IFNω species (Van Pesch et al., 2004, Kepler et al., 2010). A large number of IFNω is not out of the ordinary, as this has also been observed in cows (*Bos taurus*) which possess 26 intact IFNω

genes. IFNω has been previously demonstrated to exhibit anti-proliferative and antiviral effects, therefore the apparent expansion of IFNω in bats could potentially aid in their innate immune defence against viruses (Li et al., 2017). IFNδ identified in bats is not present in humans, but exists in sheep, horses and pigs (Cochet et al., 2009). In *P.vampyrus*, 14 assemblies with 5 intact ORFs, 2 partial ORFs and 7 pseudogenes were recorded for IFNδ. The first complete transcriptome analysis of IFNs in any bat species was conducted in *P.alecto* by Zhou et al. (2016), whereby 10 type I IFNs were identified, including only 3 IFNα genes, in comparison to the 14 that humans and mice possess (Pestka et al., 2004). A single IFNβ and IFNε gene and five IFNω genes were also identified. Furthermore, a single IFNκ gene was also identified, but within a separate *P.alecto* scaffold, alongside a further 8 IFNα pseudogenes. Studies have shown that IFN signalling in *P.alecto* cells is highly dependent on IFNAR2, as depletion of this receptor halts IFN signalling in bats and was shown to increase H1N1 influenza virus replication (Zhang et al., 2017). The contraction of the IFNα locus was also observed in other bat species, with *P.vampyrus* only possessing 7 IFNα genes and *M.lucifugus* containing IFNα pseudogenes only, but it is worth noting that these two datasets were retrieved from two low coverage bat genome sequences (Van Pesch et al., 2004, Kepler et al., 2010). These results highlight a restricted type I IFN locus within several bat species, containing fewer IFNα genes than other mammals (Zhou et al., 2016). Contraction of the type I IFN locus is not present in all bat species however, as other research has identified the expansion of type I IFNs in *R. aegyptiacus*, consisting of 12 IFNα genes, a single IFNβ, IFNε and IFNκ, but also 9 IFNδ and 22 IFNω genes (Pavlovich et al., 2018). The contrast in the contraction and expansion of different type I IFNs not only highlights the differences in type I IFN loci between bats and humans, but also shows high variability in type I IFNs between different bat species, warranting further investigations into the functionality of type I bat IFNs and how these changes

influence the antiviral actions of bat immunity (Corrales-Aguilar and Schwemmle, 2020).

Type III IFNs have also been characterised in *M.lufigugus* and *P.alecto*, identifying the presence of a single IFNλ gene and two IFNλ genes (IL28a and IL29) respectively, which appear to show homology to other mammals displaying similar loci and sequence length, indicating a potential functional conservation (Virtue et al., 2011). Furthermore, two chains comprising the type III IFN receptor complex have also been identified in *P.alecto* and IFNλR1 has been demonstrated as a functional receptor (Zhou et al., 2011a, Zhou et al., 2011b). Interestingly, the type III IFN receptor complex in bats is distributed in a wider range of tissues, consistent with a more significant role in bats compared to humans, whereby IFNλ1R is mainly localised to epithelial cells (Sommereyns et al., 2008, Witte et al., 2010, Zhou et al., 2011a).

Several studies in Pteropid bat cells and cell lines have confirmed that bat IFN production in response to stimulation with synthetic TLR ligands, including poly(I:C) and lipopolysaccharide (LPS) is functional (Stewart et al., 1969, Kepler et al., 2010, Zhou et al., 2011b, Crameri et al., 2009, Baker et al., 2013). Research has also identified the induction of the bat IFN response by viral infection via both *in vivo* and *in vitro* studies, which also suggest different roles for IFN responses in bats and the potential for viruses to evade the bat IFN response (Baker et al., 2013). The first study investigating IFN induction in bats infected brain and spleen tissues from the microbat *Triatoma brasiliensis* with Japanese B encephalitis (JE) virus whereby IFN was detected in both tissues after one week of infection, but then interestingly only in the brain tissue after week two (Stewart et al., 1969). *In vitro* infection of *P.alecto* splenocyte cells with a bat paramyxovirus named Tioman virus, resulted in the unusual downregulation of type I IFN, whilst simultaneously inducing the upregulation of type III IFNs, stressing the potential significance of type III IFNs in bat antiviral

responses (Zhou et al., 2011b). Contrastingly, experimental infection of both Pteropid bat and human cells with henipavirus, induced the production of both type I and III IFNs (Virtue et al., 2011, Zhou et al., 2011b). An investigation by Kepler et al. (2010) highlighted the conservation of IFN signalling between bats and other mammals through stimulation of *P.vampyrus* cells, whereby infection with Vesicular stomatitis virus (VSV) resulted in a delay in IFN response, compared to the rapid induction of IFNs by poly(I:C) or LPS, consistent with what occurs in humans. Collectively, this research shows that bat IFNs are successfully induced by both viruses and synthetic viral ligands but differ in their response to one another and to humans, which may prove significant in their ability to control viral replication.

Fascinating research by Zhou et al. (2016) characterised the contraction of the type I IFN locus in *P.alecto*, but also revealed that IFNα genes in bats are constitutively expressed in unstimulated cells and tissues, whereby IFNα levels remain unaffected by viral infection with bat-borne viruses (HeV and Pulau virus). This expression pattern is interesting and appears unique, as the constitutive activation of type I IFN has seldom been observed in any other species. Constitutive activation of IFNα was further confirmed in *Cynopterus brachyotis* indicating that this expression pattern was not exclusive to *P.alecto* (Zhou et al., 2016). Furthermore, IFNα functionality was confirmed via the successful induction of ISGs in bats in the presence of all three IFNα species and supporting evidence by Shaw et al. (2017) confirmed high basal transcription levels of type I IFNs in bat cells from both suborders, in comparison with other mammals (Zhou et al., 2016). These findings exhibiting the constitutive activation of functional IFNα suggests that bats possess a primed IFN response with high basal levels of IFNα, as opposed to the traditional upregulation of IFNs following viral infection commonly observed in humans and other mammals. Evolution of an ‘always on’ type I IFN response may confer bats with the advantageous immune mechanism to rapidly and immediately respond to viral infection. Furthermore,

constitutive IFNα expression coupled with the contraction of the type I IFN locus in bats, is consistent with the 'less is more' theory that natural selection can produce mutations that favour a reduction in the number of functional genes, but provides a heightened advantage to the host (Olson, 1999). Despite these interesting findings, further investigations into bat IFNs are necessary to gain a better understanding of IFN induction and expression in bats and whether they play a key role in their antiviral immunity or if other influencing factors shape their antiviral activity (Baker et al., 2013).

1.4.4 The Bat Interferon System

1.4.4.1 Induction of Bat Interferons

Although bat immune studies remain somewhat limited, research has indicated that bats share several key features of innate immune signalling with humans and other mammals, including the induction of IFNs. For example, bat cells have been shown to mount an antiviral response to RNA viruses such as Newcastle disease virus (NDV) and Sendai virus, in addition to the response mounted upon transfection of synthetic stimulants such as poly(I:C) (Cowled et al., 2012, Liang et al., 2015, Li et al., 2015a, Glennon et al., 2015). These viral stimulants are detected by TLRs (TLR 3, 7, 8 or 9) or the cytosolic receptors RIG-I and MDA5. The activation of these receptors results in the further activation of downstream adaptor proteins such as the mitochondrial antiviral signalling protein (MAVS), Toll/IL-1R domain-containing adaptor-inducing IFNβ (TRIF) and TNF receptor-associated factor (TRAF3), which in turn activate cellular kinases such as TANK-binding kinase 1 protein (TBK1). TBK1 can then activate the transcription factors interferon regulatory factor 3 or 7 (IRF3/IRF7), nuclear factor kappa-light-chain-enhancer of activated B cells (NF-κB) and activating protein 1 (AP-1) by orchestrating the assembly of multi-protein complexes. Once activated, IRF3/7, NF-κB and AP-1 translocate to the cell nucleus to stimulate the

transcription of IFNs, such as IFNα, β, ω, κ and λ, which are secreted from the infected cell to bind its cognate receptor complex via autocrine or paracrine manners (Figure 1.6).

In human cells, virus recognition and signalling utilise IRF3 and IRF7 to drive the induction and expression of IFNs (Collins and Mossman, 2014, Honda et al., 2005, Janeway Jr and Medzhitov, 2002). IRF3 sequences have been identified in bats, but appear evolutionarily distinct in sequence to human IRF3 (Banerjee et al., 2019). IRF3 from *E.fuscus* cells was identified to mediate the antiviral signalling response of bat cells against MERS-CoV and poly(I:C) stimulations, whereby knockdown of IRF3 highly reduced the production of IFNβ in response to viral stimulation (Banerjee et al., 2019). IRF7 functionality has also been investigated in bats, acting in a similar manner to IRF3 in *E.fuscus* cells, whereby knockdown of IRF7 in *P.alecto* cells greatly reduced the induction of IFNβ to infection with Sendai virus (Zhou et al., 2014). Furthermore, in both *P.alecto* and *E.fuscus* bat cell lines, IRF7 was successfully induced in response to poly(I:C) stimulation (Banerjee et al., 2017, Zhou et al., 2014). IRF7 appears an interesting area of study in bat innate immunity, due its conserved activation of IFNs in addition to its observed widespread tissue distribution and constitutive activation in bats, which could potentially provide bats with the advantage to respond more rapidly to viral infection (Zhou et al., 2014). The TLR and cellular kinase adaptor proteins that activate IRF3 and IRF7 currently remain unexplored in bats but could provide valuable insight into the signalling pathways leading to IFN induction.

MAVS is a protein adaptor utilised by IRF3 and NF-κB for nuclear translocation, to induce type I IFNs and has been identified as functionally conserved between bats and humans, after the investigation of MAVS signalling in two bat species; *Rhinolophus sinicus* and *Eidolon helvum* (Seth et al., 2005, Feng et al., 2019). Experimental knockout of MAVS in human cells and replacement with bat MAVS

resulted in the successful activation of IRF3 after Sendai virus infection and the induction of the IFNβ promoter and ISG expression of IFN-induced protein with tetratricopeptide repeats 1 (IFIT1) (Feng et al., 2019). These studies proved useful in highlighting the conserved functionality of MAVS between bats and other mammals, yet downstream signalling pathways and other molecules potentially involved in MAVS-mediated signalling remain uncharacterised and warrant future study (Banerjee et al., 2020).

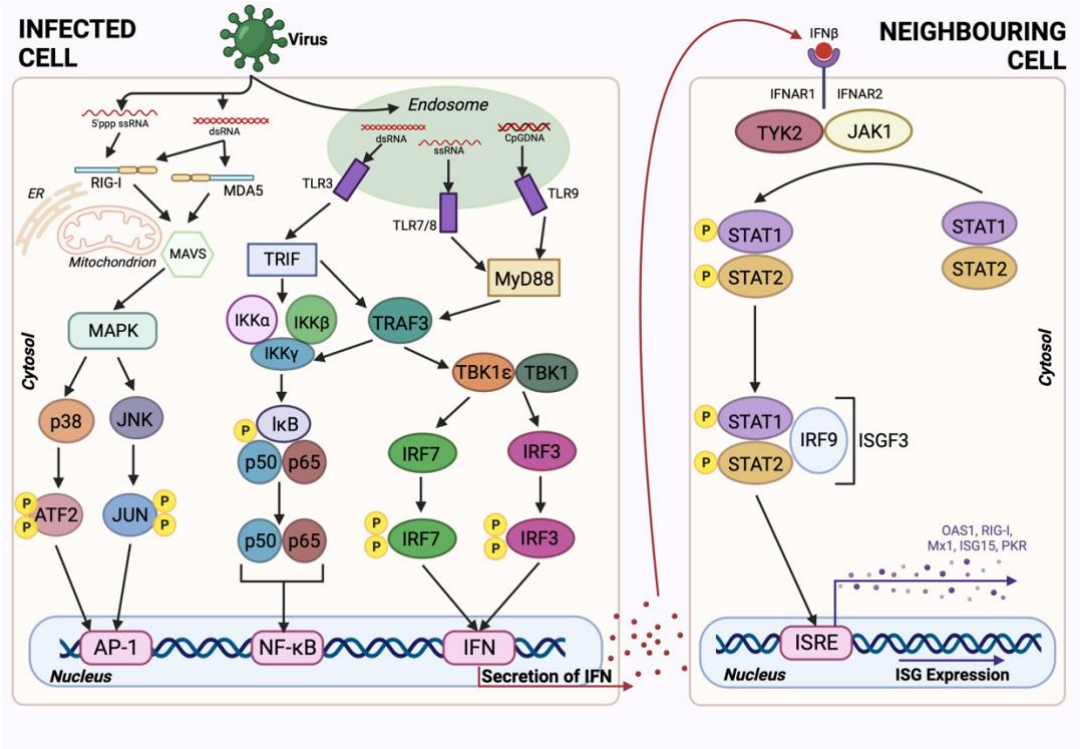

Figure 1.6 - The induction of interferons and the antiviral state they elicit in bat cells. *Viral RNA species such as dsRNA and ssRNA, are detected by TLRs, RIG-I or MDA5, initiating the signalling of downstream adaptor proteins; MAVS, TRIF and TRAF3. Adaptor proteins activate cellular kinases such as TBK1, which in turn activate IRF3/7, NF-κB, and AP-1 by orchestrating the assembly of multimeric protein complexes. Once activated, IRF3/7, NF-κB and AP-1 translocate to the cell nucleus to stimulate the expression of IFNs such as IFNs α, β, ω, κ, and λ. IFNs then bind to their cognate receptor complex (IFNAR) on infected or neighbouring cells to activate the JAK-STAT pathway via kinases such as Jak1 and Tyk2 that phosphorylate STAT proteins. Phosphorylated STAT proteins (STAT1 and STAT2) merge with IRF9, collectively forming the ISGF3 transcription factor. ISGF3 is translocated to the nucleus to initiate the transcription of genes present in ISRE promoters known as ISGs. ISGs such as Mx1, OAS1 and ISG15 are expressed and work to subsequently establish an antiviral state against the invading pathogen. Figure was generated based on findings in the bat IFN pathway which shows high conservation to human, but several pathways and molecular homologs in the bat IFN response still require characterisation. Adapted from Clayton and Munir (2020) and Banerjee et al. (2020) and created with Biorender.com.*

1.4.4.2 The Bat Interferon Signalling Pathway

Upon IFN induction in the mammalian response to viral infection, typically, type I and III IFNs bind their cognate receptors and activate the same signalling pathway, known as the JAK-STAT pathway, to ultimately result in the transcription of ISGs and other antiviral molecules to establish an antiviral state in cells (Baker et al., 2013). Type I IFN signalling takes place via the binding of IFNs to IFNAR comprised of two proteins with transmembrane domains (IFNAR1 and IFNAR2), whereas type III IFNs bind the IFNL1 receptor which is composed of the type III IFN-specific IL-28RA and IL10R2 chains (Kotenko et al., 2003, Sheppard et al., 2003).

Despite differences between the binding of type I and type III, they share similar subsequent intracellular signalling whereby binding of these IFNs to their cognate receptors recruits specific protein kinases such as Janus kinase1 (JAK1) and tyrosine kinase 2 (TYK2) that activate upon extracellular IFN binding to the receptors. These kinases phosphorylate the signal transducer and activator of transcription (STAT) proteins (Gad et al., 2009, Miknis et al., 2010). The phosphorylated STAT1 and STAT2 proteins dimerize and recruit IRF9 to form the interferon stimulated gene factor 3 (ISGF3) complex (Fujii et al., 2010). The ISGF3 transcription factor then translocates to the cell nucleus to bind the IFN-stimulated response element (ISRE) sequence, to initiate the transcription of several ISGs such as Mx1 and OAS1 which work to establish an antiviral state against the invading pathogen (Figure 1.6) (Samuel, 2001). Only a select few studies have been devoted to investigating the IFN signalling pathway following IFN induction and the STAT1 protein is the only component of IFN signalling that has been characterised in bats, whereby STAT1 was identified in *R.aegyptiacus*. The phosphorylation of STAT1 and subsequent translocation to the cell nucleus after stimulation with IFNα is consistent with the activation of type I IFN signalling in humans and other mammals (Samuel, 2001, Fujii et al., 2010). STAT1 is antagonised in rabies infection in both bat and human cells,

preventing its translocation to the nucleus and subsequent induction of antiviral ISGs (Brzózka et al., 2006, Fujii et al., 2010).

1.4.4.3 Bat Interferon-stimulated Genes

Upon viral infection, bat IFN production is activated to induce the transcription of hundreds of ISGs which have essential roles in eliciting an antiviral state in infected and neighbouring cells. ISGs are crucial to vertebrate antiviral immunopathology due to their roles in instigating antiviral processes which work to target almost every step in the viral life cycle (Schoggins and Rice, 2011, Sadler and Williams, 2008). There are around 50-1000 ISGs that have been identified in humans, which vary based on cell type and duration of IFN stimulation, whereas the full ISG repertoire of bats has not yet been established (Banerjee et al., 2020, Schoggins and Rice, 2011). Each mammal possesses their own unique repertoire of ISGs which consists of ISGs that are commonly shared with other mammalian species, in addition to a collection of ISGs that are often species or lineage-specific (Shaw et al., 2017). Banerjee et al. (2020) suggests that due to the large volume of bat species and the high diversity observed within the two bat suborders, it is more than likely that bats possess both unique and parallel ISGs to one another and to other mammals and although studying homologs of human ISGs in bats is very useful, it may not be fully representative of the potential capacity of ISGs in bats. Valuable research by La Cruz-Rivera et al. (2018) confirms the presence of both unique and conserved ISG expression profiles between bats and other mammals. La Cruz-Rivera et al. (2018) further describe the alternative ISG expression levels in bats to humans, which despite exhibiting similar early induction kinetics, possess distinct late phase decline. This indicates that a rapid induction of ISGs is often followed by a rapid decline in transcript level within *P.alecto* cells treated with IFNα (La Cruz-Rivera et al., 2018). This is contrasting to human ISGs which lack this decline phase and hence remain elevated for longer periods of time. The quicker decline of ISGs after IFN stimulation

in bats may underlie the control of viral replication and reduced viraemia observed in bats. Basal ISGs in unstimulated *P.alecto* cells were also expressed more highly than their human counterparts, suggesting that bat ISGs could provide some residual antiviral protection even once IFN signalling is returned to basal levels, also suggesting the potential of species-specific differences in viral susceptibility in bats (La Cruz-Rivera et al., 2018).

1.4.4.3.1 Conserved Bat ISGs

Many ISGs present in humans have been identified in bats, for example the *in vitro* stimulation of *P.alecto* cells with Pteropine ortheovirus (PRV) resulted in the induction of protein kinase R (PKR), 2-5-oligoadenylate synthetase 1 (OAS1) and orthomyxovirus-resistant gene 1 (Mx1 GTPase) in an IFN dose-dependent manner, which are also found in humans and other mammals (Zhou et al., 2013a). These three ISGs are the most represented in bat literature and are involved in the major antiviral pathways raised against an invading viral pathogen (Clayton and Munir, 2020). Experimental stimulation of *E.fuscus* kidney cells with poly(I:C) also resulted in the expression of several conserved mammalian ISGs: MDA5, RIG-I, radical S-adenosyl methionine domain-containing 2 (RSAD2), IRF7, OAS1, IFN-inducible protein 6 (IFI6) and myxovirus resistance 1 (Mx1) (Banerjee et al., 2017). Interesting findings show that the OAS1 gene promoter identified in *P.alecto* cells possesses two ISREs, in comparison to a single ISRE present in humans (Zhou et al., 2013a). This additional ISRE element implies that OAS1 may play an important role in antiviral activity in *P.alecto* and *E.fuscus*. An additional study showed that the ectopic expression of Mx1 from six different bat species, resulted in a decreased replication of both Ebola and influenza A virus in human embryonic kidney (HEK293T) cells *in vivo* (Fuchs et al., 2017). Mx1 is an ISG of great interest in bats, due to research showing the residues within the Mx1 protein in at least 13 bat species are positively evolving, indicating their high importance in controlling antiviral activity in bats (Fuchs

et al., 2017). Other research revealed that interferon stimulated gene 54 (ISG54) and interferon stimulated gene 56 (ISG56) were both induced by type I IFN in Pteropid bat cell lines and stimulation with type III IFN in bat cells also showed the induction of ISG56, alongside RIG-I (Zhou et al., 2011a, Virtue et al., 2011). The induction of 2'5'-oligoadenylate-synthetase 2 (OAS2) has also been detected in *P.vampyrus* cells when infected with VSV or stimulated with LPS or poly(I:C) (Kepler et al., 2010). Collectively, these results highlight the high degree of similarity in signalling molecules and ISGs downstream to IFN induction between bats and other mammals (Baker et al., 2013).

1.4.4.3.2 Novel Bat ISGs

In addition to the characterisation of ISGs in bats that were conserved with human, gene expression profiling analyses by La Cruz-Rivera et al. (2018) also identified several ISGs that had not been previously recorded in any other mammal and thus appear unique to bats. One significant novel ISG identified in *P.alecto* cells is the highly inducible ribonuclease L (RNase L), which although is present in humans, is not IFN-inducible (La Cruz-Rivera et al., 2018). RNase L encodes a 2'5'-oligoadenylate synthetase-dependent RNase, which has been uncovered to have roles in the antiviral immune response against viruses by degrading products produced by the OAS family of enzymes during infection. Knock-out studies have exhibited that the IFN-stimulated induction of RNase L in *P.alecto* confers heightened antiviral protection in bats, as when absent, *P.alecto* cells showed an enhanced susceptibility to viral infection (La Cruz-Rivera et al., 2018). Only proteins upstream of OAS are induced by IFNs in humans as RNAse L itself is not directly induced, therefore the direct induction of RNase L in *P.alecto* could prove significant in providing a more efficient impairment of viral replication before it can spread to neighbouring cells (La Cruz-Rivera et al., 2018). Additional non-canonical ISGs were found in stimulated *P.alecto* cells, including; ER membrane receptor complex subunit

2 (EMC2), filamin A interacting protein 1 (FILIP1), TL17RC, OTOGL, solute carrier family 10 member 2 (SLC10A2) and solute carrier family 4 member 1 (SLC4A1) (La Cruz-Rivera et al., 2018).

Another study investigating ISGs in bats infected *P.vampyrus* cells with NDV and identified the expression of canonical ISGs including RIG-I, interferon stimulated gene 15 (ISG15), interferon regulatory factor 1 (IRF1) and MDA5. However, the upregulation of another set of ISGs was observed; RND1, SERTA-domain containing 1 (SERTAD1), ChaC glutathione specific gamma-glutamylcyclotransferase 1 (CHAC1) and MORC3 (Glennon et al., 2015). These genes are NDV-dependent as IFN treatment alone did not successfully induce this set of ISGs, therefore these results raise questions about the potential of virus-specific antiviral genes in bats that are induced irrespective of IFN stimulation. This set of ISGs identified in *P.vampyrus* have not been previously reported in humans or other mammals and so appear to be novel to bats. The identification of a subset of ISGs unique to bats directs towards the ability of bats to utilise a different ISG repertoire to humans to infer antiviral activity in bat cells. However, the effects and molecular mechanisms generated via expression of these novel bat ISGs remains unknown. Understanding atypical antiviral immune responses in bats may prove fruitful in identifying alternate therapeutic targets in humans and other animals in order to activate antiviral pathways to offset infection caused by pathogenic viruses (Banerjee et al., 2020). In summary, although studies have identified several typical and novel ISGs in bats, these observations are limited to a select few species and cell lines. For a better representation of the global ISG response in different bat species, the responses induced in *in vivo* model systems would prove valuable in addition to virus-induced bat transcriptome analyses which allows for the identification of all antiviral ISGs via RNA sequence analysis.

1.5 Unique Mechanisms of Immune Tolerance in Bats

1.5.1 Bats Exhibit Dampened DNA Virus Sensing

1.5.1.1 Sensing of DNA Viruses

Bats that are both naturally and experimentally infected with viruses display an immune tolerance in which viral infection does not affect the bat host or cause clinical signs of disease (Swanepoel et al., 1996, Watanabe et al., 2010, Munster et al., 2016, Middleton et al., 2007). A substantial amount of focus within bat research has been focussed on RNA viral tolerance in bats, due to the importance of several RNA viruses as highly pathogenic zoonotic pathogens known to affect human populations. However, this has led to a slower understanding in the interactions of bat immunity and viral tolerance with DNA viruses, which are just as valuable to identify (Banerjee et al., 2020). Only a selection of limited studies investigating DNA sensors and signalling in bats have been undertaken, despite the knowledge that bat cells are likely at a greater risk of cytosolic DNA exposure (Xie et al., 2018). Numerous DNA viruses have been characterised in bats, including; poxviruses, herpesviruses, adenoviruses, hepadnaviruses and polyomaviruses, yet a full understanding of their detection in bats is lacking (Host and Damania, 2016, Shabman et al., 2016, Subudhi et al., 2018, Mendenhall et al., 2019, Drexler et al., 2013, O'Dea et al., 2016, Fagrouch et al., 2012, Misra et al., 2009). Detection of DNA viruses and self-DNA in humans occurs through the endosomal receptor TLR9 and cytosolic receptors belonging to the PYRIN and HIN domain (PYHIN) family such as cGAS, AIM2 and IFI16 (Kawai and Akira, 2006, Schattgen and Fitzgerald, 2011, Li et al., 2013, Ni et al., 2018). Detection of DNA viruses thus occurs both within the cell cytoplasm by cGAS for example, and also within endosomes by TLR9. Following detection of DNA via these sensors, downstream pathways are activated which lead to the expression of both antiviral and pro-inflammatory cytokines (Kawai and Akira, 2006).

Research investigating the DNA sensor TLR9, identified the evolution under purifying selection and mutations in the ligand-binding domains of TLR9 from 8 bat sequences (Escalera-Zamudio et al., 2015). Further *in vitro* observations deduced that bat cells do not respond as well to stimulation of the TLR9 DNA sensor in comparison to humans cells and computational analyses supports the notion that bat TLR9 has evolved altered ligand specificity (Banerjee et al., 2017, Escalera-Zamudio et al., 2015). The functional roles of all TLRs in bats remain undefined, but the mutations in TLR9 that result in differential ligand binding to traditional TLR9 in other mammals may suggest a degree of specificity in bat TLR9 and the types of DNA it can sense (Banerjee et al., 2020).

1.5.1.2 STING Mutation and Reduced Response

Despite evidence that bats have evolved mechanisms to detect and control RNA virus infections, preliminary studies have demonstrated that their responses to DNA viruses appear dampened (Ahn et al., 2016a, Xie et al., 2018). STING is an essential adaptor protein in numerous DNA sensing pathways that mediates IFN signalling and thus plays key roles in infection, inflammation and cancer (Barber, 2015). A significant study exploring immune tolerance in bats demonstrated that STING has undergone a point mutation within a conserved residue in several bat species, resulting in the reduction of STING-dependent signalling (Xie et al., 2018). Sequence alignment of STING from a total of 30 different bat species revealed a common point mutation in the highly conserved serine residue at position 358 (S358) in bats which was replaced by a selection of alternate residues including; D, F, H, N, P and R (Xie et al., 2018). The S538 residue was markedly identified as highly conserved among other mammals where it acts as a key phosphorylation site critical in the downstream activation of IFNs (Xie et al., 2018). Therefore, the mutation of this residue within bats suggests there may be a weakened response of STING in the context of IFN response to DNA viruses (Liu et al., 2015, Tanaka and Chen, 2012, Tsuchida et al.,

2010). To examine the effect of the S358 mutation in bats on IFN induction and the antiviral response, *P.alecto* cells were infected with the DNA virus herpes simplex virus (HSV), which consequently displayed higher replication levels due to STING mutation, however upon reversing this mutation at position 358 in STING, HSV replication was then significantly inhibited in the bat cells, indicating that STING-induced IFN induction had been restored upon replacement of the S358 residue (Ni et al., 2018). The STING mutation evident in bats could be evolutionarily driven to provide bats with the capacity to tolerate the overactivation of STING by self-DNA produced as a result of powered flight. However, the influence of dampened STING responses to infection with bat-borne RNA species including those produced as by-products of viral DNA infection, have not been investigated and require further mechanistic investigations to fully characterise the action of STING in bats (Irving et al., 2021, Li et al., 2015b).

1.5.2 Controlled Inflammasome Response

1.5.2.1 Absence of PYHIN gene family

Recent genomic analysis has identified the loss of the entire PYHIN gene family in both megabat and microbat species (Ahn et al., 2016b). As previously mentioned, members of the PYHIN family, such as AIM2 and IFI16, are essential immune sensors for the recognition of intracellular DNA that activates the inflammasome and IFN response (Schattgen and Fitzgerald, 2011, Brunette et al., 2012). PYHIN proteins possess an N-terminus PYRIN domain in addition to one or occasionally two C-terminal HIN domains, and all PYHIN genes are located at the same locus (Brunette et al., 2012). The PYHIN family is found within all other major groups of placental mammals, which tend to possess at least one PYHIN gene member, although numbers can be variable. Contrastingly, the universal loss of PYHIN genes was recorded in the genomes of 10 bat species, representative of four out of five major bat lineages (Ahn et al., 2016a). The presence of viral DNA triggers a protective

immunological response in host cells, however the self-DNA produced in mammals during periods of stress can also cause excessive inflammation and autoimmune mechanisms. Subsequently, the secretion of inflammasome cytokines upon viral infection must be tightly regulated to reduce excessive activation and immunopathology. Bats appear unique in their universal evolutionary loss of the PYHIN family which could provide beneficial ramifications in their ability to control inflammation.

1.5.2.2 Dampened NLRP3 Inflammasome Response

Recent investigations into mechanisms of immune tolerance in bats have revealed the dampening of inflammation in bats in response to RNA virus infection (Ahn et al., 2019). NLR family pyrin domain containing 3 (NLRP3) is an important inflammasome sensor that has essential roles in both age-induced and viral-stimulated inflammation. NLRP3 recognises viral and bacterial infections along with cellular stresses such as oxidized DNA species, mitochondrial damage and the presence of extracellular adenosine triphosphate (ATP) (Shimada et al., 2012, Mariathasan et al., 2006, Iyer et al., 2013, Sha et al., 2014, Kuriakose and Kanneganti, 2017). NLRP3 in bats has been described as dampened at both the transcriptional and protein level in comparison with human or mouse counterparts. Significantly, the dampened action of NLRP3 resulting in the reduction in inflammation in infected bats in response to RNA viruses did not influence the viral loads, which supports the ability of bats to tolerate viral replication whilst restricting the effects of inflammation (Irving et al., 2021). A diverse range of emerging viruses are sensed by NLRP3, including coronaviruses, influenza A virus (IAV) and rabies virus (Lupfer et al., 2015, Chakrabarti et al., 2015, Tong et al., 2012, Lawrence et al., 2013, Johnson et al., 2010, Ahn et al., 2019, Chen et al., 2019, Nieto-Torres et al., 2015). As the NLRP3 inflammasome is central to infection and aging in mammals, the dampened NLRP3-mediated inflammatory response observed in bats signifies differences in inflammasome responses between

bats and other mammals and supports the theory that bats possess an enhanced immune tolerance, as opposed to an enhanced antiviral defence (Ahn et al., 2019). The dampened stress and viral-related inflammatory responses in bats support their longevity and capacity to tolerate disease, in contrast to pathogenesis caused by bat-borne viruses in spillover infections.

Overall, the high metabolic demands and body temperatures associated with powered flight in bats results in the release of harmful by-products such as ATP, cytosolic DNA and reactive oxidation species, all known to trigger an inflammasome reaction. The evolutionary loss of PYHIN genes and the dampened actions of NLRP3 and STING in DNA sensing pathways in bats likely contribute to the reduction in self-DNA-mediated immunopathology, which in turn influence viral DNA detection. These unique immune mechanisms permitting bats to manage inflammation from viral infection or from flight, largely influence their immune tolerance and unique qualities as viral reservoirs. Due to the ability of bats to carry several DNA viruses without exhibiting signs of illness, it is speculated whether DNA sensing pathways in bats are globally dampened or are specific to DNA species. Thus, more investigations are warranted to determine whether bats possess novel mechanisms to differentially sense and respond to self and exogenous DNA (Hayman, 2016).

1.6 Learning from Bats

Until recently, bats have remained one of the least extensively researched mammals, yet recent advances have been made over the past few decades allowing researchers to gain a valuable insight into their roles as important reservoir hosts for emerging viruses. The capacity of bats to host zoonotic viruses that are highly pathogenic when transmitted to humans and other animals, without exhibiting any overt signs of disease, has led to studies into the evolution of antiviral responses in bats, with a particular focus directed towards their novel immune tolerance mechanisms (Schountz, 2014).

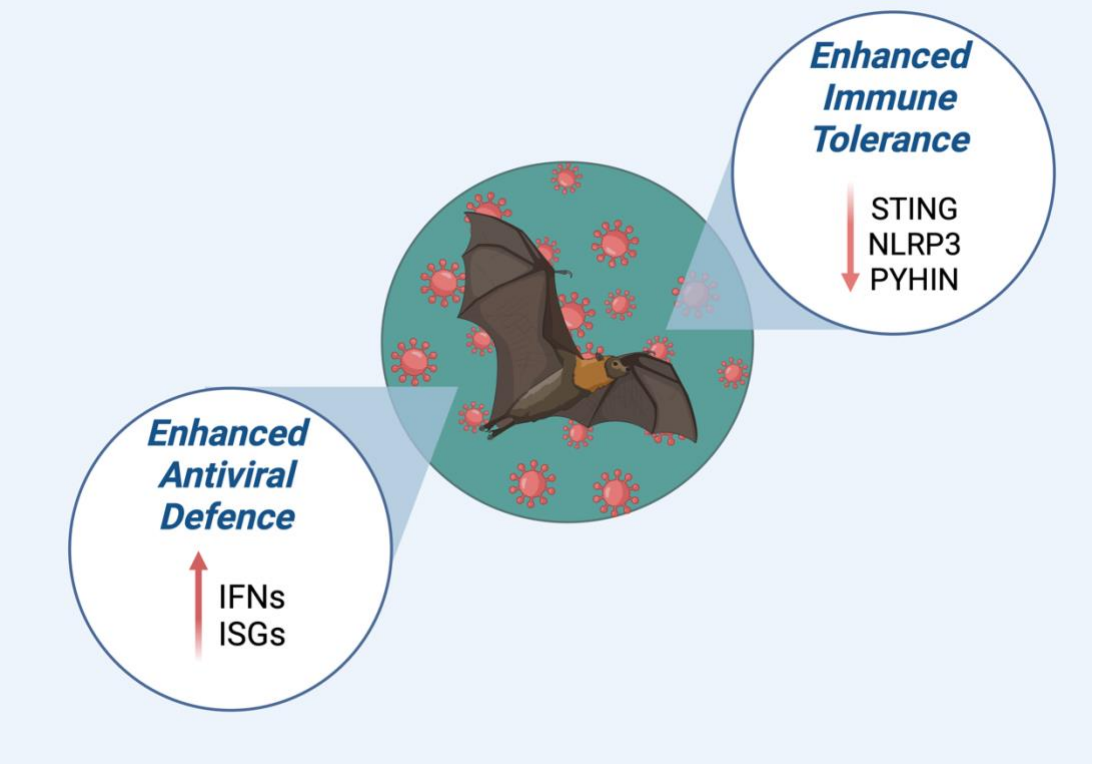

Figure 1.7 - The unique adaptations of bats as viral reservoirs that enable them to balance antiviral host defences and immune tolerance mechanisms. *The ability of bats to host viruses without exhibiting any clinical symptoms of disease is owing to a unique balance between host defence and immune tolerance. Antiviral host defences in bats include the constitutive activation of IFNs and expression of antiviral ISGs. Whereas the dampening of STING and suppression of inflammasome pathways mediated by dampened NLRP3 and loss of PYHIN contribute to immune tolerance in bats. Adapted from Irving et al. (2021) and created with Biorender.com..*

Bats are unique mammals, owing to the myriad of characteristics and attributes that they possess such as powered flight, echolocation and extreme longevity (O'shea et al., 2014). It is theorised that several key features that bats have evolved, facilitate, and underline their viral reservoir status. Several adaptations have been identified in bats that enable them to mount a robust antiviral immune response against RNA viruses, allowing them to co-exist in a viral-host equilibrium. Contrastingly, studies have also shown that the bat immune response to DNA viruses appears somewhat dampened, this is likely due to the evolution of flight and the accompanying risk of DNA damage driving inflammation and immunopathology in the host. Overall, it can be deduced that bats have established a reserve of special immune mechanisms that

allow them to thrive as viral reservoirs, exhibiting a unique host-virus relationship (Figure 1.7).

Collective research has demonstrated that bats have innate immune systems that are highly conserved with humans and other mammals, but also possess their own set of unique immune tolerance mechanisms (Banerjee et al., 2020). Genome-wide comparisons of immune-related genes confirmed the close phylogenetic relationship between bats and humans, which is closer than that between humans and rodents (Gamage et al., 2020). The high degree of conservation and close relationship between bats and humans suggests the prospective valuable role of bats as model species for the investigation of viral diseases and pathology, in addition to studies on cancer and ageing (Irving et al., 2021). Fully characterising bat immunity and the tolerance mechanisms they exhibit against emerging pathogenic viruses, may unveil novel treatment options and therapeutic targets in cases of human disease that can be explored and employed. Additionally, a comprehensive examination of bat immunity and their roles as leading viral reservoirs may aid in the understanding of viral spillover into human populations and support the discovery of potential barriers that could be implemented to prevent future outbreaks of viral diseases. Overall, by gaining valuable insights into the bat immune tolerance of viruses and their roles as viral source reservoirs, approaches can be developed and implemented into improving the global One Health status (Gibbs, 2014).

Although the field of bat immunology is currently progressing at a much faster rate than in previous years, for significant advances in the field to be achieved, a major effort in bat research must be launched. Substantial challenges are encountered in bat research due to the large species diversity in bats, alongside the lack of availability of tools and reagents. For example, the limited repertoire of susceptible bat cell lines and the propagation of bat viruses in non-host cell lines due to difficulties endured in cell harvesting and maintenance (Banerjee et al., 2018,

Paweska et al., 2016, Munster et al., 2016). An enhanced approach driven towards bat research generating the expansion of available reagents and knowledge within the field, will enable future investigations exposing bat immunology. Despite caveats encountered, the field of bat research and study of bat immunology is continually developing, allowing researchers to determine their roles as viral reservoirs and discover novel adaptations in bat immunity, which continues to redefine our understanding of mammalian immune responses (Foley et al., 2018, Jebb et al., 2018, Banerjee et al., 2020, Laing et al., 2019).

Chapter 2. Materials and Methods

2.1 Mammalian Cell Culture

2.1.1 Growing Mammalian Cells

Growing and passaging of cells was performed in a laminar flow hood using appropriate aseptic technique. HEK293T cells (ATCC) and VeroE6 cells (Public Health England, now DHSA), were all grown in Gibco Dulbecco's modified eagle medium (DMEM) + GlutaMAX (10% (v/v) FBS (Gibco), 1% (v/v) penicillin streptomycin (Gibco)). *Pteropus alecto* brain (PaBr) cells (Crameri et al., 2009) originally generated by and sourced from the University of São Paulo, Brazil, were grown in Gibco DMEM/F-12 + GlutaMAX (5% (v/v) FBS, 1% (v/v) penicillin streptomycin (Gibco), 1% non-essential amino acids (Gibco)).

A Panasonic CO_2 incubator was used. Cells were grown at 37°C, 5% CO_2.

2.1.2 Passaging Mammalian Cells

Cells were passaged every 2-3 days. Media was removed via aspiration and washing in 10ml PBS. Cells were then incubated in 3mL of trypsin (Gibco) or trypsin-versene (Gibco) at 37°C until cells no longer adhered to the base of flasks. Equal parts of growth media to dissociation reagent were added to neutralise trypsin activity and cells were pelleted at 500 x g for 5 minutes in a centrifuge. Pelleted cells were resuspended and generally passaged at a 1:3 ratio for cell maintenance, or alternatively used to prepare plates for experiments.

2.1.3 Freezing Mammalian Cells

Cells were grown to approximately 50% density in T75 flasks. Cells were washed with 5mL PBS and trypsinised as described in section 2.1.2. Growth medium was added to neutralise the trypsin. The cell suspension was centrifuged at 500 x g for 5 minutes and supernatant was removed from the pelleted cells. The cell pellet was resuspended in 500µl of freezing medium (250µl dimethyl sulfoxide (DMSO) (Sigma), 250µl DMEM growth media). Cells were then decanted into 1ml cryotubes. Cryotubes

were added to a Mr.Frosty™ freezing container (Thermo-Scientific) and frozen overnight at -80°C before being transferred to liquid nitrogen for long-term storage.

2.1.4 Transient Transfection

Cells were seeded into wells to reach 80% confluency. 100µl of Opti-MEM reduced serum media (Thermo-Scientific) was added to a 1.5ml tube containing the desired plasmid to be transfected. Plasmid amount was independently calculated for each experiment. In a separate tube, 100µl Opti-MEM was added to transfection reagent. Transfection reagents used were dependent on target cell line and included Viafect (Promega), Lipofectamine 2000 (Thermo-Scientific) and Turbofect (Thermo-Scientific) and Fugene 4K (Promega). A 1:3 ratio of plasmid DNA to transfection reagent was generally used. Both plasmid and transfection tubes were incubated at room temperature for 5 minutes. Plasmid and transfection reagent tubes were then combined, mixed by pipetting, and incubated at room temperature for 30 minutes. Media was aspirated from cell-containing wells and replaced with fresh growth medium for the cell line used. After 30 minutes, transfection mixtures were added dropwise to the corresponding wells and rocked back and forth by hand to ensure an even distribution of reagent. Cells were then incubated at 37°C, 5% CO_2 for 24 hours to allow sufficient expression of protein of interest. After 24 hours, transfection media was removed from cells and replaced with fresh growth medium.

2.2 E. coli

2.2.1 Bacterial Transformation

For transformations, 1µl of plasmid was added to 30µl of competent DH5α (Thermo-Scientific) on ice for half an hour. Following incubation, the transformation mixture was heat shocked at 42°C on a heat block for 2 minutes. Samples were then transferred to ice for 2 minutes. Samples were mixed with 250µl of LB broth media (Thermo-Scientific) and incubated whilst shaking at 37°C for 1 hour. Following incubation, around 80µl of transformation mixture was spread onto LB agar plates

(Thermo-Scientific) supplemented with appropriate antibiotics (100µg/ml ampicillin or 50µg/ml kanamycin). Agar plates were then incubated at 37°C overnight to allow time for colony growth.

2.2.2 Purifying Plasmid DNA from *E.coli*

E. coli were prepared from glycerol stocks or fresh transformations (see section 2.2.1), supplemented with appropriate antibiotic (4µl antibiotic: 1ml LB broth ratio). Generally, 9ml of bacteria were grown overnight at 37°C in LB broth. Bacteria were harvested by centrifugation at 6,800 x g for 3 minutes at room temperature (15-25°C). Plasmid DNA was subsequently isolated following the protocol outlined in the QIAprep Spin Miniprep Kit (Qiagen). When higher concentrations of DNA were required, plasmids were eluted in a reduced 25µl of elution buffer.

2.2.3 Quantifying DNA Concentration

DNA concentration was measured using a NanoDrop 2000c spectrophotometer (Thermo-Scientific) following manufacturer's instructions.

2.2.4 Isopropanol Precipitation

DNA concentrations were increased following miniprep or gel extraction via isopropanol precipitation. Firstly, 100µl of room temperature isopropanol was added to the DNA solution and mixed well. Samples were incubated at 4°C for 3 hours then centrifuged at 15,000 x g for 30 minutes at 4°C. Supernatant was then decanted and the pelleted DNA was rinsed with 500µl of room temperature 70% ethanol. Samples were centrifuged at 15,000 x g for 20 minutes at 4°C. The supernatant was removed and pellets were air dried for 20 minutes to allow the remaining ethanol to evaporate. DNA was then dissolved in 20µl of elution buffer (Qiagen) and concentration was subsequently measured via Nanodrop as described in section 2.2.3.

2.3 Bat Interferon Propagation

The following interferon-encoding plasmids were sourced from GeneArt, Thermo-Fisher, Germany and generated using interferon sequences taken from the Australian Black Flying Fox (*Pteropus alecto* (pa)) accessible from the NCBI database. These plasmids were subsequently used for the *in vitro* production of bat interferons (Table 2.1).

Table 2.1 - List of bat interferons.

Interferon	**IFN Type**	**Plasmid Name**
paIFNα	Type I	pcDNA3.1_paIFNα
paIFNβ	Type I	pcDNA3.1_paIFNβ
paIFNδ	Type I	pcDNA3.1_paIFNδ
paIFNκ	Type I	pcDNA3.1_paIFNκ
paIFNγ	Type II	pcDNA3.1_paIFNγ
paIFNλ1	Type III	pcDNA3.1_paIFN λ1
paIFNλ2	Type III	pcDNA3.1_paIFN λ2

HEK293T cells were grown in 6-well plates to 80% confluency before being transfected with 2µg of IFN at a 1:3 ratio with Lipofectamine 2000 as described in section 2.1.4. At 24 hours post-transfection, supernatant was collected, and growth media was replaced. At 48 hours post-transfection, supernatant was collected again and pooled with the previous 24-hour supernatant. The combined supernatant was centrifuged at 500 x g for 5 minutes to pellet any cell debris. This IFN-containing supernatant was then aliquoted into 1ml tubes and stored at -80°C, to be used in subsequent IFN-stimulation studies.

2.4 Generation of paIRF7-mRFP Constructs

2.4.1 paIRF7 Primer Design

Table 2.2 – List of primers used in paIRF7-mRFP construct design. *All primers were ordered from Thermo-Scientific.*

Primer	Sequence
PA-IRF7-WT-F	ATATGGTACCCCACCATGGACTACAAAGACGATGACGAC
PA-IRF7-WT-R	ATATGCGGCCGCCCGGCGGGCTGCTCCACCTCCATC
PA-IRF7ΔID-R	ATATGCGGCCGCCCCTTGTACATGATGGTCACGTCC
PA-IRF7-ΔVAD+ID-R	ATATGCGGCCGCCCCTGGGGCTGTGACCTGGGGCTGGC
PA-IRF7-DBD-R	ATATGCGGCCGCAAAGGGCCTTGTGCTCCCCCTGG

2.4.2 PCR Amplification of paIRF7 and its fragments

The full-length open reading frame (ORF) of paIRF7:

NCBI accession number: Gene ID: 102897349

ATGGCCGCCGCCCGCGATAGGGGGGCCCCGCGCGTGCTGTTCGCAGACTGGC

TTCTGGGCGAGGTCAGCAGCGGCCGCTACGAGGGGCTGCGGTGGCTGGACGA

GGCCCGCACACGCTTCCGAGTGCCCTGGAAGCACTTTTCGCGGAAGAACCTGG

GCGAGGCCGACTCGCTCATCTTCAAGGCCTGGGCCATCGCCCGCGGCAGGTG

GCCGCTCAGCAGCGGCCCAGGCAACCCGCCAATCCGCGAAAGTGCACTCCGA

GCCGGCTGGAAAACCAACTTCCGCTGCGCACTGCGCAGCACTCAGCGCTTCGT

CATGCTGCACGACAATTCCGCGGACCCCGCCGACCCGCATAAAGTGTATGAGC

TCAGCTCCGAACCGCCGTGGAGAGAAAGTCCAGGCATTAACCAGGGGGAGCAC

AAGGCCCTTGAGGATGCCTCATCCTGGAGGGGTGGGCTCCCTAGGCCACATCT
GGTAGATGCTGGTGAGAGGCTGGGGCCTGCGCCCAGTGCCCCAAGCCCCGGC
CTGGCAGGCTCCACGGGGGACCTTCTGCTCCAGGCTCTGCAGCAGAGCCACCT
GGAGGACCATCTGCTGGACGGTGCCCAGGAGGTGGACCCAGTCCCCCTAGAG
GCTCCTGGCCCAGAGCTCCCTGCTGAGCAACCATACCTGCCGTGGGCCATGGA
GGTGGCCGCCAGCCCCAGGTCACAGCCCCAGGCCGCAATGACAGATGCAGGC
CCCGCCCCAGAGCCCTGGCAGCCCCTACAGGAGACGGAGCCGTCCACCCAAG
TGGTGGGGCCCAGCCACCCACAGCCCAGTCTGCACGTGGAGTCTGGCCTGGG
GACCCTGGACGTGACCATCATGTACAAGGGCCGAACAGTGCTGCAGGAGGTGG
TGGGGCGCCCGCGCTGTGTGCTGCTCTACGGGCCCCCTGGTCTAGCCAGCGA
GGCCAGAGAGCCCCAAGAGCCCCAGATGGTGGCCTTCCCCAGCCCAGCCGAG
CCCCCTGACCAGAAGCAGCTGCACTACACAGAGAAGCTGCTGCAGCACGTGGC
CCCGGGCCTGCAGCTTGAGCTCCGGGGGCCTGGGCTGTGGGCCCGGCGCCTG
GGCAAGTGCAAGGTCTACTGGGAGGTGGGCGGCCCGCTGGGCTCCGACAACC
CCTCCACACCGGCCCGCCTGCTGCAAAGGAACTGTGACACCCCCATCTTTGATT
TTGGCACCTTCTTCCGAGAGCTGGTGGAGTTCCGGACTCGGCAGCGCCGAGGC
TCTCCACACTACACCATCTACCTGGGCTTCGGGCAGGACCTGTCGGCTGGGAG
GTCCAAGGACAGGAGCCTGGTTCTGGTGAAGCTGGAGCCGTGGCTGTGCCGC
GCATACCTGGAGAGCGTGCAGCGGGAAGGTGTGTCCTCCCTGGACAGCAGCA
GCTTCAGCTCTGCTCTGTCTAGCTCCAACAGCCTATATGAGGACCTGGAACAC
TTCCTGGAGCACTTCCTGATGGAGGTGGAGCAGCCCGCCTAG was chemically synthesized (GeneArt, Thermo-Fisher, Germany) and cloned into pCAGGs. To construct RFP-fused fragments, full length paIRF7 (WT) and its fragments (ΔID, ΔID+VAD and DBD) were amplified using primers mentioned in Table 2.2 and pCAGGs-IRF7 plasmid as template. The amplified fragments were cloned in fusion with mRFP in the pcDNA3.1-mRFP plasmid (Addgene plasmid ID: 13032https://www.addgene.org/13032/). Specific paIRF7 domain constructs were amplified from paIRF7-pCAGGs plasmid DNA as described in Table 2.3 below.

Table 2.3 - PCR setup for paIRF7.

Component	**25µl Reaction**	**Final Concentration**
5X Q5 Reaction Buffer (50µM Na+)	5µl	1X
10µM dNTPs	0.5µl	200µM
10µM Forward Primer	1.25µl	0.5µM
10µM Reverse Primer	1.25µl	0.5µM
Template DNA	1µl	<1000ng
Q5 High-Fidelity DNA Polymerase	0.25µl	
5X Q5 High Fidelity DNA Polymerase	5µl	1X
Nuclease Free Water	To 25µl	

Reactions were set up on ice, mixed by pipetting up and down and spun to collect liquid at bottom of each reaction tube. PCR reactions were transferred to a PTC-200 Thermal Cycler (Marshall Scientific) and run under the thermocycling conditions described below in Table 2.4.

Table 2.4 - Cycling conditions for PCR reaction.

Step	**Temperature**	**Time**
Initial Denaturation	98°C	30 seconds – 3 minutes
25-35 Cycles	98°C 65°C 72°C	5-10 seconds 10-30 seconds 15-30 seconds per kb
Final Extension	72°C	2 minutes
Hold	4°C	

2.4.3 Restriction Digestion for palRF7 Construct Generation

Restriction enzymes (KpnI-HF and NotI-HF) were obtained from New England Biolabs and digestions were performed in 25µl reaction volumes (Table 2.5). The reactions were performed according to the manufacturer's instructions in terms of restriction temperature, duration, and deactivation protocols. Briefly, following restriction digestion for 4 hours at 37°C, the digested products were cleaned using the GeneJET™ Gel Extraction Kit without heat inactivation, as described in section 2.4.5. The cleaned up digested products were then used in ligation reactions as outlined in section 2.4.6.

Table 2.5- Restriction digest conditions for palRF7 vector pcDNA3.1-mRFP plasmid.

Component	**Reaction**
DNA	800ng (vol equivalent to)
10X Cutsmart Buffer	2.5µl
KpnI-HF	1µl
NotI-HF	1µl
Nuclease Free Water	Up to 25µl

2.4.4 Agarose Gel Electrophoresis

Restriction digest products were run on a 1% agarose gel to confirm the presence of desired DNA bands. DNA samples were prepared in 6X DNA loading buffer (NEB), mixing one part loading buffer with 5 parts of DNA sample. Agarose gels were prepared by dissolving 0.5g of ultrapure agarose (Thermo-Scientific) in 50ml of Tris-acetate EDTA solution (TAE) (Thermo-Scientific). Agarose was dissolved by heating in a microwave. Subsequently, 0.01% (v/v) gel red (Thermo-Scientific) was added once the agarose solution had cooled sufficiently. Agarose was poured into a gel tank and left to set, with an appropriate comb added. Samples were loaded into wells along with a DNA ladder of GeneRuler 1kb (Thermo-Scientific). Gels were run in TAE

buffer at 100V for 60 minutes, or until the dye reached the end of the gel. Gels were imaged using the Bio-Rad GelDoc EZ Imager (Bio-Rad) or DNA fragments were visualised using the GelDoc UVP Dual-intensity Transilluminator (Bio-Rad).

2.4.5 Clean Up of paIRF7 Digest Product

DNA fragments were excised from the gel using a clean scalpel under the UVP Dual-Intensity Transilluminator and placed into a pre-weighed 1.5ml tube whereby gel slice weight was recorded. DNA was then extracted from the gel using the GeneJET™ Gel Extraction Kit (Thermo-Scientific) according to manufacturer's instructions. The purified DNA was eluted in 35µl elution buffer and stored at -20°C.

2.4.6 DNA Ligation of paIRF7 Fragments and pcDNA3.1-mRFP Vector Plasmid

The DNA ligation kit was obtained from New England Biolabs and the reactions were performed according to the manufacturer's instructions. The following reaction was set up in a microcentrifuge tube per sample on ice as shown in Table 2.6 below.

Table 2.6 - Ligation conditions for paIRF7.

Component	**25µl Reaction**
Vector DNA (pcDNA3.1-mRFP)	1µl
Insert DNA (paiRF7 construct)	5µl or 3µl
T4 Ligase Buffer (10X)	2.5µl
T4 DNA ligase	1µl

A 1:3 ratio of vector DNA (pcDNA3.1-mRFP https://www.addgene.org/13032/): insert DNA (paIRF7) was used for the reaction. The amount of each plasmid required at this ratio was calculated using NEBcalculator to generate a total 50ng. Reactions were incubated for 12 hours at 24°C then a further 12 hours at 4°C.

2.4.7 Transformation of Ligated paIRF7 Construct DNA

Ligated DNA was transformed according to section 2.2.1, whereby 5µl of ligation mixture was added to 30µl of competent DH5α cells. The following day, liquid cultures were made for each plasmid as stated in section 2.2.2 for amplification of ligated DNA.

2.4.8 Verification of paIRF7 Plasmid Constructs

Plasmid DNA was isolated as described in section 2.2.2 and plasmid concentration was measured using Nanodrop as described in section 2.2.3. Restriction digestion and gel electrophoresis were repeated using the final eluted DNA product to provide confirmation of accurate cloning.

2.5 qRT-PCR Quantification of paIFIT5

Table 2.7 - Primers used for paIFIT5 RT-qPCR. *All primers were ordered from Thermo-Scientific.*

qPA-IFIT5-F	GGATCCCGCTCCTGAGAAAG
qPA-IFIT5-R	GTCTGAGTGTTCACGCTGGA
qPA-18S-F	CGGCTACCACATCCAAGGAA
qPA-18S-R	GCTGGAATTACCGCGGCT

PaBr cells seeded in 6-well plates were treated with either a total of 200 units of paIFNβ generated as described in section 2.3 and calculated as previously described using a VSV-based bioassay (Santhakumar et al., 2017), 150µg of polyI:C (Thermo-Scientific) or were infected with recombinant NDV (produced in house) at an MOI of 1.0. Untreated cells were used as a control. Total RNA was extracted using TRIzol

reagent (Thermo-Scientific) according to manufacturer's instructions. Quantity and quality of RNA was assessed via Nanodrop as described in section 2.2.3. A total of 200ng of RNA was then used in PCR reactions using SuperScript™ III Platinum™ SYBR™ Green One-Step qRT-PCR Kit (Thermo-Scientific). The reaction was carried out in ABI 7500 light cycler using the paIFIT5 targeting and housekeeping gene primers listed in Table 2.7 which were designed and used considering MIQE guidelines (Johnson et al., 2014). The following thermo-profile was used; 50 °C for 5 minutes hold, 95 °C for 2 minutes hold, followed by 40 cycles of 95 °C for 3 seconds and 58 °C for 30 seconds. Melting curve was determined at 95 °C for 15 seconds, 60 °C for 1 minute, 95 °C for 15 seconds and 60 °C for 15 seconds. Quantification of paIFIT5 was performed using 2(-Delta Delta CT) method (Livak and Schmittgen, 2001).

2.6 Immunostaining

2.6.1 Western Blotting

2.6.1.1 Casting SDS-PAGE Gels

Gels were cast using the Bio-Rad Mini-PROTEAN tetra handset system. Separating gels were prepared using 30% (v/v) acrylamide with bis (Bio-Rad), 1.5M Tris-HCl (pH 8.8), 10% sodium dodecyl sulphate (SDS) and 10% (w/v) ammonium persulphate (APS) (Sigma). 4µl of Tetramethylethylenediamine (TEMED) was added prior to pouring. Gels were poured between spacer plates and a thin layer of isopropanol was added on top to remove bubbles. After the resolving gel had set, isopropanol was removed using filter paper. A stacking gel was prepared with 30% acrylamide with bis, 0.5M Tris-HCl (pH 6.8), 10% w/v SDS and 10% (w/v) APS. Directly prior to pouring, 4µl of TEMED was added. Stacking gel was added on top of the separating gel and a 10-well comb was added before then allowing the gel to set. Gels were used immediately after setting.

2.6.1.2 SDS-PAGE

HEK293T cells were transfected with varying quantities (1, 2 or 4µg) of paIFI35-pCAGG plasmid or 1µg of an empty pCAGG plasmid as described in section 2.1.4. At 24 hrs post-transfection, growth medium was removed, and cells were washed twice with PBS. Cells were then lysed using 200µl/well of NP40 lysis buffer supplemented with protease inhibitor. Cells were incubated in lysis buffer on ice for 1 hour on a rocking platform before being scraped, transferred into 1.5ml microfuge tubes and centrifuged at 180 x g for 5 minutes to pellet any cell debris. Supernatants containing the cell lysates were transferred into fresh microfuge tubes for use in SDS-PAGE. For SDS-PAGE, 15µl of SDS sample buffer (containing 10% of β-mercaptoethanol) (Sigma-Aldrich) was added to 15µl of cell lysate in a microfuge tube and incubated at 98°C for 5 minutes on a pre-warmed heat block. Samples were then loaded onto the SDS-PAGE gel alongside 5µl of pre-stained protein ladder (Abcam).

Samples were run on 10% self-cast resolving gels with 5% stacking gels as prepared in section 2.6.1.1. Gels were run in a Mini-PROTEAN Tetra Cell Tank (Bio-Rad) at 80V for 30 minutes and then 100V for approximately 1 hour, or until sample dye reached the base of the gel.

2.6.1.3 Transferring Protein to PVDV Membrane

For Western blot analysis, proteins were run on SDS-PAGE then transferred to a PVDF Western blotting membrane (Thermo-Scientific) using a semi-dry trans-blot turbo transfer system (BioRad). 6 pieces of filter paper and 1 piece of PVDF membrane were cut for each gel (9cm x 7cm per gel). Filter paper was soaked in transfer buffer (50mL of SDS 10X running buffer, 200mL of methyl alcohol (Sigma-Aldrich), dissolved in 800mL of distilled water and pH adjusted to 8.3. Total volume was made up to 1l with ddH_2O) for 2 minutes. PVDF membrane was soaked in methanol (Sigma-Aldrich) for 5 minutes. Filter paper in 3 layers was stacked on the base of the transfer system, then the PVDF membrane, SDS-PAGE gel, and the final

3 layers of filter paper. A roller was used on top of the stack to ensure removal of air bubbles. Protein transfers were run at 1.3A, 25V for 10 minutes.

2.6.1.4 Probing Membranes

Following transfer, membranes were blocked for 1 hour within 50ml falcon tubes in 10ml blocking buffer (PBST (PBS + 0.5% Tween), 3% skim milk powder) on a roller at room temperature. Following blocking, membranes were incubated with primary antibody at appropriate concentrations (Table 2.9) in blocking buffer overnight at 4°C on a roller. After the primary antibody incubation, membranes were washed 3 times for 5 minutes in 5ml PBST followed by the addition of 5ml of an appropriate concentration of HRP-conjugated secondary antibody in blocking buffer which was incubated for 2 hours (Table 2.9). Membranes were washed a final 3 times with 5ml PBST.

Blots were developed using Pierce enhanced chemiluminescence (ECL) Western Blotting Substrate (Thermo-Scientific) at a 1:1 ratio for 3 minutes with agitation. Western blots were imaged with either the Bio-Rad Chemidoc MP imaging system or iBright750 imaging system (Thermo-Scientific). Developing times varied across different antibodies and samples.

2.6.1.5 Normalising Loads Across Western Blot Samples

Normally, protein levels are equalised across Western blots by comparing the levels of actin or tubulin in cellular samples. For the paIFI35 Western blot analysis this was not completed, but samples should normally be loaded onto SDS-PAGE gels at equal volumes, typically 14µl. SDS-PAGE gels are prepared and separated protein transferred to a PVDF membrane. Blots should then be probed for actin or tubulin and developed. The signal intensity can then be compared via image-lab software (Bio-Rad).

2.6.2 Immunofluorescence labelling

Cells grown on Nunc™ Thermanox™ coverslips (VWR,UK) in 24-well plates (Thermo-Scientific) were washed with 300µl PBS. Cells were then fixed in 500µl 4% paraformaldehyde in PBS (Thermo-Scientific) for 1 hour on a rocker and washed with 300µl PBS. Following this, 500µl of 0.1% Triton X100 (Thermo-Scientific) was added for 10 minutes only and then removed. Wells were washed again with PBS and then 500µl 0.5% bovine serum albumin (BSA) (Sigma-Aldrich) was added to block non-specific binding for 1 hour on a rocker. Primary antibody solutions were prepared at appropriate concentrations in 0.5% BSA whereby 500µl of primary antibody solution was firstly added to each well and incubated on a rocker for 1 hour 30 minutes. Wells were then washed in PBS three times, for 5 minutes each time. Secondary antibodies were also prepared at an appropriate concentration in 0.5% BSA and 500µl of secondary antibody was added to wells and incubated on a rocker for 1 hour 30 minutes whilst covered in foil to protect from light. Wells were washed in PBS three times, for 5 minutes each time. To stain for nuclei, 300µl of DAPI 1:10000 (Thermo-Scientific) was added to each well for 15-30 minutes whilst covered in foil to protect from light. Coverslips were then directly mounted onto glass microscope slides using Vectashield mounting medium (Vector) and sealed with clear nail polish. Slides were visualised and imaged on the Zeiss LSM 880 confocal microscope.

2.7 Virus Experiments

2.7.1 Virus Propagation

VeroE6 cells were grown to 80% confluency in a T75 flask. For infection, 100µl of VSV-GFP-VLPs (sourced from Peter Staheli, Germany) were added to the flask and incubated at 37°C, 5% CO_2 for 2 hours. Infection media was replaced with growth media and cells incubated for 24 hours. Supernatant was collected at 24 hours post-infection and replaced again with growth medium. Supernatant was further collected at 48 hours post-infection and pooled with the 24 hours supernatant. Combined

supernatant was centrifuged at 500 x g for 5 minutes to remove any cell debris. This supernatant containing the propagated VSV-GFP and was subsequently quantified via plaque assay as described in section 2.7.3, and then stored at -80°C to be used in subsequent infection studies.

2.7.2 Viral Infection

Cells were infected with virus amount as calculated according to the desired MOI for each independent experiment. Infections were made up in DMEM media without serum. Growth media was aspirated from wells and the virus subsequently added to cells, which were incubated at 37°C, 5% CO_2 for 1 hour 30 minutes. Plates were rocked back and forth every 30 minutes to ensure even distribution of virus. After incubation, viral supernatant was removed and replaced with fresh growth media and cells incubated for 24 hours.

2.7.2.1 Infection of HEK293T and VeroE6 cells with VSV-GFP for Immunolabelling

To observe the influence on cellular location of WT paIRF7 or paIRF7-mRFP constructs by VSV-GFP *in vitro*, HEK293T or VeroE6 cells seeded in 24-well plates were transfected with 2µg of the appropriate paIRF7 plasmid. At 24 hours post-transfection, cells were infected with VSV-GFP at an MOI of 1.0 according to section 2.7.2 and subsequently stained for immunofluorescence as described in 2.6.2.

2.7.2.2 Infection of VeroE6 cells with VSV-GFP for Assessment of *P.alecto* ISG Antiviral Activity

In order to assess potential *in vitro* antiviral activity of different *P.alecto* ISGs, in three independent experiments VeroE6 cells were seeded in 12-well plates and transfected with 2µg of either paIFIT5, paIRF7 or paIFI35 plasmid alongside accompanying controls of paMx1 and non-transfection control. At 24 hrs post-transfection, cells were infected with VSV-GFP at an MOI of 0.25 according to section 2.7.2 and subsequently assessed for antiviral activity via plaque assay analysis.

2.7.3 Plaque Quantification of Infectious Viral Titres

VeroE6 cells were counted and grown in 12-well plates to reach 100% confluency before using for plaque assay analysis. Ten-fold serial dilutions of virus or viral supernatant taken from infection experiments were prepared from 10^{-1} through to 10^{-6} diluting in 450µl DMEM without serum and using 50µl of virus in serial dilution. Working one plate at a time, growth media was removed from VeroE6 monolayers which were then washed with 500µl PBS. The 10-fold viral dilutions were added to the monolayer, working from lowest to highest concentration, and plates were rocked back and forth to ensure equal distribution of viral supernatant. A media only control was also included in one well for each sample used. Cells were incubated at 37°C, 5% CO_2 for 1 hour 30 minutes, ensuring plates were rocked back and forth every 30 minutes. Following incubation, infection media was removed, and cells were washed with 500µl PBS and 1.5ml of complete overlay media (Table 2.11) was added to each well, ensuring no air bubbles were present and cells were incubated for 3 days at 37°C, 5% CO_2. Cells were fixed with 1ml 4% paraformaldehyde for 1 hour on a rocker. Supernatant was aspirated and 500 µl of 0.2% crystal violet solution (Sigma-Aldrich) was added for 1 hour on a rocker to stain adherent cells. Wells were washed to remove excess dye and left to dry. Plaques were counted in the dilution factor that yielded 5-100 plaques per well. Viral titre (in PFU/ml) was calculated as the average number of plaques per well / (dilution x infection volume).

2.7.4 Viruses and Viral Systems

Table 2.8 - List of viruses and viral systems.

Name	Source
VSV-GFP-VLPs	Peter Staheli, Germany
rNDV-GFP (LaSota)	Produced in Lancaster University by Professor Munir's group.
rCedPV-GFP	Produced and provided by Christopher C. Broder's group, USA.
H17N10 VLPs	Georg Kochs, Germany
RVFV Minigenome	Georg Kochs, Germany

2.7.5 H17N10 VLP System

H17N10 virus-like particles (VLPs) (Georg Kochs, Germany) were produced and measured as previously described in (Fuchs et al., 2017) in the presence of paIFIT5. HEK293T cells were transfected in a 12-well format with expression plasmids coding for PB2 (50ng), PB1 (50ng), PA (10ng) and NP (100ng) of H17N10. In addition, expression plasmids encoding the viral minigenome Pol-I FF-Luc (50ng) as well as HA (100ng), neuraminidase (NA; 100ng), M1 (125ng), M2 (20ng) and nuclear export protein (NEP) (25ng) of SC35M (H7N7) were transfected as previously described (Fuchs et al., 2017), together with 300ng quantities of the paIFIT5 constructs. As a negative control, the HA plasmid was omitted. At 48 hours post-transfection, the firefly luciferase activity in the lysates of the VLP-producing cells was measured on the TECAN luminometer.

2.7.6 RVFV Polymerase Assay

To determine the influence of paIFIT5 on RVFV polymerase activity, HEK293T cells were transfected with expression plasmids, encoding paIFIT5 (250ng), RVFV L, M and N (250ng each), a minigenome construct coding for the full-length RVFV segment with the NSs ORF replaced by *Renilla* luciferase (250ng) and firefly

luciferase under the control of the constitutively active SV40 promoter (50ng). As a control, the paIFIT5 plasmid was replaced with an empty vector. At 4 hours post-transfection, luciferase activities were determined. The activity of *Renilla* luciferase was normalised to firefly luciferase and the empty vector control with RVFV L omitted was set to 100%.

2.7.7 *In vitro* Transcription of 5' biotinylated Synthetic RNA

In vitro transcription and biotinylation methods were conducted as previously described by Santhakumar et al. (2018). The 7SK-as plasmid, encoding for antisense non-coding 7SK RNA, was first linearized using BamHI (NEB) restriction digestion overnight at 37°C, and the purified DNA was used to generate *in vitro* transcribed RNA in the presence of bioin-16-UTP using RiboMAX™ Large Scale RNA Production System-SP6 (Promega, Cat# P1280) as reported previously (Habjan et al., 2013). Briefly, 100µl reactions were generated containing 20µl SP6 buffer, 10µl NTP-bioUTP mixtures, 5µg linearized plasmid and 10µl enzyme mix. The reaction mixture was then incubated at 37 °C for 3 hours. The reaction was treated with RNase-free DNAse (Thermo-Scientific) for another 30 minutes at 37°C, to remove undigested DNA remnant. The biotin-16-UTP was incorporated during *in vitro* transcription. Following *in vitro* transcription, RNA was run on agarose gel electrophoresis to assess RNA quality and subsequently purified using RNeasy MinElute Cleanup Kit (Qiagen). A 30µl reaction of the purified *in vitro* transcribed and biotinylated ppp-RNA was then dephosphorylated using alkaline phosphatase (FastAP, Fermentas) to remove 5′ triphosphate (ppp), leaving an OH group, or mock-treated. The biotinylated RNA samples were purified with RNAeasy MinElute Cleanup Kit and eluted in 35µl nuclease-free water for further use in RNA-protein interactions.

2.8 RNA Protein Immunoprecipitation

To purify IFIT5-binding RNAs, streptavidin affinity resin was incubated at 4°C for 60 minutes with either 1µg ppp-RNA or 1µg OH-RNA as previously described

(Santhakumar et al., 2018). To prepare paIFIT5 protein, HEK293T cells (1×10^6) were transfected with 5µg V5-tagged paIFIT5 plasmid for 48 hours and lysed with TAP buffer in the presence of protease and RNAse inhibitors. A total of 2.0 mg of paIFIT5 protein lysate was incubated with the RNA-coated beads (bearing either ppp-RNA or OH-RNA) for 4 hours at 4 °C on a rotary wheel and washed three times to remove unbound proteins. These beads were mixed with loading buffer and transferred directly on SDS before probing for anti-V5 primary antibodies (Sigma-Aldrich), and with IRDye-labelled secondary antibodies (Li-Cor BioSciences). Signals were acquired and assessed Odyysey infrared imaging system (Li-Cor Biosciences).

2.9 Antibodies

Table 2.9 - List of primary antibodies used for immunofluorescence (IF) and Western blotting (WB).

Primary Antibody	Animal Raised-In	Concentration	Supplier	Product Code	Application
Monoclonal Anti-FLAG	Mouse	1:1500	Sigma-Aldrich	F3165	WB
Monoclonal Anti-FLAG	Rabbit	1:1500	Sigma-Aldrich	F2555	WB
Monoclonal Anti-αtubulin	Mouse	1:1500	Abcam	ab7291	WB
Monoclonal Anti-βactin	Mouse	1:1500	Cell Signalling Technology	8H10D10	WB
Monoclonal Anti-HA	Mouse	1:1500	Abcam	ab1424	IF
Monoclonal Anti-HA	Rabbit	1:1500	Abcam	ab9110	IF
Monoclonal Anti-FLAG	Mouse	1:1500	Abcam	ab18230	IF
Monoclonal Anti-FLAG	Rabbit	1:1500	Sigma-Aldrich	F7425	IF
Monoclonal Anti-V5	Rabbit	1:1500	Abcam	ab309485	IF

Table 2.10 - List of secondary antibodies used for immunofluorescence (IF) and Western blotting (WB).

Secondary Antibody	Animal Raised-In	Concentration	Supplier	Product Code	Application
Polyclonal Anti-Mouse IgG (HRP)	Goat	1:3000	Abcam	ab205719	WB
Polyclonal Anti-Rabbit IgG (HRP)	Goat	1:3000	Abcam	ab6721	WB
Polyclonal Anti-Mouse IgG (HRP)	Rabbit	1:3000	Abcam	ab6728	WB
Alexafluor 568 Anti-Mouse IgG	Goat	1:3000	Thermo-Scientific	A-11004	IF
Alexafluor 488 Anti-Mouse IgG	Goat	1:3000	Thermo-Scientific	A-10680	IF
Alexafluor 568 Anti-Rabbit IgG	Goat	1:3000	Thermo-Fisher	A-11011	IF
Alexafluor 488 Anti-Rabbit IgG	Goat	1:3000	Thermo-Fisher	A-11008	IF

2.10 Buffers and Solutions

Table 2.11 - List of buffers and reagents.

Solution	**Recipe**
TAE (10X)	48.5g Tris base, 11.4ml glacial acetic acid (17.4M), 20mL 0.5M EDTA (pH 8.0), ddH_2O to 1l
PBS (10X)	8g NaCl, 0.2g KCl, 1.44g $Na_2HPO_4 \cdot 2H_2O$, 0.24g KH_2PO_4, ddH_2O to 1l (pH 7.4)
SDS Running Buffer (10X)	30.3g Tris-base, 144.4g glycine, 10g SDS adjust pH to 8.3 and add ddH_2O to 1l
LB Broth	20g LB Broth, ddH_2O to 1l
Blocking Solution	5ml PBST, 0.15g skim milk powder
Resolving Gel Tris Buffer (4X)	181.5g Tris base, 850ml ddH_2O, and adjust pH to 8.8 with 6M HCl
PBST	100ml 10X PBS, 900ml ddH_2O, 1ml Tween 20 reagent
10X Transfer Buffer	30.3g Tris base, 144g glycine, ddH_2O to make 1l
NP-40 Cell Lysis Buffer	30ml of 5M NaCl, 100ml 10% NP-40, 50ml of 1M Tris (pH 8.0), adjust volume to 1L with ddH_2O + protease inhibitor tablet
0.5% Gelatine	2.5g gelatine, 500ml ddH_2O
4% Paraformaldehyde	40g Paraformaldehyde, 1l ddH_2O

0.2% Crystal Violet Solution	0.2g crystal violet powder, 80ml ddH_2O, 20ml methanol
2.4% (w/v) Carboxymethylcellulose (CMC) Solution	20mg CMC solution (Sigma-Aldrich)
2X Overlay Media	142ml sterile bottled water, 50ml 10X MEM, 15ml sodium bicarbonate solution (7.5%), 5ml glutamax, 5ml antibiotic/antimycotic, 5ml non-essential amino acids, 13ml HEPES (1M), 20ml FCS (heat inactivated).
Complete Overlay Media 1X	1:1 mixture of 2X overlay media with 2.4% CMC solution
Triton X-100 Stock (1%)	1ml Triton X-100, 250ml ddH_2O
BSA 1% Stock	1g BSA, 100ml PBS
6X DNA Loading Dye	15ml glycerol, 12.5mg bromophenol blue, 12.5mg xylene cyanol, make up to 50ml with ddH_2O
10% APS	5g ammonium persulphate (APS), make up to 50ml with ddH_2O
0.5M EDTA pH 8	93.05g $EDTA.2H_2O$, adjust pH to 8 with NaOH, add ddH_2O to make up to 500ml
1.5M Tris-HCl pH 8.8	90.75g Tris base, add ddH_2O to make up to 500ml
0.5M Tris-HCl pH 6.8	30.35g Tris base, adjust pH to 6.8 with HCl, add ddH_2O to 500ml

2.11 Bioinformatic Analyses

2.11.1 Sequence Data Mining

In this work, the direct comparison of nucleotide sequences was performed between selected bat immune genes and a pool of representative species. To retrieve the reference sequences from a selection of species, each gene was independently retrieved from the NCBI database (www.ncbi.nlm.nih.gov) in FASTA format containing only coding sequences.

2.11.2 Amino Acid Alignment

Multiple sequence alignment (MSA) analysis was used to directly compare aligned amino acid sequences between studied genes and to identify mutations. The FASTA sequences for each gene were imported into the BioEdit software (Hall, 1999) whereby MSA was performed using the Clustal W algorithm with a neighbour-joining bootstrap value of 1000.

2.11.3 Weblogo

To generate graphical representations of aligned amino acid sequences, FASTA sequences were imported into the Weblogo database (V2.8.2) (Crooks et al., 2004) to generate frequency plots. This graphical MSA representation displays the frequency of a given amino acid present at each residue position within aligned sequences, allowing the observation of sequence conservation and mutations within short stretches sequence of genes from different species.

2.11.4 Phylogenetic Analysis

Evolutionary analysis was performed to estimate the time of divergence between genes from different species. Sequences previously aligned using MSA in BioEdit were saved in Fas format and imported into MEGA 11.0 software. Phylogenetic trees were then generated using the Maximum-likelihood method with a bootstrap value of 1000.

2.11.5 Pairwise Identity Matrix

Fas files previously generated in BioEdit containing aligned amino acid sequences were imported into the Sequence Demarcation Tool (SDT) software (Muhire et al., 2014) for analysis of pairwise identity. The software takes the input file of aligned sequences and aligns every unique pair of sequences and calculates pairwise identity similarity scores, represented by a colour-coded matrix. Our sequence similarity scores were generated using the MUSCLE algorithm which uses a rooted neighbour joining phylogenetic tree to cluster closely related sequences based on similarity scores. SDT calculates pairwise identity scores as 1-(M/N), where M is the number of mismatching nucleotides and N it the total number of positions along the alignment at which neither sequence has a gap character.

2.11.6 Protein Domain Prediction

The NCBI conserved domains tool (NCBI Conserved Domain Search (nih.gov)) was used to determine the location of selected immune genes from a group of representative species chosen for analysis. Nucleotide sequences previously retrieved from the database as described in section 2.11.1 in FASTA format were imported and used for conserved domain prediction. Domain hits were displayed for conserved domains and the sequence interval they belong to.

2.11.7 Syntenic Analysis

Selected immune genes from different species were searched for using the NCBI database gene's function (www.ncbi.nlm.nih.gov). Data was retrieved from genomic region, transcripts, and products to firstly determine the chromosomal location of the gene to allow comparison between genes from different species. Following this, manual exploration of the annotated chromosome or gene scaffold was undertaken, noting the genes that flank the gene of interest both upstream and downstream to also be compared between species.

2.11.8 3D Protein Annotation

Nucleotide sequences for immune genes retrieved as described in section 2.11.1 were submitted onto the I-Tasser online server (Yang and Zhang, 2015) for protein structure prediction. Completed prediction files were then downloaded and imported into the PyMOL software (Schrodinger, 2015) for visualisation of 3D protein structure and subsequent domain labelling.

2.12 Transcriptomic Analyses

2.12.1 Infection or stimulation of PaBr cells

For transcriptomic analysis, PaBr cells were seeded in T75 flasks for two independent experiments. Each study was performed in triplicate whereby 3 T75 flasks were infected/stimulated and another 3 T75 flasks remained uninfected or unstimulated as a control. One set of bat cells were infected with VSV-GFP at an MOI of 1.0 whilst the other was stimulated with 200 units of paIFNλ, both sets were incubated at 37°C 5% CO_2 for 1.5 hrs before replacing infection/stimulant media with fresh growth medium for further incubation at 37°C 5% CO_2 for 24 hrs. At 24 hrs post-infection or stimulation, growth media was removed, and wells were washed with PBS. Total RNA was isolated from the PaBr cells using TRIzol reagent (Thermo-Scientific) according to manufacturer's instructions and RNA quality was assessed via Nanodrop as described in section 2.2.3. Total RNA was subsequently sent to GENEWIZ, Azenta Life Sciences, (www.GENEWIZ.com) for RNA sequencing.

2.12.2 RNA-seq Analysis

Paired-ended 150 bp long reads were generated by strand-specific RNA-sequencing with polyA selection. Read quality assessment was performed using FastQC and reads with Phred score < 20 were removed via Trim Galore (Krueger, 2015). Transcript abundance level in terms of transcripts per million (TPM), was estimated using *Pteropus alecto* reference transcriptome via Salmon (Patro et al.) as described in

Figure 2.1. The transcript level expression data and low expressed transcripts were filtered and normalized to remove the technical biasness.

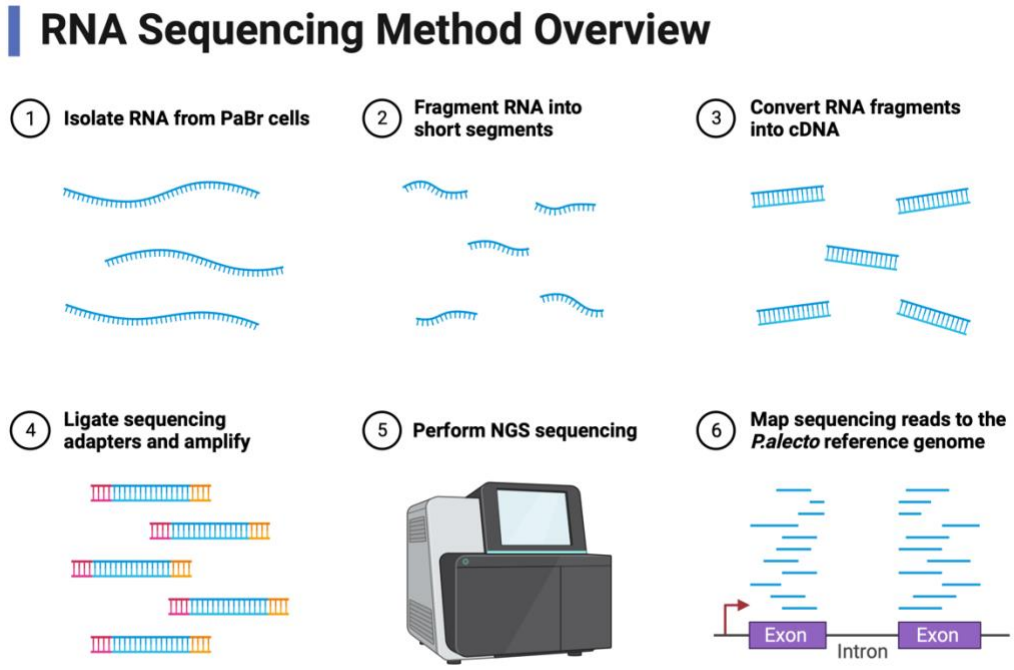

Figure 2.1 - RNA Sequencing Method Overview. *Following stimulation of PaBr cells in triplicate T175 flasks, total RNA was collected and fragmented to subsequently generate cDNA. Ligation and amplification was then followed by next-generation sequencing (NGS) and the mapping of sequence reads to the reference genome of P.alecto. Figure generated from template on Biorender.com.*

The pairwise comparison was performed on normalized values to detect differentially expressed genes (DEGs) using DESeq2 (Love et al., 2014). The DEGs were further filtered (adjusted p-value<0.05; absolute log2fold change>1) to identify significant DEGs. The expression dataset was also used to estimate the alternative splicing events and their percent spliced in (psi) values. The PSI values across the conditions were compared to perform the differential splicing using SUPPA (Alamancos et al., 2015). The differentially spliced alternative splicing events were filtered based on FDR ≤0.05 to identify the significant events. Gene ontology (GO) enrichment pathway analysis was performed using the ShinyGO software (Ge et al., 2020).

Moreover, the filtered transcript expression dataset was used to statistically identify the isoforms involved in the isoform switching using IsoformSwitchAnalyzeR (ISAR) (Vitting-Seerup and Sandelin, 2019). The differential isoform usage of filtered isoforms was estimated using DEXSeq (Anders et al., 2012) as a measure to detect the isoform switching. To further gain detailed insight into functional consequences of isoforms involved in switching, the coding potential was calculated using the Coding Potential Calculator 2 (CPC2) tool (Kang et al., 2017). Signal peptides were detected via SignalP (Teufel et al., 2022) and protein domains were detected using Pfam (Sonnhammer et al., 1997). The intrinsically disordered regions (IDR) were identified via NetSurfP-2 (Klausen et al., 2019) and sensitivity to Non-sense Mediated Decay (NMD) was predicted based on knowledge of isoform positions for the CDS/ORF.

2.13 Statistical Analyses

When analysing two independent groups in qRT-PCR analysis of paIFIT5 induction (section 5.2.3), means were compared using an unpaired Students *t*-test. Likewise, an unpaired Students *t*-test was used in H17N10 and RVFV minigenome assays (section 5.2.5) to assess the level of minigenome viral transcription in the presence or absence of paIFIT5. A one-way analysis of variance (one-way ANOVA) was used when multiple comparisons were required for a single factor in the analysis of antiviral plaque assays for paIFIT5 where n=3 (section 5.2.4). Remaining antiviral plaque assays of paIRF7 constructs and paIFI35 were only conducted once and thus could not be analysed here for statistical significance (section 6.2.1.2 and 6.2.2.2). All statistical analyses performed were completed using Graphpad Prism 8 Software which was also used to generate the figures presented.

Chapter 3. CedPV-Induced Transcriptomes of Cells from the Megabat *Pteropus alecto*

3.1 Introduction

3.1.1 Bats as Henipavirus Reservoirs

The emergence of zoonotic viruses from bats continues to pose a significant threat to public health and with the increasing knowledge of viral diversity in bat species globally, further bat-borne pathogens are predicted to emerge in the near future (Marsh et al., 2012). Members of the henipavirus genus remain some of the most important and pathogenic bat-borne viruses to be discovered in recent history. Hendra virus (HeV) and Nipah virus (NiV) are highly pathogenic henipaviruses, belonging to the Paramyxoviridae family that result in severe and often fatal respiratory and/or neurological disease. HeV was first discovered in 1994 after investigations of serious disease outbreaks in Australia, which infected twenty-one horses and two humans who handled the horses (Murray et al., 1995). Four additional outbreaks followed which resulted in the death of five horses and one human, with a second non-fatal human infection also recorded (Field et al., 2000, Hooper et al., 1996, O'sullivan et al., 1997, Rogers et al., 1996, Selvey et al., 1995). Recently, Peel et al. (2022) have discovered a novel HeV variant in October 2021 following the death of a horse in New South Wales, Australia, stemming from spillover from Pteropus flying foxes where the variant was also detected in their tissue and urine. NiV was first recognised in 1999 during a disease outbreak amongst pig farmers in Malaysia which was initially attributed to Japanese encephalitis (Paton et al., 1999). This was believed until March 2023, when the novel paramyxovirus was isolated from the cerebrospinal fluid of an encephalitic patient from this time and soon confirmed as the aetiological agent responsible for the outbreak (Chua et al., 1999, Chua et al., 2000). NiV was also recognised in Bangladesh in 2001 and further outbreaks occur annually in eastern India. NiV is transmitted by Pteropus bat species, the natural reservoir host, into pigs which act as a secondary species and an intermediate for transmission from bats to humans, although human-to-human transmission has also been documented (Singh et al., 2019). A total of 639

human cases of NiV infection have been collectively recorded in Bangladesh, India, Singapore, Philippines and Malaysia (Eaton et al., 2006).

Cedar virus (CedPV) is a more recently characterised paramyxovirus that appears closely related to the other known Henipaviruses, sharing significant features such as genome size and organization, and use of the same receptor molecule (ephrin-B2) for entry during infection (Marsh et al., 2012). Two additional henipaviruses include Mojiang virus and Ghanaian bat virus, which were both established via viral RNA detection, as appose to conventional isolation of the virus itself (Drexler et al., 2009, Wu et al., 2014). Unlike HeV and NiV, there is currently no evidence that CedPV, Mojang and Ghanaian bat viruses are pathogenic to humans (Weatherman et al., 2018). The natural reservoir of henipaviruses (HeV, NiV and CedPV) has been successfully recognized as fruit bats belonging to the genus Pteropus, commonly known as flying foxes (Halpin et al., 2011). It is also worth noting that serological evidence suggests the circulation of these viruses in non-pteropid bats (Li et al., 2008, Hayman et al., 2008). HeV antibodies were first identified in *Pteropus poliocephalus* and *P. alecto* in 1996 (Young et al., 1996, Halpin et al., 2000). NiV antibodies were then identified as present in Pteropus species common in Malaysia; *Pteropus hypomelanus* and *Pteropus vampyrus* (Yob et al., 2001, Chua et al., 2002, Rahman et al., 2010). CedPV virus was isolated via the collection of urine from colonies of *P.alecto* and some *Pteropus poliocephalus* bats (Marsh et al., 2012). Transmission of henipaviruses between bats occurs via direct or environmental contact as they shed the viruses in their urine, which is often used in grooming, and henipaviruses have also been detected in throat and rectal swabs (Halpin et al., 2011, Middleton et al., 2007, Edson et al., 2015, Williamson et al., 2000). This viral shedding permits the ease of transmission between bats and also to secondary hosts which may come into contact with their urine, such as horses and pigs, which then act as amplifying hosts to transmit the virus further into human populations (Weatherman et al., 2018).

Despite the pathogenic and fatal infections observed in human upon henipavirus infection, bats do not show any clinical signs of disease when experimentally challenged with HeV and NiV, although it is worth noting that little is currently known about the effect of henipavirus infection in naturally-infected bats (Weatherman et al., 2018, Halpin et al., 2011, Middleton et al., 2007, Williamson et al., 2000, Williamson et al., 1998). The absence of pathology in bats infected with henipaviruses aligns with the assumption that bats can co-exist with viruses in an equilibrium, whereby viral replication and shedding takes place but at a level that does not cause disease in the reservoir host. However, knowledge of the dynamics behind this ability of bats to maintain these viral infections without illness is currently limited, but may prove invaluable to the field of emerging infectious diseases (Eaton et al., 2006, Hess et al., 2011, Wynne et al., 2014). Previous research in bats has highlighted the potential link between their innate immune systems and their ability to host and maintain viruses, including HeV, without exhibiting traditional signs of disease (Halpin et al., 2011, Papenfuss et al., 2012). Furthermore, investigations have demonstrated that genes involved in innate immunity have undergone positive selection in *P.alecto*, the reservoir host for henipaviruses, indicative of a co-evolutionary relationship (Zhang et al., 2013b). It is therefore imperative that the bat gene repertoire induced upon viral infection is explored in order to understand potential antiviral mechanisms that permit the bats to host viruses, including henipaviruses, without displaying clinical signs of disease.

3.1.2 Transcriptomic Analysis in Bats

Transcriptomic analysis encompasses the investigation of the complete collection of RNA transcripts that are produced by the genome, under explicit circumstances in a specific cell. Transcriptomics allows researchers to explore the complete gene repertoire of an organism which can be very useful when investigating certain responses, for example upon infection or external stimulation. Significant advances in

bat-virus interactions have been made in recent decades, expanding our understanding of their roles as novel viral reservoirs. Whole transcriptome and genome sequencing has been essential in gaining key insights into the bat immune response (Zhang et al., 2013b, Moreno-Santillán et al., 2019, Hölzer et al., 2019). *P.alecto* is regularly employed as a bat model species due to the accessibility of resources from this species, including cell lines and reagents (Papenfuss et al., 2012, Ng et al., 2016). Previous transcriptomic work has provided insights into the co-evolution of bats and the array of viruses that they host, whilst also enabling studies into novel bat transcripts that are induced during times of stress and infection. The availability and quantity of transcriptomic investigations and resources in bats has significantly improved in recent years, supplemented by the sequencing and assembly of numerous tissues and organs from bats including heart, brain, lung, liver, kidney, spleen, thymus and lymph (Papenfuss et al., 2012, Lee et al., 2015, Lei et al., 2014, Shaw et al., 2012). However, despite progress, the contribution of bat innate immunity and particularly their IFN response towards their ability to host viruses without showing clinical signs of disease, remains unclarified (Hölzer et al., 2019). Previous work has endeavoured to unearth the global transcriptional response in bats to infection with several viruses including NiV, HeV, Ebola, Marburg, Tacaribe virus, bat adenovirus and NDV (Kuzmin et al., 2017, Wynne et al., 2014, Hölzer et al., 2016, Glennon et al., 2015). An additional prominent study by Wynne et al. (2014) used an integrated approach of proteomics with transcriptomics to measure and directly compare the response of bat and human cells to HeV. This study was successful in detecting crucial cellular pathways in which differential gene activation correlates with outcome in PaKiT03 (*P.alecto* kidney) cells and human HEK293T on a transcriptomic coupled to proteomic basis. However, there remain limited studies investigating the global transcriptional and antiviral response of Pteropid bat cells to infection with viruses.

3.1.3 CedPV-Induced Transcriptomes in Bats

In this study, we aim to measure global transcriptomic data via infection of the immortalised Pteropid bat cell line known as PaBr (*P.alecto* brain cells) with CedPV (Figure 3.1). CedPV is a known bat henipavirus belonging to the same family as HeV and NiV, therefore by investigating the transcriptomic response of bat cells in response to CedPV infection, we can not only understand their response to CedPV, but potentially apply our findings to the henipavirus group as a whole. Furthermore, CedPV is non-pathogenic to humans, unlike HeV and NiV which are BSL-4 pathogens, so it is therefore safer to use for experimental infection of mammalian cells and can be used at BSL-2. Additionally, there remains limited information regarding the antiviral genes induced by CedPV in bat cells, thus deeming worthy investigation. Transcriptomic analyses into the differentially expressed genes, differential splicing and isoform switching events induced by CedPV infection of bat cells, will hopefully permit an in-depth understanding into the response of *P.alecto* to henipavirus infection at the molecular level.

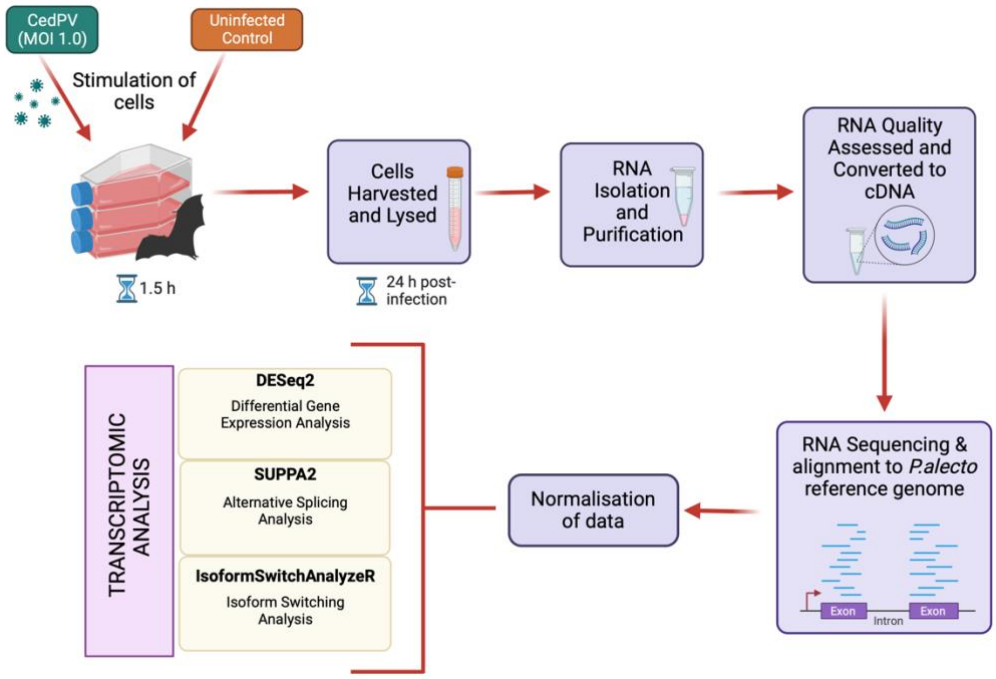

Figure 3.1 - Flow diagram showing the process of our transcriptomic study. *PaBr cells were infected with either CedPV ar an MOI of 1.0 or remained uninfected. Cells were harvested and lysed at 24hpi and total RNA was isolated. Purified RNA was quality-assessed and converted to cDNA before processing for RNA-sequencing. RNA-seq results were used for transcriptomics analysis. Pre-processing of data and differential gene expression (DEG) analysis was carried out using DESeq2 software, alternative splicing analysis was completed using SUPPA2 and analysis of isoform switching events used IsoformSwitchAnalyzeR. Figure created with Biorender.com.*

3.2 Results

3.2.1 Pre-processing of RNA-seq data

Total RNA was extracted from PaBr cells that were infected with CedPV (MOI 1.0) or were uninfected from three biological replicates and used for comparative RNA-seq analysis. Before investigations into transcript expression and abundance in infected PaBr cells, we first normalised the dataset to ensure that there was no variance or bias in the analysis. This was first achieved by generating transformed counts from counts per gene (Figure 3.2A) which were subsequently used for normalisation of counts (Figure 3.2B) using DESeq2 software.

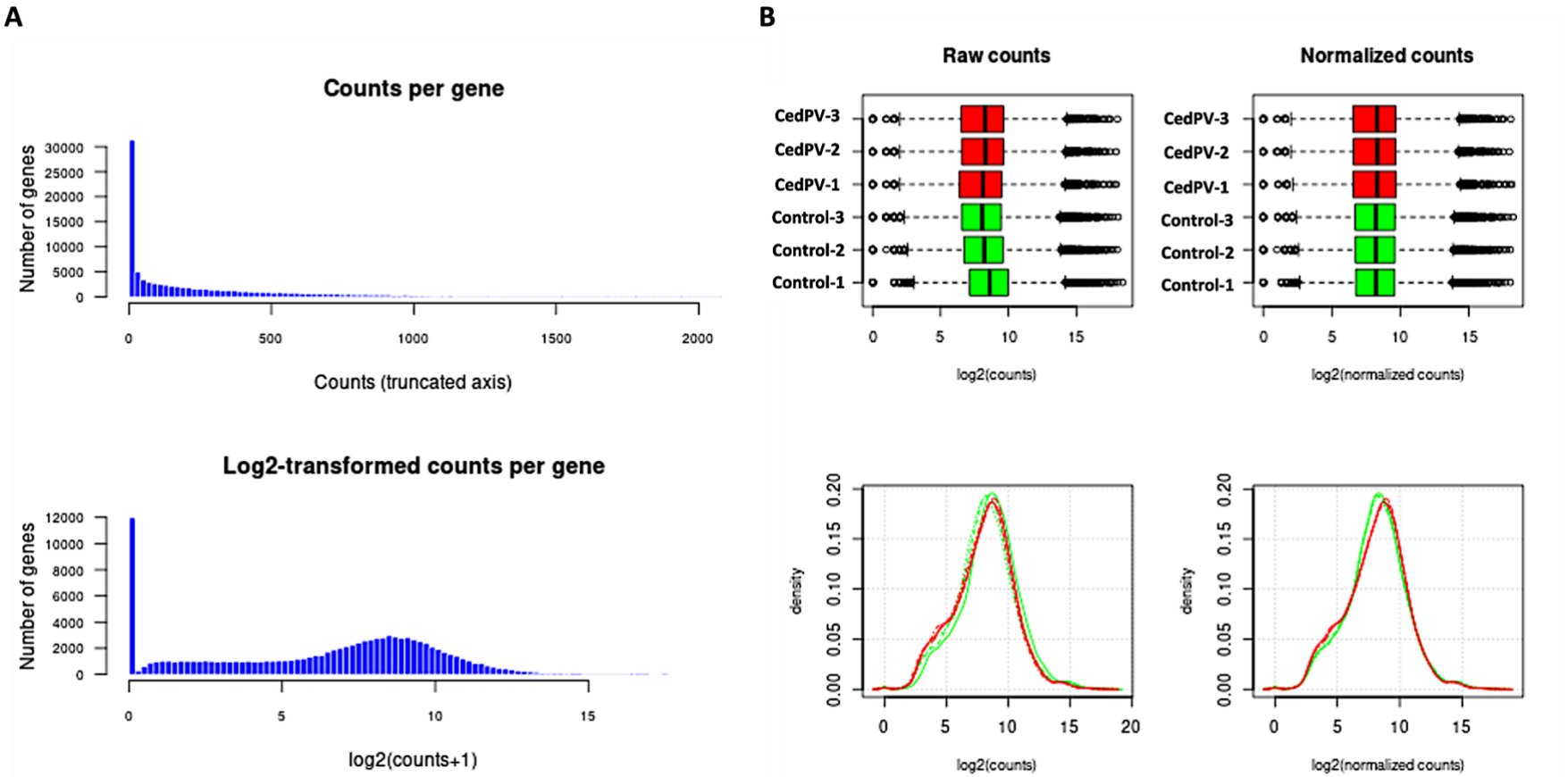

Figure 3.2 - Pre-processing of transcriptomic RNA-seq data for analysis. (A) *Raw read counts per gene and generation of log2(counts+1) transformed counts per gene.* ***(B)*** *Normalisation of the transformed counts from raw RNA-seq data represented by box plots and plotted against density.*

To determine the degree of variation in RNA-seq data, a dispersion estimation plot was generated using DESeq2 (Figure 3.3). Dispersion is a measure of variability in the dataset, whereby dispersion estimates reflect variance in gene expression for a given mean count value. Data from our experiment fits the dispersion plot, whereby gene dispersion estimates are generally spread around the curve and dispersion decreases as mean expression levels of normalised counts increase.

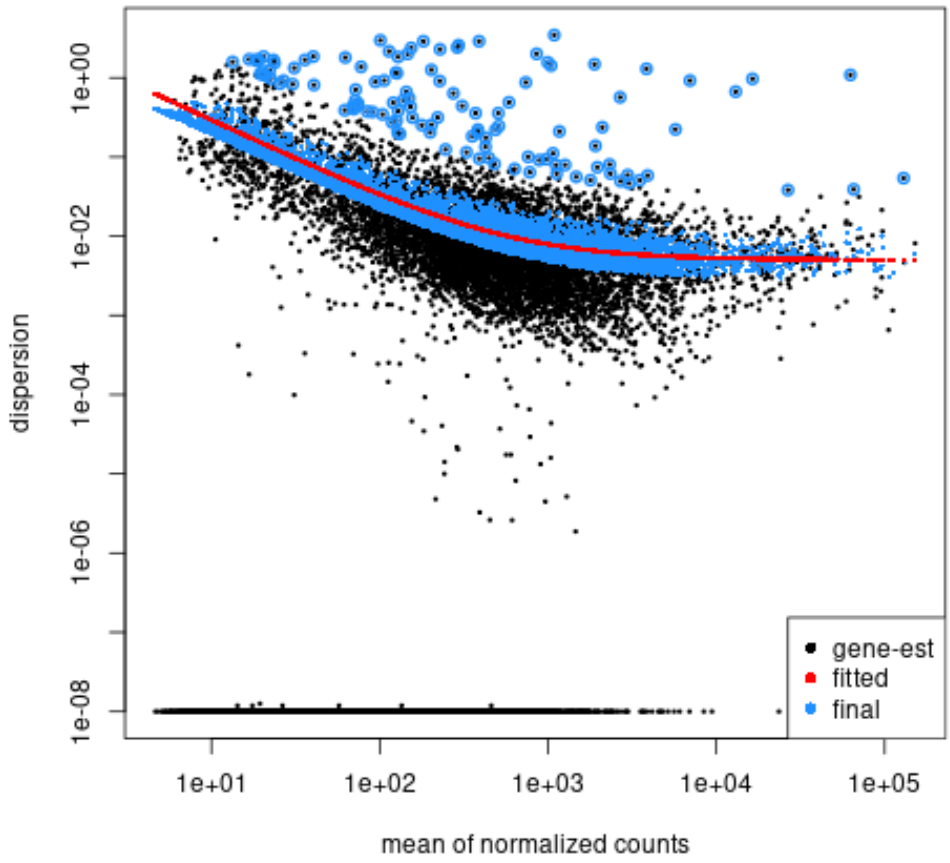

Figure 3.3 - Dispersion estimation plot generated in DESeq2 showing the final estimates shrunk from the gene-wise estimates towards the fitted estimates. *Estimated gene dispersions are represented by black dots, the fitted dispersion estimate curve is in red and the adjusted gene dispersions shrunk towards the curve are represented by blue dots. Black dots with blue circles around them are genes estimates with high dispersion values that have not been shrunk towards the curve.*

Lastly, to further confirm the overall variability within the normalised sample counts and to determine if biological replicates clustered together, we performed principal component analysis (PCA) whereby the triplicate biological replicates of uninfected and CedPV-infected PaBr cells were analysed (Figure 3.4). Our PCA results display

the close clustering of biological replicates for both treatment groups. The PCA revealed that the transcriptomes of uninfected samples clustered closely together as expected of a control group. A higher variance was observed (PC1 with 97%) in the CedPV-infected biological replicates, but these too displayed relatively close clustering, whereby two of the replicates clustered closely, with the third displaying a slightly lower variance (PC2 with 1%).

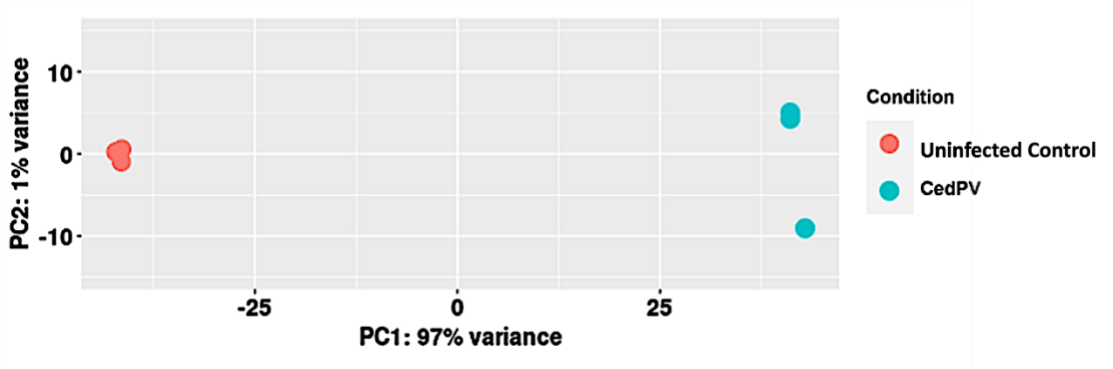

Figure 3.4 - Principal component analyses (PCA) for uninfected and CedPV-infected cells performed using DESeq2 normalised RNA-seq data. *X-axis represents PC1 at 97% variance, with the Y-axis representing PC2 at 1% variance. Infection was carried out in biological triplicates for each treatment. Uninfected cells are represented by red dots and cells infected by CedPV are represented by blue dots.*

3.2.2 CedPV-induced Differential Gene Expression Analysis

Differential gene expression (DGE) analysis is a common and useful application of RNA-seq data which was conducted on our normalised data sets because this analysis permits the elucidation of differentially expressed genes across two or more different conditions or treatment types, which for our samples were either mock or CedPV-infected PaBr cells. RNA-seq analysis identified 38,154 total gene counts which when filtered based on expression left 12,649 genes. Of these genes, 7,890 were DEGs (3,963 up-regulated and 3,927 down-regulated). A final filtering was applied to identify significant DEGs for analysis, of which there were 3,004 significant DEGs between uninfected and CedPV-infected samples (Figure 3.5A). This significance was calculated as genes with an adjusted p-value of <0.05 and an absolute log2 fold change of >1.

Significant DEGs were visualised using a volcano plot (Figure 3.5B), where the threshold of the volcano plot was $-\log_{10}$ (adjusted p-value) and plotted against the Log_2 fold change. The most significant DEGs between uninfected and CedPV-infection (at both p-value and $\log_2$ fold change) are represented by a red dot, genes significant at only the $\log_2$ fold change are represented in green, and non-significant DEGs by grey dots. Genes significant at only the p-value are also listed here in blue but are masked on the volcano plot as the red dots encompass these genes anyway. DEGs located on the left-hand side of the volcano plot represent downregulated genes, contrasting to DEGs on the right-hand side which are upregulated during CedPV infection in comparison to absence of infection. DEGs with the highest $-\log_{10}$ adjusted p-value located and labelled at the top of the volcano plot, are deemed the most highly significant and thereby the most up or down-regulated. The most up-regulated significant DEGs in the context of innate immunity included BTG1, IFI6, MX1, IFIT2, CCL5, IFIT3 and CXCL8 (Table 3.1). Significant DEGs that were largely downregulated included MATN3, ACTG2, TIMP3 and CALD1.

Table 3.1- List of the most significant up-regulated and down-regulated genes. *Gene significance was determined at the Log2 fold-change value.*

Gene	**Log2FC**
Upregulated DEGs	
CXCL8	12.195675
IFIT3	11.64170625
CCL5	10.8537734
IFIT2	10.1738609
MX1	6.199079619
IFI6	3.288553557
BTG1	3.00717309
Downregulated DEGs	
MATN3	-8.644923413
ACTG2	-7.667132826
TIMP3	-6.402151591
CALD1	-3.363742834

To further understand the changes in gene expression observed between the two treatment types, an investigation into the most variable genes was undertaken to recognise which genes presented the highest change in expression upon infection of PaBr cells with CedPV in comparison to the uninfected control. The variability of genes represents the amount by which each gene deviates in a specific sample from the average of the genes across all samples. Figure 3.5C denotes the 25 most variable genes identified between the two treatment types, representing the genes that differed in their expression the most between the two treatment groups. A deeper blue colour

represents higher gene expression, whereas a lighter green shade indicates the gene is expressed less. When assessing the difference between the two treatment types, the larger the difference in colour, the larger the difference in gene expression between treatment groups, as represented in the colour key and histogram. At first glance, results exhibit a selection of genes that appear more highly variable in between CedPV-infected and uninfected cells. Notable genes which display the largest variability between treatment groups and show the highest expression, represented by a deep blue colour under CedPV conditions, includes LOC1028843, LOC1028983, IFIT3, IFIT2 and ISG15 whereby a high variability is observed between uninfected and CedPV groups. The large increase and difference in expression of these genes during viral infection compared to uninfected cells, corresponds with the identified roles of these genes in the mammalian immune response to viral infection, whereby immune gene levels increase in response to viral invasion. Additionally, the uncharacterised scaffolds LOC1028843 and LOC1028983 present in *P.alecto* are also highly expressed during CedPV infection when compared to uninfected conditions but these genes are currently unknown and require further annotation to decipher their function before we can conclude their significance in viral infection here. Contrastingly, some genes displayed higher expression in uninfected PaBr cells in comparison to CedPV infection. These include TAGLN and to a minor degree, MYL9, CST6, PTN and MATN3 whereby a difference in their expression is observed between the two treatment groups, remaining slightly higher in uninfected cells. These genes do not have functional roles in immunity but are involved in various other processes such as muscle contraction, bone development and homeostasis. Further studies into why this selection of genes are either downregulated during CedPV infection or accordingly upregulated in uninfected cells may shed light onto their potential roles in viral infection. These observations highlighting the most highly variable significant DEGs between uninfected cells and CedPV-infection, allow us to gain a valuable insight into the types of genes that are more highly differentially expressed in response to henipavirus infection in bat cells.

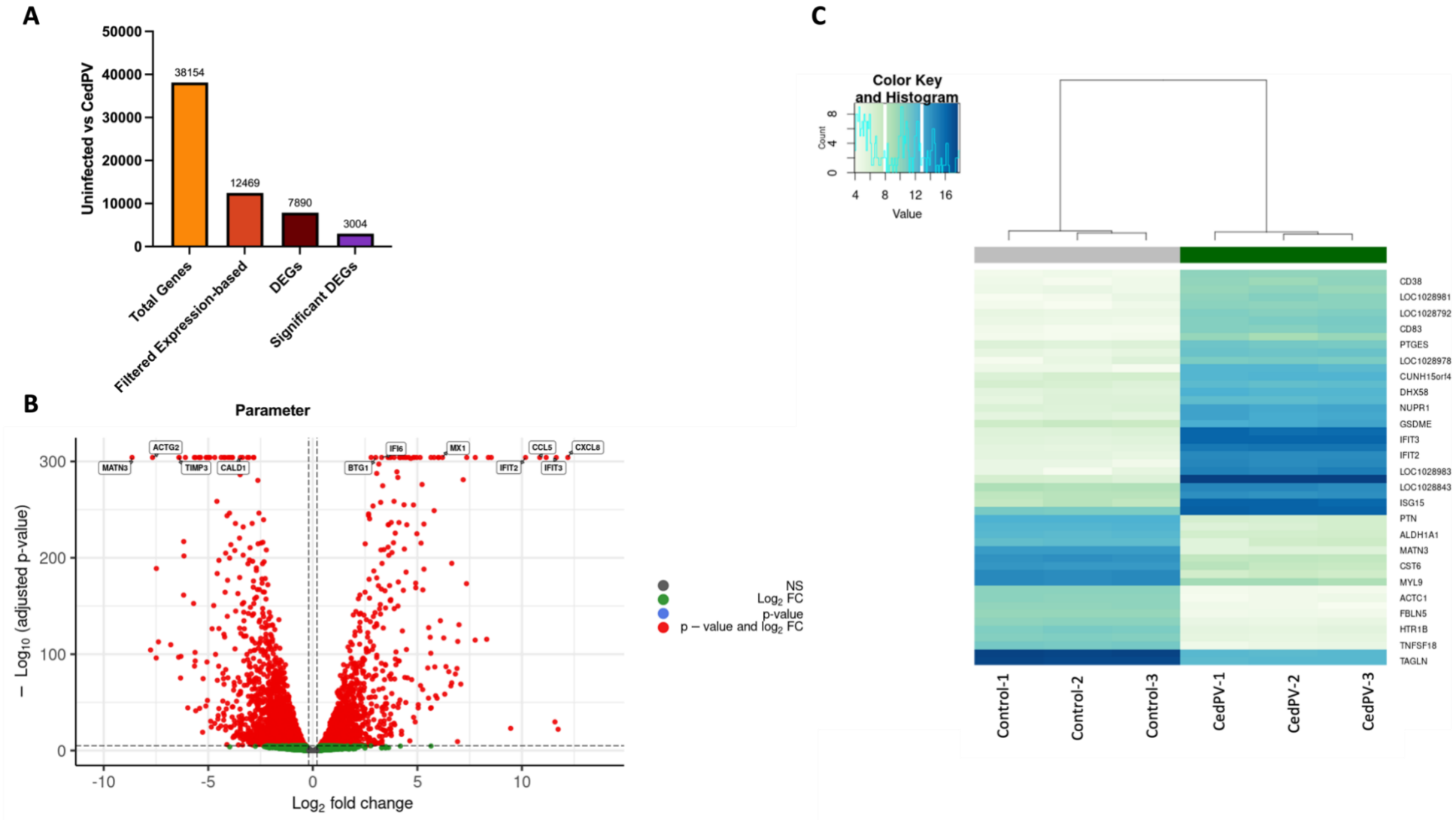
A
Uninfected vs CedPV
50000
40000
30000
20000
10000
0
38154
12469
7890
3004
Total Genes
Filtered Expression-based
DEGs
Significant DEGs
B
Parameter
ACTG2
MATN3
TIMP3
CALD1
IFI6
MX1
BTG1
IFIT2
CCL5
CXCL8
IFIT3
300
200
100
0
− Log10 (adjusted p-value)
-10
-5
0
5
10
Log2 fold change
NS
Log2 FC
p-value
p − value and log2 FC
C
Color Key and Histogram
Count
0
4
8
4
8
12
16
Value
CD38
LOC1028981
LOC1028792
CD83
PTGES
LOC1028978
CUNH15orf4
DHX58
NUPR1
GSDME
IFIT3
IFIT2
LOC1028983
LOC1028843
ISG15
PTN
ALDH1A1
MATN3
CST6
MYL9
ACTC1
FBLN5
HTR1B
TNFSF18
TAGLN
Control-1
Control-2
Control-3
CedPV-1
CedPV-2
CedPV-3

Figure 3.5 - ***Analysis of differentially expressed genes between uninfected and CedPV-infected PaBr cells (A)*** *Bar chart representing the filtering process of total genes to identify significant differentially expressed genes (DEGs) between uninfected vs CedPV-infected PaBr cells. Significance was calculated as genes with an adjusted p-value of <0.05 and absolute log2 fold change >1.* ***(B)*** *Volcano plot showing differentially expressed genes in uninfected vs CedPV-infected PaBr cells. Y-axis denotes –log10 P values, whilst X-axis shows log2 fold change values. Red dots represent significant differentially expressed genes at both p value and log2 FC, blue dots denote genes with significant p values only, green represent genes with only log2 FC value and grey dots represent non-significant DEGs. The most upregulated genes between uninfected vs CedPV-infected cells are represented on the right-hand side of the plot, with downregulated genes on the left-hand side. Differentially expressed genes that display the highest statistical significance are located at the top of the plot where their gene names are annotated.* ***(C)*** *Heatmap showing the top 25 most variable genes between uninfected vs CedPV-infected (GFP) PaBr cells. Heatmap was generated using log2 expression of counts normalized to transcript size and million mapped reads (FPMK values). Y-axis denotes the gene name of interest, while X-axis represents the treatment type delivered in triplicate to the PaBr cells. Expression values are represented by the colour key and histogram, whereby a deeper blue colour indicates higher expression and lighter green represents lower expression for the given treatment type.*

As previously mentioned, former research has directed efforts towards investigating innate immune-related genes in *P.alecto* due to their projected potential to underlie their roles as viral reservoirs. Therefore, in concurrence with chapters 5 and 6 of this thesis, we aimed to analyse the influence of CedPV infection on several innate immune genes present in *P.alecto*. The selected genes are known to play key roles within the mammalian antiviral innate immune response and therefore commanded further analysis into the differential expression of this set of immune genes from the RNA-seq data. Figure 3.6 demonstrates the distribution of normalised counts for our selected innate immune genes, obtained for the biological replicates from uninfected and CedPV-infected treatment groups. It is apparent that for all six genes examined here (Figure 3.6 (A) IRF7, (B) IFIT5, (C) IFI35, (D) IFIT2, (E) IFIT3 and (F) IFI6), a higher normalised count of these innate immune genes is observed upon CedPV infection in comparison to non-infected controls.

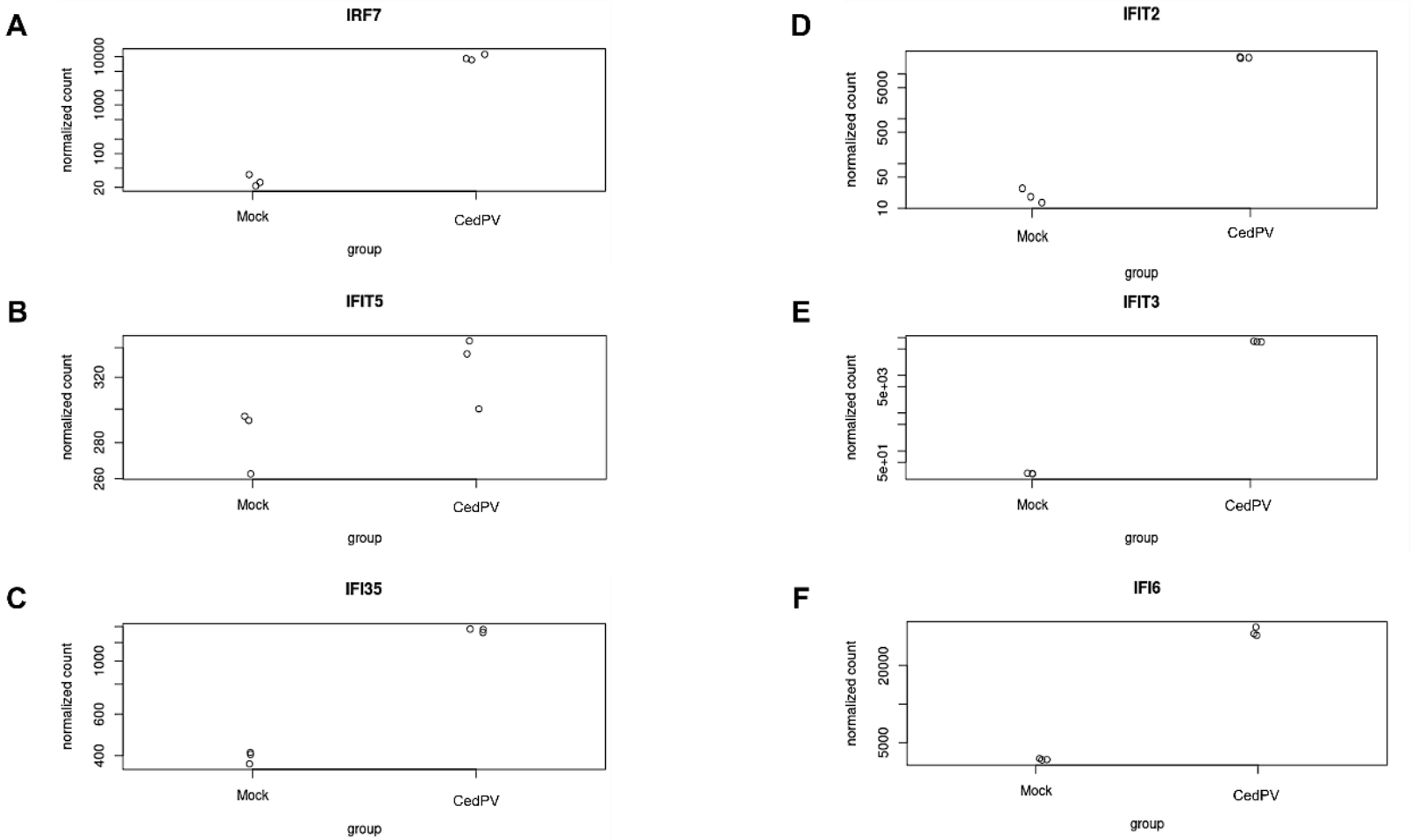

Figure 3.6 - Differential gene expression box plots for genes in <u>P.alecto</u> associated with innate immunity. *The normalised counts of the differentially expressed gene for each of the three biological replicates is represented for uninfected and CedPV-infected treatment groups.* ***(A)*** *IRF7,* ***(B)*** *IFIT5,* ***(C)*** *IFI35,* ***(D)*** *IFIT2,* ***(E)*** *IFIT3 and* ***(F)*** *IFI6 normalised counts are all increased upon CedPV infection in comparison to the uninfected control.*

Functional enrichment analysis of DEGs was performed. Differentially expressed genes were identified using the DESeq-2 package in R, which were then used in the ShinyGO software to perform gene enrichment and pathway analysis. The significant DEGs were categorised into the functional groups including cellular component (CC), molecular function (MF) and biological process (BP). The gene ontology (GO) analyses described in Figure 3.7 (A-C) collectively represent the top 10 GO terms for each category, as represented by their p-value.

The CC analysis shows that based on their p-adjust values, the most significant cellular components involved in the differential expression of genes in uninfected vs CedPV-infection were in the condensed chromosome, followed closely by the extracellular space (Figure 3.7A). MF results show that the DEGs were most significantly associated with the molecular functions of transcription regulator activity, chemokine receptor binding and chemokine activity, as shown in Figure 3.7B. The highest count of genes in MF were shown to partake in nucleic acid binding and other non-specified molecular functions, as represented by the largest circles on the plot. In BP, DEGs are shown to be largely associated with the regulation of cell death, followed closely by other biological processes including response to stress and significantly, the innate immune response (Figure 3.7C). Further insight into the biological processes that DEGs are classified into and are most involved with, were examined via functional enrichment analysis. The most significant biological processes that DEGs partake in are represented by bright green nodules and include the immune response, the defence response, and the response to an external stimulus or other organism (Figure 3).

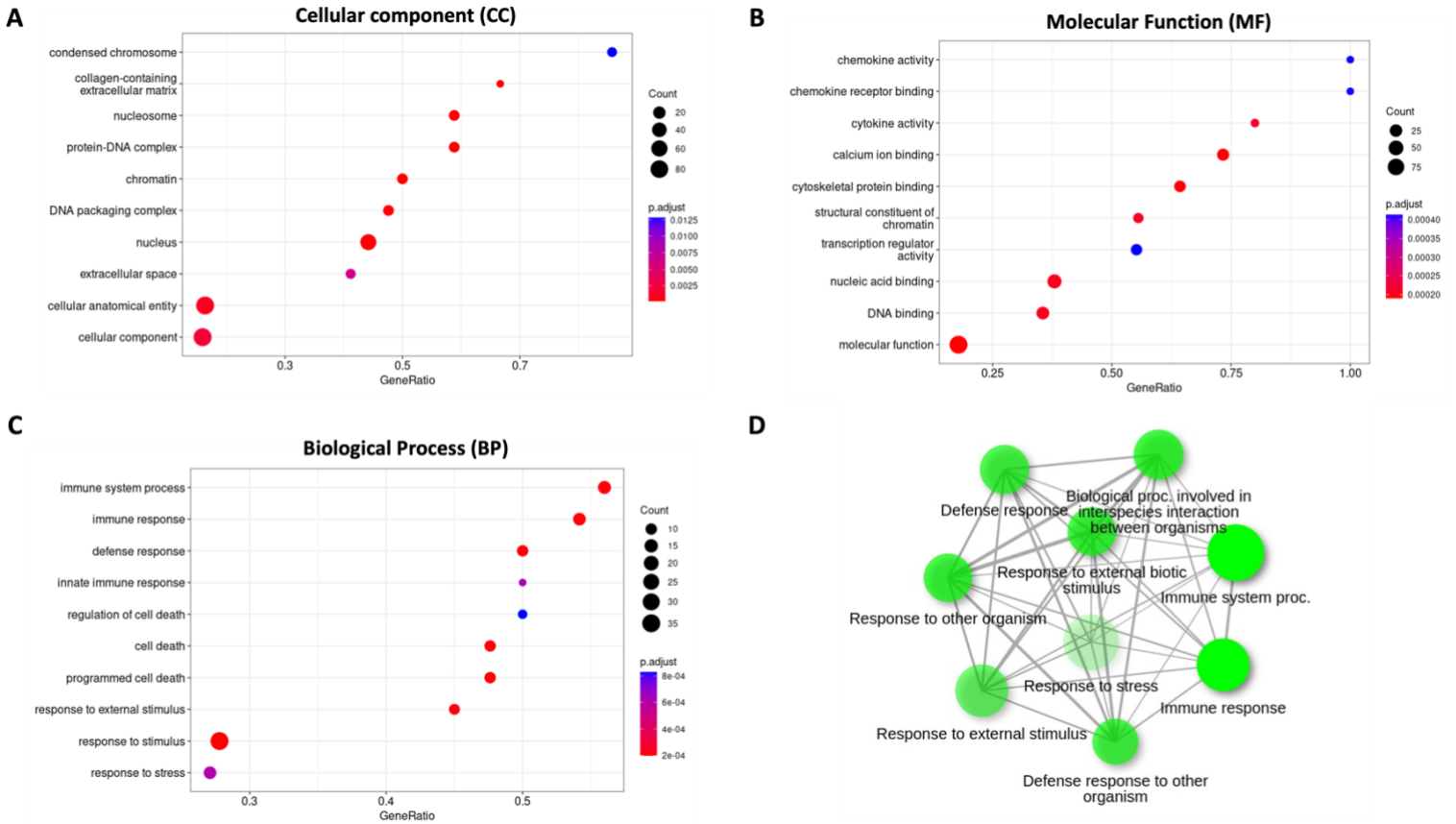

Figure 3.7 - Gene ontology analysis of significant DEGs in uninfected control vs CedPV-infection of PaBr cells. (A-C) *Dot plots generated using gene ontology (GO) enrichment analysis (ShinyGO tool) to show the top ten most significant cellular components (CC), molecular functions (MF) and biological processes (BP) in significant DEGs between uninfected and CedPV-infection. Counts are represented by circles whereby circle size represents the number of individual significant differentially expressed genes belonging to the category. Significance is represented by the colour intensity of the p-adjust value, whereby a deep blue represents the most significant and red the least significant. Gene ratio represents the amount of genes from the total significant DEGs in each select category.* ***(D)*** *Functional enrichment analysis was performed for all DEGs using the ShinyGO software. Assigned GO terms were used to classify functions of DEGs based on biological processes only. The brighter green nodes represent a higher degree of significance, whereas the more faded green nodes are less significant.*

3.2.3 CedPV-induced Alternative Splicing and Isoform Switching Analysis

Of the 3,004 significant DEGs identified previously in uninfected vs CedPV-infected PaBr cells, SUPPA2 software identified 470 of these genes to undergo differential splicing at a p-value of <0.05. Differential splicing analysis between the CedPV-infected and uninfected conditions is represented in the form of a volcano plot to show the magnitude of splicing change across the two conditions (Figure 3.8A). Delta PSI (ΔPSI) values plotted on the Y axis represent the difference of the mean percent spliced in (PSI) value between conditions. PSI value is defined as the ratio of the relative abundance of all isoforms containing a certain exon, over the relative abundance of all isoforms of the gene containing the exon (Schafer et al., 2015). This ΔPSI value is plotted against the average transcript abundance on the X axis. Significant differential splicing events are represented by blue dots and non-significant by grey dots on the volcano plot. Gene ontology enrichment analysis was performed for alternative splicing events occurring between uninfected and CedPV-infected PaBr cells. Significant alternative splicing events were categorised into CC, MF and BP whereby gene ontology (GO) analyses show the top GO terms for each category, as represented by lollipop plots in Figure 3.8(B-D). CC analysis shows that based on their $-\log_{10}$(FDR) value, the most significant cellular components involved in alternative gene splicing in uninfected vs CedPV-infected PaBr cells are located in the ribonucleoprotein complex, cell-substrate junction, focal adhesion, contractile actin filament bundle and stress fibre, which all had a high significance with a $\log_{10}$(FDR) value of 2.5 or more, as represented in red in Figure 3.8B. The highest number of genes that partake in differential splicing during CedPV infection have roles in RNA binding. Genes involved in other molecular functions such as double stranded RNA binding and nuclease activity also undergo alternative splicing here, but only RNA binding displays the highest $\log_{10}$(FDR) value of 7 (Figure 3.8C). BP

analysis shows the most significant genes that partake in differential splicing are related to the biological processes of RNA metabolic processes with the highest $\log_{10}$(FDR) value of 5 (Figure 3.8D). Additionally, it is evident that the groups representing the negative regulation of sphingolipid biosynthetic processes and lipoprotein particle receptor catabolic processes display a high fold enrichment during CedPV infection.

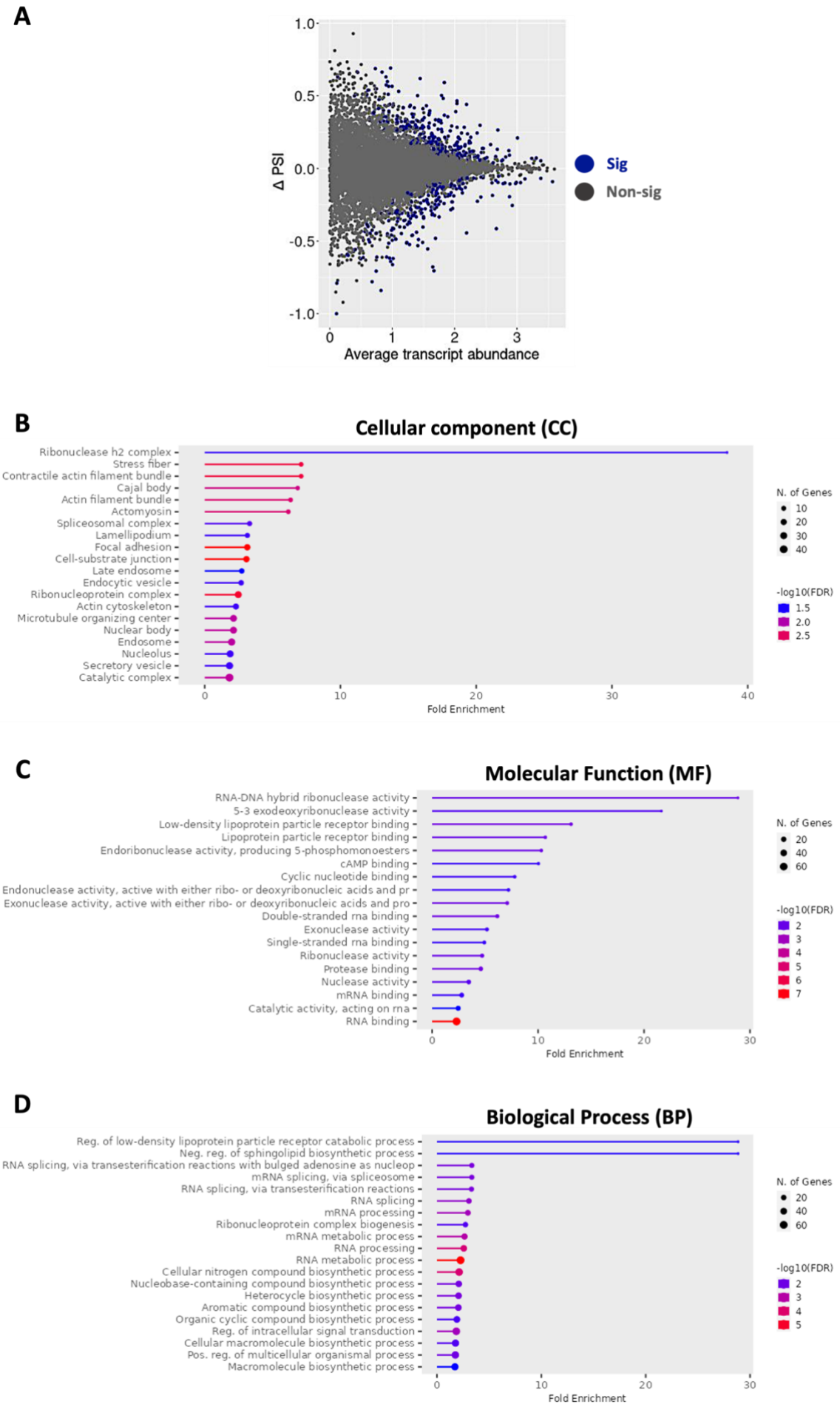
A
1.0
0.5
0.0
-0.5
-1.0
Δ PSI
0
1
2
3
Average transcript abundance
Sig
Non-sig
B
Cellular component (CC)
Ribonuclease h2 complex
Stress fiber
Contractile actin filament bundle
Cajal body
Actin filament bundle
Actomyosin
Spliceosomal complex
Lamellipodium
Focal adhesion
Cell-substrate junction
Late endosome
Endocytic vesicle
Ribonucleoprotein complex
Actin cytoskeleton
Microtubule organizing center
Nuclear body
Endosome
Nucleolus
Secretory vesicle
Catalytic complex
0
10
20
30
40
Fold Enrichment
N. of Genes
10
20
30
40
-log10(FDR)
1.5
2.0
2.5
C
Molecular Function (MF)
RNA-DNA hybrid ribonuclease activity
5-3 exodeoxyribonuclease activity
Low-density lipoprotein particle receptor binding
Lipoprotein particle receptor binding
Endoribonuclease activity, producing 5-phosphomonoesters
cAMP binding
Cyclic nucleotide binding
Endonuclease activity, active with either ribo- or deoxyribonucleic acids and pr
Exonuclease activity, active with either ribo- or deoxyribonucleic acids and pro
Double-stranded rna binding
Exonuclease activity
Single-stranded rna binding
Ribonuclease activity
Protease binding
Nuclease activity
mRNA binding
Catalytic activity, acting on rna
RNA binding
0
10
20
30
Fold Enrichment
N. of Genes
20
40
60
-log10(FDR)
2
3
4
5
6
7
D
Biological Process (BP)
Reg. of low-density lipoprotein particle receptor catabolic process
Neg. reg. of sphingolipid biosynthetic process
RNA splicing, via transesterification reactions with bulged adenosine as nucleop
mRNA splicing, via spliceosome
RNA splicing, via transesterification reactions
RNA splicing
mRNA processing
Ribonucleoprotein complex biogenesis
mRNA metabolic process
RNA processing
RNA metabolic process
Cellular nitrogen compound biosynthetic process
Nucleobase-containing compound biosynthetic process
Heterocycle biosynthetic process
Aromatic compound biosynthetic process
Organic cyclic compound biosynthetic process
Reg. of intracellular signal transduction
Cellular macromolecule biosynthetic process
Pos. reg. of multicellular organismal process
Macromolecule biosynthetic process
0
10
20
30
Fold Enrichment
N. of Genes
20
40
60
-log10(FDR)
2
3
4
5

Figure 3.8 - Differential splicing analysis from RNA-seq data in uninfected vs CedPV-infected PaBr cells. (A) *Volcano plot to show the magnitude of splicing change for differential splicing events. The magnitude of splicing change (ΔPSI) was calculated across the two conditions of uninfected or CedPV-infected PaBr cells in triplicate, as represented on the Y-axis as a function of the average transcript abundance represented on the x-axis in -log$_{10}$(TPM + 0.01) scale. The alternative splicing events were filtered based on FDR with a p value <0.05 according to SUPPA2 to identify the significant splicing events which are represented by a blue dot and grey dots represent non-significant differential splicing events.* ***(B-D)*** *Lollipop plots of the top ten significantly different cellular components (CC) and molecular functions (MF) and biological processes (BP) identified by Gene Ontology (GO) fold-enrichment analysis. Circle size represents the number of significant genes partaking in differential splicing belonging to that category and significance is represented by the colour intensity of the –log10(FDR) value, with red representing the most significant and blue the least.*

Isoform filtering and ISAR prediction was carried out on RNA-seq data using the IsoformSwitchAnalyzeR software, which identified 46,921 total isoforms within 38,154 genes in uninfected vs CedPV-infected PaBr cells. After ISAR filtering, based on default values of ISAR, 15,994 isoforms remained, and the final set of isoforms was 18,749 (Figure 3.9A). Isoform switching analysis revealed 411 genes, showing significant 502 switching events involving 640 isoforms (Figure 3.9B). Interestingly, 195 genes (47%) have an isoform switching event with downstream consequences influencing the functional properties of 307 isoforms. Consequence enrichment analysis revealed that the switching events implicated in these isoforms was generally due to the use of ES (exon skipping), MES (multiple exon skipping) and ATSS (alternative transcription start site) gain (Figure 3.9C). When considering each type of alternative transcription event with isoform consequence separately, we can determine that the most frequent changes in alternative splicing in significant isoforms are the utilisation of an alternative transcription start site (ATSS) and exon skipping (ES) (Figure 3.9D). Despite a lower number of significant isoforms than ATSS and ES, multiple exon skipping (MES) appeared to occur slightly more often in the isoform used less. Little to no difference was observed for the use of A3, A5, ATT, IR and MEE alternative splicing events which all also only exhibited a low number of significant isoforms.

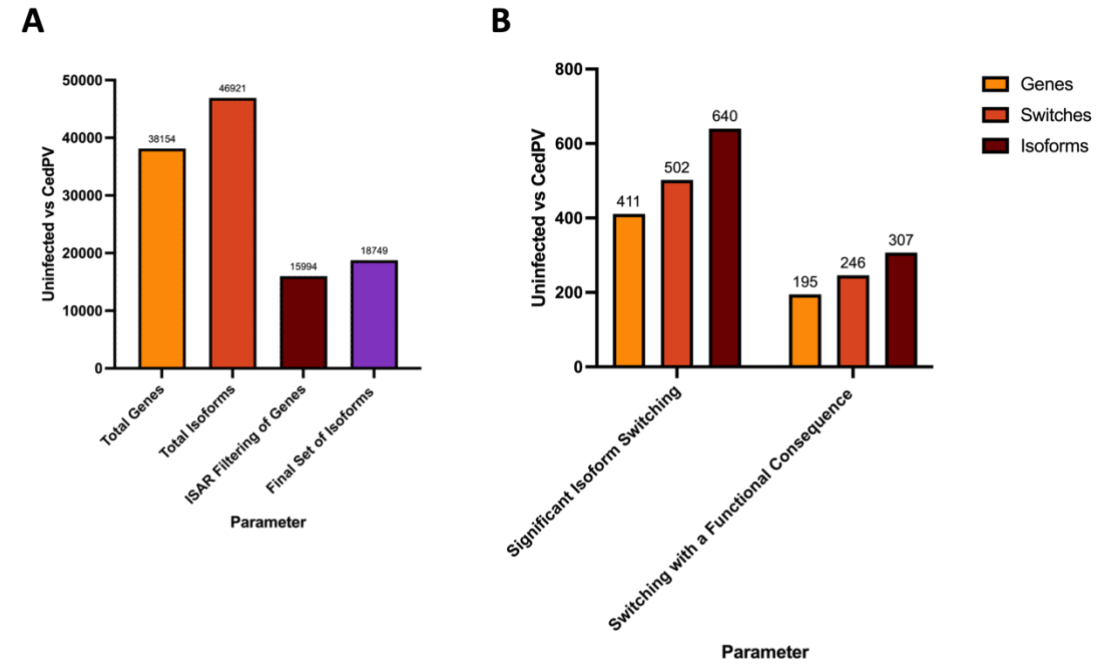
A
Uninfected vs CedPV
50000
40000
30000
20000
10000
0
38154
46921
15994
18749
Total Genes
Total Isoforms
ISAR Filtering of Genes
Final Set of Isoforms
Parameter
B
Uninfected vs CedPV
800
600
400
200
0
411
502
640
195
246
307
Genes
Switches
Isoforms
Significant Isoform Switching
Switching with a Functional Consequence
Parameter

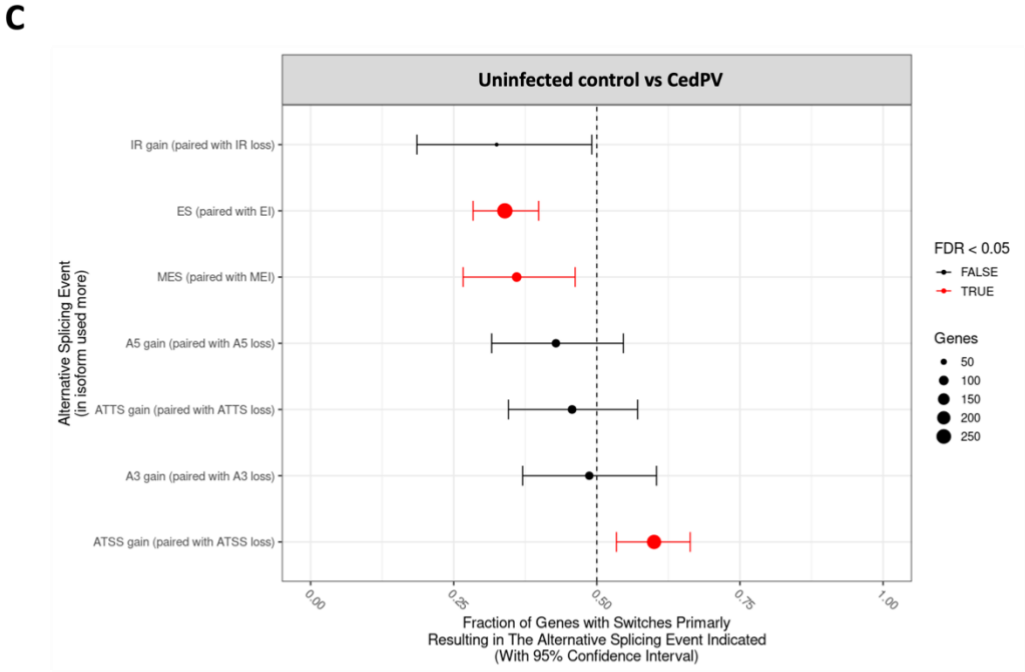
C
Uninfected control vs CedPV
IR gain (paired with IR loss)
ES (paired with EI)
MES (paired with MEI)
A5 gain (paired with A5 loss)
ATTS gain (paired with ATTS loss)
A3 gain (paired with A3 loss)
ATSS gain (paired with ATSS loss)
Alternative Splicing Event
(in isoform used more)
0.00
0.25
0.50
0.75
1.00
Fraction of Genes with Switches Primarly
Resulting in The Alternative Splicing Event Indicated
(With 95% Confidence Interval)
FDR < 0.05
FALSE
TRUE
Genes
50
100
150
200
250

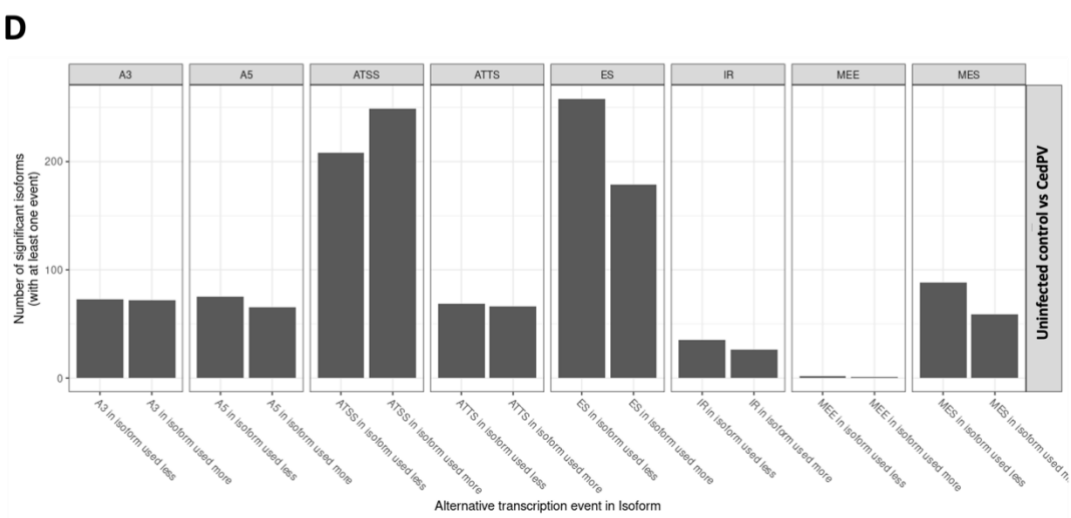
D
A3
A5
ATSS
ATTS
ES
IR
MEE
MES
Number of significant isoforms
(with at least one event)
200
100
0
Uninfected control vs CedPV
A3 in isoform used less
A3 in isoform used more
A5 in isoform used less
A5 in isoform used more
ATSS in isoform used less
ATSS in isoform used more
ATTS in isoform used less
ATTS in isoform used more
ES in isoform used less
ES in isoform used more
IR in isoform used less
IR in isoform used more
MEE in isoform used less
MEE in isoform used more
MES in isoform used less
Alternative transcription event in Isoform

***Figure 3.9 - Isoform switching analyses in uninfected vs CedPV-infected PaBr cells**. **(A)** Bar chart to show the filtering process of total genes to identify significant isoforms between uninfected vs CedPV-infected cells. **(B)** Bar chart illustrating the measure of genes, switches and isoforms involved in significant isoform switching events and significant isoform switching events with a functional consequence, in uninfected vs CedPV-infected PaBr cells.**(C)** Enrichment of specific splice events for each set of opposing events (e.g. IR gain vs loss) as determined by analyzing the fraction of events associated with each type of consequence. The X axis represents the fraction of genes showing enrichment of a specific alternative spicing event upon CedPV infection whereby a value of 0.5 corresponds with no systematic change occurring, represented by the dotted line through the centre of the plot. Y axis denotes the alternative splicing event that has taken place in the most used isoform of that gene. Circle size represents the number of genes for each splicing event and true significance of splicing is represented in red, determined to have an FDR value of <0.05. **(D)** Global splicing analysis to observe alternative splicing events in different isoforms. Splicing events presented here are A3 (alternative 3' splice-site), A5 (alternative 5' splice-site), ATSS (alternative transcription start site), ATTS (alternative transcription termination site), ES (exon skipping), IR (intron retention), MEE (mutually exclusive exons) and MES (multiple exon skipping).*

Using a built-in function of the ISAR package, a total of 195 genes were identified to undergo significant isoform switching with functional consequence, resulting in a total of 307 isoforms from these genes. Further in-depth analysis into individual genes concerned here provided an insight into the type of isoform switching taking place in each gene. Overall, genes undergoing isoform switching belonged to several diverse processes within the bat host. However, for our investigations into understanding bat innate immunity, we selected four immune-related genes (DHX9, IL1R1, IL23A and TRAF1) which exhibited isoform switching with a functional consequence for further investigation here (Figure 3.10 A-D). These genes were selected as the top four most significant genes that are concerned with innate immunity for our investigations, out of the total 195 genes that undergo isoform switching with a functional consequence.

Overall, gene expression was increased more highly in the CedPV-infected cells compared to uninfected (Figure 3.10 B,C,D), except for DHX9, whereby gene expression appears slightly less in the infected cells (Figure 3.10A). DHX9 encodes an RNA helicase which has roles in unwinding double-stranded RNA and transcriptional regulation. Isoform switching analysis showed that DHX9 possesses two protein coding isoforms (XM_006907755 and XM_006907756) which differed in their expression between uninfected and CedPV-infection. The IL1R1 gene, which encodes a cytokine receptor, important in mediating cytokine-induced immune and

inflammatory responses, was shown to possess five protein-coding isoforms (Figure 3.10B). Two of these isoforms represented a significant difference in expression and usage between uninfected and CedPV-infected cells, whereby isoform XM_006920783 is used more in absence of infection, whereas XM_015596292 shows increased upon infection of CedPV. IL23A which encodes a cytokine that aids in the production of IFNγ, also possesses five protein coding isoforms. Isoform XM_025044701 displayed increased usage in CedPV infection and isoform XM_025044700 was significantly favoured in uninfected cells (Figure 3.10C). Three protein-coding isoforms were identified in TRAF1, a gene which has important roles in signal transduction for NF-κB activation (Figure 3.10D). Isoform usage was significant for all three of these isoforms, whereby CedPV infection favoured expression of isoforms XM_025050438 and XM_025050439 and the remaining isoform XM_006917075 was used more in uninfected cells. Overall, an observable preference for alternative isoform usage was exhibited in both the presence and absence of infection within these four genes, whereby certain isoforms were used more in infected cells than in uninfected cells and vice versa.

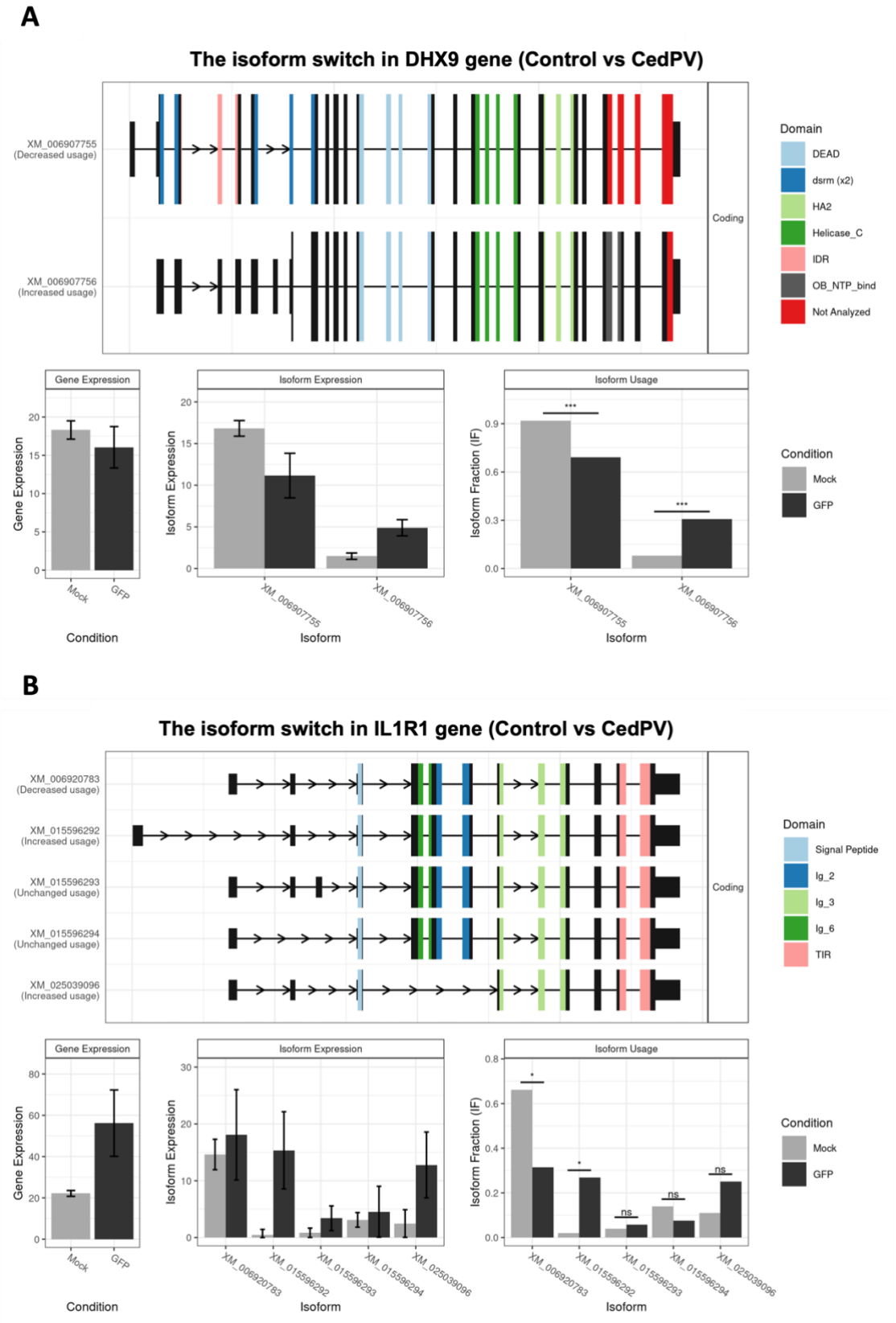
A
The isoform switch in DHX9 gene (Control vs CedPV)
XM_006907755
(Decreased usage)
XM_006907756
(Increased usage)
Coding
Domain
DEAD
dsrm (x2)
HA2
Helicase_C
IDR
OB_NTP_bind
Not Analyzed
Gene Expression
Isoform Expression
Isoform Usage
Gene Expression
Isoform Expression
Isoform Fraction (IF)
Mock
GFP
Condition
XM_006907755
XM_006907756
Isoform
Condition
Mock
GFP
B
The isoform switch in IL1R1 gene (Control vs CedPV)
XM_006920783
(Decreased usage)
XM_015596292
(Increased usage)
XM_015596293
(Unchanged usage)
XM_015596294
(Unchanged usage)
XM_025039096
(Increased usage)
Coding
Domain
Signal Peptide
Ig_2
Ig_3
Ig_6
TIR
Gene Expression
Isoform Expression
Isoform Usage
Gene Expression
Isoform Expression
Isoform Fraction (IF)
Mock
GFP
Condition
XM_006920783
XM_015596292
XM_015596293
XM_015596294
XM_025039096
Isoform
ns
Condition
Mock
GFP

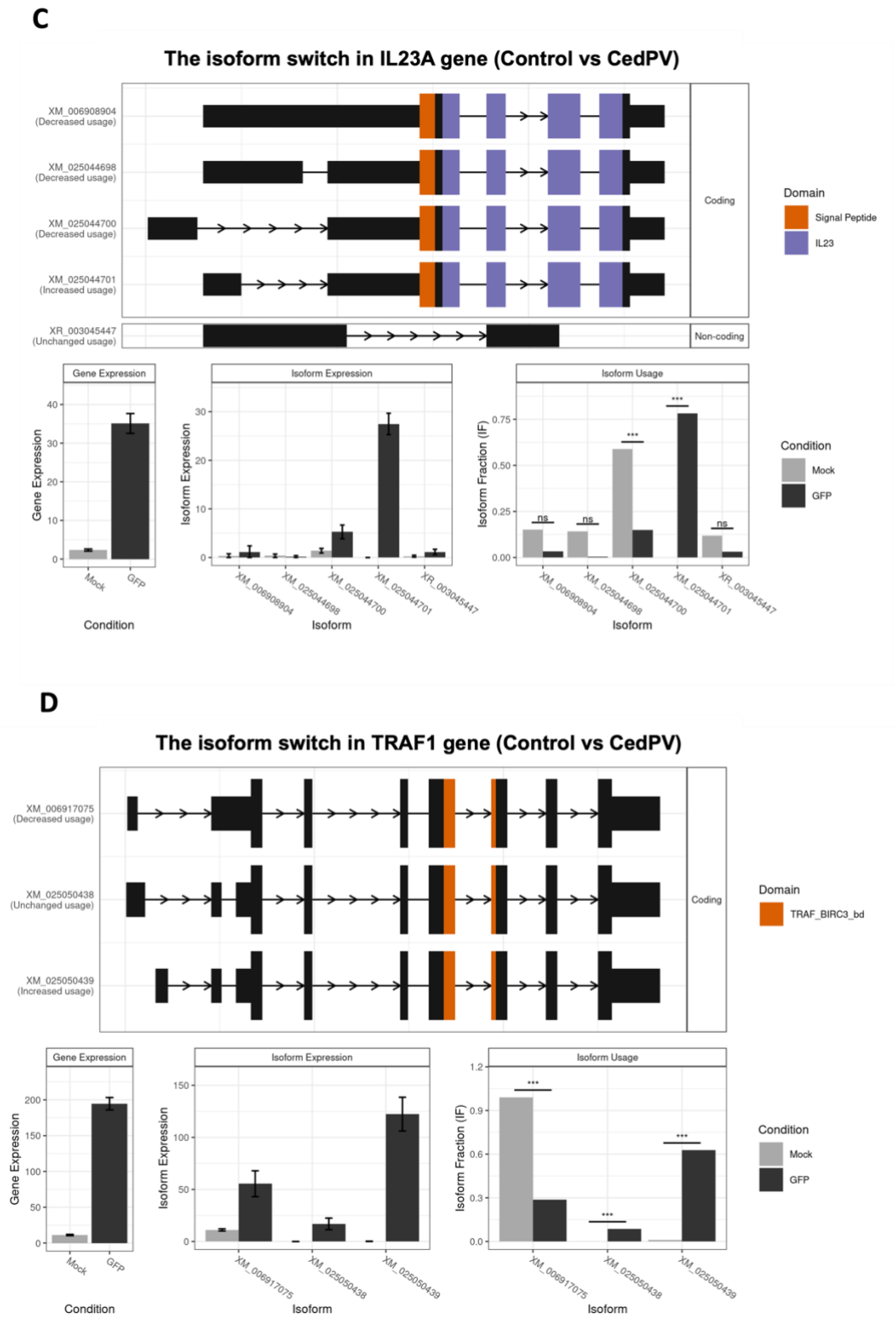

Figure 3.10 - Isoform switching events in genes that undergo switching with functional consequence in uninfected vs CedPV-infected PaBr cells. *Isoform switching events with a functional consequence in four representative immune-related genes;* ***(A)*** *DHX9,* ***(B)*** *IL1R1,* ***(C)*** *IL23A and* ***(D)*** *TRAF1 were identified by RNA-seq.*

Whilst some genes only undergo one type of alternative splicing to produce alternative isoforms, genes can also partake in different splicing events to result in isoform switching, as shown in Figure 3.11. The difference between the isoforms involved in an isoform switch can result from changes within the three distinct biological mechanisms; aTSS, aTTS and AS. Therefore, we aimed to observe which combination of these mechanisms gives rise to the difference between the two isoforms involved in an isoform switch and perceive any commonality of genes within these mechanisms. Results show that 10 genes are capable of alternative splicing by all three aTSS, aTTS and AS methods. Furthermore, results indicate a relatively higher importance of the combination of aTSS with AS than aTTS with AS for example, as represented by a higher number of genes (103) undergoing both aTSS and AS together.

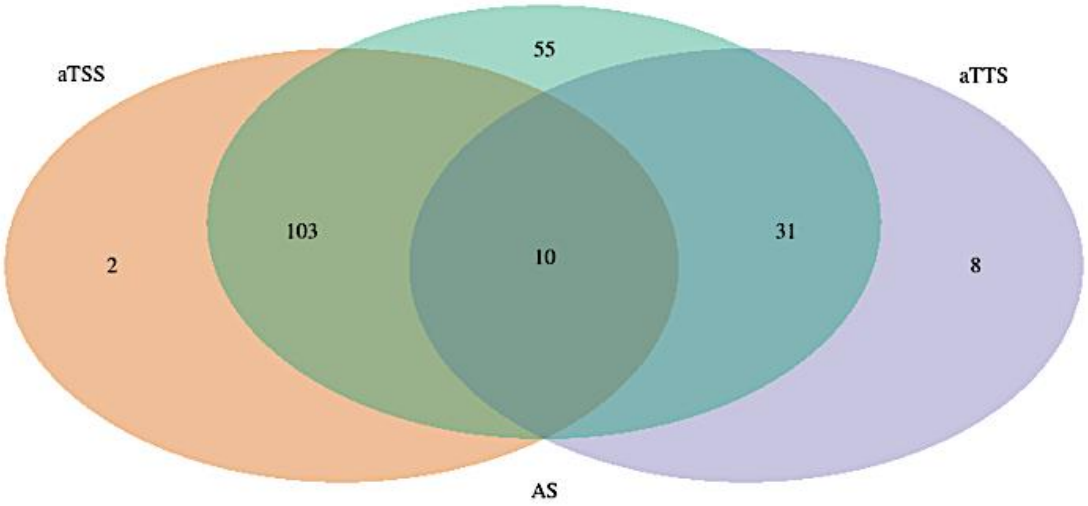

Figure 3.11 *-* ***Venn diagram representing gene counts undergoing discrete alternative splicing events that result in isoform switching.*** *Counts of genes which undergo alternative splicing to express different isoforms are categorised here into aTSS (alternative transcription start site), aTTS (alternative transcription termination site) and AS alternative splicing).*

Taken together, the investigations using RNA-seq analysis can help to map the transcriptomic response of cells to stimuli such as CedPV infection used here, which is beneficial in expanding our understanding and knowledge of differential gene expression and behaviour induced upon viral infection in bats. Figure 3.12A displays the number of genes that are associated with each of the three RNA-seq analysis methods used here; differential gene expression, differential/alternative splicing and isoform switching analyses. Results indicate that some genes are universally involved in two or more events, with 89 genes partaking in both differential gene expression and differential splicing, 54 genes undergo differential splicing and isoform switching and 32 genes undergo both differential expression and isoform switching. Notably, 22 genes are common within all three parameters, as represented in the centre of the Venn diagram and the relative functions of these genes are described in Figure 3.12B.

A

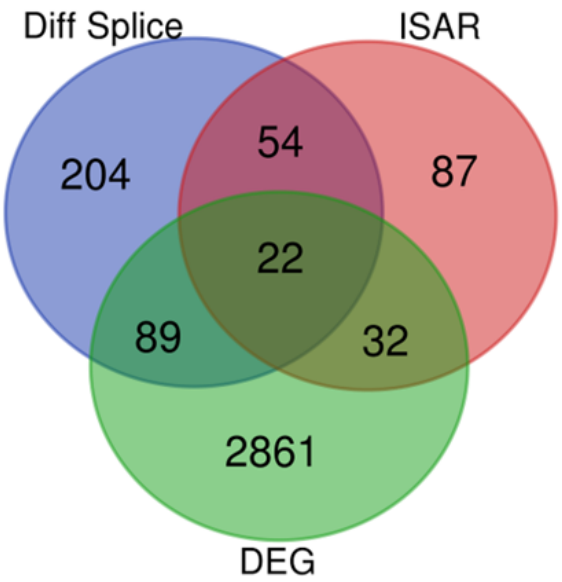

B

Gene	Full Gene Title	Function
MAX	MYC Associated Factor X	Regulation of cell proliferation, differentiation and apoptosis
PRPF3	Pre-mRNA Processing Factor 3	Role in pre-mRNA splicing involved in spliceosome assembly
IL23A	Interleukin 23 Subunit Alpha	Important in inflammatory and immune responses against infection
TEX10	Testis Expressed 10	rRNA processing in nucleus and cytosol and processing of capped intron-containing pre-mRNA
DEPDC1	DEP Domain Containing 1	Enables GTPase activator activity and involved in negative regulation of transcription
TMX3	Thioredoxin Related Transmembrane Protein 3	Catalyze protein folding and thiol-sulfide interchange reactions
YARS	Tyrosyl-tRNA synthetase cytoplasmic	Catalyze aminoacylation of tRNA by their cognate amino acid
CALD1	Caldesmon 1	Plays essential role in the regulation of smooth muscle and nonmuscle contraction
ABHD14A	Abhydrolase Domain Containing 14A	Predicted to enable hydrolase activity
IL1R1	Interleukin 1 receptor type I	Important mediator involved in many cytokine induced immune and inflammatroy responses
PDLIM5	PDZ and LIM domain protein 5	Involved in cytoskeleton organization, cell lineage specification, organ development and oncogenesis
DDAH1	Dimethylarginine Dimethylaminohydrolase 1	Encoded enzyme plays a role in nitric oxide generation
ARIH2	Ariadne RBR E3 Ubiquitin Protein Ligase 2	Polyubiquitinates some proteins, tagging them for degredation and also upregulates p53 in some cancer cells
RHBDD2	Rhomboid Domain Containing 2	Involved in intramembrane proteolysis and overexpressed in some breast cancers
TPM1	Tropomyosin 1	Involved in contractile system of striated and smooth muscles and the cytoskeleton of non-muscle cells
RIMKLB	Ribosomal Modification Protein RimK Like Family Member B	Predicted to enable N-acetyle-L-aspartate-L-glutamate ligase activity and citrate-L-glutamate ligase activity
CLK1	Dual Specificity Protein Kinase	Phosphorylates serine/arginine-rich protein involved in pre-mRNA processing, releasing them into the nucleoplasm
BST2	Bone Marrow Stromal Cell Antigen 2	Involved in growth and development of B-cells
TRAF1	TNF Receptor Associated Factor 1	Associate with and mediate signal transduction from receptors of TNFR superfamily and required for activation of NF-kappaB
ANKRD12	Ankyrin Repeat Domain 12	Inhibition of transcriptional activity of nuclear receptors through recruitment of histone deacetylases
RNASEH2A	Ribonuclease H2 Subunit A	Endonucleolytically cleaves ribonucleotides
TMED4	Transmembrane P24 Trafficking Protein 4	Involved in positive regulation of I-kappaB kinase/NF-kappaB signalling

Figure 3.12 - Gene distribution identified in RNA-seq parameters. (A) *Venn diagram displaying genes which are common between the different RNA-seq analysis methods of differential gene expression (DEGs), differential splicing and isoform switching analysis (ISAR). A total of 22 genes identified in uninfected vs CedPV-infected PaBr cells partake in differential expression, splicing and isoform switching.* ***(B)*** *Table showing the full title and function of the 22 identified genes.*

3.3 Discussion

Previous transcriptomic studies investigating the gene repertoire induced upon viral infection in bats remain limited, and to our knowledge, the transcriptomes induced by the bat henipavirus CedPV remain unexplored. Transcriptomic analysis is an invaluable technique used to investigate all RNA species within a host, a cell, or a collection of cells, the latter of which we examined in this study. Transcriptomics encompasses gene transcription, expression, location, trafficking and degradation events, alongside the examination of transcript structure, their splicing patterns and resultant isoform switching events (Milward et al., 2016). These transcriptomic analysis methods utilise high-throughput techniques to examine gene expression and events under different physiological conditions or external treatments. The observation of the host transcriptomic response under varying circumstances allows researchers to gain a valuable insight into the action of transcripts and gene expression patterns induced under different conditions and how they may vary in their RNA signature. We therefore adopted a transcriptomic approach with the aim of illustrating the gene expression patterns and host processes induced upon CedPV infection in PaBr cells from the natural reservoir of this virus, *P.alecto.* By investigating the transcriptomic events taking place within the henipavirus natural host during CedPV infection, we sought to unearth potential gene expression patterns and splicing mechanisms taking place, with a substantial focus directed towards their antiviral immune response, and how these differences in expression may provide an advantage to bats in regulating virus-mediated pathology.

RNA-seq data were first normalised and assessed via a dispersion plot (Figure 3.3). Dispersion is a measure of variability in the dataset, whereby dispersion estimates reflect variance in gene expression for a given mean count value. Dispersion estimates generated in DESeq2 are inversely related to the mean and directly related to variance. Based on this, for large mean counts dispersion is lower and for small

read counts it is higher and dispersion estimates for genes with the same mean will only differ based on their variance (Anders and Huber, 2012). For each gene, an initial dispersion was generated using maximum likelihood estimation, which was plotted in function of the mean expression level (mean of normalised counts of replicates), whereby each gene is represented by a black dot. A curve was then fitted to the gene-wise dispersion estimates (as represented by a red line on plot), which represent the estimate for the expected dispersion value for genes of a given expression level. This is beneficial in demonstrating individual genes possess different levels of variability, but overall, there will be a distribution of acceptable dispersion estimates. To obtain final dispersion estimates, the initial gene-wise dispersion estimates were shrunk towards the fitted curve. The adjusted dispersion values are represented by blue dots in the dispersion plot. Shrinkage of dispersion estimates is important in reducing the risk of false positives in subsequent differential expression analysis. Adjustment of dispersion value results in an increase for some genes, which limits the potential for false positives that could appear from an underestimated dispersion. Furthermore, dispersion estimates that sit slightly above the plotted curve are also shrunk towards it. However, it is also important that dispersion estimates that have very high values are not shrunk towards the curve here, as this could result in false positives (Love et al., 2014). These genes are represented by blue circling on the dispersion plot. Data from our experiment fits the dispersion plot, whereby gene dispersion estimates are generally spread around the curve and dispersion decreases as mean expression levels of normalised counts increases.

Additionally, to further confirm the overall variability within the normalised sample counts and to determine if biological replicates clustered together, we performed principal component analysis (PCA) whereby the triplicate biological replicates of uninfected and CedPV-infected PaBr cells were analysed (Figure 3.4). We undertook

PCA analysis, which is an unsupervised test of variability, whereby no prior information is applied to the dataset for analysis. Instead, PCA utilises a dimensionality reduction technique that identifies the largest amounts of variation within a dataset and assigns it to principal components. The first principal component (PC1) accounts for the principal direction along which samples display the greatest amount of variation and the second principal component (PC2) is calculated in the same manner with the condition that is uncorrelated with the first principal component and is orthogonal to the PC1 axis, accounting for the next highest variance (Kassambara, 2017). Generally, we plot PC1 and PC2 against each other as representatives of the largest variation in the dataset. Generally, biological replicates are expected to cluster closely together, and the different sample groups tend to cluster apart from one another within the PCA plot. Overall, our PCA results showed the close clustering of biological replicates for both treatment groups. The PCA revealed that the transcriptomes of uninfected samples clustered closely together as expected of a control group. A higher variance was observed (PC1 with 97%) in the CedPV-infected biological replicates, but these too displayed relatively close clustering, whereby two of the replicates clustered closely, with the third displaying a slightly lower variance (PC2 with 1%). These PCA results confirm the expected scenarios of this study, whereby uninfected controls tend to show little to no variation and CedPV-infected transcriptomes group closely but can vary slightly due to the different outcomes achieved following viral infection.

The normalised RNA-seq results obtained from mock vs CedPV-infected PaBr cells were then used for differential expression analysis. Differential gene expression is a technique useful in determining which genes are expressed at different levels between two or more sets of conditions. Results highlighting the varied expression, including the up or down-regulation of genes, offer key insights into the biological processes influenced by the varying conditions or stimuli. Our study sought to identify

significant differentially expressed genes in PaBr cells induced upon CedPV infection to understand the transcript-level response and possibly how these genes may prove advantageous in the role of bats as viral reservoirs. Results showed that several significant upregulated DEGs in CedPV infection are associated with the innate immune response mounted towards viral infection (Figure 3.5B). IFI6, Mx1, IFIT2 and IFIT3 are all IFN-inducible genes known to display antiviral activity by collectively targeting several stages of the virus life cycle including replication and signalling (Zhou et al., 2013b, Sajid et al., 2021, Verhelst et al., 2013). Other significant DEGs upregulated upon CedPV infection include the cytokines CCL5 and CXCL8, which both have immunoregulatory roles and are mediators of the inflammatory response, alongside BTG1 which negatively regulates cell proliferation. Investigations into the most variable DEGs between conditions also denoted the strong association of immune-related genes upregulated during CedV infection. The ISGs, IFIT2 and IFIT3, were shown to display higher expression during infection than in uninfected cells, alongside another ISG named ISG15, which is also known to possess antiviral activity (Figure 3.5C). Notably however, two of the most variable genes observed between CedPV infected and uninfected PaBr cells included LOC1028843 and LOC1028983, which displayed higher expression in CedPV infection and represent unannotated transcripts in *P.alecto*. As the name and function of these genes are unknown, further annotation of the *P.alecto* genome in the future may allow us to identify these genes and thus their potential influence upon viral infection in bats. Collectively, the upregulation and high contrast in variability of significant DEGs in comparison to uninfected cells observed here during CedPV infection, comprises several innate immune genes together with inflammatory and immunoregulatory genes which potentially act as the first line of defence to viral infection by demonstrating a balanced response within *P.alecto* cells.

In addition to the study of upregulated genes, DEG analysis successfully identified DEGs which were downregulated during CedPV infection, including MATN3, CALD1, ACTG2 and TIMP3 (Figure 3.5B). These genes have differing roles related to processes such as muscle contraction, bone development and inhibition of ECM degradation. Moreover, some DEGs were shown to display a higher expression in uninfected cells compared to CedPV infected cells as represented by variability between the two treatment groups (Figure 3.5C). These DEGs include, but are not limited to, TAGLN, MATN3, PTN, CST6 and MYL9 which are associated with a variety of processes such as muscle contraction, bone maintenance and the regulation of cell growth. The combined downregulation of these genes during CedPV infection and/or their high basal expression warrant further functional annotation to understand why the expression of these genes is altered between viral infection and uninfected cells and additionally any benefits this may provide to the bat host.

Alongside individual DEGs of interest, several pathways and biological processes concerning the innate immune response to viral infection were heavily implicated during functional enrichment analysis investigations obtained from our RNA-seq data. The molecular functions shown to possess the highest significance during CedPV infection of PaBr cells when compared to the untreated group include the regulation of transcription activity and chemokine activity/receptor binding (Figure 3.7B). As chemokines are essential mediators for inflammation and control of viral infection, the high number of DEGs partaking in this function may aid in the shaping of the bat immune response to CedPV infection. Furthermore, actions facilitated by transcriptional regulatory activity highlighted in MF analysis, may mediate the transcription of genes involved in the antiviral immune response to CedPV infection, but further analysis into the functionality of these molecular roles is required. The importance of DEGs associated with innate immune mechanisms observed in this study were supported via BP GO analysis, whereby significant processes included

the regulation of cell death, response to stress and the innate immune response (Figure 3.7C). Additionally, most biological processes identified here encompass the immune response to viral infection, such as immune and defence responses and the response to stress and external stimuli, all representing BP categories that exhibit high significant DEG counts. Additionally, the increased negative regulation of sphingolipids during CedPV infection may be due to their role in the immune response (Figure 3.7C). As sphingolipids are located in cellular membranes, they have been previously demonstrated to influence viral replication, including at the point of fusion of virus with the plasma membrane (Avota et al., 2021). The increased reduction in their regulation observed here may perhaps be a mechanism employed by CedPV to allow for ease of viral entry. Functional enrichment network analysis further displayed the key significant functions in which DEGs partake in, which were all related to the innate immune defence (Figure 3.7D).

Generally, DEG analysis demonstrated the significant role of several DEGs and their associated molecular processes to partake in the innate immune response to CedPV infection. In accordance with these observations from our RNA-seq data, we aimed to further identify the change in expression of important mammalian DEGs often involved in the antiviral response. The selected immune genes were identified within the *P.alecto* transcriptome obtained from our RNA-seq results and subsequently chosen for further analysis due to their key antiviral roles in shaping the mammalian innate immune response. Although there are several hundred conserved and novel ISGs induced in bats upon viral infection, we centred our focus around these six due to their prior examination in other mammalian species and their well-characterised innate immune activity. Upon observation of normalised counts of the selected immune genes, as represented in triplicate in uninfected control and CedPV-infection, all six immune genes display a much higher normalised gene count upon CedPV infection in comparison to uninfected cells (Figure 3.6(A-F)). Therefore, these results

demonstrate the increased usage of the mammalian innate immune genes (IRF7, IFIT5, IFI35, IFIT2, IFIT3 and IFI6) in bat cells upon infection with CedPV, signifying their capacity to mount an antiviral immune response. Profound analysis into other immune-related genes present within the *P.alecto* transcriptome, alongside research into their functional roles in bats, could provide a valuable insight into the nature of the innate immune response mounted by bats when challenged with viral infection.

Using our RNA-seq data from CedPV-infected vs uninfected PaBr cells, we aimed to assess the alternative splicing events occurring in infected bats. Alternative splicing is a process by which different proteins are produced from a single pre-mRNA via regulation of exons that are included within the mature transcript. It is a fundamental process that generates transcriptomic diversity, whereby spliced variants of the same gene can differ in their structure, function, and localisation, successively influencing protein outcomes. Over 90% of human genes that are expressed undergo alternative splicing, which is hence recognised to play important roles in cellular processes such as the regulation of immune responses, in addition to a range of pathogenic processes that underlie disease and pathologies including cancer and neurological disorders (Wang et al., 2008, Raj and Blencowe, 2015, Dredge et al., 2001). Chauhan et al. (2019) describes how growing evidence suggests that the regulation and precision of splicing is essential to the well-being of cells, as when altered or disrupted, pathological outcomes can arise. For example, viral infection can cause global changes in the pattern of alternative splicing, either directly or indirectly, which can alter the immune responses mounted against the invading pathogen. Therefore, by observing the alternative splicing events induced in PaBr cells upon infection of the henipavirus CedPV, we can contribute to the current understanding of viral influence and disruption of host alternative splicing events in bats.

Previous research has demonstrated that several viruses are capable of hijacking host splicing machinery during infection including HIV, Zika and dengue virus, which

are believed to also partake in widescale infection-mediated disruption of host response machinery (Machiels et al., 2013, De Maio et al., 2016, Hu et al., 2017). Although these studies are currently limited, they present a new perspective on host-pathogen interactions of viral infection. Little is understood about the processes and patterns of alternative splicing in bats upon viral challenge and any implications or potentially advantages these events may provide to bats as viral hosts. Therefore, we aimed to characterise alternative splicing events in CedPV-infected PaBr cells to better understand their transcriptomic response to infection.

A total of 470 genes in CedPV vs uninfected PaBr cells were identified to undergo differential splicing (Figure 3.8A). Gene enrichment analysis also revealed the most significant cellular components, molecular functions and biological processes implicated in these alternative splicing events in PaBr cells (Figure 3.8(C-E)). Several components displayed high significance and are hence likely associated with alternative splicing of genes involved in these processes. Genes located within the ribonucleoprotein complex, cell-substrate junction, focal adhesion, and stress fibres for example were identified to undergo significant differential splicing (Figure 3.8C). The method of alternative splicing and the influence it may have on the role of genes within these cellular structures during viral infection require further functional and computational investigation. Similarly, significant alternative splicing events involved in molecular functions and biological processes such as RNA binding, double stranded RNA binding and RNA metabolism require further characterisation in bats to understand the molecular outcomes of these splicing events and their influence on the bat host (Figure 3.8D). Additional biological processes affected by alternative splicing upon CedPV infection included RNA and mRNA processing, alongside regulation of intracellular signal transduction, cellular nitrogen compound biosynthetic processes and mRNA metabolic processes (Figure 3.8E). Although the roles of these processes in CedPV infection of bats have not been identified, it is plausible that viral

infection regulates these processes for successful hijacking of the cellular RNA processing machinery for the benefit of virus replication.

Some genes have more than one pattern of splicing and undergo alternative splicing, which can give rise to different mRNA and therefore proteins which have a slightly different sequence, resulting in different isoforms of the same gene or transcript. Isoforms are thus versions of the same protein that possess similar but not identical amino acid sequences. Isoforms are generated from a single gene by the use of alternative splicing methods such as the use of a different alternative transcriptional start site and termination sites (Chen et al., 2022). Eukaryotic cells have the facility to determine which isoform to express at a given time which is often dependent on factors such as regulatory signals, in order to switch from expressing one isoform of a gene to an alternative, this is known as isoform switching. Results from our RNA-seq data identified the most significant modes of alternative splicing in CedPV-infected PaBr cells were exon skipping (ES), multiple exon skipping (MES) and the use of an alternative transcription start site (ATSS) (Figure 3.9C). Often, the expression of an alternative isoform results in an altered function of the encoded protein, occurring via the gain or loss of protein domains and signal peptides and loss of protein coding sequence (Chen et al., 2022). We identified 195 genes to undergo 246 alternative splicing events, resulting in 370 different isoforms that have a functional consequence (Figure 3.9B). Future studies examining these alternatively spliced genes and their resultant consequences on protein function could uncover the impact on the functionality of proteins in bats and resultant beneficial or detrimental effects on the wellbeing and viral reservoir potential of the bat host.

Due to our interest in observing the innate immune response induced in bats upon CedPV infection, we selected four immune-related genes from the 195 genes already identified within the RNA-seq dataset, that were exhibited to undergo significant isoform switching with a functional outcome (Figure 3.10(A-D)). DHX9 senses and

binds to several DNA and RNA species, including those produced by viruses, such as rotavirus, whilst also having roles in mRNA translation (Figure 3.10A) (Jain et al., 2010, Zhang and Grosse, 1997, Zhang et al., 1999, Jain et al., 2013, Zhu et al., 2017). Interestingly, whilst this gene has been shown to enhance HIV-1 transcription, it also plays a role in viral MyD88-dependent DNA and RNA sensors in dendritic cells, inducing antiviral innate immune responses here (Fujii et al., 2001, Xing et al., 2014, Kim et al., 2010, Zhang et al., 2011). Therefore, it is plausible that the usage of an alternative isoform in CedPV-infected bat cells, could provide beneficial roles within the antiviral immune response, but requires functional characterisation via knock out experiments for example. IL1R1 encodes a cytokine receptor that mediates the activation of NF-κB, MAPK and other pathways important to the cytokine-induced immune and inflammatory responses (Figure 3.10B) (Mosley et al., 1987). Isoform switching of this gene with a functional consequence could prove beneficial in the control of inflammatory responses balanced with the immune response in bats. IL23A is another cytokine investigated here, which also results in the activation of the NF-κB and MAPK pathways and has a key role in activating the transcription factor STAT4 to stimulate the production of IFNγ and pro-inflammatory cytokines (Figure 3.10C) (Oppmann et al., 2000, Parham et al., 2002). Again, the preference for an alternative isoform in the presence of viral infection may be adopted by bat hosts to enable them to balance inflammatory and immune responses and thus requires further exploration. Lastly, the gene TRAF1 is also imperative in the activation of NF-κB and MAPK8/JNK, mediated by TNFα and is also found to be induced upon Epstein-Barr virus (EBV) infection (Figure 3.10D) (Guo et al., 2009, Lavorgna et al., 2009, Greenfeld et al., 2015, Siegler et al., 2003). We theorise that the alternative isoforms expressed in the CedPV-infected PaBr cells for each of these immune genes, holds the potential to provide advantageous immune regulatory qualities, contributing to the ability of bats to host viruses without displaying any overt signs of disease. However, substantial investigations are necessary to determine this and work should be

directed towards the characterisation of the impact of alternative isoform usage on the immune and inflammatory mechanisms involved in CedPV infection in bats.

Our research has generated investigative RNA-seq data representative of the bat response to henipavirus infection. Transcriptomic analysis methods including DEG, alternative splicing and isoform switching have provided a preliminary insight into various genes of interest in bats and the potential benefits they may confer to the bat host in controlling virus-mediated immunopathology. Although our data has been derived from a single bat cell line and may not be representative of all bat species due to their extremely large diversity, it provides an initial framework and transcriptomic characterisation of the global response of bat cells to infection with CedPV, which had previously remained unexplored. The identification of 22 genes in CedPV-infected vs uninfected PaBr cells significant in all three transcriptomic analyses utilised here is of great interest, as subsequent experimental investigations into the functional role of these genes in bats could aid in the understanding of their significance during henipavirus infection (Figure 3.12(A-B)). Notably, several significant genes identified within our RNA-seq analysis were unannotated scaffolds and hence their role in the bat response to viral infection could not be determined here. Further exploration is therefore essential to generate a complete genomic annotation of *P.alecto* to allow for subsequent investigations into the functionality of these genes in bats. In summary, our RNA-seq data will provide valuable for future studies exploring the functional annotation of genes in the megabat species *P.alecto* and expectantly permit an improved understanding of the unique roles of bats as key viral reservoirs.

Chapter 4. paIFNλ-Induced Transcriptomes of Cells from the Megabat *Pteropus alecto*

4.1 Introduction

4.1.1 IFN-Induced Transcriptomic Analysis in Bats

Transcriptomic work in bats is continuing to advance, allowing the observations of global transcriptomic responses of bat cells to an array of viruses as described in section 3.1.2. However, Hölzer et al. (2019) have illuminated the fact that the full immune capacity of the viral response in bats remains indefinite because almost all previous studies in both megabat and microbat species utilised wild-type viruses for infection which are only weak inducers of the IFN response, with the exception of NDV (Glennon et al., 2015). Therefore, to avoid the issue of weak IFN induction by viral infection, the stimulation of bat cells directly with IFN could allow for a better understanding in the IFN response induced in bats.

There remain limited studies exploring the IFN-induced transcriptomic profile in bats and whether this may contribute to their roles in controlling viral replication. Previous transcriptomic analyses using IFN stimulation in bats are restricted to studies on the megabats *P.alecto* and *P.vampyrus* and the microbats *M.lucifugus* and *Myotis daubentonii* which explored IFN-stimulated expression profiles in bats (Hölzer et al., 2019, La Cruz-Rivera et al., 2018, Zhang et al., 2017, Shaw et al., 2017). These studies investigated the bat transcriptome apparent upon type I IFN induction by IFNα and notably, with the exception of Zhang et al. (2017) who used a bat-derived IFNα3, the stimulation of bat cells for transcript analysis was undertaken using universal or pan-species IFNα. Overall, transcriptomic studies in bats remain restricted to certain species and the IFN-induced transcriptomes of bat are either underrepresented due to the weak induction of the IFN response by wild-type virus infection, or alternatively, the stimulation of bat cells directly with IFN are restricted to type I IFNs (IFNα) and commonly use universal IFNs that are not unique to bats.

4.1.2 Type III IFNs in *P.alecto*

Similar to type I IFNs, type III IFNs share a similar production and use the same signalling pathways, which result in the induction of ISGs with key antiviral roles in combatting infection from viral pathogens (Ank and Paludan, 2009, Ank et al., 2006, Uzé and Monneron, 2007). It remains unknown why two IFN systems have evolved with similar antiviral activities, but they are known to possess some differences making them distinct from one another, such as their receptor expression patterns whereby type III IFN receptors are predominantly expressed in epithelial cells, compared to the widespread expression of the type I IFN receptor (IFNAR) (Sommereyns et al., 2008). The epithelial expression of the type III IFN receptor (IFNLR) is theorised to provide a more specialised role in the immediate immune response to viral infection, due to their presence within the tissues that correspond to sites of viral entry (Kotenko et al., 2003, Sheppard et al., 2003, Ank and Paludan, 2009, Sommereyns et al., 2008). Both type I and type III IFNs are often expressed simultaneously, however recent research suggests potential alternative mechanisms may influence their regulation and result in differential expression of both IFN types (Ank et al., 2006, Uzé and Monneron, 2007). Further research is required to uncover if type III IFNs possess functions not shared with type I IFN and to expose their full antiviral gene repertoire.

Type III IFN has been previously reported in bats via *in silico* analysis in the microbat genome (Fox et al., 2009), which was followed by the successful functional characterisation of IFNλ in *P.alecto* (Zhou et al., 2011b). Research has identified two IFNλ genes in *P.alecto*, designated IFNλ1 and IFNλ2, whilst also providing confirmation that *P.alecto* IFNλ genes possess antiviral activity via induction of ISGs, demonstrating the important role of type III IFNs in the early innate immune response to viral infection in bats (Zhou et al., 2011b). Despite previous evidence confirming the presence and functional capacity of type III IFNs in *P.alecto*, there currently

remains limited studies on transcriptomics in bats, with no studies previously undertaken to investigate the global transcriptional cell responses to type III IFN stimulation in bats at the time of writing this thesis (Zhou et al., 2011b). Therefore, we have chosen to undertake this study and fill in the gaps of type III IFN-induced transcriptomes in *P.alecto* to gain a better understanding of the immune gene repertoire and transcript dynamics involved in their IFN response (Figure 4.1). Furthermore, we have stimulated PaBr cells with IFNλ from *P.alecto* (paIFNλ), generated as described in section 2.3, in hopes of providing a more biologically relevant outlook on IFN-induced genes in this bat species, as opposed to using universal IFNs. The characterisation of the IFNλ-induced transcriptome in *P.alecto* could provide essential framework for understanding the nature of type III IFN responses in bats, which could shed light into potential mechanisms utilised by bats to host viruses without exhibiting clinical signs of illness.

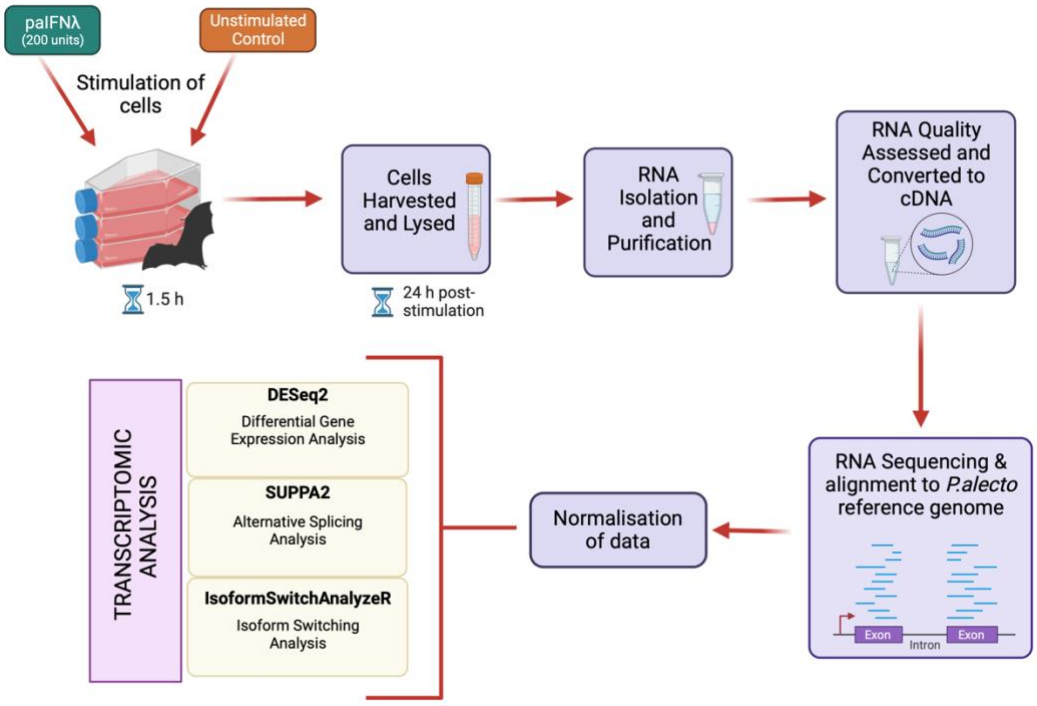

Figure 4.1 - Flow diagram showing the process of our transcriptomic study. *PaBr cells were stimulated with 200 units of paIFNλ or left unstimulated. At 24hrs post-stimulation, cells were harvested and lysed, and total RNA was isolated. Purified RNA was quality assessed and converted to cDNA before processing for RNA-sequencing. RNA-seq results were used for transcriptomics analysis. Pre-processing of data and differential gene expression (DEG) analysis was carried out in DESeq2, alternative splicing analysis was completed using SUPPA2 and analysis of isoform switching events used IsoformSwitchAnalyzeR. Figure created with Biorender.com.*

4.2 Results

4.2.1 Pre-processing of RNA-seq data

Total RNA was extracted from PaBr cells that were stimulated with paIFNλ or mock-treated, from three biological replicates and used for comparative RNA-seq analysis. Before investigations into transcript expression and abundance in stimulated PaBr cells can take place, we first had to normalise the dataset to ensure there was no variance or bias to our results. This was first achieved by generating transformed counts per gene (Figure 4.2A) which were subsequently used for normalisation of counts (Figure 4.2B) via DESeq2 software.

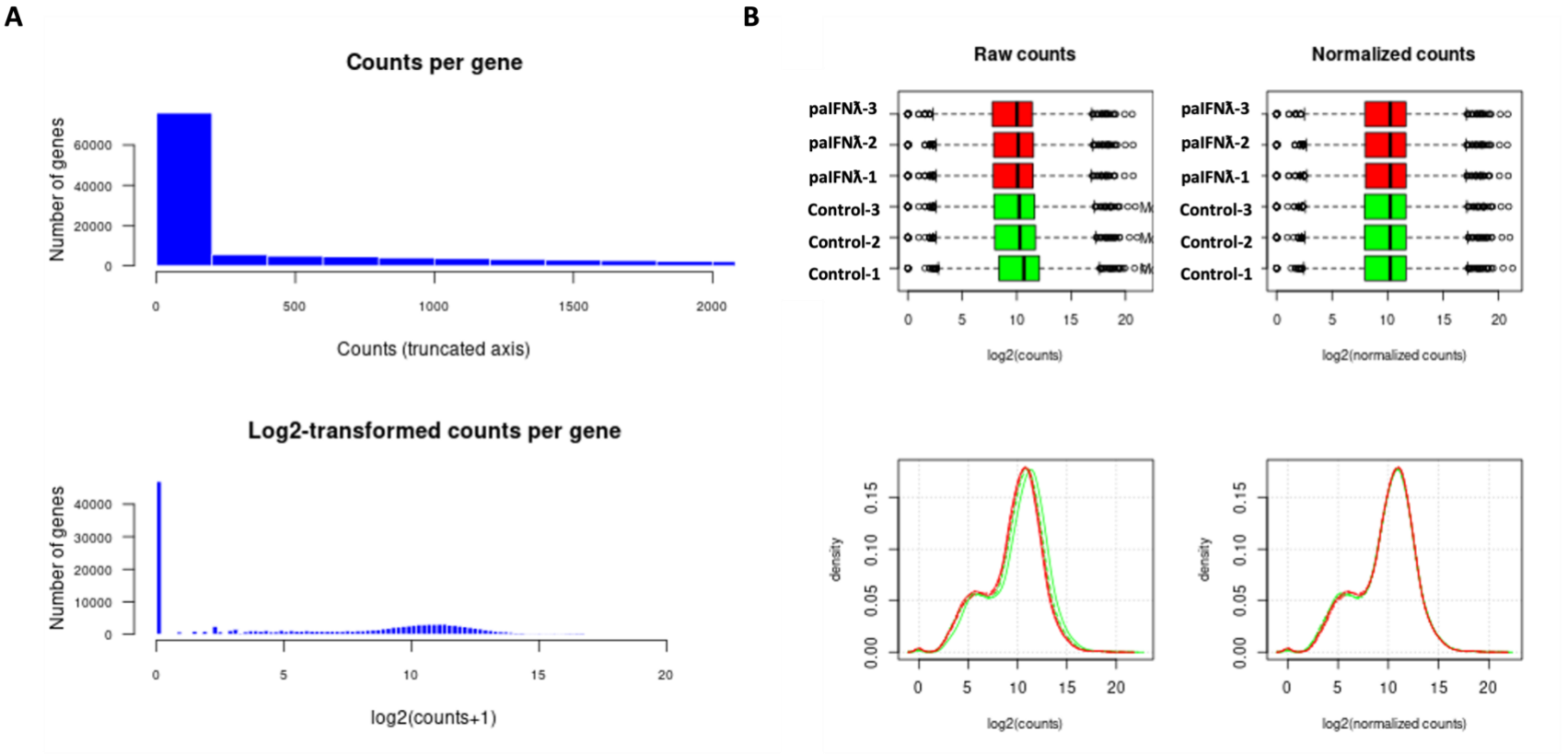

Figure 4.2 - Pre-processing of transcriptomic RNA-seq data for analysis. (A) *Raw read counts per gene and generation of log2(counts+1) transformed counts per gene.* ***(B)*** *Normalisation of the transformed counts (log2) from raw RNA-seq data represented by box plots and plotted against density.*

To determine the degree of variation in our RNA-seq data, a dispersion estimation plot was generated using DESeq2 (Figure 4.3). Dispersion is a measure of variability in the dataset, whereby dispersion estimates reflect variance in gene expression for a given mean count value. Data from our experiment fits the dispersion plot, whereby gene dispersion estimates are generally spread around the curve and dispersion decreases as mean expression levels of normalised counts increase.

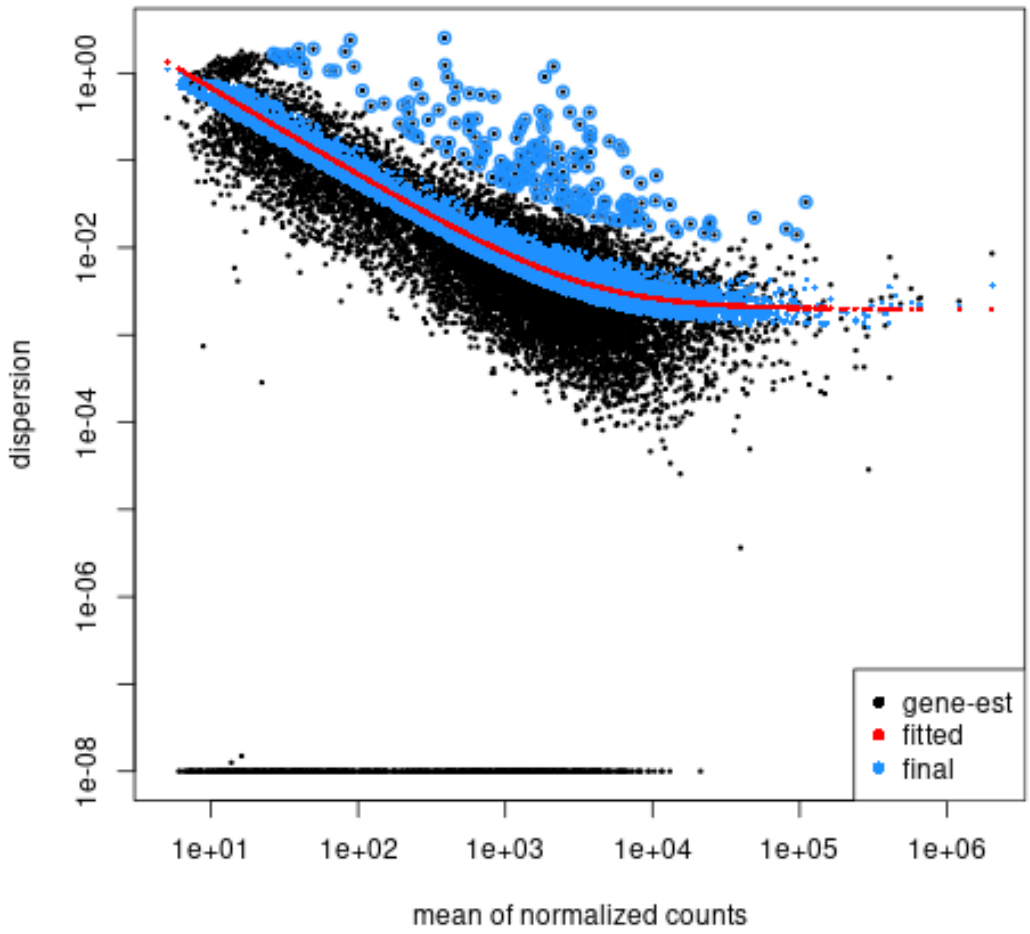

Figure 4.3 - Dispersion estimation plot generated in DESeq2 showing the final estimates shrunk from the gene-wise estimates towards the fitted estimates. *Estimated gene dispersions are represented by black dots, the fitted dispersion estimate curve is in red and the adjusted gene dispersions shrunk towards the curve are represented by blue dots. Black dots with blue circles around them are genes estimates with high dispersion values that have not been shrunk towards the curve.*

Lastly, to further confirm the overall variability within the normalised sample counts and to determine if biological replicates clustered together, we performed principal component analysis (PCA) (Figure 4.4). The triplicate biological replicates of the transcriptomes of unstimulated and paIFNλ-stimulated PaBr cells were analysed.

PCA results show a general clustering of unstimulated samples but a wider distribution and thus variation in the paIFNλ-stimulated replicates along both the PC1 and PC2. A higher variance was observed (PC1 with 59%) in the paIFNλ-stimulated biological replicates and their distribution was highly varied. These PCA results somewhat align with the expected clustering of unstimulated samples which display only slight variation, however the large variation observed for the paIFNλ-stimulated transcriptomes indicates significant variation between samples investigated here and should be taken into consideration when interpreting transcriptomic results.

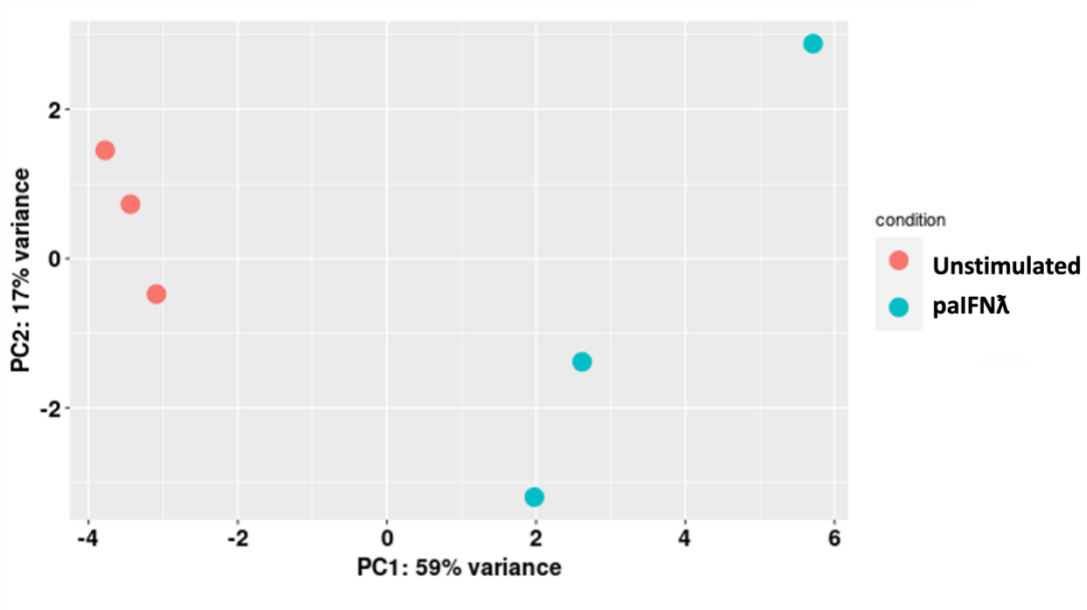

Figure 4.4 - Principal component analyses (PCA) for unstimulated and paIFNλ stimulated cells performed using DESeq2 normalised RNA-seq data. *X-axis represents PC1 at 59% variance, with the Y-axis representing PC2 at 17% variance. Infection was carried out in biological triplicates for each treatment. Unstimulated cells are represented by red dots and cells stimulated with paIFNλ are represented by blue dots.*

4.2.2 Differential Gene Expression Analysis

Differential gene expression analysis was carried out using the normalised RNA-seq data from paIFNλ-stimulated and unstimulated PaBr cells in triplicate (Figure 4.5A). RNA-seq analysis identified a total of 23,474 total genes, 14,082 genes remained after expression-based filtering and 1,249 significant DEGs were identified (623 up-regulated and 626 down-regulated). Significant DEGs were confirmed as genes with an adjusted p value of <0.05 and absolute log2 fold change >1.

The up and down-regulation of DEGs was further explored via the use of a volcano plot with a threshold of -log10(adjusted p-value) plotted against log2 fold-change (Figure 4.5B). The most significant DEGs at the p and log_2 FC values are represented by red dots, DEGs significant at log_2 FC only, are represented by green dots and non-significant DEGs in grey. DEGs located on the left-hand side of the volcano plot were downregulated upon paIFNλ stimulation, and those located on the right-hand side of the plot are upregulated. Noteworthy DEGs located at the top of the volcano plot represent the most significant and possess the highest log10 p-value. Although there were no labelled immune genes that were significantly upregulated with p-value and log2FC significance which are of interest for our studies, there are still genes within this bracket that haven't been labelled by name on the volcano plot. Additionally, significantly downregulated genes of interest include MATN3, TIMP3 and CALD1. Further genes labelled on the volcano plot displaying significance at log2 FC value only, include IFI6 (Log2 FC of 1.19) and IFIT3 (Log2 FC of 1.63) which were slightly upregulated. All other labelled genes of interest here (Mx1, CCL5, IFIT2, BTG1 and CXCL8) represented in grey were deemed non-significant in their differential expression during paIFNλ stimulation.

To observe the changes in gene expression in PaBr cells upon paIFNλ stimulation, a heatmap displaying the top 25 most variable genes between the two conditions in triplicate was generated (Figure 4.5C). The 25 most variable genes between the two

treatment types are represented here, whereby a deeper blue colour represents higher gene expression, and a lighter green shade indicates lower expression within each condition. Results show that genes such as HSPA1B,IFI6, NFKBIZ and ZFAND2A appeared slightly more highly expressed in the presence of paIFNλ compared to unstimulated conditions. Alternatively, some genes appeared to be expressed more in the unstimulated cells, such as PIP4K2A. Overall however, there were no stark contrasts in expression levels and thus evident variability observed between the unstimulated and paIFNλ-stimulated PaBr cells. Additionally for this study, it appears the biological repeats also differ in their values for some genes, whereby their expression under that condition may not be significant and hence strong conclusions on gene relevance under stimulation cannot be made from this dataset alone.

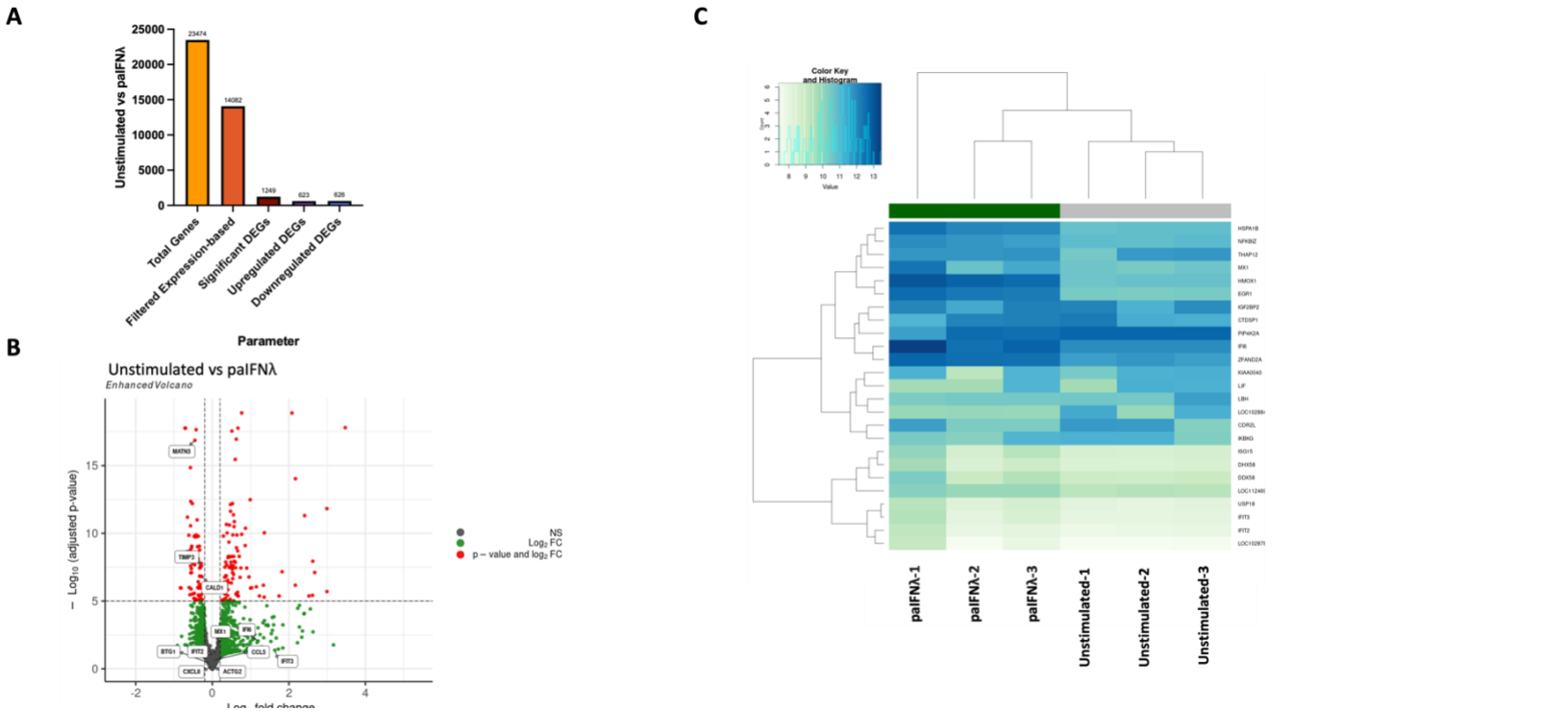

Figure 4.5 - Analysis of differentially expressed genes between unstimulated and paIFNλ-stimulated PaBr cells (A) *Bar chart representing the filtering process of total genes to identify significant differentially expressed genes (DEGs) between unstimulated vs paIFNλ- stimulated cells. Significance was calculated as genes with an adjusted p-value of <0.05 and absolute log2 fold change >1 to identify 69 significant DEGs (69 up-regulated, 0 down-regulated).* ***(B)*** *Volcano plot showing differentially expressed genes in unstimulated vs paIFNλ- stimulated PaBr cells. Y-axis denotes –log10 P values, whilst X-axis shows log2 fold change values. Red dots represent significant differentially expressed genes at both p-value and log2 FC, green dots show genes with significance at log2FC only and grey dots represent non-significant DEGs. The most upregulated genes between unstimulated vs paIFNλ- stimulated cell are represented on the right-hand side of the plot, with downregulated genes on the left-hand side. Differentially expressed genes that display the highest statistical significance are located at the top of the plot where their gene names are annotated.* ***(C)*** *Heatmap showing the top 25 most variable genes between unstimulated and paIFNλ- stimulated cells. Heatmap was generated using log2 expression of counts normalized to transcript size and million mapped reads (FPMK values). Y-axis denotes the gene name of interest, while X-axis represents the treatment type delivered in triplicate to the PaBr cells. Expression values are represented by the colour key and histogram, whereby a deeper blue colour indicates higher expression and lighter green representing lower expression.*

Functional enrichment analysis of DEGs in paIFNλ-treated and unstimulated PaBr cells was undertaken to observe the major cellular components (CC), molecular functions (MF) and biological processes (BP) that these DEGs belong to and partake in. CC analysis revealed that based on their p-adjust values, the most significant cellular components concerning differential gene expression in treated vs untreated cells were largely located in the protein-containing complex, as represented by a deep blue colour on the gene ontology plot (Figure 4.6A). DEGs concerning membrane location were also highlighted as significant in CC ontology analysis whereby the membrane, integral component of membrane and intrinsic component of membrane all also showed a high p-value as demonstrated by a purple colour on the plot. Higher gene counts were represented in other components such as the nucleus and membrane bound/intracellular organelles, but with a low significance value. MF analysis revealed only a select few molecular functions concerned with DEGs in unstimulated vs paIFNλ-stimulated PaBr cells. The most significant functions were involving transcription (transcription regulator activity and DNA-binding transcription factor activity) which both displayed a high p-adjust value as represented by a deep blue colour (Figure 4.6B). It is worth noting however, that the counts for the most significant functions here are low at less than 2 genes each. Other molecular functions identified during paIFNλ stimulation included nucleic acid and DNA binding, alongside catalytic activity at lower significance values. Lastly, functional enrichment analysis into the biological processes in which DEGs partake in, highlighted several processes such as transcription, gene expression and biosynthetic processes to all possess the same p-adjust value of significance and all had a gene count of 2 (Figure 4.6C).

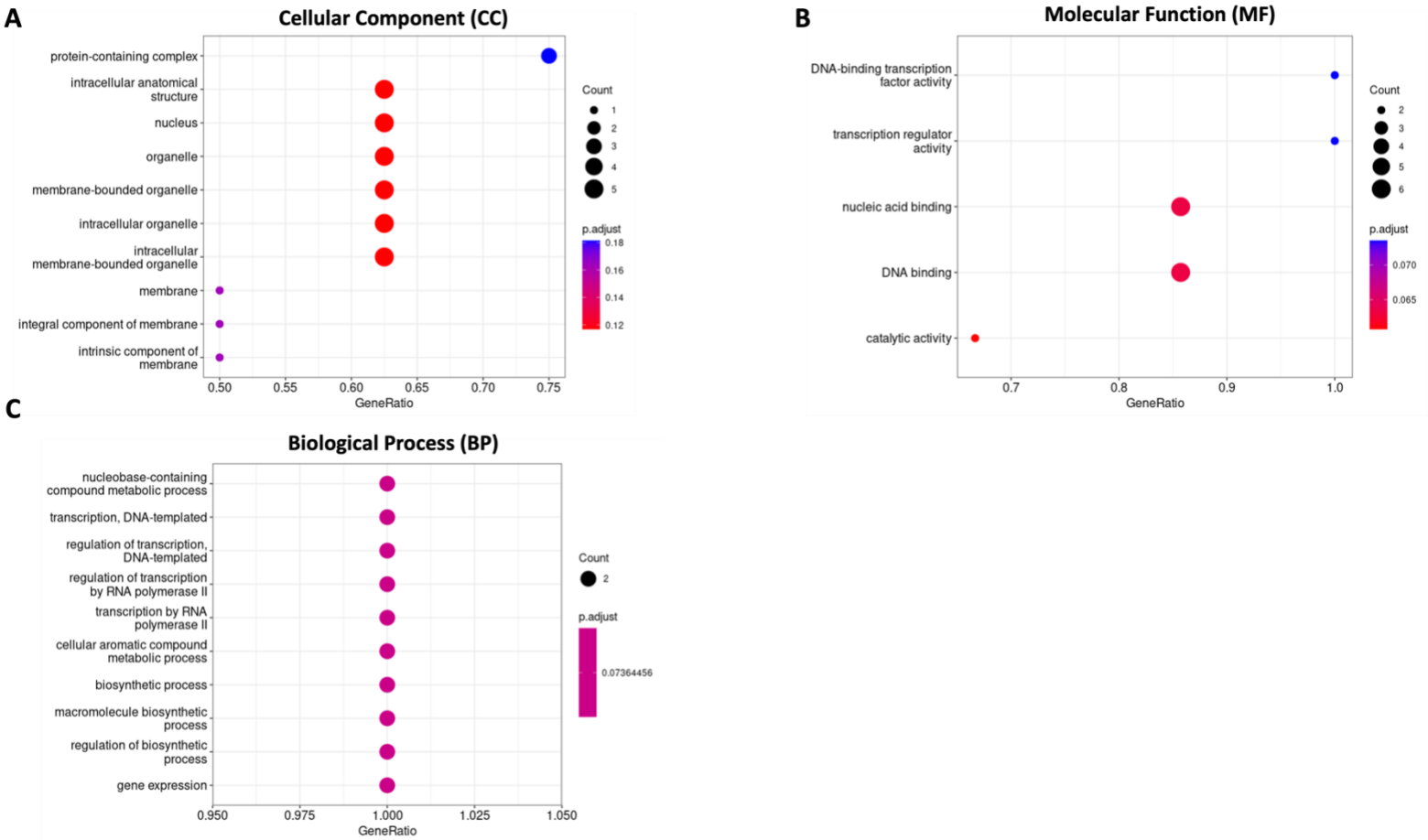

Figure 4.6 - Gene ontology analysis of significant DEGs in unstimulated vs paIFNλ-stimulated PaBr cells. (A-C) *Dot plots generated using gene ontology (GO) enrichment analysis to show the top ten most significant cellular components (CC), molecular functions (MF) and biological processes (BP) in significant DEGs between mock and paIFNλ stimulation. Counts are represented by circles whereby circle size represents the number of individual significant differentially expressed genes belonging to the category. Significance is represented by the colour intensity of the p-adjust value, whereby a deep blue represents the most significant and red the least significant. Gene ratio represents the number of genes from the total significant DEGs in each category.*

4.2.3 Alternative Splicing and Isoform Switching Analysis

As previously described in Chapter 3, alternative splicing encompasses the process by which combinations of different exons are joined together during or after transcription to produce more than one mRNA from a single gene, resulting in different proteins that vary in their sequence.

In paIFNλ-stimulated vs unstimulated PaBr cells, we observed 27,184 differential splicing events in 6,984 genes. Upon filtering of these genes to identify splicing events with a significance at an FDR value of ≤ 0.1, 338 genes were identified to produce 448 differential splicing events (Figure 4.7A). Differential splicing analysis was further observed via representation in a volcano plot (Figure 4.7B), whereby the magnitude of splicing change across the paIFNλ-treated and unstimulated conditions is evident. ΔPSI values plotted on the Y axis represent the difference of the mean percent spliced in (PSI) value between conditions. PSI value is defined as the ratio of the relative abundance of all isoforms containing a certain exon, over the relative abundance of all isoforms of the gene containing the exon. This ΔPSI value is plotted against the average transcript abundance on the X axis. Filtering here was based on FDR≤ 0.05 to identify splicing events at this significance value. Significant differential splicing events here are represented by blue dots and non-significant by grey dots on the volcano plot. Results show that at this significance value, there are only few significant splicing events, in comparison to non-significant. Gene ontology analysis was performed for the genes undergoing differential splicing events at the FDR value of ≤0.1 to identify the main processes implicated in differential spicing events in paIFNλ-stimulated PaBr cells. CC analysis revealed only four individual components that genes undergoing differential splicing belong to and based on their $\log_{10}$(FDR) value, the most significant cellular component was the ribonucleoprotein complex, with a value of 2.7 (Figure 4.7C). The remaining components were nuclear protein-containing complex, the ATPase complex and the SWI/SNF superfamily-type

complex but at lower significance values. The molecular functions containing the most significant genes concerning differential splicing consisted of mRNA metabolic processes, RNA processing, cellular amide metabolic processes and cell cycle processes, as represented in red on the lollipop plot with the highest -log10(FDR) value of 1.6 (Figure 4.7D). Cell cycle, organonitrogen compound and amide biosynthetic processes were also represented but at a lower -log10(FDR) significance value. Meiosis I cell cycle process was also identified in only a small number of genes. BP analysis only identified four processes that are implicated by differential splicing events in genes during paIFNλ-stimulation. The most significant genes identified to partake in differential splicing events were those involved in RNA binding, with the highest -log10(FDR) value of 4, and contained the highest number of genes, as shown in Figure 4.7E. Other processes included cupric reductase, ferric-chelate reductase (NADPH) and single-stranded DNA endodeoxyribonuclease activities but only displayed a low gene count and low significance value.

A

Parameter	Unstimulated control vs paIFNλ
Total Differential Splicing Events	27184
Total Number of Genes	6984
Significant Differential Splicing Events (FDR ≤0.1)	448
Number of Significant Genes (FDR ≤0.1)	338

B

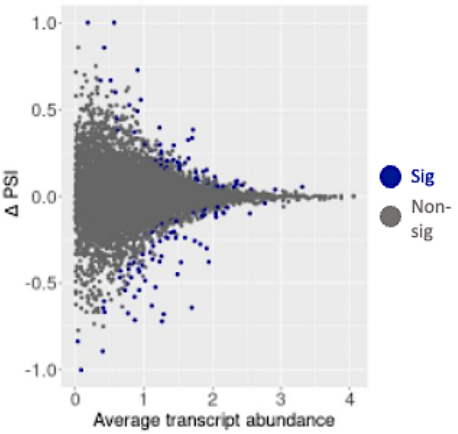

C

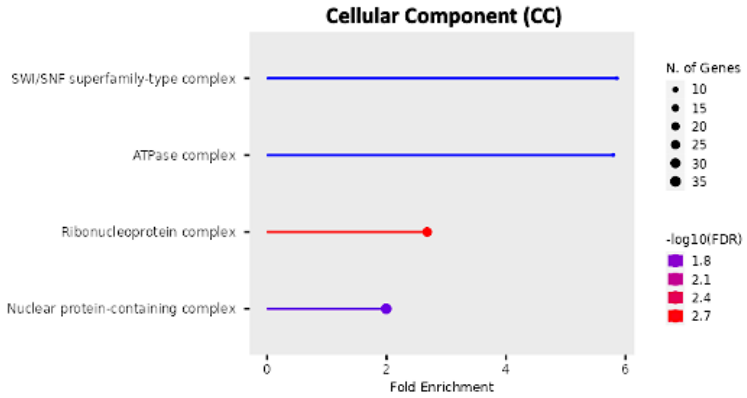

D

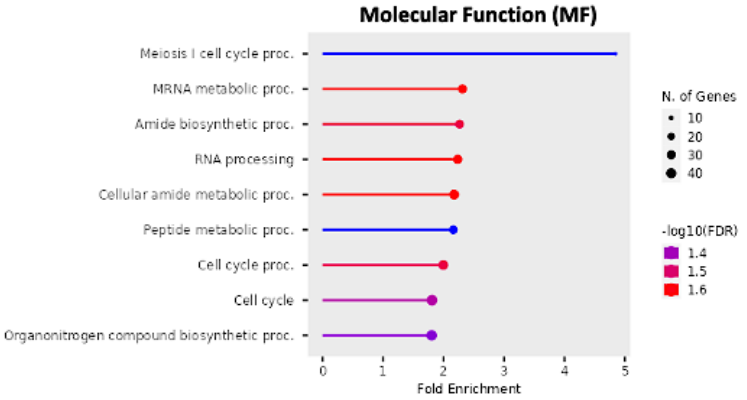

E

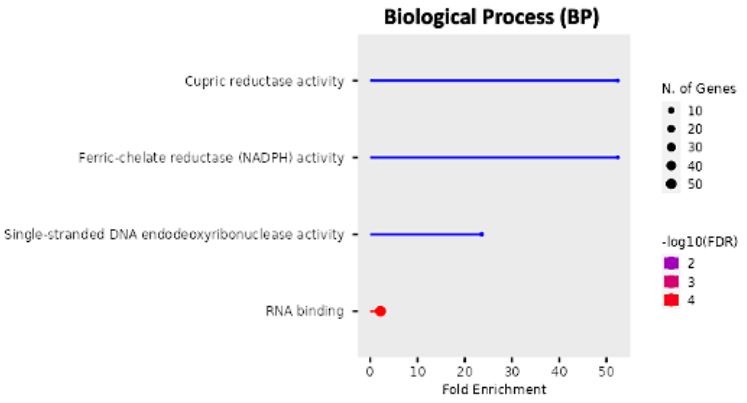

Figure 4.7 - Differential splicing analysis from RNA-seq data in unstimulated vs paIFNλ-stimulated PaBr cells. (A) *Table displaying the total number of splicing events and the number of genes they were possessed by. Filtering for significant splicing events at FDR ≤0.1 identified 448 splicing events in 338 genes.* ***(B)*** *Volcano plot to show the magnitude of splicing change for differential splicing events. The magnitude of splicing change (ΔPSI) was calculated across the two conditions of unstimulated or paIFNλ-stimulated PaBr cells in triplicate, as represented on the Y-axis as a function of the average transcript abundance represented on the x-axis in -log_{10}(TPM + 0.01) scale. The alternative splicing events were filtered based on FDR with a p value <0.05 according to SUPPA2 to identify the significant splicing events which are represented by a blue dot and grey dots represent non-significant differential splicing events.* ***(C-E)*** *Lollipop plots of the top ten significantly different cellular components (CC) and molecular functions (MF) and biological processes (BP) identified by Gene Ontology (GO) fold-enrichment analysis. Circle size represents the number of significant genes partaking in differential splicing belonging to that category and significance is represented by the colour intensity of the –log10(FDR) value, with red representing the most significant and blue the least.*

The process of alternative splicing results in the potential for multiple isoforms of a protein to arise from a single gene. Isoforms generated from a single gene vary in their amino acid sequence which can often influence their functionality. Using the RNA-seq data obtained from paIFNλ-stimulated and unstimulated PaBr cells, isoform filtering analysis was performed using the software IsoformSwitchAnalyzeR. A total of 38,154 genes were identified to give rise to 46,921 isoforms. Upon ISAR filtering, 34,411 genes remained that result in a final set of 18,964 isoforms (Figure 4.8A). Further isoform switching analysis identified 63 genes to undergo 87 switching events, resulting in 72 different isoforms. From these genes, 23 of them undergo 33 individual switching events to result in a final 27 isoforms, whereby isoform switching results in a functional consequence to the protein (Figure 4.8B). Alternative isoforms are a result of differential splicing events taking place and the final isoform encoded can differ in their signal peptides and protein domains which impacts its function. Investigation into the types of switching events taking place that influence isoform outcome was undertaken using consequence enrichment analysis. Results were filtered based on an FDR value of <0.05 and no significant ('true') results were observed here at this significance level (Figure 4.8C). However, it is evident that the switching events taking place in the largest number of genes here are exon skipping (ES) and gain of an alternative transcription start site (ATSS), as denoted by a larger circle representative of gene count. Other alternative splicing events were detected,

but ES and ATSS were the most prominent in the paIFNλ-stimulated vs unstimulated PaBr cells. These results are reflected in Figure 4.8D, when observing the degree of each type of alternative transcription event taking place separately, the most significant frequent changes in alternative splicing are ES and ATSS. The number of isoforms utilising ATSS was slightly higher in the isoform used more, whereas for isoforms produced by ES, these alternative splicing events were more prominent in the isoform used less. Other alternative splicing events appear to occur in genes during paIFNλ stimulation including A3, A5, ATTS, IR, MEE and MES but with a lower number of significant isoforms that ATSS and ES events.

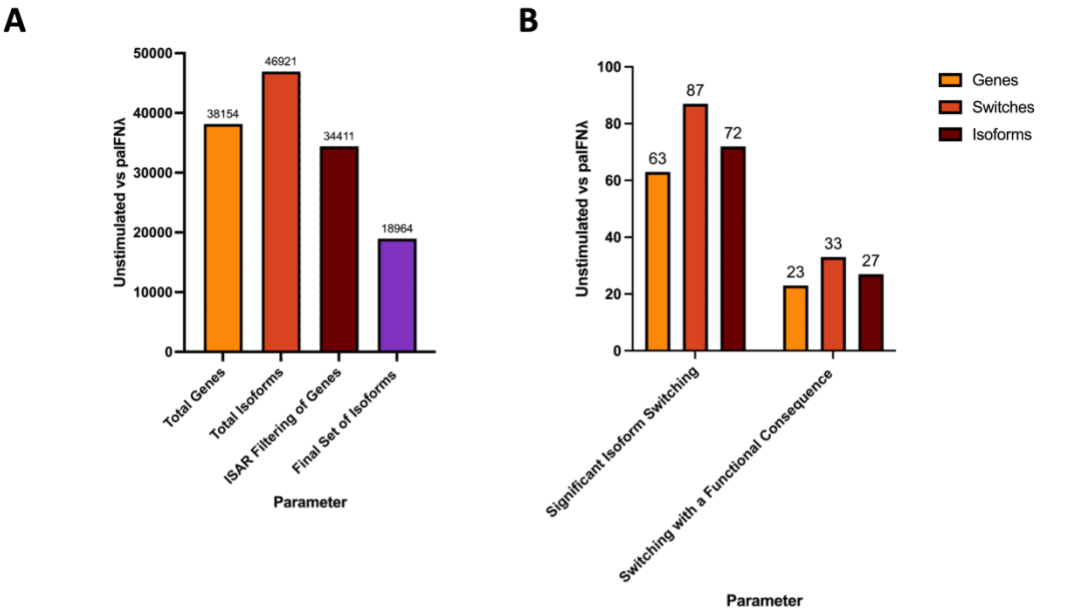
A
Unstimulated vs paIFNλ
50000
40000
30000
20000
10000
0
38154
46921
34411
18964
Total Genes
Total Isoforms
ISAR Filtering of Genes
Final Set of Isoforms
Parameter
B
Unstimulated vs paIFNλ
100
80
60
40
20
0
63
87
72
23
33
27
Genes
Switches
Isoforms
Significant Isoform Switching
Switching with a Functional Consequence
Parameter

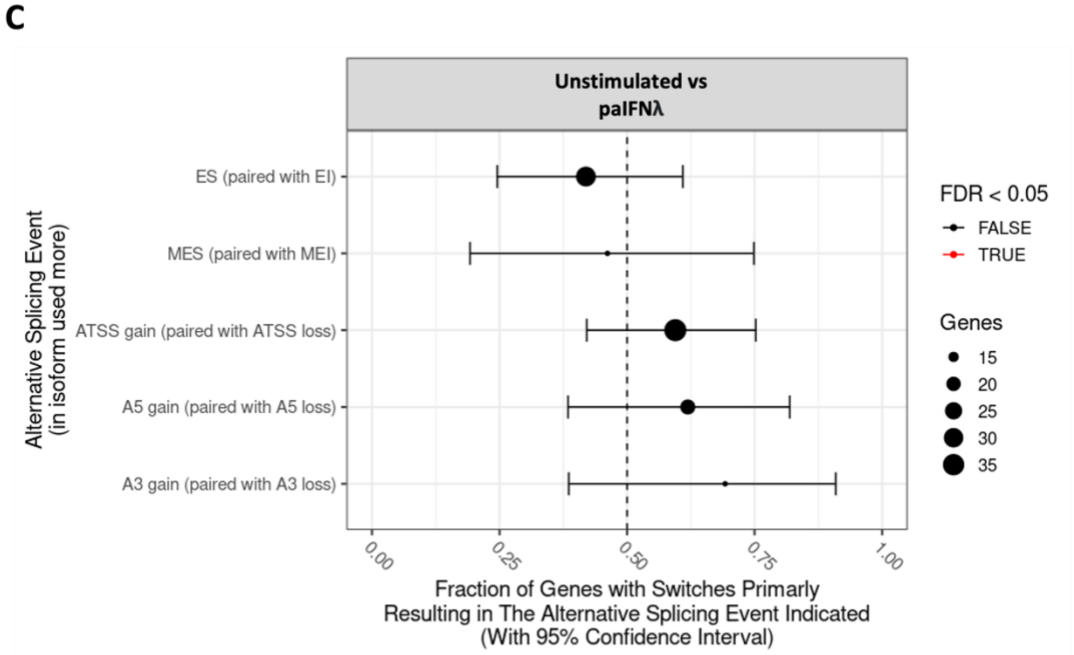
C
Unstimulated vs paIFNλ
ES (paired with EI)
MES (paired with MEI)
ATSS gain (paired with ATSS loss)
A5 gain (paired with A5 loss)
A3 gain (paired with A3 loss)
Alternative Splicing Event (in isoform used more)
0.00
0.25
0.50
0.75
1.00
Fraction of Genes with Switches Primarly Resulting in The Alternative Splicing Event Indicated (With 95% Confidence Interval)
FDR < 0.05
FALSE
TRUE
Genes
15
20
25
30
35

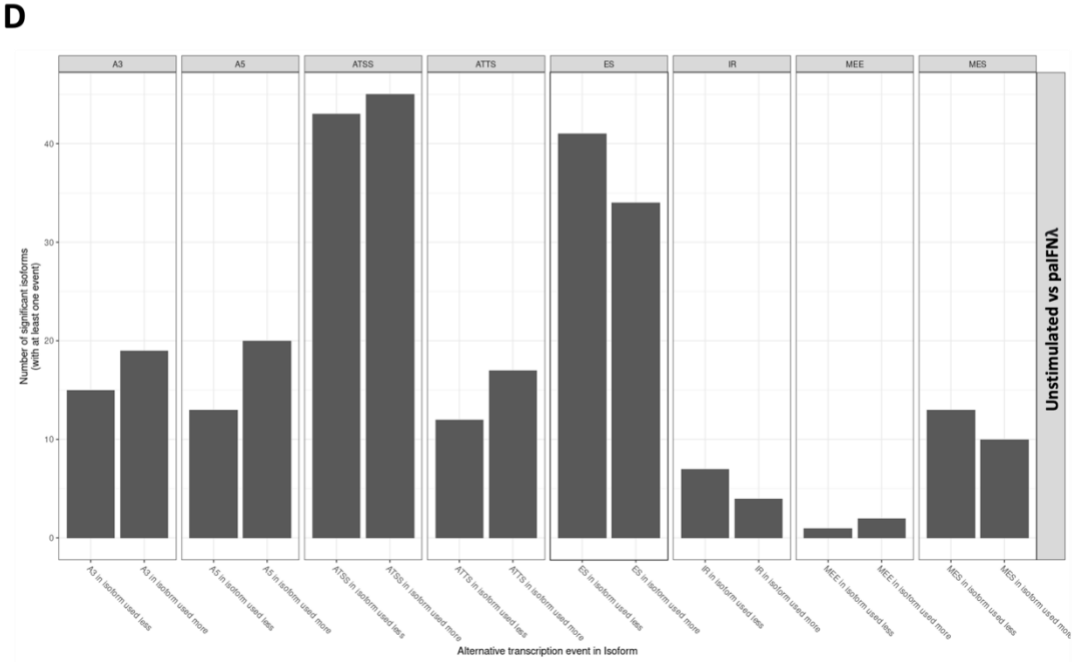
D
A3
A5
ATSS
ATTS
ES
IR
MEE
MES
Number of significant isoforms (with at least one event)
Unstimulated vs paIFNλ
Alternative transcription event in Isoform

***Figure 4.8 - Isoform switching analyses in unstimulated vs paIFNλ-stimulated PaBr cells**. **(A)** Bar chart to show the filtering process of total genes to identify significant isoforms between unstimulated vs paIFNλ-stimulated cells. **(B)** Bar chart illustrating the measure of genes, switches and isoforms involved in significant isoform switching events and significant isoform switching events with a functional consequence.**(C)** Enrichment of specific splice events for each set of opposing events (e.g. A5 gain vs loss) as determined by analyzing the fraction of events associated with each type of consequence. The X axis represents the fraction of genes showing enrichment of a specific alternative spicing event upon paIFNλ stimulation, whereby a value of 0.5 corresponds with no systematic change occurring, represented by the dotted line through the centre of the plot. Y axis denotes the alternative splicing event that has taken place in the most used isoform of that gene. Circle size represents the number of genes for each splicing event and true significance of splicing is represented in red, determined to have an FDR value of <0.05. None of the alternative splicing events for paIFNλ stimulation were deemed significant at this value.(**D)** Global splicing analysis to observe alternative splicing events in different isoforms. Splicing events presented here are A3 (alternative 3' splice-site), A5 (alternative 5' splice-site), ATSS (alternative transcription start site), ATTS (alternative transcription termination site), ES (exon skipping), IR (intron retention), MEE (mutually exclusive exons) and MES (multiple exon skipping).*

The 23 genes which undergo alternative splicing resulting in isoform switching with a functional consequence are of specific interest when investigating isoform usage in the presence and absence of paIFNλ stimulation of PaBr cells, as these genes may prove integral to the cellular response occurring under stimulation in bat cells. Figure 4.9 represents the top four most significant genes out of the total 23 which result in isoform switching with a functional consequence. TCF4, also known as transcription factor 4, was the most significant gene to undergo significant isoform switching with functional consequence during unstimulated vs paIFNλ stimulation (Figure 4.9A). This gene has roles in binding immunoglobin enhancers and is involved in the initiation of neuronal differentiation. There are 10 isoforms expressed from this single gene, however only one of them (XM_015590844) appears significant in its differential expression. This isoform is expressed more highly in unstimulated cells and is seemingly not expressed at all during paIFNλ treatment. For this gene, the overall gene expression in the presence of paIFNλ appears slightly less than in the unstimulated cells. Figure 4.9B represents isoforms in the CEP57L1 gene, known as centrasomal protein 57-like 1, which plays roles in enabling identical protein binding and microtubule attachment to centrosomes. Five isoforms are present from this gene, but only two of these are significant in their usage. Isoform XM_015600126 displays the highest significance, whereby its expression is utilised substantially more

in the absence of paIFNλ stimulation and is contrastingly not used at all in its presence. The other significant isoform XM_025042384 displays opposite expression patterns and is increasingly used during paIFNλ treatment than in unstimulated conditions and upon observation of the protein domains involved in this isoform, this is the only isoform that appears to lack an IDR (intrinsically disordered region), which may underlie its preferred usage during paIFNλ treatment. SSBP4 (single-stranded DNA binding protein 4) represents the third most significant gene to undergo isoform switching with a functional consequence which has roles in single stranded DNA binding and the regulation of transcription by RNA polymerase II (Figure 4.9C). Out of the four isoforms present in this gene, only the isoform XM_015587204 is significant in its usage and displays an increased use during paIFNλ treatment in comparison to not being used at all during unstimulated conditions. This isoform is the only isoform out of the four from this gene to possess an addition SSDP (single stranded DNA binding protein) domain. Lastly, TCEANC also known as transcription elongation factor A N-terminal and central domain containing protein possesses five isoforms and only one significant isoform (XM_015589153) is preferred during paIFNλ stimulation, which is absent in unstimulated conditions (Figure 4.9D).

A

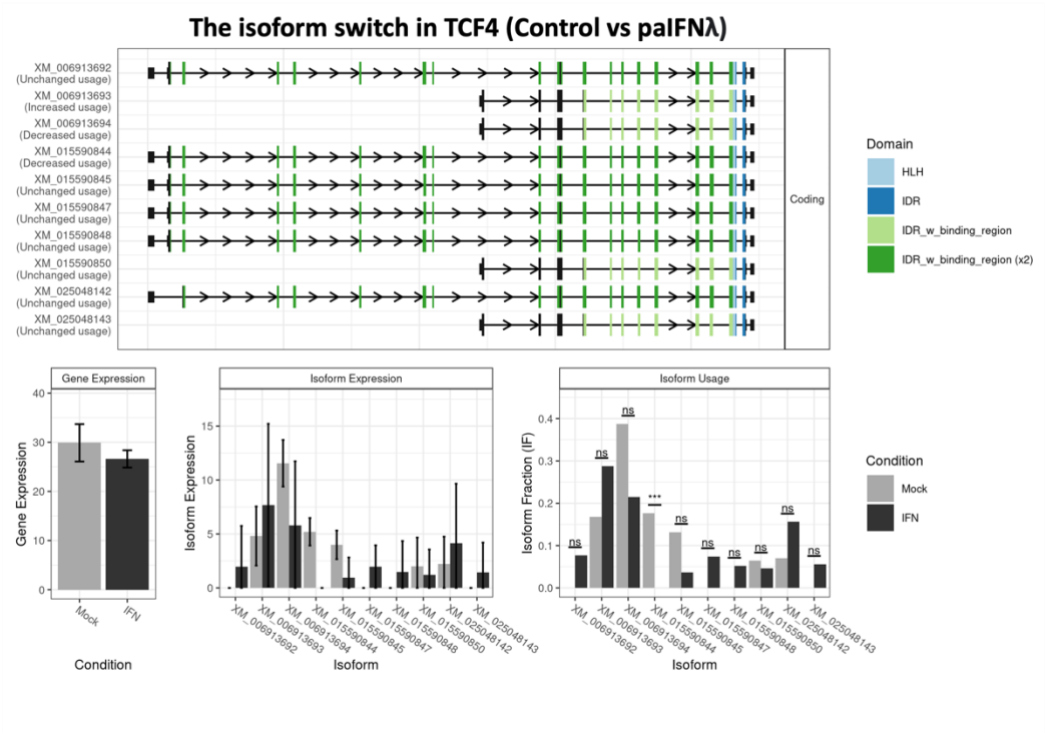
The isoform switch in TCF4 (Control vs paIFNλ)
XM_006913692 (Unchanged usage)
XM_006913693 (Increased usage)
XM_006913694 (Decreased usage)
XM_015590844 (Decreased usage)
XM_015590845 (Unchanged usage)
XM_015590847 (Unchanged usage)
XM_015590848 (Unchanged usage)
XM_015590850 (Unchanged usage)
XM_025048142 (Unchanged usage)
XM_025048143 (Unchanged usage)
Coding
Domain
HLH
IDR
IDR_w_binding_region
IDR_w_binding_region (x2)
Gene Expression
Isoform Expression
Isoform Usage
Isoform Fraction (IF)
Condition
Mock
IFN
Isoform

B

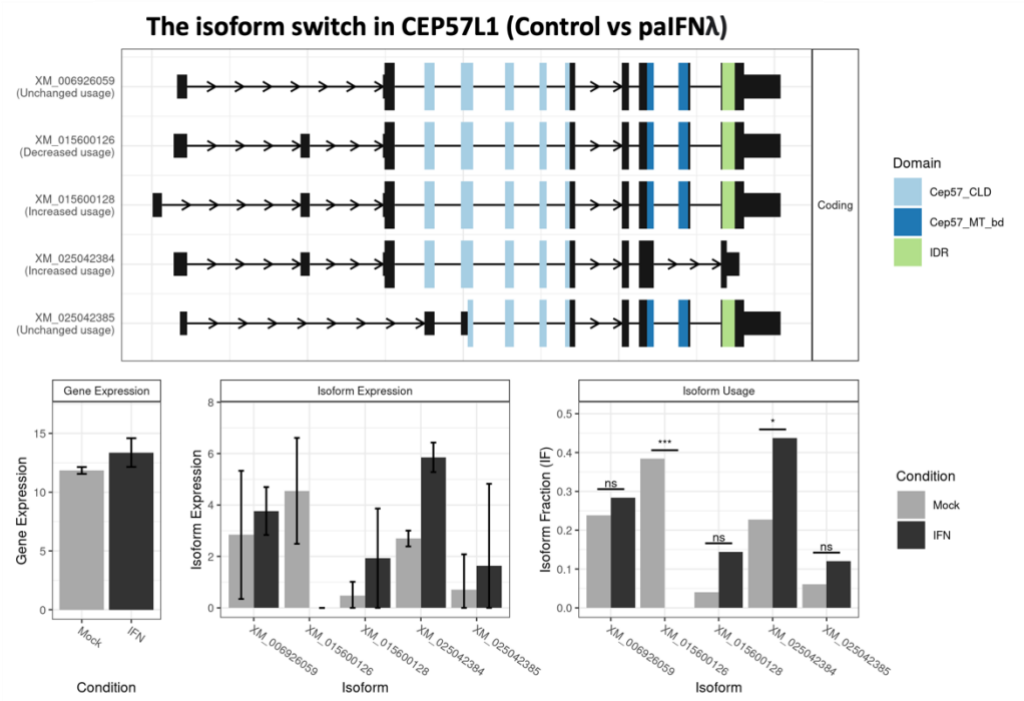
The isoform switch in CEP57L1 (Control vs paIFNλ)
XM_006926059 (Unchanged usage)
XM_015600126 (Decreased usage)
XM_015600128 (Increased usage)
XM_025042384 (Increased usage)
XM_025042385 (Unchanged usage)
Coding
Domain
Cep57_CLD
Cep57_MT_bd
IDR
Gene Expression
Isoform Expression
Isoform Usage
Isoform Fraction (IF)
Condition
Mock
IFN
Isoform

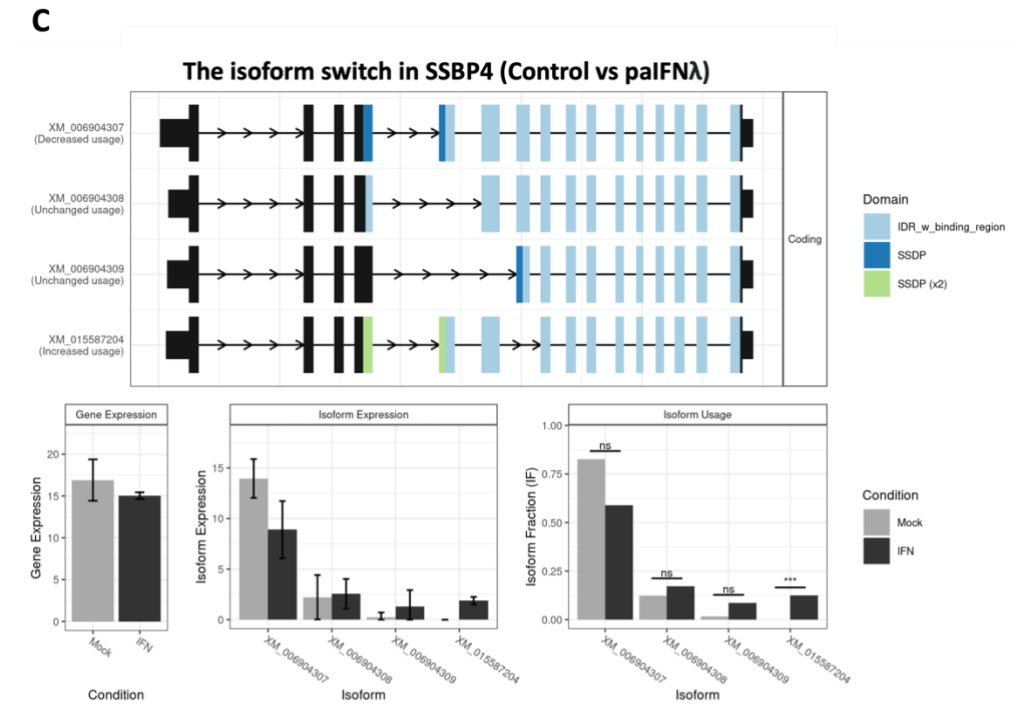

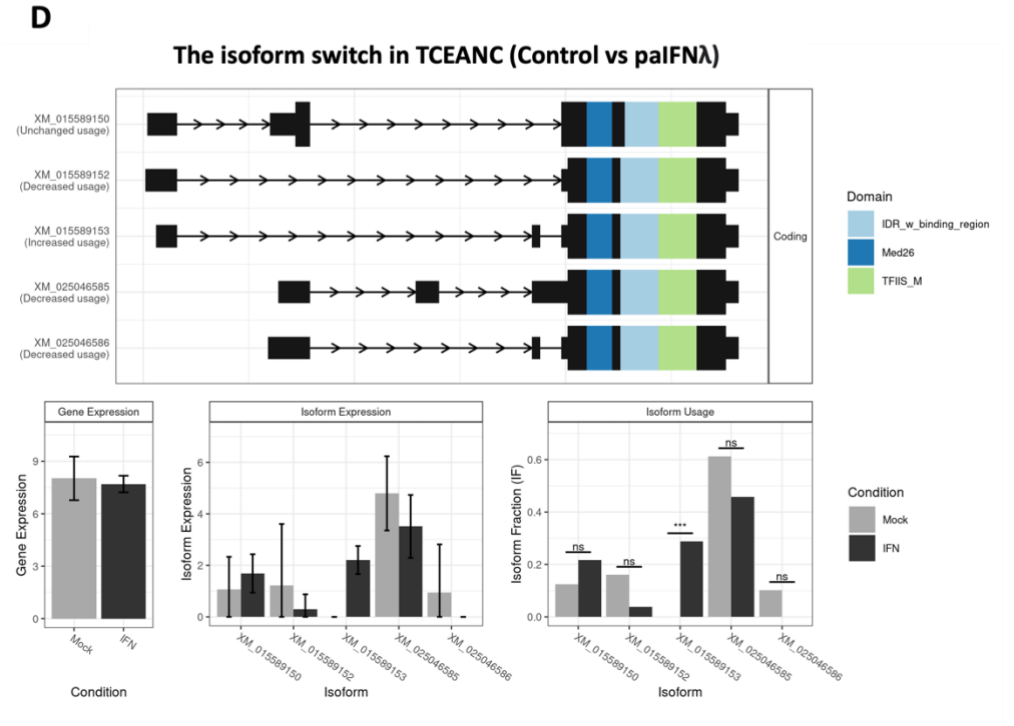

Figure 4.9 - Isoform switching events in genes that undergo switching with functional consequence in unstimulated control vs paIFNλ-stimulated PaBr cells. *The top four genes which undergo isoform switching events with a functional consequence were selected* ***(A)*** *TCF4,* ***(B)*** *CEP57L1,* ***(C)*** *SSBP4 and* ***(D)*** *TCEANC.*

Some genes only undergo one type of alternative splicing to result in different isoforms, however, others can also partake in more than one splicing event during isoform switching. Figure 4.10 shows the number of genes partaking in aTSS, aTTS and all other alternative splicing events (AS). Results show that 2 genes during paIFNλ stimulation of PaBr cells undergo all three aTTS, aTSS and AS events.

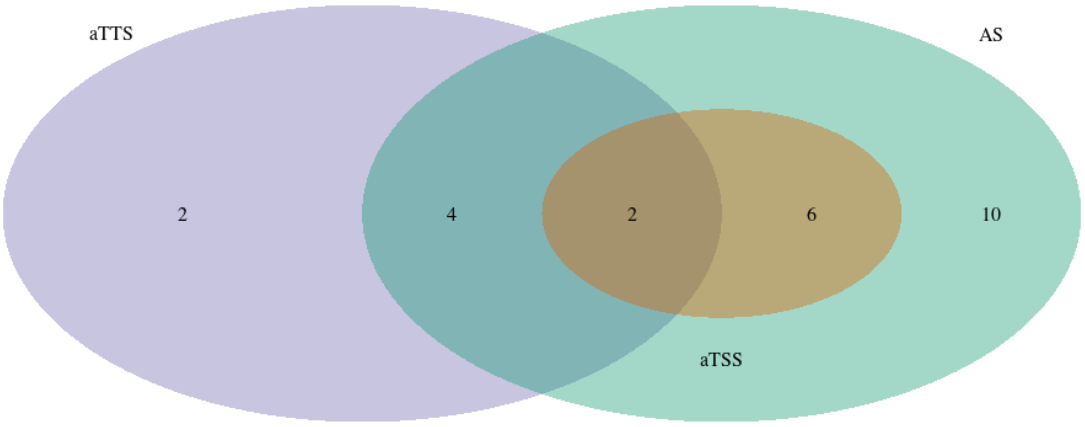

Figure 4.10 - Venn diagram representing gene counts undergoing discrete alternative splicing events that result in isoform switching. *Counts of genes which undergo alternative splicing to express different isoforms are categorised here into aTSS (alternative transcription start site), aTTS (alternative transcription termination site) and AS (representative of all other methods of alternative splicing).*

4.3 Discussion

Previous research exploring the transcriptomic response in bats upon IFN stimulation remains limited and largely restricted to investigations of the type I IFN response. In addition to type I IFNs, type III IFNs, which also partake in the innate immune response to viral infection have also been successfully identified in bats, yet the transcriptome of bat cells stimulated with type III IFN remains uncharacterised. Therefore, we aimed to observe the gene repertoire induced by type III IFN in bats by stimulating PaBr cells from the model species *P.alecto* with paIFNλ, a type III IFN isolated from *P.alecto* itself. Transcriptomic analysis allows for the investigation of all RNA species in a host under different conditions and subsequently permits a direct comparison of responses between the two conditions. By comparing the variation in the expression and usage of RNA species in PaBr cells under mock conditions with those stimulated with paIFNλ, we aim to gain a valuable insight into the transcriptomic response mounted in bats and how it may differ during the presence and absence of type III IFN stimulation.

Notably for this study, during normalisation of RNA-seq results obtained from unstimulated vs paIFNλ-stimulated PaBr cells, the PCA analysis identified a large variation in the paIFNλ stimulated cells (Figure 4.4). Although variation in PCA value is expected in biological replicates of a treatment group, this wide distribution may influence the results obtained and hence should be considered when interpreting results. Accordingly, unlike in the previous chapter whereby CedPV infection of PaBr cells was compared with uninfected cells and the PCA values for uninfected conditions clustered closely together (Figure 3.4), during this transcriptomic study, the unstimulated samples appeared slightly more widely distributed, yet still exhibited some clustering.

Dispersion estimates were also generated for our dataset using DESeq2 software for data normalisation. These estimates are inversely related to the mean and directly

related to variance. Based on this, for large mean counts dispersion is lower and for small read counts it is higher and dispersion estimates for genes with the same mean will only differ based on their variance (Anders and Huber, 2012). For each gene, an initial dispersion was generated using maximum likelihood estimation, which was plotted in function of the mean expression level (mean of normalised counts of replicates), where each gene is represented by a black dot. A curve was then fitted to these gene-wise dispersion estimates (as represented by a red line on plot), which represent the estimate for the expected dispersion value for genes of a given expression level. This is beneficial in showing that individual genes possess different levels of variability, but overall, there will be a distribution of acceptable dispersion estimates. To obtain final dispersion estimates, the initial gene-wise dispersion estimates were shrunk towards the fitted curve. The adjusted dispersion values are represented by blue dots in the dispersion plot. Shrinkage of dispersion estimates is important in reducing the risk of false positives in subsequent differential expression analysis. Adjustment of dispersion value results in an increase for some genes, which limits the potential for false positives that could appear from an underestimated dispersion. Furthermore, dispersion estimates that sit slightly above the plotted curve are also shrunk towards it. However, it is also important that dispersion estimates that have very high values are not shrunk towards the curve here, as this could result in false positives (Love et al., 2014). These genes are represented by blue circling on the dispersion plot. Our experimental data fits the dispersion plot, whereby gene dispersion estimates are generally spread around the curve and dispersion decreases as mean expression levels of normalised counts increases.

Following the normalisation of RNA-seq data, we were able to use this dataset to investigate the differential gene expression observed between unstimulated and paIFNλ-stimulated PaBr cells. DEG analysis is a useful technique in determining the level of gene expression in two or more conditions. Our results identified a set of

1,249 DEGs in unstimulated vs paIFNλ stimulated PaBr cells which exhibited an almost equal distribution of up and downregulation. The total significant DEGs identified here are much lower in comparison to those identified in the transcriptomic study of CedPV infection in the previous chapter (3.004). The reduced volume of DEGs identified during paIFNλ treatment is potentially due to the role of paIFNλ as a type III IFN, which is a slower acting stimulant of the interferon response than type I IFNs. Therefore, despite generally inducing a similar set of ISGs, type I IFN signalling activates a faster and stronger ISG response in addition to the induction of pro-inflammatory cytokines. Accordingly, during CedPV infection assessed in Chapter 3, the immediate type I response coupled with the type III IFN response are likely both being stimulated, resulting in a more heightened observable transcript induction than observed here for type III IFN only. When DEG expression is conveyed via volcano plot, the distribution of significant DEGs at different confidence levels is more evident, as here genes were filtered and categorised based on two levels of significance (p-value and log2 FC value respectively). There were only a select few DEGs of interest to our study with significance at both p-value and log2 FC here which included the downregulated genes MATN3, TIMP3 and CALD1 which have varying roles including the homeostasis of bone and tissue, inhibition of matrix metalloproteinases and regulation of smooth muscle contraction, respectively (Figure 4.5B). Results obtained from the DEG volcano plot also exhibit the genes IFI6 and IFIT3, which are both involved in innate immunity, as significant at the log2 FC value only. Notably, unlike in CedPV infection investigated previously which highlighted several other immune-related genes as significantly upregulated during infection, upon paIFNλ stimulation several of these labelled immune genes were actually found to be nonsignificant including the ISGs Mx1 and IFIT2, which are annotated in grey on the DEG volcano plot.

Variability in gene expression was also measured in DEGs between unstimulated and paIFNλ treatment to identify the influence paIFNλ stimulation has on certain genes. Results indicated that some genes, such as HSPA1B, IFI6, NFKBIZ and ZFAND2A displayed higher expression in the presence of paIFNλ treatment, whereas other genes such as PIP4K2A displayed the opposite and appeared slightly more highly expressed in the absence of paIFNλ (Figure 4.5C). Although there were slight trends demonstrating the overall higher gene expression in the presence of paIFNλ stimulation for the most variable genes assessed here, the general variability of genes between the two conditions appears minimal and additionally for certain genes, there is substantial variation within the biological replicates measured here. Therefore, it is difficult to draw any substantial conclusions here on the influence of paIFNλ on changes in gene expression in bat cells from the top 25 most variable genes. Functional enrichment analysis using DEGs between unstimulated and paIFNλ stimulated cells was carried out to observe the components and functions that these genes partake in (Figure 4.6(A-C)). Results demonstrated that the most significant cellular components concerned with DEGs in unstimulated vs paIFNλ treatment belonged to protein containing complexes and membrane components (Figure 4.6A). Gene counts were also identified in other cellular components including the nucleus or other organelles. Investigations of the molecular functions of these genes in unstimulated vs paIFNλ treated cells identified only five functions that DEGs are classified into. The most significant functions included DNA binding transcription factor activity and transcription regulator activities in addition to other functions such as nucleic acid and DNA binding alongside catalytic activity (Figure 4.6B). The small collection of molecular functions that DEGs partake in here implies limited roles of the genes induced during paIFNλ stimulation of PaBr cells but requires further elucidation to confirm if DEGs in unstimulated vs paIFNλ treatment are limited to these functions only. Curious results were observed for the classification of DEGs into distinct biological processes, as several processes were

implicated, such as those concerning transcription alongside biosynthetic and metabolic processes and remarkably, all genes exhibited the same significance level and contained only two genes in each category (Figure 4.6C). The even distribution of genes into a broad selection of biological processes may be due to the limited total gene count observed for the gene ontology in the presence and absence of paIFNλ stimulation.

Further to differential gene expression analysis, we investigated the alternative splicing events occurring in unstimulated vs paIFNλ stimulated cells using our RNA-seq data. Prior research has shown that several components of the type I and type III IFN response encode different isoforms that are generated via alternative splicing in order to regulate the activation of the IFN response and function. Liao and Garcia-Blanco (2021) resourcefully summarises some of the alternative isoforms produced in human cells and their influence on the host IFN response, as represented in Figure 4.11. These previous studies demonstrate the importance of alternative splicing in regulating the IFN system in mammals, alongside the effect that alternative isoform expression has on IFN-mediated antiviral signalling. Therefore, we aimed to characterise the differential splicing events and isoform switching occurring in bats during paIFNλ stimulation to hopefully shed some light on the genes involved and their influence in the response to type III IFN treatment in bats.

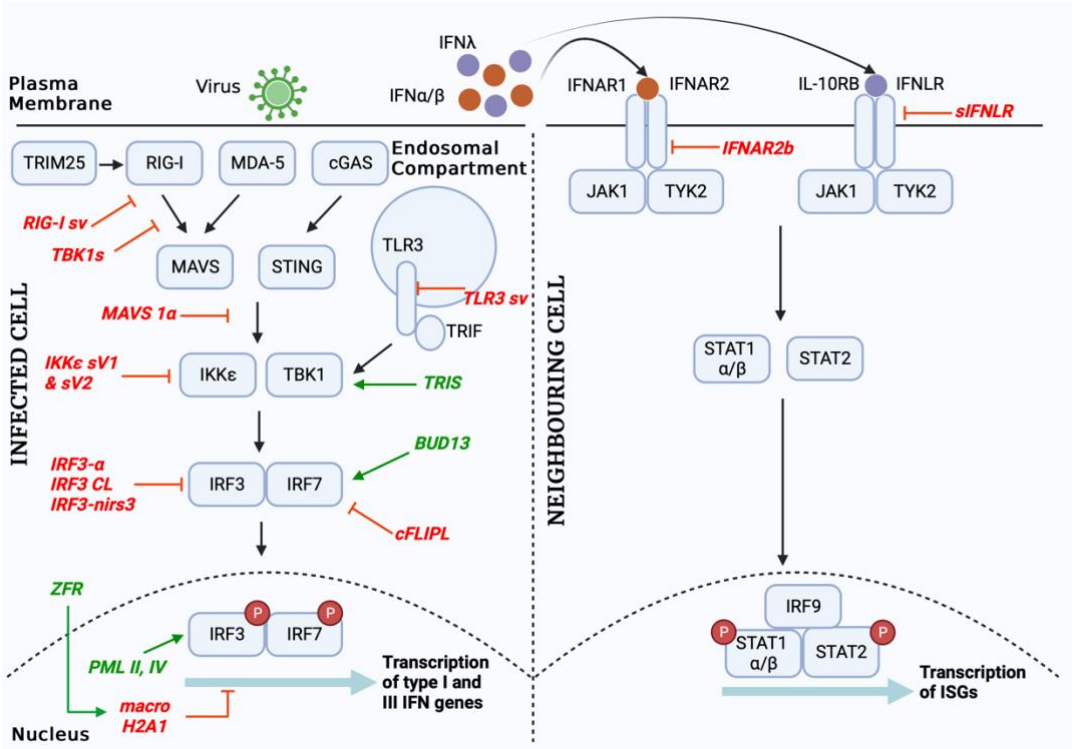

Figure 4.11 - Diagram representing the influence of alternative splicing on the human type I and type III IFN response. *Isoforms produced from alternative splicing events that are known to upregulate the antiviral response are represented in green, whereas those that downregulate the antiviral response are in red. Figure adapted from Liao and Garcia-Blanco (2021)* and created with Biorender.com.

Alternative splicing analysis identified 27,183 differential splicing events occurring within 6,984 genes and upon subsequent filtering of genes with an FDR value of ≤0.1, 338 genes were identified as significant to undergo 448 distinct differential splicing events. It is evident that from the total genes undergoing alternative splicing in unstimulated vs paIFNλ stimulated cells, only a small fraction of them (4.8%) were found to be significant. Gene ontology analysis was also used to investigate the potential roles that genes undergoing alternative splicing may possess (Figure 4.7(B-D)). Only four cellular components were implicated during alternative splicing, the most significant being the ribonucleoprotein complex, which is integral to several biological functions including transcription, translation, and the regulation of gene expression (Figure 4.7B). Therefore, it is plausible that the alternative splicing of genes in the ribonucleoprotein complex during paIFNλ treatment may influence the

roles of these genes during the type III IFN response in bats but warrants future studies. Alternative splicing in the context of molecular function was also determined and results identified several significant molecular functions including RNA metabolism, RNA processing, cellular amide metabolic processes and the cell cycle (Figure 4.7C). Lastly, the analysis of biological processes found only four processes, the most significant being RNA binding (Figure 4.7D). Again, the alternative transcription occurring in genes that partake in these molecular functions and biological processes during unstimulated vs paIFNλ stimulation could result in the production of alternative isoforms that influence the type III IFN response in bats and future work perceiving their function in bats is required.

The alternative splicing of transcripts produces different isoforms from the same gene. We conducted isoform switching analysis to observe alternative isoform expression in our RNA-seq data, as the expression of alternative isoforms often results in an altered function of the encoded protein (Chen et al., 2022). In unstimulated vs paIFNλ stimulated PaBr cells, we identified 63 genes that produced 72 isoforms from 87 switching events and 23 of these genes resulted in 27 isoforms generated via 33 alterative splicing events that have a functional consequence (Figure 4.8B). Analysis of isoform switching identified the most common alternative splicing events taking place in unstimulated vs paIFNλ stimulation of PaBr cells were ATSS and ES which represented the highest gene count, however at the FDR value of <0.05, no alternative splicing events were deemed significant (Figure 4.8C). Therefore, although we can observe the alternative splicing events that were favoured more during isoform switching, we cannot conclude their significance at this value. Within the genes identified to undergo isoform switching with a functional consequence, there were no immune-related genes highlighted here for our examination. Therefore, we alternatively explored the four most significant genes that were identified to undergo alternative splicing to result in isoform switching with a

functional consequence. Our study of these genes identified varying expression patterns and isoform usage (Figure 4.9(A-D)). Results exhibited the preferred usage of certain isoforms within these single genes either during paIFNλ treatment or alternatively in its absence which warrants further research. Additional investigations examining the alternative splicing of the genes identified in unstimulated vs paIFNλ-treated PaBr cells and the isoforms they produce, particularly those concerned with functional consequences, may allow researchers to gain an enhanced insight into the heightened or dampened functionality of a wide range of proteins induced during type III IFN stimulation and their contribution to the bat IFN response.

Although we initially expected to observe immune-related genes within our differential expression, alternative splicing and isoform switching analyses, as we stimulated PaBr cells with an interferon known to induce the type III IFN pathway, the results failed to highlight many immune-related genes in the context of paIFNλ stimulation. The lack of observed immune genes as mentioned previously, is likely because unlike in our previous study using CedPV infection (Chapter 3), which is known to stimulate several immune pathways including the type I IFN pathway, the use of paIFNλ in this case only activates a single (type III) IFN pathway. Additionally, the type I IFN response is rapidly induced and is considered to mount a robust antiviral response in bats via the generation of antiviral ISGs, and although the type III IFN pathway still composes part of the first line of defence to infection, the type III IFN response acts in a much slower manner, yet notably remains sustained for longer durations (Jilg et al., 2014, Marcello et al., 2006). The type III IFN response is also known to result in the delayed production of ISGs in comparison to type I IFNs which work early during infection and this delay may underlie the reduced number of total genes and alternative splicing events observed in the stimulation of PaBr cells with paIFNλ in comparison to viral stimulation (Manivasagam and Klein, 2021). Furthermore, despite both type I IFN and type III IFNs acting through the same

downstream signalling pathways, they bind via different receptors which largely differ in their cellular expression and distribution in mammals (Wells and Coyne, 2018). Rapid type I IFN induction occurs via IFNAR which are ubiquitously expressed in mammalian cells, whereas the IFNLR-mediated induction of ISGs is restricted to certain cells such as epithelial cells, neutrophils and the endothelial cells of the blood-brain barrier (Sommereyns et al., 2008, Read et al., 2019, Broggi et al., 2017). It is worth considering that although the PaBr cells that we stimulated were originally isolated from the brains of *P.alecto* bats, the sufficient expression of IFNLR type III IFN receptors within these cells *in vitro* has not been previously defined and ideally should have been confirmed prior to our investigations. Therefore, a potentially minimal expression of the type III IFN receptor in the PaBr cells may hinder the true representation of paIFNλ stimulation in bats and thus warrants future study utilising bat cells previously recognised to sufficiently express IFNLR receptors. Overall, our research mapping the gene repertoire and splicing events induced in PaBr cells in response to paIFNλ stimulation provides the first characterisation of the transcriptomic response of bat cells to stimulation with a type III bat IFN. Although our data is derived from an individual bat cell line and may not be representative for all bat species, the differential gene expression, alternative splicing, and isoform switching analyses investigated here provide a preliminary insight into the transcriptomic response in bats during type III IFN treatment and highlights potential genes of interest for future investigation.

Chapter 5. paIFIT5 Displays a Broad Virus Inhibition Activity Mediated Through Binding 5'ppp RNA

5.1 Introduction

5.1.1 IFIT5 and its Antiviral Ability

Interferon induced proteins with tetratricopeptide repeats (IFITs) are well-studied ISGs that are known to play essential roles in antiviral responses, nucleic acid sensing and protein translation in humans, whereby they can directly recognise viral RNA molecular signatures (Abbas et al., 2013). All IFIT proteins contain a characteristic feature of several tetratricopeptide repeats (TPRs), a motif composed of 34 amino acids in a helix-turn-helix structure to allow for protein-protein interactions (D'Andrea and Regan, 2003). Under basal conditions, IFIT proteins are not expressed in most cells, however upon viral infection, IFIT genes are rapidly transcribed to reach high levels. Moreover, IFIT gene expression can also be induced directly via PAMP recognition such as dsRNA, a common by-product of viral infection, which occurs independently without IFN stimulation (Sarkar and Sen, 2004). In this case, these genes are often referred to as viral stress-inducible genes (VSIG), which are often induced directly by IRF3, which is activated following viral infection (Grandvaux et al., 2002b). The IFIT family is comprised of four proteins in humans (IFIT1, IFIT2, IFIT3 and IFIT5) which are all located on chromosome 10q23 and are induced via IFNs, viral infection or PAMP recognition (Figure 5.1) (Diamond and Farzan, 2013). Human IFIT1, IFIT2 and IFIT3 possess analogous functions as interacting heterodimers or oligomers to bind directly to eukaryotic initiation factor 3 (eIF3). These IFIT genes are well characterized and are known to potentiate diverse antiviral processes (Katibah et al., 2013, Zhou et al., 2013b). IFIT5 however, remains less well-understood and does not partake in the association of IFIT1, IFIT2 and IFIT3 and in fact lacks any other interacting protein partner (Pichlmair et al., 2011, Katibah et al., 2013).

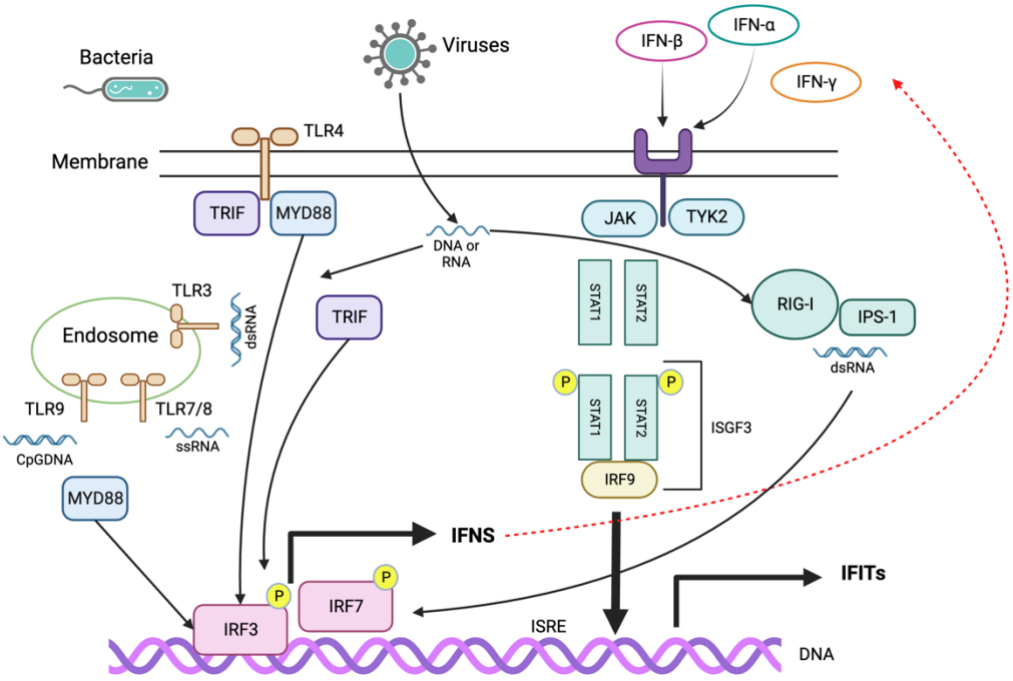

Figure 5.1 - Signalling pathway resulting in IFIT gene induction*. Pattern recognition receptors (PRRs) such as Toll-like receptors (TLRs) and RIG-I-like receptors (RLRs) recognise pathogen-associated molecular patterns (PAMPs) which trigger signalling. Briefly, following sensing of stimuli, intracellular signalling pathways activate IRF3 and IRF7 via phosphorylation, which then bind DNA to stimulate IFN expression. IFNs are secreted and then act in an autocrine or paracrine manner to bind IFNAR receptors and signal via the JAK-STAT pathway where ultimately, ISGF3 binds the ISRE elements in the promoter of IFIT genes and stimulates IFIT gene expression. Figure adapted from Zhou et al. (2013b) and generated using Biorender.com.*

The IFIT5 gene is present in human cells, but absent in mice and rats (Schoggins and Rice, 2011) and is the only IFIT protein present in opossums, chickens, frogs and zebrafish (Zhou et al., 2013b). Previously, IFITs have been known to commonly restrict viral replication via the alteration of protein synthesis, yet recent studies have found that some IFIT proteins including IFIT5, can act in an explicit manner via the direct binding of viral RNA possessing a 5' triphosphate group (5'ppp) at their 5' terminus (Zhou et al., 2013b). IFIT5, in addition to IFIT1, is able to distinguish between cellular and viral mRNA via the detection of this particular feature at the 5' terminus (Katibah et al., 2013). IFIT5 is able to distinguish viral RNA from host RNA such as ribosomal RNAs (rRNAs) and transfer RNAs (tRNAs) as host RNAs tend to carry a cap structure at their 5' termini consisting of a N7-methylguanosine linked to the first transcript nucleotide via a 5'-5' triphosphate bridge which is important for

initiating translation (Shatkin, 1976). Methylation occurs at the 2'-0 position of the first or second base yielding cap1 or cap2 (m^7GpppNmN, m^7GpppNmNm respectively), and although these are not essential for translation, human IFIT1 and theoretically IFIT5, can inhibit translation of mRNA lacking cap1 (Leung and Amarasinghe, 2016). Several viruses are known to mimic these features as immune evasion strategies. However, negative-sense single-stranded RNA viruses such as NDV and IAV do not possess any cap structures, therefore IFIT5 can directly recognise this as foreign RNA and bind to the 5'ppp group (Abbas et al., 2013, Santhakumar et al., 2018). These PAMPs are recognised by PPRs on host cells which initiate innate immune responses in order to limit viral replication (Randall and Goodbourn, 2008). Recent research has suggested that alongside its direct interaction with 5'ppp, human IFIT5 has further antiviral capacity in synergizing the interaction of IRF3 and NF-κB to mediate gene expression (Zhang et al., 2013a). IFIT5 has been identified in several animal species including bats but remains poorly characterised both genetically and functionally.

Genomic and transcriptomic analyses in bats have identified a high degree of conservation of their immune systems with that of humans and other mammals, such as the presence of PRRs, IFNs and notably, also ISGs (Pamela et al., 2018, Schountz et al., 2017). Despite bats sharing several immunological features with other mammals, there has been little research directed towards understanding their immune mechanisms and antiviral responses, largely due to the limited availability of resources required for bat immune studies (Schountz, 2014, Baker et al., 2013). Due to the observed conservation of bat immune pathways with that of humans, in addition to the antiviral capabilities of human IFIT5, we sought to uncover the genetic and functional implication of bat IFIT5 in interfering with the replication of viruses, specifically those bearing a 5'ppp molecular signature. Moreover, we previously identified the clear upregulation of paIFIT5 during viral infection in bats, as described

in Figure 3.6, which implicates a potentially antiviral role of this gene warranting further exploration.

5.2 Results

5.2.1 Genomic, Structural and Evolutionary Characterization of paIFIT5 Locus

IFITs have been identified in several species, including most mammalian species. However, functional characterization of IFIT genes has only been undertaken in a select few species (Diamond and Farzan, 2013). IFIT genes are encoded in bats genome (Ensembl Database), specifically IFIT5, but its sequence conservation and homology to IFIT5 homologues in other species had not yet been explored.

To evaluate conservation of gene collinearity among IFIT5 homologues on a chromosomal level, we selected mammalian species of interest commonly used for gene comparison studies, such as human, horse and dog and compared alongside chicken, representative of a non-mammalian group for a broader insight. Distribution of IFIT5 homologues showed that they were allocated in various chromosomes in different species, with the chromosomal number denoted next to each species, as shown in Figure 5.2A. It is worth noting that in both investigated bat species, the chromosomal location of IFIT5 still remains unknown due to lack of genetic mapping and annotation within these species. Syntenic analysis demonstrated that IFIT5 is commonly flanked upstream by IFIT3 and/or FAS genes and downstream by KIF20B in most studied species (Figure 5.2A). Overall, synteny remained largely conserved between the mammalian species, with loss of synteny observable in chicken due to the absence of common neighbouring genes to IFIT5. *M.davidii* also only displayed a limited number of genes which is likely due to incomplete genomic annotation within this bat species. Phylogenetic analysis of *Pteropus alecto* IFIT5 (paIFIT5) with other species demonstrated paIFIT5 to cluster closely with mammalian species; the microbat species *M.davidii*, and also closely with horse and human IFIT5 (Figure 5.2B). The close phylogenetic relationship between bats and horses has been previously described, classing both species into a superorder named Pegasoferae,

encompassing Chiroptera, Periossodactyla, Carnivora and Pholidota (Nishihara et al., 2006). Therefore, the close phylogenetic relationships observed between bat and horse IFIT5 is expected because genome wise, bats are more closely related to horses than they are to humans (Nishihara et al., 2006).

Further confirmation of this cluster was examined via pairwise identity analysis to analyse amino acid homology between IFIT5 sequences. Percent identity between all mammalian species remained high (over 96%), whilst chicken expectedly displayed a much lower percentage identity to paIFIT5 and other mammalian species (less than 64%) (Figure 5.2C). Based on the observed clustering patterns and homology, it is apparent that paIFIT5 is highly conserved with IFIT5 genes present in other mammalian species, the closest being the microbat species *M.davidii*, closely followed by horse, human and dog. Collectively, gene syntenic analysis, phylogenetic and pairwise annotations indicate that paIFIT5 is highly genetically analogous to IFIT5 genes of other mammals (*M.daviddi*, horse and human).

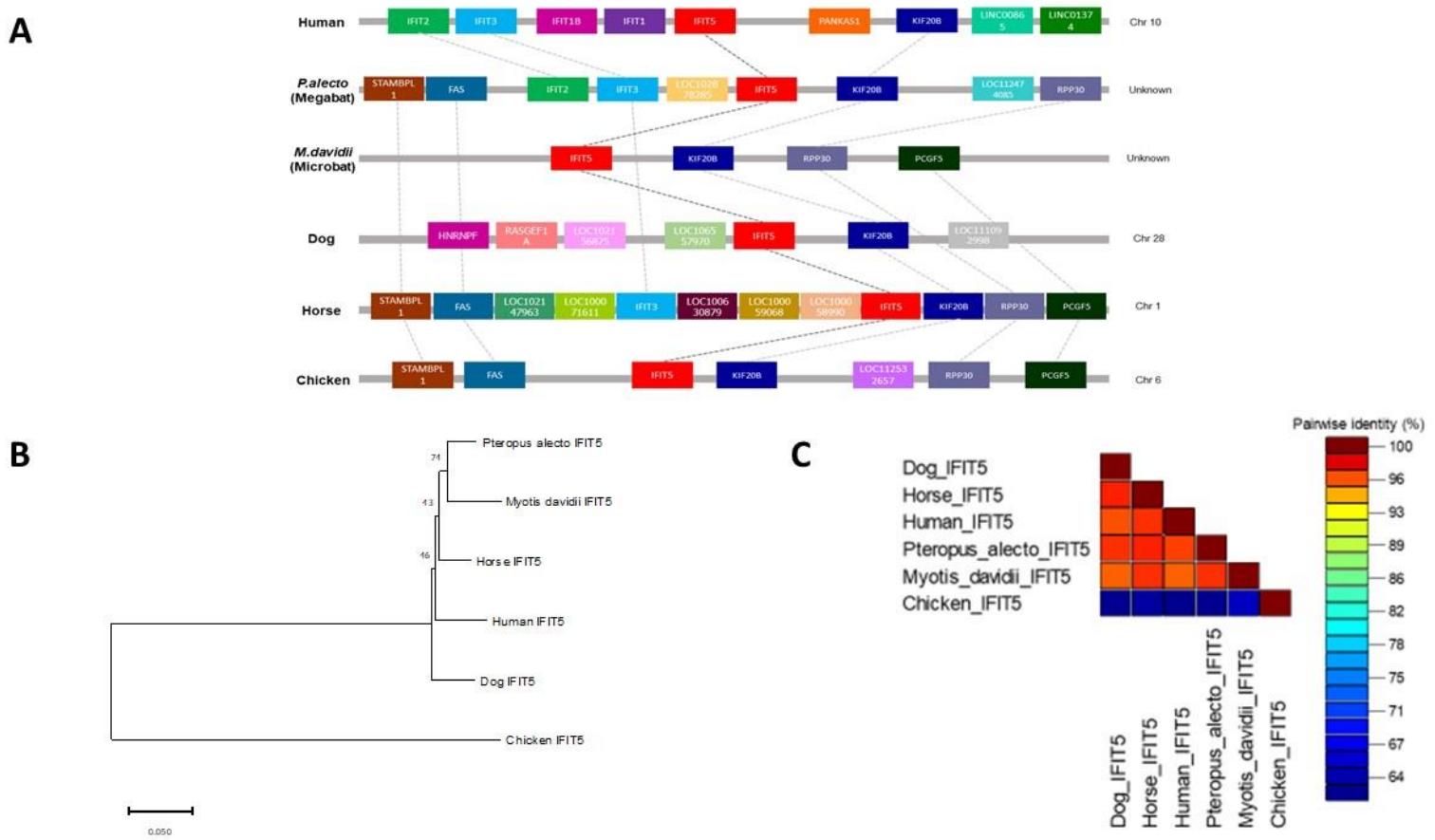

Figure 5.2 - Genomic analysis and loci identification of IFIT5 genes in human, megabat and microbat, dog, horse and chicken. (A) *Direct syntenic analysis of P.alecto IFIT5 with other species commonly known to possess IFIT5. The IFIT5 gene lies on the forward strand and is commonly flanked upstream by IFIT3 and/or FAS, and downstream by KIF20B.* ***(B)*** *Phylogenetic analysis of IFIT5 genes in different species. Bootstrap probabilities are denoted at the branch nodes. The scale bar at the bottom represents the error rate.* ***(C)*** *Pairwise % identity analysis of IFIT5 genes shows a high conservation of bat IFIT5 with horse, dog and human.*

TPRs are a defining structural characteristic of all IFIT proteins, including IFIT5 (Vladimer et al., 2014). TPRs consist of degenerate helix-turn-helix motifs comprised of 34 amino acids which extend throughout the length of the IFIT protein as tandem arrays and are largely responsible for protein-protein interactions (Main et al., 2003, Abbas et al., 2013). The consensus human IFIT5 (huIFIT5) and paIFIT5 sequences were used to predict TPRs using NCBI's Conserved Domain Database for a direct comparison of TPR homology between the two species. The TPR number and position are highly conserved between paIFIT5 and huIFIT5, however, paIFIT5 was shown to possess an additional TPR located after TPR3 and before TPR4 which was hence tentatively labelled as TPR3b (Figure 5.3A). Subsequently, 3D-structures were generated using Pymol software and individual TPR sequences were coloured and labelled. paIFIT5 is shown to adopt the same basic tertiary structure as huIFIT5, revealing the presence of a potential binding pocket (Figure 5.3B). Overall, the protein sequence of paIFIT5 appears highly conserved with its huIFIT5 analogue, only differing by a select few amino acids (Figure 5.3C). Taken together, these results highlight the high degree of sequence conservation between huIFIT5 and paIFIT5 in addition to the characterisation of their TPR repeats.

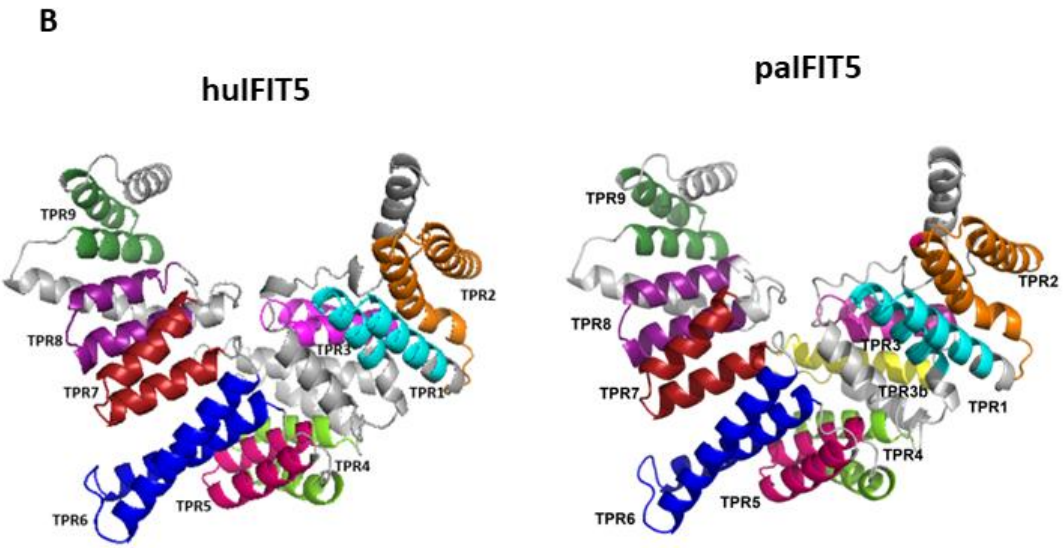

huIFIT5

MSEIRKDTLKAILLELECHFTWNLLKEDIDLFEVEDTIGQQLEFLTTKSRLALYNLLAYV
KHLKGQNKDALECLEQAEEIIQQEHSDKEEVRSLVTWGNYAWVYYHMDQLEEAQK
YTGKIGNVCKKLSSPSNYKLECPETDCEKGWALLKFGGKYYQKAKAAFEKALEVEPD
NPEFNIGYAITVYRLDDSDREGSVKSFSLGPLRKAVTLNPDNSYIKVFLALKLQDVHAE
AEGEKYIEEILDQISSQPYVLRYAAKFYRRKNSWNKALELLKKALEVTPTSSFLHHQM
GLCYRAQMIQIKKATHNRPKGKDKLKVDELISSAIFHFKAAMERDSMFAFAYTDLAN
MYAEGGQYSNAEDIFRKALRLENITDDHKHQIHYHYGRFQEFHRKSENTAIHHYLEA
LKVKDRSPLRTKLTSALKKLSTKRLCHNALDVQSLSALGFVYKLEGEKRQAAEYYEKA
QKIDPENAEFLTALCELRLSI

paIFIT5

MSEIPKDSLKAVLLELECHFTWNLLKEDIDLFDVEDTIGQQLEFLTTKSRLTLYNLLAFV
KHLKGQNKDALDCLEQAEEIIQREHSDKEEVRSLVTWGNYAWVYYHMDHLKEAQK
YIDKVGNVCKKLSSPFNYKLECPEIDCEKGWALLKFGGKYYQKAKAAFEKALEVEPD
NPEFNIGYAITVYRLDDSDREGSIKSFSLGPLRKAVTLNPDNTYIKVFLALKLQDVHAE
AEGEKYIEEILDQISSQPYVLRYAAKFYRRKNSWDKALELLKKALEVTPTSSFLHHQM
GLCYRAQMIQIKKATRNRPKGKDKLKVDGLITSAIFHFKAAVERDSMFAFAYTDLAN
MYAEGGQYSNAEDIFQKALRLENITDDHKHQIHYHYGRFQEFHRKSENTAIHHYLEA
LKVKDRSSLRSKLTSALKKLATKRLGHNALDVQSLSALGFVYKLEGEKRQAAEYYERA
QKIDPENAEFLTALCELRLSI

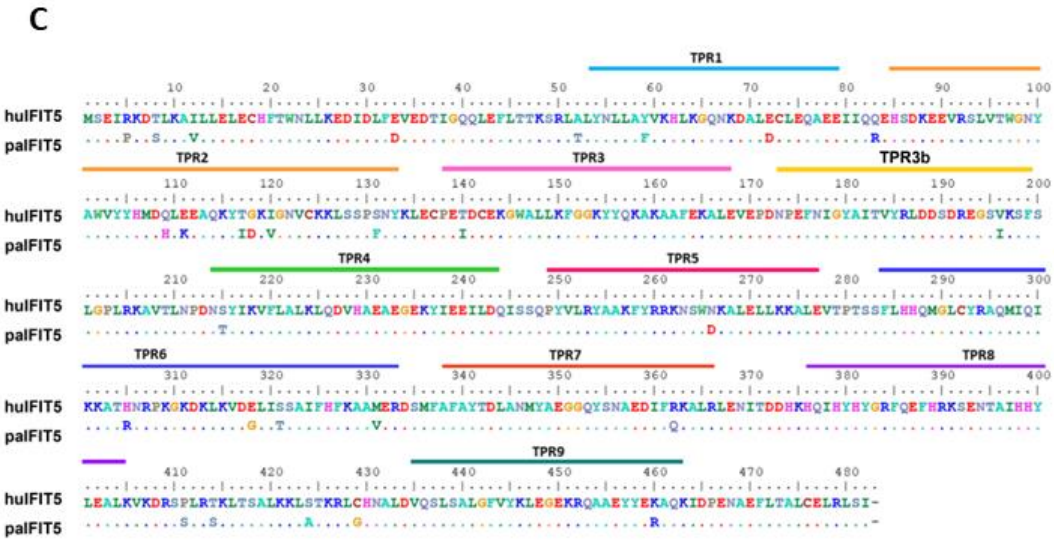

Figure 5.3 - Structural overview and sequence conservation of bat (P.alecto) IFIT5 with human IFIT5. (A) *TPR numbers and positions in huIFIT5 and paIFIT5.* ***(B)*** *Three-dimensional (3D) protein structure and sequence comparison between huIFIT5 and paIFIT5 displays putative homology of TPR repeats.* ***(C)*** *Sequence alignment of the entire IFIT5 protein between human and Pteropus alecto, displaying homology between the two proteins and the location of TPR repeats in IFIT5 gene sequence. Amino acids in paIFIT5 sequence are represented by a dot if conserved with huIFIT5 or alternatively labelled if they differ at that position. Alignment was generated in BioEdit using the ClustalW multiple sequence alignment with a bootstrap value of 1000.*

5.2.2 Subcellular Distribution of paIFIT5 Protein

There is limited information available on the cellular location of huIFIT5. Preliminary analysis predicts an intracellular location of huIFIT5 along with its potential localisation with the plasma membrane of cells when expressed in A-431 and SK-MEL-30 cell lines (Uhlén et al., 2015, TheHumanProteinAtlas, 2023). paIFIT5 subcellular location also remains entirely unspecified. Therefore, we aimed to identify and compare the subcellular locations of both paIFIT5 and huIFIT5 protein in mammalian (VeroE6) cells (Figure 5.4). After transfection of IFIT5 proteins, both paIFIT5 and huIFIT5 were fixed and then stained for immunofluorescence using primary antibodies directed towards the FLAG tag. Nuclei were then stained blue using DAPI nuclear stain before mounting of coverslips onto microscope slides for confocal imaging and analysis. huIFIT5 was investigated alongside paIFIT5 here to allow for a direct comparison between the two proteins. Analysis of the subcellular distribution patterns revealed that both huIFIT5 and paIFIT5 were expressed throughout the cells in which their expression appeared predominantly within the cell nucleus and also in the cell cytoplasm in VeroE6 cells.

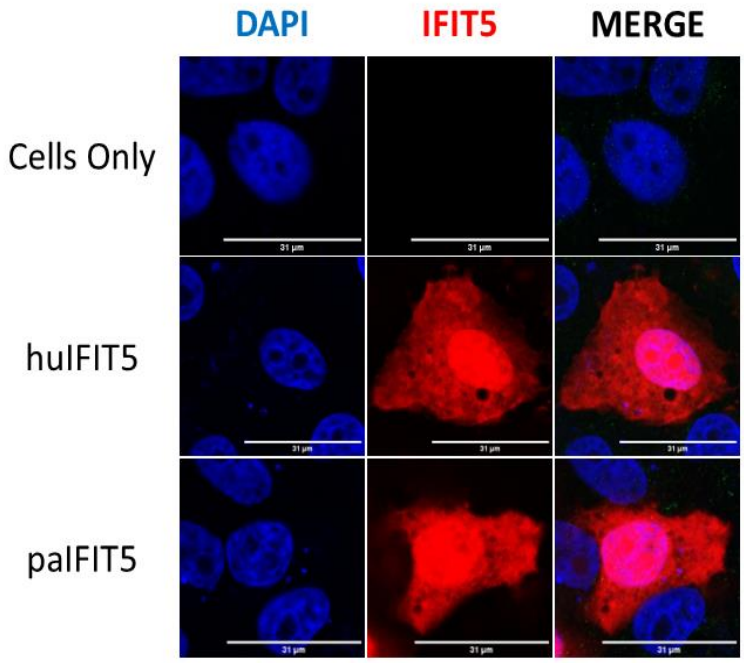

Figure 5.4 - Subcellular distribution of paIFIT5 and huIFIT5 proteins expressed in VeroE6 cells. *VeroE6 cells were transfected with 2µg of FLAG-tagged paIFIT5 or huIFIT5 for 24 hours before fixation, staining for nucleus (DAPI) and IFIT5 (RFP). Scale bar represents 31µm.*

5.2.3 paIFIT5 is Interferon and Virus-Inducible

Previous studies have suggested that the potential antiviral activity of huIFIT5 against viruses is attributed to the viral 5'ppp molecular signature (Pichlmair et al., 2011, Abbas et al., 2013). However, before any antiviral activity of paIFIT5 could be considered, we first needed to determine whether IFIT5 was transcriptionally activated by virus infection and/or interferon. huIFIT5 has been previously described as both interferon and virus-inducible (Zhou et al., 2013b). Therefore, we aimed to investigate the transcriptional activation of paIFIT5 under the stimulation of interferon and viral ligands via qRT-PCR. IFNβ from *P.alecto* (paIFNβ) generated as described in section 2.3, (Figure 5.5A) was chosen as it is a type I IFN which directly induces the transcription of IFIT5, whereas NDV (Figure 5.5B) and poly I:C (Figure 5.5C) are stimuli which also induce the transcription of IFIT5 indirectly via IFN expression and signalling. paIFIT5 was successfully induced in the presence of all three stimuli when

compared to the untreated controls. However, amongst all, the highest induction of paIFIT5 (3.5-fold) was observed by the NDV (Figure 5.5B). NDV transcriptional activation of paIFIT5 is likely to occur principally though the activation of IFNs, since paIFNβ also successfully induced the transcription of paIFIT5 almost 3-fold (Figure 5.5A). It has previously been identified that negative-sense RNA viruses, such as NDV, produce dsRNA intermediates during their replication cycle (Santhakumar et al., 2018), which in turn could mediate the transcription of paIFIT5. Therefore, poly I:C activation of paIFIT5 was also determined. Poly I:C is a synthetic analogue of dsRNA which is used as a surrogate to mimic viral infection and antiviral responses in cells through the production of interferons. Poly I:C is first recognised by Toll-like receptor 3 (TLR3), present within endosomes of cells, which in turn activates IRF3 which leads to the production of IFNs. As paIFIT5 was also successfully induced by poly I:C at over 3-fold (Figure 5.5C), like with NDV, this is likely due to the production of interferons which then led to the transcriptional activation of paIFIT5. Collectively, these results confirm that paIFIT5 is both interferon and virus inducible.

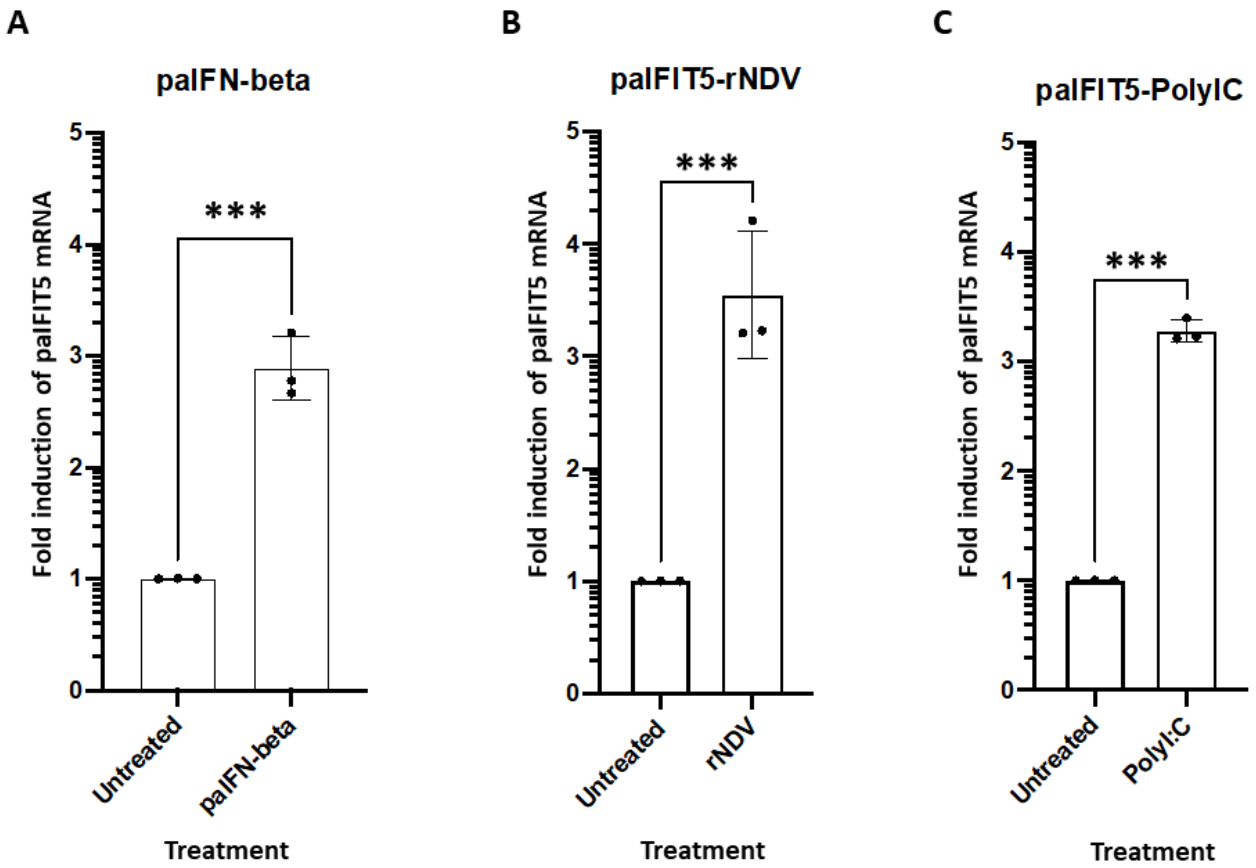

Figure 5.5 – qRT-PCR Expression of paIFIT5. *Quantitation of paIFIT5 mRNA in PaBr cells stimulated with either; 200 units of P.alecto IFNβ (paIFNβ)* ***(A)****, 1.0 MOI of NDV* ***(B)****, or 150 µg PolyI:C* ***(C)*** *for 24 hours before RNA extraction and analysis for qRT-PCR using primers specific for the P.alecto IFIT5 gene. Significance was determined at p ≤0.05 (***) and was calculated and figure was generated using an unpaired t test in Graphpad Prism 8 software.*

5.2.4 paIFIT5 Exerts Potent Antiviral Effects *in vitro*

To further explore the potential antiviral ability of paIFIT5 against the replication of viruses, a plaque assay was performed in VeroE6 cells expressing paIFIT5 and infected with VSV (Figure 5.6 A-B). VSV was chosen as it is a known negative-sense RNA virus that bears the 5'ppp molecular signature that IFIT5 is believed to recognize (Abbas et al., 2013). Furthermore, VSV is well-characterised for purpose in plaque assay quantifications in VeroE6 cells and producing countable plaques (Santhakumar et al., 2017). VeroE6 cells were transfected with 2µg of either paIFIT5 or paMx1-expressing plasmids for 24 hours before infection with VSV-GFP at an MOI of 0.25 or mock-infection. paMx1 was used as a positive control for this experiment as Mx1 is an ISG known for its antiviral activity (Fuchs et al., 2017). After 24 hours, viral supernatant was collected from VeroE6 cells and used for plaque quantification via the generation of serial dilutions applied onto VeroE6 cells in a 12-well plate format and incubated in overlay media for 72 hours. Cells were fixed and stained for plaque counting and quantification. Results indicate that paIFIT5 displays significant antiviral activity against VSV-GFP, due to its lower viral titre than the infected cells control. Cells infected with VSV-GFP resulted in a PFU/ml of around 5×10^8, whereas when paIFIT5 was expressed in cells, viral titre was much lower at less than 2×10^8 PFU/ml. The observed lower viral titre suggests that the presence of paIFIT5 results in less replication of VSV-GFP. Therefore, the mechanisms by which IFIT5 can inhibit viral replication require further analysis. IFIT5 is known to act in an antiviral manner, but it requires elucidation as to whether this effect is from the interaction with 5'ppp present on negative-sense RNA viruses, or if it is acting in a broader manner against other viruses.

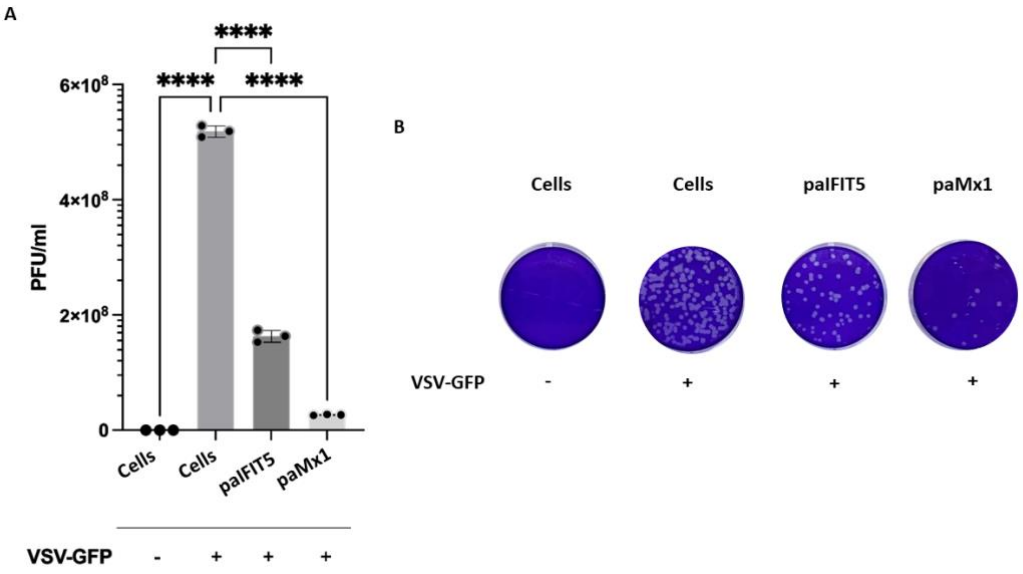

Figure 5.6 - The antiviral activity of paIFIT5 measured against VSV-GFP replication*. VeroE6 cells were transfected with 2µg of paIFIT5, paMx1 or left non-transfected for 24 hours. Cells were then infected with VSV-GFP at an MOI of 0.25 or left uninfected for 24 hours before **(A)** quantification via plaque assay analysis in VeroE6 12-well plates. Significance was calculated using a one-way ANOVA and was determined at p ≤0.01 (****) (n=3). **(B)** Plaques were counted at the 10^{-5} dilution. Figure was generated using Graphpad Prism 8 software and significance was calculated using a One-Way ANOVA.*

5.2.5 paIFIT5 Specifically Inhibits Negative-Sense RNA Viruses

After the previous observation of prospective antiviral activity of paIFIT5 against VSV, we next aimed to investigate if paIFIT5 exhibited antiviral activity against endogenous bat viruses. Bats have been shown to host several viral pathogens, including influenza A-like viruses such as the H17N10 subtype in central American fruit bats (Calisher et al., 2006). Influenza A-like viruses are negative-sense single stranded RNA viruses which possess the 5'ppp signature which is recognized by IFIT5 (Lee et al., 2016). Hence, we selected this bat influenza virus to investigate potential antiviral activity of paIFIT5 mediated via the interaction of paIFIT5 with 5'ppp. Attempts to isolate the H17N10 virus have so far been unsuccessful (Tong et al., 2012, Tong et al., 2013). Therefore, in order to mimic the action of H17N10, we used artificial replication-deficient but transcriptionally active VLPs to observe the effect of paIFIT5

on this bat influenza virus as previously described (Fuchs et al., 2017). The VLPs carry a firefly luciferase minigenome, the polymerase subunits and NP of the bat (H17N10) virus, in addition to all other structural proteins of an H7N7 influenza virus. HEK293T cells were used to produce the H17N10 VLPs which were co-transfected with paIFIT5. At 48 hours post-transfection, supernatants were collected which contained the VLPs and the cell lysates were used to measure firefly luciferase activity which was defined as a measure of the viral polymerase activity of H17N10 (Figure 5.7A). Analysis of the transcriptional activity of H17N10 assay revealed that paIFIT5 significantly reduced reporter gene expression to 14 RLU (average values), compared to the empty vector control of 302 RLU (average values). The reduction in luciferase activity in the presence of paIFIT5 indicates a significant antiviral ability of the protein against H17N10.

As previously mentioned, bats can host a broad range of emerging pathogens, including bunyaviruses, which are negative-sense RNA viruses known for causing severe disease in humans and animals. These viruses are often transmitted by arthropod vectors, however studies have also shown bunyaviruses such as hantavirus, nairovirus and phenuivirus to be harboured by small mammalian hosts including rodents and bats (Weiss et al., 2012, Guo et al., 2013, Müller et al., 2016, Saeed et al., 2021, Brinkmann et al., 2020). We therefore chose to assess potential antiviral function of paIFIT5 against bunyaviruses, as they too possess the 5'ppp signature we theorise interacts with paIFIT5 (Laudenbach et al., 2021). To investigate this, a minireplicon system for RVFV was utilised, as previously described (Habjan et al., 2009, Fuchs et al., 2017). HEK293T cells were co-transfected with the paIFIT5 encoding plasmid, alongside expression constructs coding for the viral L, M and N proteins of RVFV and a *Renilla* luciferase-encoding minigenome construct. As a control, IFIT5 was omitted and replaced with an empty vector (EV). Results showed that in the presence of paIFIT5, viral polymerase activity of RVFV appeared very

slightly increased compared to the EV control, however statistical analysis deemed these results non-significant (Figure 5.7B).

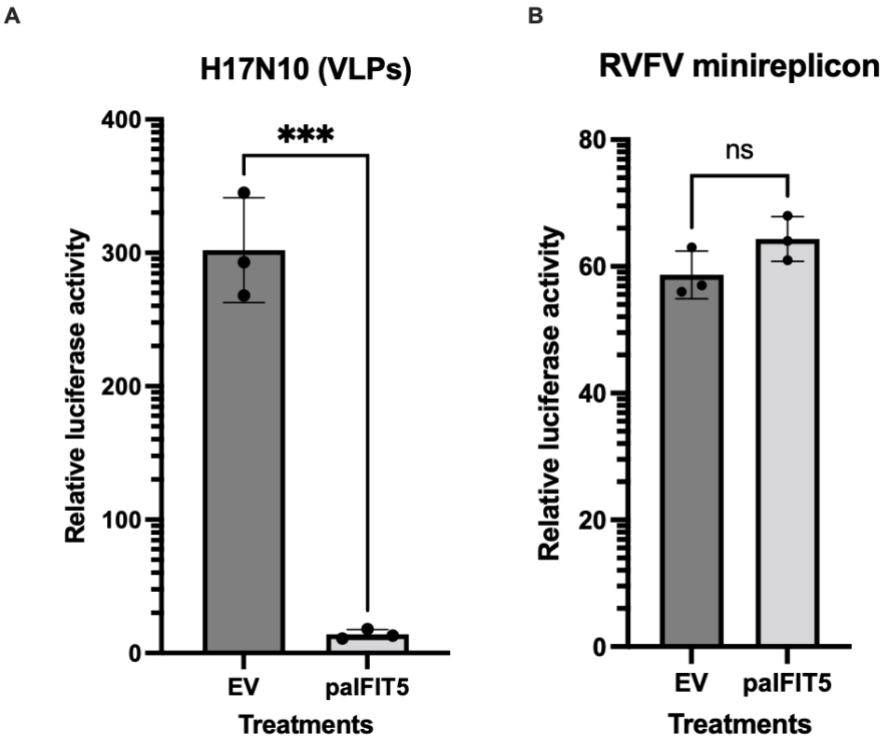

Figure 5.7 - The influence of paIFIT5 on the polymerase activity of bat influenza (H17N10) and Rift-valley Fever Virus (RFV). (A) *FLUAV (H17N10) VLP minireplicon system consisting of 10ng of PB2, 10ng of PB1, 10ng of PA, 10ng of NP, and 50ng of Pol-I FF-Luc was co-transfected alongside helper plasmids encoding the additional structural proteins from the H7N7 virus, in addition to 300ng of paIFIT5 expression plasmids, or empty vector (EV) control plasmid. At 48h hours post-transfection, supernatants were collected, and the cell lysates were analysed for firefly luciferase activity. The empty vector control was set to 100% and significance was calculated using a student's t test (n=3) where *** represents significance at $p \leq 0.05$.* ***(B)*** *HEK293T cells were transfected with 250ng of paIFIT5 alongside plasmids encoding RVFV N, L and M proteins and the Renilla luciferase-encoding minigenome (250ng each). At 48 hours post transfection cells were lysed and used to measure the Renilla luciferase activity. As a control, the paIFIT5 plasmid was replaced with an EV. The activity of the empty vector control was set to 100% and statistical significance was calculated using a student's t test (n=3).*

5.2.6 paIFIT5 Interacts Specifically with 5'ppp-bearing RNA

IFIT proteins in human are known to interact with RNA carrying modifications at their 5' ends and notably IFIT5 has been shown to interact with a 5'ppp molecular signature (Diamond and Farzan, 2013, Abbas et al., 2013). Since huIFIT5 has been shown to directly interact with 5'ppp, we therefore aimed to explore whether the

antiviral effects of paIFIT5 are attributed to its interaction with 5'ppp-bearing RNA. As aforementioned, paIFIT5 appears highly conserved in its structure to its human counterpart. huIFIT5 has been structurally characterised by Abbas et al. (2013) whereby huIFIT5 displays novel arrangement of TPR domains that bind specifically to ppp-RNA in a non-sequence-specific manner. We generated a predicted 3D crystallised structure of full-length paIFIT5 (Figure 5.8A) which appears highly conserved in structure with the previously described huIFIT5 (Abbas et al., 2013) and seems to possess a similar pocket which may be involved in binding 5'ppp. To determine the molecular mechanisms involved in the recognition of 5'ppp by paIFIT5, we generated RNA species bearing either the 5' triphosphate (5'ppp-RNA) group or alternatively a hydroxyl (5'OH-RNA) group at their N-termini. These RNA, simulating viral RNA ends, were then biotinylated and coupled with agarose beads which were subsequently incubated with HEK293T cells expressing V5-tagged paIIFT5 or huIFIT5. The ribonucleoproteins were then purified and the interaction of paIFIT5 or huIFIT5 was determined by immunostaining for IFIT5 (Figure 5.8B). paIFIT5 did not interact with the 5'OH-RNA species, but both paIFIT5 and huIFIT5 recognized RNA carrying the 5'ppp signature. The molecular structures of the alternative RNA ligands generated and investigated for IFIT5 binding (5'ppp and OH), are illustrated in Figure 5.8C.

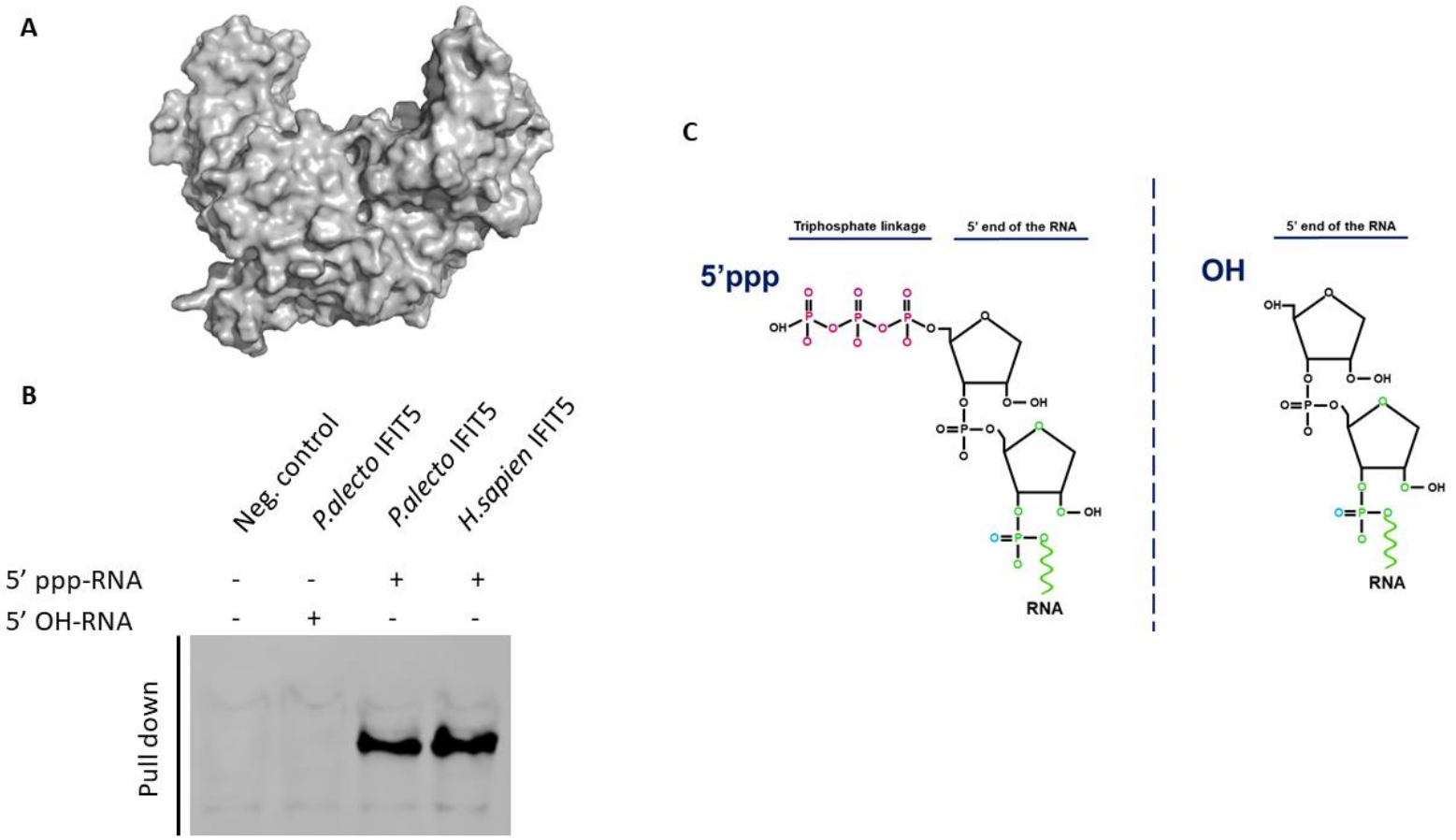

Figure 5.8 - The interaction of palFIT5 with RNA carrying modifications in their 5' termini using RNA-protein immunoprecipitation. (A) *The 3D structure of paIFIT5.* ***(B)*** *Pull-down of biotinylated RNA interacting with paIFIT5 indicated that both huIFIT5 and paIFIT5 interacted with RNA carrying 5'ppp structures.* ***(C)*** *The genomes of negative-sense RNA carry a triphosphate linkage (5'ppp) in the first transcribed base of the RNA.*

5.3 Discussion

ISGs provide an essential branch of the innate immune response whereby they act in an antiviral manner by targeting several stages of viral replication (Schoggins and Rice, 2011). IFIT proteins are a family of ISGs which are major players in innate immunity, due to their substantial antiviral responses mounted against viral and IFN stimuli (Vladimer et al., 2014, Diamond and Farzan, 2013). Significant advances have been made in the knowledge and characterisation of IFIT proteins in human and mouse, however the understanding of IFIT proteins in other mammalian species such as bats currently remains understudied (Diamond and Farzan, 2013, Fensterl and Sen, 2015). The characterisation of IFIT proteins in bats is crucial in gaining a better understanding of their innate immune responses, which have previously been highlighted as somewhat unique in aiding bats to host viruses without displaying any clinical symptoms of illness (Banerjee et al., 2020). Unearthing the role of ISGs such as IFIT proteins in the bat antiviral immune response, would allow for a better understanding of their roles as viral reservoirs and potentially provide a basis to regulate the common emergence and spillover of zoonotic pathogens from bat hosts. The functions of IFIT1/IFIT2/IFIT3 have been extensively investigated in comparison to IFIT5 (Zhang et al., 2013a). Notably, IFIT5 has recently been discovered in humans to possess antiviral activity parallel to IFIT1, in directly recognising and binding to RNA possessing a 5'ppp molecular signature (Abbas et al., 2013, Zhang et al., 2013a, Zhou et al., 2013b). Therefore, IFIT5 was selected as an initial gene of interest that warrants further investigation in bats to identify if bat IFIT5 is also capable of 5'ppp RNA recognition and subsequent antiviral activity.

The IFIT5 gene of the Australian Black flying fox (*P.alecto*) was chosen for analysis as it remains one of the few whole-bat genomes that have been sequenced and annotated (Zhang et al., 2013b). Furthermore, *P.alecto* are the natural reservoir hosts for several pathogenic viruses, including henipaviruses, deeming them an appropriate

representative species of bat that warrants investigation (Peel et al., 2022, Field, 2009, Wong et al., 2007). To explore bat IFIT5, we first employed a bioinformatic approach to compare the *P.alecto* IFIT5 gene (paIFIT5) with that of other animals, assessing their gene synteny, sequence conservation and phylogenetic relationship (Figure 5.2(A-C)). Based on these results, paIFIT5 appeared highly conserved with IFIT5 homologues in other mammals. Interestingly bat IFIT5 displayed a closer phylogenetic relation and pairwise percentage of 74% to horse IFIT5, than to human IFIT5 (Figure 5.2(B-C)). This supports the notion that alternative to bats previously belonging to, and diverging from, the same group as primates, bats may actually belong to the super-order named Pegasoferae, which also contains horses (Tsagkogeorga et al., 2013). However, due to the large species diversity of bats, these results are likely not representative of IFIT5 in all bat species but are useful in understanding IFIT5 from *P.alecto*.

We directly compared the sequence and TPR repeats of paIFIT5 with huIFIT5, due to the recent findings of the role of IFIT5 in humans, in addition to their observed sequence homology (Zhang et al., 2013a). Observations demonstrate high conservation in the protein sequence and three-dimensional structure of paIFIT5 with that of huIFIT5, differing by only a few amino acids (Figure 5.3C). Interestingly, the two IFIT5 proteins differ only slightly in their TPR repeats, due to the presence of an additional TPR (TPR3b) apparent in paIFIT5 (Figure 5.3(A-B)). TPRs are characteristic of IFIT proteins and have key structural roles the responsibility of binding a diverse range of ligands, such as protein and peptide recognition and with the recent discovery of RNA-binding IFIT proteins and also nucleic acids (Vladimer et al., 2014, Abbas et al., 2013). Studies by Abbas et al. (2013) examined the crystal structure of huIFIT5 and determined a novel arrangement of TPR domains that are able to directly bind 5'ppp-RNA in a non-sequence-specific manner. Conservation of TPR positioning between paIFIT5 and huIFIT5 may suggest a sustained ability of

paIFIT5 to bind similar ligands, including 5'ppp-RNA. However, the extra TPR present (TPR3b) in paIFIT5, potentially requires further study to determine the crystallised conformational structure of paIFIT5 and whether this additional TPR in *P.alecto* influences the binding efficiency or ligand spectrum of paIFIT5. Furthermore, deletion and mutational investigations whereby TPRs in paIFIT5 are modified may be warranted to gain a valuable insight into the binding capacity of paIFIT5 and any implications that TPR positioning may have. Additionally, we aimed to observe the cellular location of the paIFIT5 protein when expressed in VeroE6 cells, as this remained previously unexplored. Moreover, there is limited information available on the cellular location of the human IFIT5 gene, therefore we investigated both IFIT5 genes in our analyses here. Upon immunofluorescence staining and imaging of paIFIT5 and huIFIT5 expression in VeroE6 cells, we observed a similar expression pattern of the two proteins within the cell cytoplasm and the nucleus (Figure 5.4). This distribution appeared generally widespread throughout the cell and did not appear to localise to specific subcellular locations. This study may indeed represent the true expression of these proteins, however, due to the expression of paIFIT5 in non-host cells, additional studies investigating paIFIT5 expression in bat cell lines should be undertaken to confirm gene expression. Additionally, investigation of the potential colocalization of IFIT5 genes with subcellular organelles and potentially the plasma membrane, may also enable a better perception of both paIFIT5 and huIFIT5 location and activity.

Known to facilitate IFN-induction, viral infection, IFN, dsRNA and lipopolysaccharides are all stimuli known to subsequently induce the transcription of human IFIT proteins (Schoggins et al., 2011, Øvstebø et al., 2008). The induction of IFIT1/IFIT2/IFIT3 by these stimuli are well-represented in the literature, whereby they are described to form multimeric complexes that demonstrate antiviral activities such as the inhibition of translation initiation (Fleith et al., 2018). The induction of IFIT5 however, remained

unknown and functionalities remained inconsistent and conflicting (Terenzi et al., 2006, Feng et al., 2013, Wacher et al., 2007). Through their research, Zhang et al. (2013a) were able to confirm that IFIT5 was significantly induced at both the protein and mRNA level by virus, poly(I:C) and IFN-stimulation. We therefore wanted to investigate if IFIT5 in bats was also induced by these stimuli. We confirmed that paIFIT5 was transcriptionally activated by NDV, poly(I:C) and paIFNβ, whereby the fold induction of paIFIT5 was consistently increased around two-fold in the presence of stimuli, compared to untreated controls (Figure 5.5(A-C)). These results confirm that IFIT5 in *P.alecto* is both virus and IFN-inducible. This however may not be the case for all bats and hence more investigations into individual bat species are required to determine if this is induction is unique to *P.alecto* or is constant in all bat species. NDV appeared to increase the activation of paIFIT5 the highest, followed by the poly(I:C) and then IFNβ. Higher induction of paIFIT5 by NDV is likely attributed to multiple factors including viral dsRNA generated during replication, sensing of viral nucleic acid by intrinsic sensors and cellular responses to viral infection. Similarly, poly(I:C) (dsRNA) can be sensed in the same manner as virus generated dsRNA, leading to an increase in the induction of paIFIT5 genes. In contrast, treatment with IFNβ can exclusively induce the paIFIT5 through JAK-STAT signalling pathway. Furthermore, although paIFIT5 was induced by the ligands used here, it is worth noting that only one virus and IFN type was used. For a broader analysis, a variety of viral stimuli should be used in addition to other IFN types, including other type I IFNs and type III IFNs which are also known to induce ISGs but were not investigated here (Mesev et al., 2019, Pervolaraki et al., 2018).

Due to research highlighting the antiviral effect of huIFIT5 displayed against the negative-sense RNA virus NDV, we wanted to observe if paIFIT5 also possesses antiviral activity towards this classification of viruses (Zhang et al., 2013a). This previous study used NDV encoding reporter GFP, in order to visualise via

fluorescence, the amount of viral replication taking place, however we aimed to quantify viral replication via an antiviral plaque assay to gain more quantifiable results. Because NDV does not form plaques when used in plaque assays, we instead used VSV, as this too is a negative-sense RNA virus possessing the 5'ppp-RNA that we are interested in exploring. Results showed that when paIFIT5 was over-expressed, VSV-GFP replication was significantly reduced, resulting in a lower viral titre (Figure 5.6 (A-B)). paMx1 also significantly reduced the replication of VSV-GFP which was used as a positive control in this study, due to its previously characterized antiviral activities, specifically in inhibiting negative-sense RNA viruses. Additionally, Mx1 is conveniently one of the most studied ISGs in bats (Zhou et al., 2013a, Fuchs et al., 2017, Verhelst et al., 2013). Notably however, it is worth considering that an empty vector control plasmid was not used here due to lack of availability. Thus, the antiviral effect we observe for both paIFIT5 and paMx1 may encompass some background IFN induction due to the transfection of plasmid DNA into cells which is known to commonly elicit an immune response. However, the differences in antiviral activity between the two ISGs transfected highlights that there is a distinct antiviral effect of each ISG and is not solely down to plasmid transfection.

To further elucidate the antiviral nature of paIFIT5, the influenza A-like bat virus (H17N10) and RVFV were selected for analysis (Figure 5.7(A-B)). Due to the high containment required for RVFV and the inaccessibility of H17N10, we could not measure the influence of paIFIT5 on the replication of these viruses via plaque assay. Minigenome assays were alternatively used to allow for the investigation of transcription and viral replication in HEK293T cells expressing paIFIT5 or an empty vector control. paIFIT5 significantly ($p<0.001$) inhibited the replication of the H17N10 viral minigenome and hence the formation of new VLPs, as defined by a reduced luciferase activity in comparison to the empty vector control (Figure 5.7A). These results demonstrating the suppression of H17N10 viral replication in bats by IFIT5,

corresponds with the understanding that bats are able to maintain viral replication at manageable levels (Schountz et al., 2017). Contrastingly, the effect of IFIT5 on the RVFV minireplicon assay resulted in non-significant outcome and thus (Figure 5.7B). These non-significant results may potentially be due to experimental issues such as human or reagent error and hence must be repeated to determine if these are true results demonstrating the lack of effect of paIFIT5 on RVFV replication.

Despite lack of reporting on IFIT5 functionality, huIFIT5 is understood to recognize a range of RNA constructs, including 5' monophosphate (5'p), double stranded DNA and RNA with CAP0 modifications and of special interest here, 5'triphosphates (5'ppp) (Abbas et al., 2013, Katibah et al., 2014, Kumar et al., 2014). By generating modified RNA constructs bearing either a 5'ppp signature or alternatively a hydroxyl (OH) group, as previously described (Santhakumar et al., 2018), we aimed to determine if paIFIT5 specifically interacts with the 5'ppp signature commonly found within in viruses possessing negative-sense single stranded RNA genomes (Figure 5.8C). RNA-protein interaction results showed that paIFIT5 specifically interacted with RNA possessing the 5'ppp signature and did not interact with OH-bearing RNA (Figure 5.8B). huIFIT5, which is already known to interact with 5'ppp-RNA, was also assessed for direct binding, as a positive control for comparison purposes. From these results, it is feasible that paIFIT5 is able to sense foreign RNA, bearing 5'ppp, a molecular signature present only within genomes of negative-sense single stranded RNA viruses and produced as an intermediate during positive-sense RNA genome replication (Iwasaki, 2012). By sensing this RNA signature as foreign, paIFIT5 may be able to distinguish this from self-RNA which instead bear monophosphate or CAP structures at their 5' end. The direct interaction of paIFIT5 with 5'ppp RNA, could potentially sequester viral RNA, inhibiting its replication and translation by host machinery.

Our results showing the interaction of paIFIT5 with 5'ppp-RNA and its antiviral activity prove useful in understanding the role of bat ISGs and their role in bat innate immunity. However, these findings warrant further experimental validation via the use of paIFIT5 knockout experiments in bat cells, to clarify the antiviral potential of endogenous IFIT5 in host cells. Furthermore, research analysing any potential influence of other IFIT proteins present in bats are required to determine if paIFIT5 acts as a monomer in directly recognising and binding 5'ppp-bearing RNA viruses, or alternatively if paIFIT5 requires assistance via the formation of multimers with other IFITs. Lastly, significant progress can be made in understanding the downstream activation of immune mechanisms caused by the recognition of 5'ppp RNA by paIFIT5 and the potential antiviral resistance this may confer to the bat hosts. Overall, our research employed both functional genomics and molecular biology to provide solid foundations for the characterisation of IFIT5 in the megabat species *P.alecto,* which had not previously been explored. Results additionally investigated the functional rationale for the antiviral capacity of paIFIT5 against viruses possessing 5'ppp RNA molecular signatures. The groundwork presented in this study justifies future investigations assessing not only the antiviral potential of paIFIT5 against a broader range of viruses (DNA and RNA), but also in other bat species and the effects that these interactions impose on bat innate immunity.

Chapter 6. The Characterisation of Fundamental Components of The Type I IFN Response in *Pteropus alecto*

6.1 Introduction

6.1.1 The IFN Response in Bats

Bats are interesting viral reservoirs due to their ability to host a cohort of viral pathogens without signs of disease and exhibit the capacity to facilitate persistent viral infection in the absence of pathophysiology (Calisher et al., 2006, Wong et al., 2007, Brook and Dobson, 2015, Schountz et al., 2017). It has been hypothesised that bats are capable of balancing viral infection without causing pathology by controlling viral replication early in the immune response via specific innate antiviral mechanisms that bats have evolved, particularly within their IFN system, which acts as the first line of defence against viral infection (Baker et al., 2013, De Weerd and Nguyen, 2012, Baker and Zhou, 2015). Studies have demonstrated the presence and functionality of several components of the innate immune response to appear conserved between bats and humans, including PRRs and their activity, the identification of IFNs and IFN signalling together with the induction of ISGs in response to viral stimulation (Baker et al., 2013, Clayton and Munir, 2020, Banerjee et al., 2020, La Cruz-Rivera et al., 2018). However, although bats appear to share most features of their innate immune system with other mammals, several studies have demonstrated a heightened innate immune response, baseline IFN signatures and basal IFN-ligand expression in bats, which are factors consistent with the hypothesis that bats have evolved novel immune features to permit their tolerance of viral infection (Zhou et al., 2016, Zhou et al., 2011a, Zhou et al., 2011b, Baker et al., 2013, Fuchs et al., 2017, Pavlovich et al., 2018, Zhang et al., 2013b, Zhang et al., 2017).

The recent availability of whole genome and transcriptome sequences in at least 18 different bat species has permitted researchers to further investigate the conservation of immune patterns between bats and other mammals (Hawkins et al., 2019, Jebb et al., 2019). Founding transcriptomic research investigating the model species *P.alecto*, identified around 3.5% of its transcribed genes (500 genes) to be

associated with immunity (Papenfuss et al., 2012). Further studies into other bat species have also proved fruitful in investigating bat immunity, whereby 2.75% of genes (around 407 genes) in *R.aegyptiacus* and 466 genes in the Jamaican fruit bat (*Artibeus jamaicensis*) were also identified as immune-related (Shaw et al., 2012, Lee et al., 2015). Additionally, the transcriptomic study in *P.alecto* has also identified several unannotated transcripts which were not conserved with human genes. It is hence plausible that these transcripts may represent a subset of bat-specific immune genes, increasing the representative transcribed immune genes of bats closer to that of human, whereby 7% of their genome consists of immune-related genes (Kelley et al., 2005, Banerjee et al., 2020).

Despite the increasing efforts into investigating and understanding bat innate immunity, the mechanisms underlying disease tolerance in bats remains largely unknown and therefore further characterisation of antiviral immune mechanisms is required. Prior research has highlighted the conservation of the bat IFN system with humans, however this remains largely uncharacterised. Subsequently, functional investigations of key components of the mammalian IFN response may enable a better understanding of bat innate immunity and whether mechanisms of the bat IFN response may confer any advantage to their roles as novel viral reservoirs. Overall, there are numerous genes involved in the innate immune cascade identified in *P.alecto* that are also present in humans and other mammals, yet they remain uncharacterised in bats and require further study to understand their role and significance in the bat immune response to viral infection. However, due to the limited availability of tools in bat research, we decided to focus solely here on IRF7 and IFI35 from the bat model species *P.alecto*, due to the availability of reagents accessible to characterise these genes, alongside the accompanying observation of the upregulation of both IRF7 and IFI35 genes during viral infection of PaBr cells as previously highlighted in Figure 3.6.

6.1.2 IRF7

IRF7 is a member of the IFN-regulatory factor (IRF) transcription factor family and was originally identified in the context of EBV infection (Zhang and Pagano, 1997). IRF7 is considered a master regulator of the type I IFN-dependent and potentially also the type III-IFN dependent immune response in mammals against pathogenic infection (Honda et al., 2005, Österlund et al., 2007). The IRF family contains nine members, however only IRF1, IRF3, IRF5, IRF7 and IRF9 are classified to have roles in type I IFN transcription and significantly, IRF3 and IRF7 are the only IRFs recognised as having antiviral roles (Paun and Pitha, 2007, Honda et al., 2006, Zhou et al., 2014). IRF7 plays a fundamental role in the induction of the IFN response to viral invasion. In brief, the latent form of IRF7 naturally resides in the cell cytoplasm, but upon pathogenic infection IRF7 is phosphorylated and translocated to the cell nucleus, whereby it forms a transcriptional complex to bind the promoter regions of target genes to induce the transcription of type I or type III IFNs to combat pathogenic infection (Ikeda et al., 2007). Due to its central role in the innate immune response, several viruses have evolved mechanisms to target IRF7 as an approach to evade the host immune response (Randall and Goodbourn, 2008).

Initial studies have highlighted key elements of bat IRF7 in innate immunity. The sequence and functional analysis by Zhou et al. (2014) using IRF7 from *P.alecto* identified that despite sequence-level differences, the functional activity of *P.alecto* is conserved with human IRF7. However, they also provided significant evidence that IRF7 in *P.alecto* displays a broader tissue distribution than its human counterpart (Zhou et al., 2014). In humans and mice, IRF7 is expressed in low levels in most cell types and tissues, with the exception of its constitutive expression in plasmacytoid dendritic cells which specialise in IFN production (Zhou et al., 2014). The distribution of IRF7 in human cells is restricted to certain tissues containing large numbers of immune cells, such as the spleen and the thymus, whereas non-immune tissues such

as the intestine exhibit undetectable levels of IRF7 (Zhang and Pagano, 1997). However, upon type I IFN-mediated signalling, human IRF7 is strongly induced in all cell types (Sato et al., 1998). In contrast to the limited constitutive expression of human IRF7 which is restricted to immune cells only, *P.alecto* IRF7 displayed constitutive expression in both immune-related and non-immune cells and organs (Zhou et al., 2014). Although further studies are required to investigate the cell types responsible for the constitutive IRF7 expression in bats, the heightened expression of IRF7 in a wider range of cells within the bat host, may enable *P.alecto* to mount a faster and stronger IFN response to viral infection (Ning et al., 2011). The functional activity of IRF7 in bats was further proven by Irving et al. (2020) who have determined that IRF7 (alongside IRF1 and IRF3) expression levels are elevated in most bat tissues and control gene expression, alongside the findings that IRF1 and IRF7 are additionally capable of basal regulation of ISG subsets in the absence of stimulation. Due to previous studies highlighting the fascinating functional conservation of bat IRF7 activity alongside its unique expression and activation patterns, we selected IRF7 from *P.alecto* for further structural and functional investigations to determine its cellular expression and further comprehend its pivotal role in bat innate antiviral immunity.

6.1.3 IFI35

Downstream to IRF7 activity and the induction of IFNs in mammals, is the production and release of ISGs, which play major roles in the innate immune defence during viral infection. In human cells, 50-1000 ISGs have been identified, which are dependent on cell type and duration of IFN stimulation, whereas the total number of ISGs in bats currently remains unknown (Schoggins and Rice, 2011, Banerjee et al., 2020).

Interferon-induced protein 35 (IFI35), otherwise known as IFP35, is an ISG that is induced in humans by the type II IFN, IFNγ, as identified by stimulation of HeLa cells and also by IFNα and IFNβ, identified in various other cells, whereby it can

translocate from the cell cytoplasm to the nucleus (Bange et al., 1994). IFI35 has also been identified in the *P.alecto* genome, yet its biological function remains largely unknown. De Masi et al. (2021) collated the known literature and identified that IFI35 acts as a pleiotropic factor influencing the activation of JAK-STAT and damage-associated molecular pattern (DAMP) pathways in innate immune-dependent inflammation, together with its involvement in the physiology and general pathology of a range of phylogenetically distant organisms. *In vitro* and *in vivo* studies on fish and mammals have established the role of IFI35 as an ISG with both antiviral and antiproliferative roles, however in a mouse model used to investigate sepsis, IFI35 was identified to act as a DAMP molecule, which contrastingly enhances inflammation (Xiahou et al., 2017, Tan et al., 2008, Wang et al., 2013). Further findings also suggest that IFI35 expression level is relevant in diseases of the central nervous system in humans such as Multiple Sclerosis and other chronic inflammatory disorders and is hence recognised as a molecule biomarker of disease activity (De Masi and Orlando, 2020).

Concurrent with our investigations into bat innate antiviral immunity, IFI35 is an ISG that is intriguingly proposed to possess both antiviral and pro-viral roles, which appear to be dependent on the type of viral infection and cell line used. Interesting findings by Das et al. (2014) have recognized human IFI35 as a factor required for VSV infection which acts as a negative regulator of the host antiviral response. These results are intriguing as the majority of ISGs are generally understood to exert antiviral functions (Panda et al., 2011). IFI35 consists of a leucine zipper domain which lacks the region required for DNA binding, yet it interacts with binding partners through N-myc-interacting domains (NIDs) and also interacts with another ISG known as N-myc interacting protein (NMI) to form a complex in response to IFNα treatment (Wang et al., 1996, Zhou et al., 2000). This IFI35-NMI interaction prevents proteasomal degradation of IFI35, however the functional consequence of its

degradation in the context of antiviral signalling remains unknown (Chen et al., 2000). During VSV infection, IFI35 was demonstrated to suppress RIG-I activation and additionally mediated its proteasomal degradation via ubiquitination. As RIG-I is an essential sensor for VSV infection, its downregulation by human IFI35 may prove advantageous in facilitating efficient VSV replication in the host (Kato et al., 2008).

Contrastingly, other studies have identified that IFI35, similar to other ISGs, does indeed act in an antiviral manner. During Bovine Foamy virus (BFV) infection, IFI35 was found to interact with the bovine Tas (BTas) regulatory protein and disrupts its ability to activate the transcription of viral genes and hence inhibits the replication of BFV (Tan et al., 2008). Furthermore, during swine (H3N2) influenza virus infection, IFI35 can inhibit replication via direct interaction with the NS1 viral protein (Yang et al., 2021). IFI35 was shown to bind to the effector domain of NS1 mechanistically and preferentially than to RIG-I, which promotes a mutual antagonism between IFI35 and NS1 and releases RIG-I from the previously identified IFI35-mediated ubiquitination and degradation. However, this study also found that during avian (H7N9) influenza infection, IFI35 does not interact with NS1 here and instead exhibits a contrasting tole to enable H7N9 replication (Yang et al., 2021).

Overall, previous research suggests a conflicting role of IFI35 that can act in the antiviral innate immune response, yet also facilitates the replication of certain viruses via the negative regulation of the viral RNA sensor RIG-I. It is apparent that further research into IFI35 is necessary to fully understand the role of this ISG in response to infection of different viral families and how this protein contributes to the pro- or anti-viral immune response of mammals. Accordingly, due to its annotation in the *P.alecto* genome, we therefore aimed to research IFI35 in bats, which to our knowledge has not been previously explored, in order to understand the role this protein delivers to bat hosts and their immunity and whether bat IFI35 activity aligns with previous findings to act in a pro or antiviral manner.

6.2 Results

6.2.1 IRF7

6.2.1.1 IRF7 Bioinformatic and Molecular Characterisation

Previous research by Zhou et al. (2014) identified a full-length IRF7 transcript in *P.alecto* via amplification of cDNA taken from bat spleens. Subsequent alignment identified the intron and exon structure of *P.alecto* IRF7 in addition to the protein domains present in human IRF7 and *P.alecto* IRF7. Using this preceding information, we labelled the protein domains present in paIRF7 and huIRF7 (Figure 6.1A). Both proteins shared domains, starting at their N-terminus with a DNA-binding domain (DBD), constitutive-activation domain (CAD), virus-activated domain (VAD) and inhibitory domain (ID) at the C-terminus. As previously highlighted by Zhou et al. (2014), the DBD of paIRF7 appears highly conserved with huIRF7 along with the majority of the ID at the C-terminus. However, there is an observed difference in protein domains evident in the VAD of paIRF7, beginning at amino acid 233 and ending at 298, whereas huIRF7 VAD starts at amino acid 246 and terminates at 305. This alteration of amino acids within the VAD also has a knock-on effect to the beginning of the ID in paIRF7, but the ID in both species ends at amino acid 468. The difference in VAD domain is prominent due to the role of this domain in binding with MyD88, TBK-1, TRAF3 and TRAF6 which are all upstream activators of IRF7 (Kawai et al., 2004, Zhou et al., 2014, Honda et al., 2004, Ning et al., 2011). Figure 6.1B displays an annotated 3D schematic of paIRF7, with labelled protein domains for visualisation. Multiple sequence alignment (MSA) of paIRF7 with huIRF7 displays the degree of amino acid conservation (Figure 6.1C). Amino acids conserved between two sequences are denoted by a dot in the sequence, but if the amino acid in paIRF7 differs with huIRF7, then the amino acid residue is alternatively shown. Analysis of these results show a high degree of amino acid conservation across the full length of paIRF7, however some clusters of amino acids that differ in paIRF7 are evident

throughout the IRF7 sequence for example, towards the end of the sequence after amino acid 235. This observed difference in amino acid residue appears to occur within the VAD and ID domains, aligning with the previous observations of difference in protein domains between paIRF7 and huIRF7.

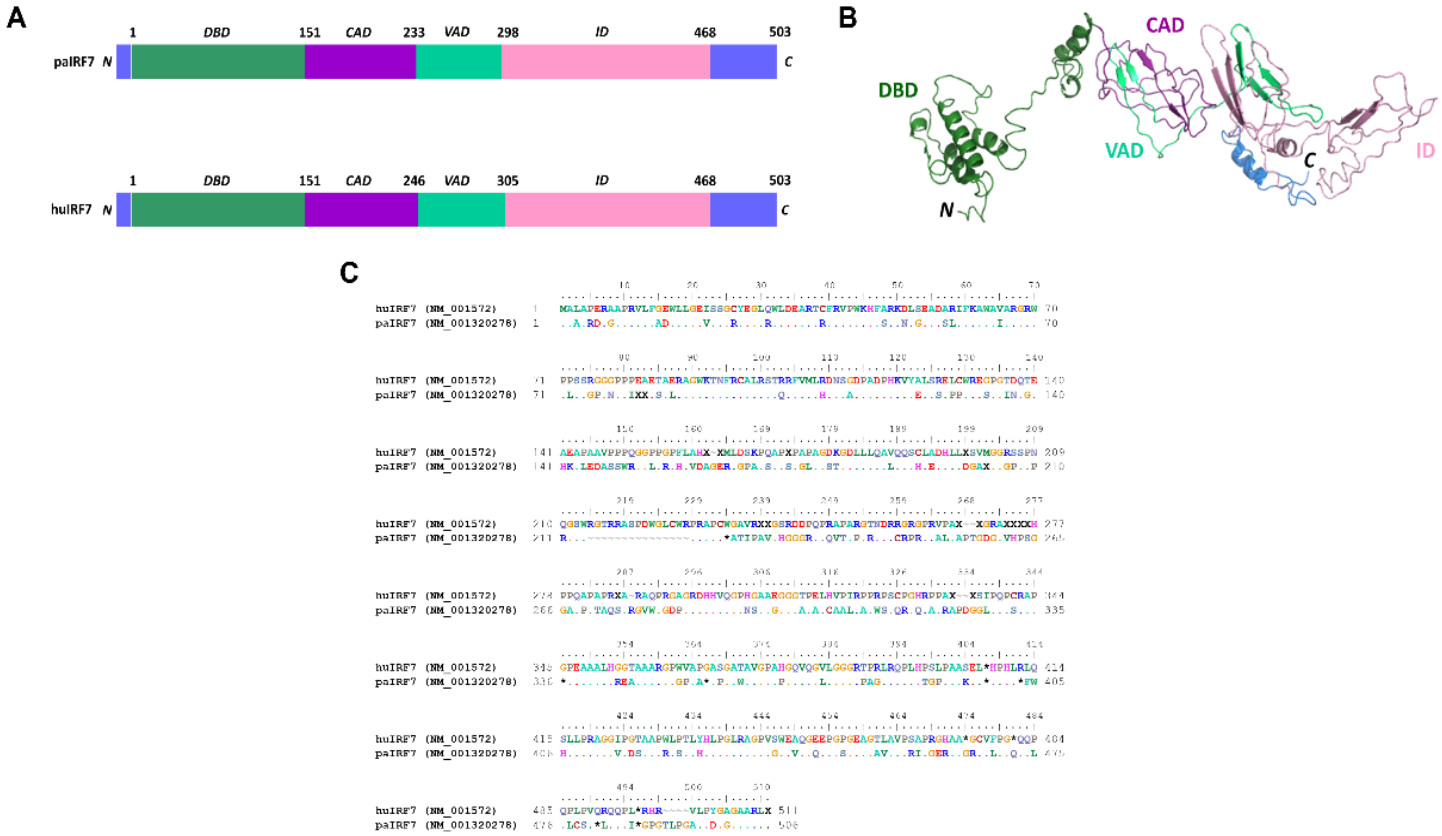

Figure 6.1 - Conservation of protein domains and sequence of paIRF7 with huIRF7. (A) *Conservation of protein domains in P.alecto IRF7 (paIRF7) and human IRF7 (huIRF7) both possessing an N-terminal DBD (DNA-binding domain), CAD (constitutive-activation domain), VAD (virus-activated domain) and an ID (inhibitory domain) at the C-terminus.* ***(B)*** *Annotated 3D schematic of paIRF7 displaying domains.* ***(C)*** *Multiple sequence alignment (MSA) of paIRF7 with huIRF7 displays sequence conservation. Conservation of residue at a position is denoted by a dot or alternatively stated if the residue differs at that position. huIRF7 and paIRF7 sequences were retrieved from the NCBI database with the accession numbers NM_001572 and NM_001320278 respectively. Alignment generated in BioEdit software.*

Phylogenetic analysis of *P.alecto* IRF7 with a selection of other species known to express IRF7, exhibited a close clustering of paIRF7 with other mammalian species (Figure 6.2A). Results indicate that paIRF7 is most closely related to IRF7 from the microbat species *M.davidii* and clustered closely with dog and horse IRF7. The close relation of genes from mammals belonging to Chiroptera, Carnivora and Periossodactyla has been previously described (Nishihara et al., 2006). A close phylogenetic relationship was also observed between paIRF7 and human IRF7, which was anticipated due to previous research identifying the conservation of innate immune genes between these species (Banerjee et al., 2020). The phylogenetic relationship of mouse and chicken IRF7 were more distant from *P.alecto* compared to other species investigated here. Pairwise identity analysis also exhibited the close relationship of *P.alecto* with other mammals; *M.davidii*, dog, horse, human and chimpanzee which all displayed high pairwise percentage scores of over 81%, representative of a high degree of residue conservation (Figure 6.2B). A lower conservation of *P.alecto* IRF7 with mouse (78%) and chicken IFI35 (63%) was observed which coincides with their more distant phylogenetic relationship.

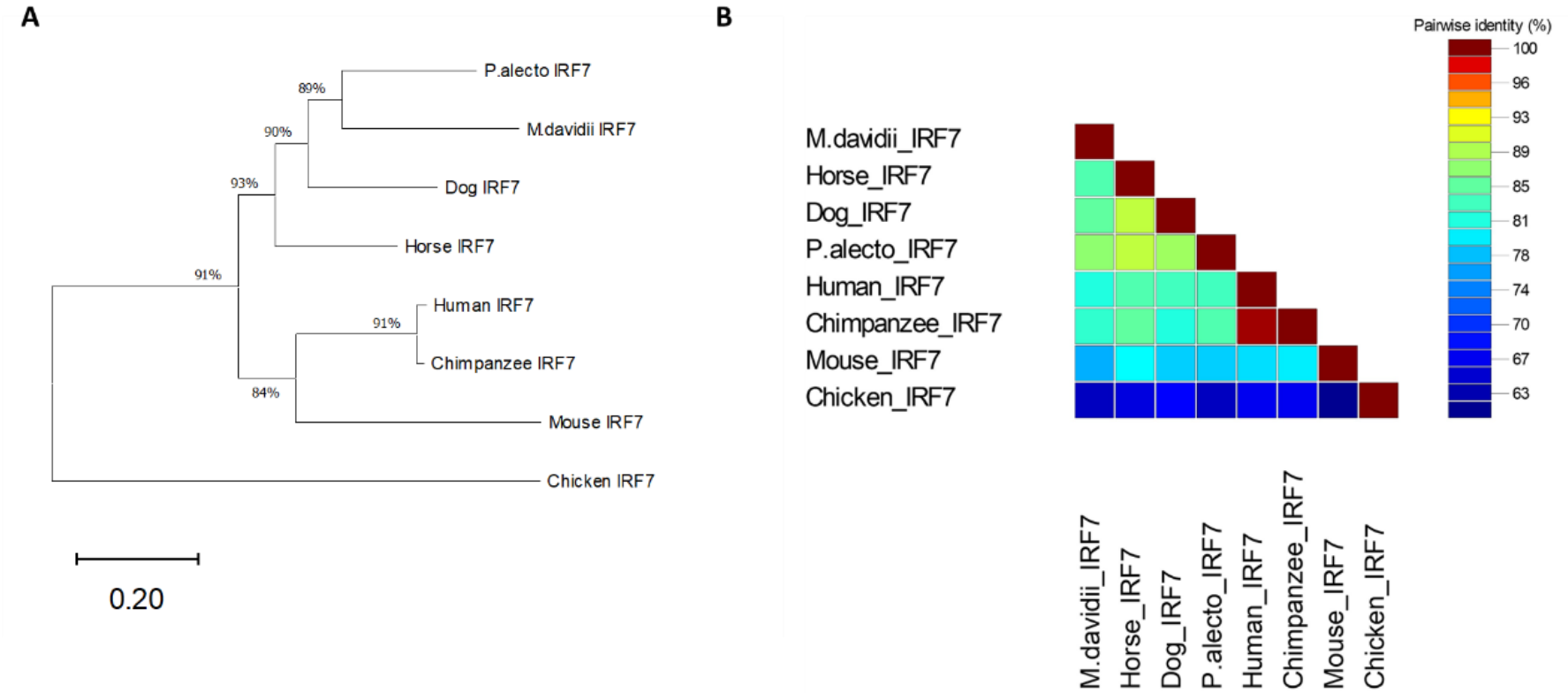

Figure 6.2 - Genomic analysis of IRF7 genes in bats, human, chimpanzee, horse, dog, mouse and chicken. (A) *Phylogenetic analysis of IRF7 genes in different species shows a strong phylogenetic relationship of paIRF7 with other mammals. Bootstrap probabilities (%) are denoted at the branch nodes and the scale bar at the bottom represents phylogenetic distance. Phylogenetic tree generated with a bootstrap of 1000 using maximum-likelihood method in MEGA11.0 software* ***(B)*** *Pairwise % identity analysis of IRF7 genes displays high sequence similarity of paIRF7 with IRF7 from other mammalian species. IRF7 sequences for all species were obtained from the NCBI database (Pteropus alecto: NM_001320278, Myotis davidii: KU161112, Human: NM_001572, Horse: XM_023654749, Chimpanzee: XM_016919997, Dog: XM_038424039, Mouse: NM_016850, Chicken: NM_205373). Pairwise identity matrix generated using the MUSCLE algorithm in SDT software.*

IRF7 plays an important role within the innate immune response functioning as a transcription factor. Human IRF7 has been well-characterised and shown to reside in the cell cytoplasm in its latent form, before activation via pathogenic infection which triggers the phosphorylation of IRF7 and its subsequent translocation into the cell nucleus whereby it stimulates transcription of target genes via binding promoter regions (Wathelet et al., 1998, Yang et al., 2003, Ning et al., 2011). Although the interestingly broad tissue distribution of bat IRF7 has been previously described, its cellular localization has not been studied in detail (Irving et al., 2020). Therefore, we aimed to observe the location of paIRF7 expressed *in vitro* and whether its translocation upon viral stimuli appears equivalent to its human counterpart. HEK293T cells were chosen as a mammalian vector cell line for paIRF7 expression analyses and were transfected with paIRF7 plasmids (Figure 6.3). Cells expressing paIRF7 were then treated with a selection of stimuli including paIFNα and paIFNλ, which represent type I and type III IFNs respectively, that had been previously generated in-house. Poly(I:C) and VSV-GFP were also used here for the stimulation of paIRF7. Results show that in unstimulated cells, paIRF7 resides solely in the cell cytoplasm, whereas upon stimulation using IFN and viral ligands, paIRF7 translocated to the cell nucleus and was subsequently observed in both the cytoplasm and nucleus of the stimulated cells. The location of paIRF7 in basal conditions alongside its translocation upon viral infection and stimulation is comparable with that of human IRF7.

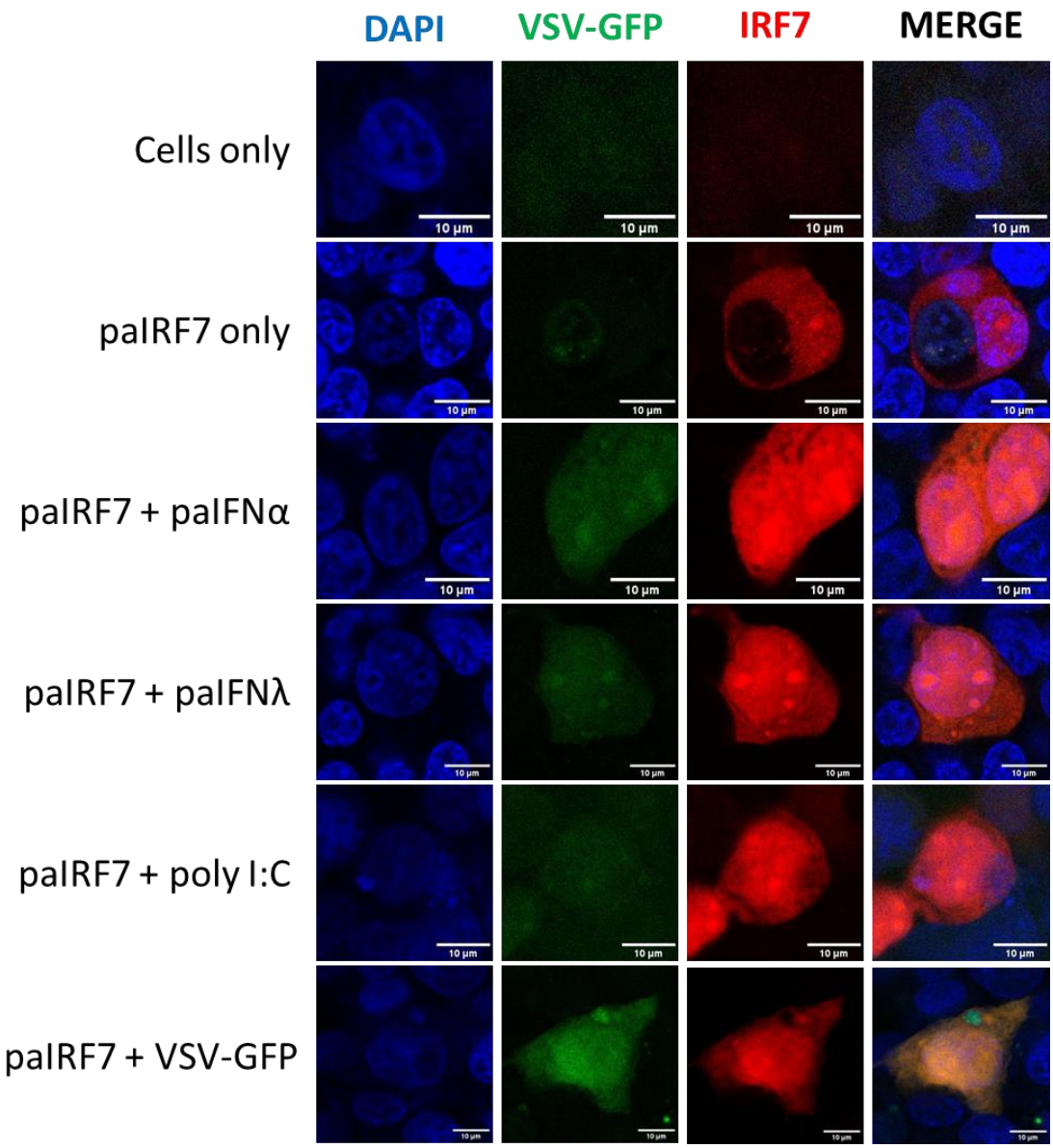

Figure 6.3 - Expression and stimulation of paIRF7 in transfected cells. *HEK293T cells were transfected with 2µg of plasmid expressing paIRF7-FLAG and 24hrs later were treated with either 200 units of paIFNα or paIFNλ, 150µg of poly (I:C) or infected with VSV-GFP at an MOI of 1.0. At 24 hours post-treatment, cells were stained for immunofluorescence using anti-FLAG primary antibodies for IRF7 and the corresponding fluorescent secondary antibody. Nuclei of cells were stained with DAPI before fixation and mounting for confocal imaging. Scale bar represents 10µm.*

6.2.1.2 An Investigation into paIRF7 Protein Domains and Their Influence on Location and Antiviral Activity

Following the observation of paIRF7 cellular localization and its translocation upon stimulation, we wanted to further assess the influence of different protein domains present in paIRF7 on its cellular location and activity. Using the previously described protein domains of paIRF7 (Figure 6.1A), we generated four distinct paIRF7 constructs which contained alternative stretches of the paIRF7 sequence and hence its protein domains, which were cloned into mRFP expression vectors for ease of visualisation (Figure 6.4A). Construct 1 (paIRF7-WT-mRFP) was generated by cloning all known protein domains in the wild type IRF7 gene into the mRFP expression plasmid. The second construct generated (paIRF7-ΔID-mRFP) lacks the ID domain whilst construct 3 (paIRF7-ΔID+VAD) lacks both the ID and VAD protein domains. Lastly, construct 4 (paIRF7-DBD-mRFP) contains only the N-terminus and DBD only. Figure 6.4B demonstrates 3D schematics of the paIRF7 protein, whereby the included protein domains for each cloned paIRF7-mRFP construct are described and labelled accordingly in the protein sequence.

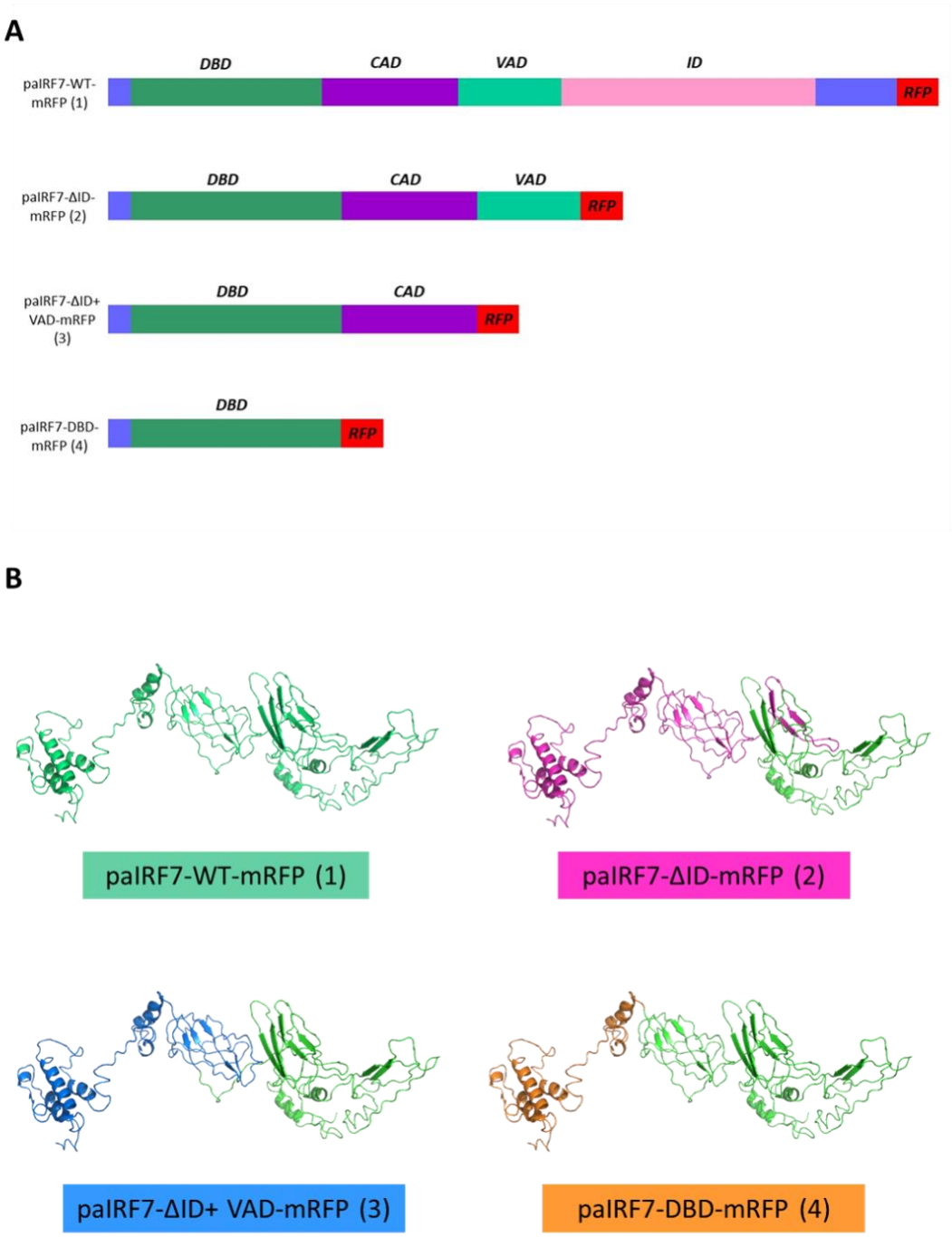

Figure 6.4 - The generation of paIRF7 clones containing distinct protein domains which were cloned into an mRFP vector expression plasmid. (A) *Schematic representation of the domains incorporated into each of the four paIRF7-mRFP constructs.* ***(B)*** *Annotated 3D diagrams representing paIRF7 protein structures. The sections of protein included within each of the four constructs are coloured and numbered accordingly, as displayed as sections of the complete protein structure.*

To examine the influence of the removal of different protein domains in paIRF7 on its cellular localization, we expressed the four distinct paIRF7-mRFP constructs in VeroE6 cells for immunofluorescence visualisation (Figure 6.5). Results showed that the first construct, containing all protein domains (paIRF7-WT-mRFP) resided solely in the cell cytoplasm of VeroE6 cells, reflecting the activity of the wild type paIRF7 protein. Construct 2 (paIRF7-ΔID-mRFP) however, which lacked the C-terminal inhibitory domain of the protein, showed expression in both the cell cytoplasm and the nucleus. The subsequent constructs 3 and 4 (paIRF7-ΔID+VAD-mRFP and paIRF7-DBD-mRFP respectively) also reflected the expression pattern of construct 2, whereby they were evident in both the cell cytoplasm and nucleus.

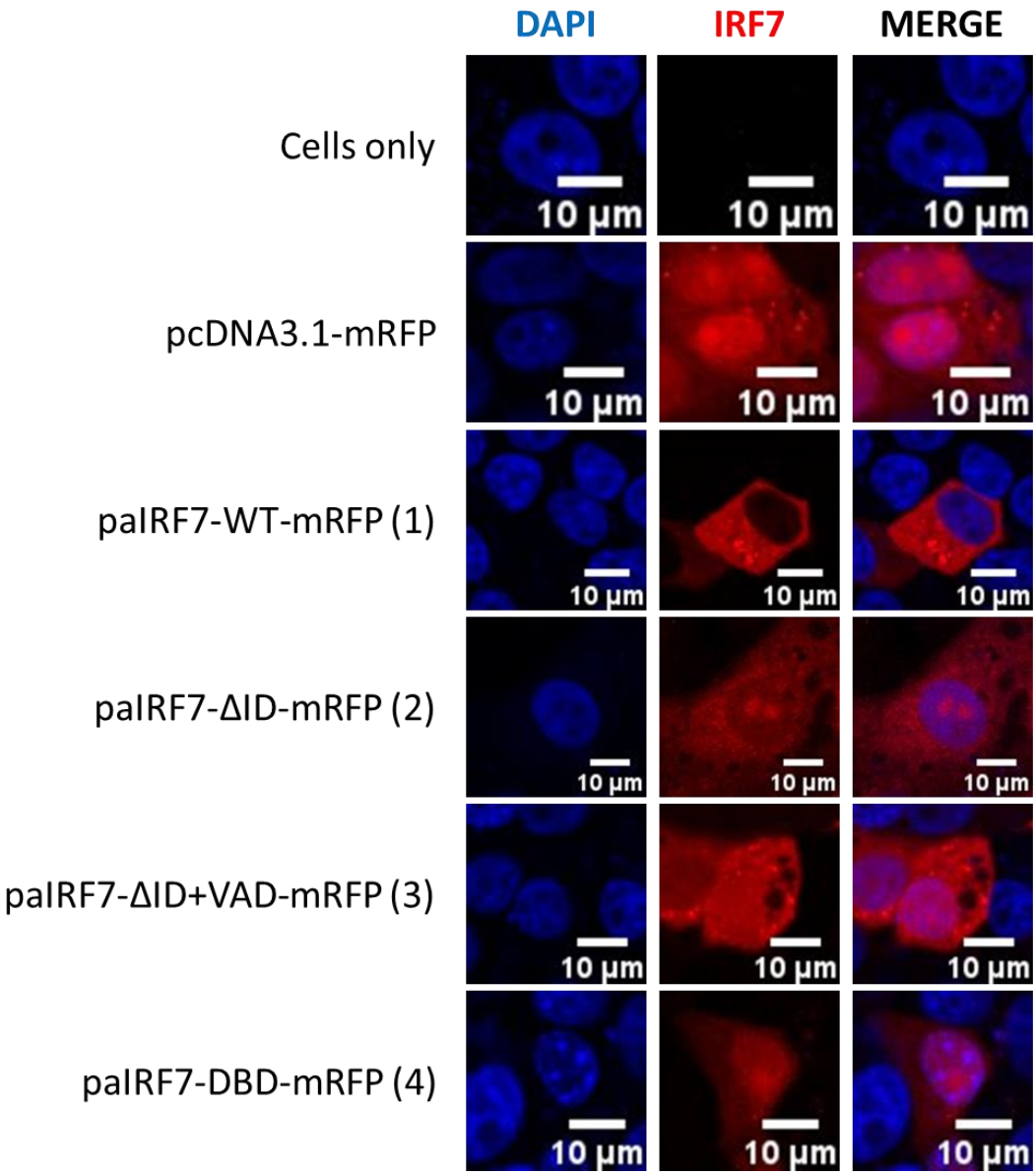

Figure 6.5 - Expression of paIRF7-mRFP protein domain constructs in transfected cells. *VeroE6 cells were transfected with the four paIRF7-mRFP constructs (paIRF7-WT-mRFP, paIRF7-ΔID-mRFP, paIRF7-ΔID+VAD-mRFP and paIRF7-DBD-mRFP) alongside a pcDNA3.1-mRFP expression control plasmid. At 24 hr post-transfection cells were stained with DAPI for visualisation of nuclei and imaged using confocal microscopy. Scale bars are displayed and represent 10µm.*

It is well recognised that wild-type IRF7 in human resides in the cell cytoplasm until a viral stimulus causes it to translocate to the cell nucleus. We previously observed this equal action of wild type paIRF7 (Figure 6.3). However, due to the previous results exhibiting the nuclear expression of paIRF7-mRFP constructs lacking the C-terminal and ID domains in absence of viral stimulation (Figure 6.5), we consequently aimed to infect cells expressing the four paIRF7-mRFP constructs to observe their activity in response to VSV-GFP infection. Figure 6.6 demonstrates the expression of all four paIRF7-mRFP constructs in both the presence and absence of VSV-GFP infection when expressed in VeroE6 cells and visualised via confocal imaging. Results show the expression of construct 1 (paIRF7-WT-mRFP) solely within the cell cytoplasm, consistent with previous findings. However, the paIRF7-WT-mRFP construct did not appear to translocate to the cell nucleus during VSV-GFP infection as initially anticipated and remained only in the cytoplasm. The expression of constructs 2,3 and 4 (paIRF7-ΔID-mRFP, paIRF7-ΔID+VAD-mRFP and paIRF7-DBD-mRFP respectively), displayed cellular expression previously observed (Figure 6.5), whereby they are present in both the cell cytoplasm and nucleus. Therefore, the stimulation of these constructs with VSV-GFP here does not appear to influence their localisation. Hence, it can be theorised that the location of constructs 2, 3 and 4 in both the cytoplasm and nucleus is irrespective of viral infection here. Consequently, the removal of the ID in paIRF7 must somewhat influence the location of the protein to the cell nucleus, as constructs 2 onwards lack this domain and all exhibit the same unprecedented nuclear expression pattern. Additionally, it should be noted that an empty plasmid control was not used here, thus the observed activity could be resultant of transfection and should be taken into consideration.

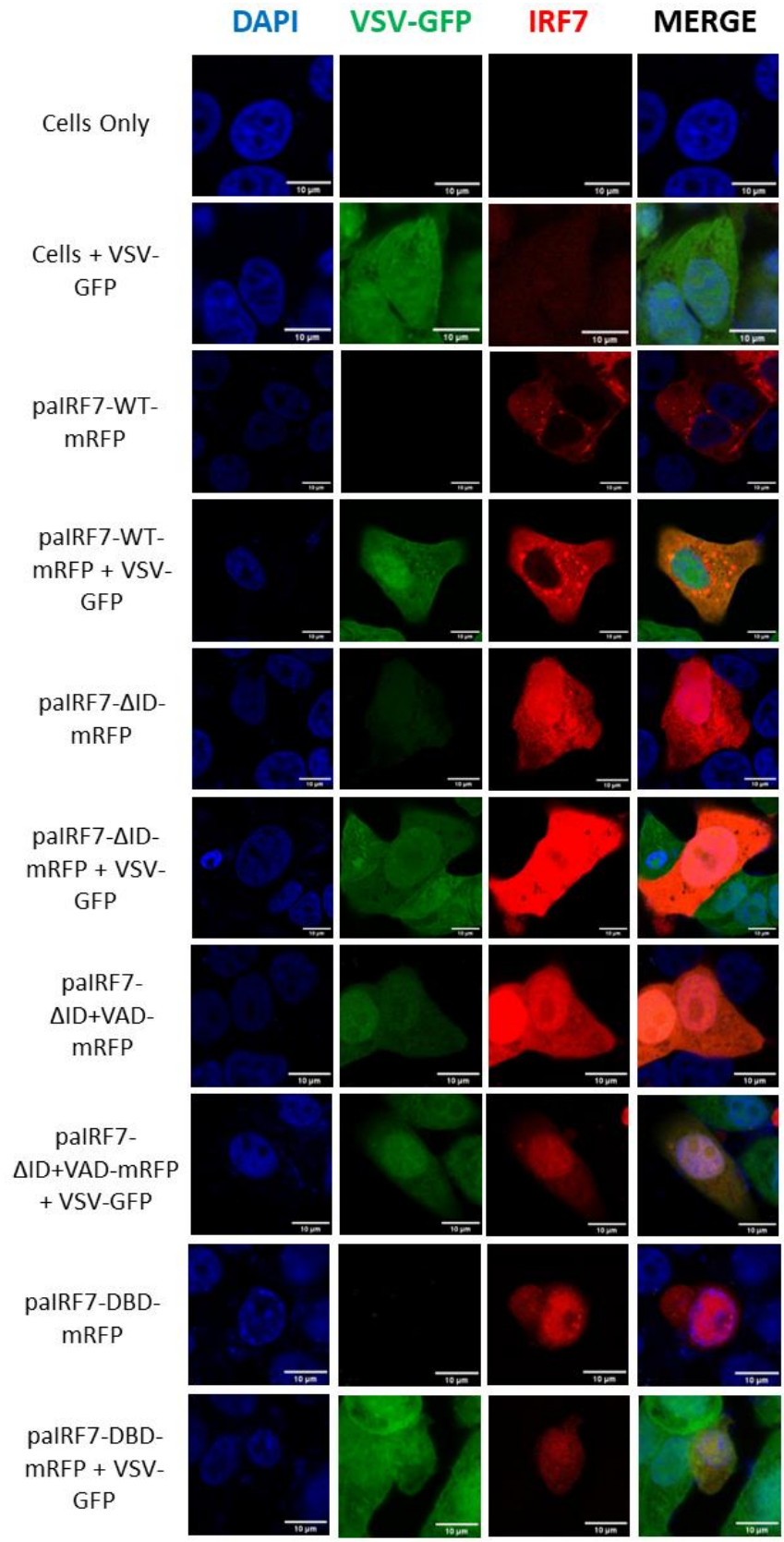

Figure 6.6 - Expression of paIRF7-mRFP protein domain constructs in transfected cells and stimulated with VSV-GFP. *VeroE6 cells were either independently transfected with 2µg of a paIRF7-mRFP construct only or at 24 hours post-transfection, were also infected with VSV-GFP at an MOI of 1.0. At 24 hours post-infection, cell nuclei were stained with DAPI and cells were fixed for confocal imaging. Scale bars represent 10µm.*

Due to the previous observation of paIRF7-WT-mRFP (construct 1) expression to remain cytoplasmic even in the presence of VSV-GFP infection (Figure 6.6), we aimed to repeat this experiment to deduce if our previous analysis was a true representation of the cellular location of the paIRF7-WT-mRFP construct. We repeated the investigation of the construct paIRF7-WT-mRFP because it contains conserved domains of the wild type protein and hence we expected to observe the translocation of this protein to the cell nucleus upon viral infection. We hypothesised that the prior lack of translocation observed in the cell we imaged in Figure 6.6 may be because IRF7 had not been activated yet or alternatively its activity was masked by a high titre of virus within that cell. Furthermore, when imaging, it was difficult to identify cells expressing paIRF7-WT-mRFP and VSV-GFP, as in most cells, the conjectured antiviral activity of the paIRF7-WT-mRFP resulted in a diminished viral signal. Upon repeating, the expression of the paIRF7-WT-mRFP construct remained solely cytoplasmic in absence of stimulation but subsequently displayed translocation to the cell nucleus upon infection of VSV-GFP as initially expected, as demonstrated in Figure 6.7. Although these results align more with the expected behaviour of the paIRF7-WT-mRFP construct under viral stimulation, they contrast the previous findings and therefore we cannot deduce the true activity of this construct without additional studies, ideally in bat cells, to confirm the true expression.

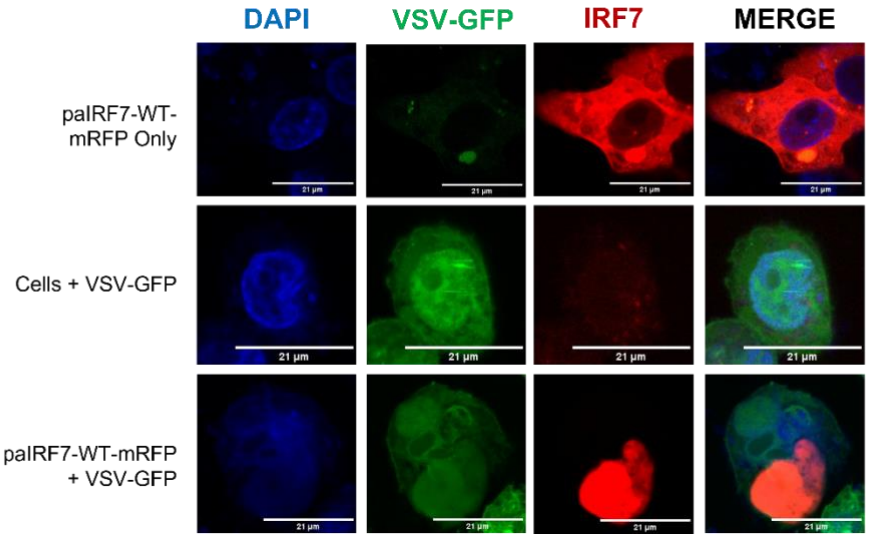

Figure 6.7 - Repeat of expression of paIRF7-WT-mRFP (construct 1) in the presence of VSV-GFP infection. *VeroE6 cells were transfected with 2µg of the paIRF7-WT-mRFP plasmid. At 24 hours post-transfection cells were either stimulated with VSV-GFP at an MOI of 1.0 or left unstimulated. DAPI was used to stain cell nuclei at 24 hours post-infection and cells were fixed for confocal visualisation. paIRF7-WT-mRFP construct appeared to translocate to the cell nucleus in presence of VSV-GFP infection. Scale bars represent 21µm.*

Our previous observations detected that paIRF7-WT-mRFP resides in the cell cytoplasm, whilst subsequent IRF7 constructs lacking their C-terminus and ID appeared to also express in the cell nucleus (Figure 6.5 and Figure 6.6). Similar investigations have been previously undertaken into human IFR7 domains, which identified a parallel expression pattern whereby the deletion of the C-terminal domain resulted in the nuclear expression of human IRF7 (Lin et al., 2000). This previous research identified the existence of a leucine-rich region present within the C-terminal domain of human IRF7 (LVLVKLEPWLCVHL) that represents a consensus for a nuclear export sequence (NES) (Lin et al., 2000). Therefore, to understand if this NES is present in *P.alecto* IRF7 and whether the removal of this sequence underlies the auto-translocation of paIRF7-mRFP constructs to the cell nucleus, we aligned the NES region of human IRF7 with the same region in *P.alecto IRF7* (Figure 6.8A). Results showed a high degree of conservation within the NES residues of human and *P.alecto* IRF7 which differed by only two residues. Figure 6.8B demonstrates the

NES region within the 3D schematic of the *P.alecto* IRF7 protein for contextualisation. To further observe variation with this NES region in other species, we aligned the stretch of IRF7 sequence representing the identified NES region in human and bat alongside other animals expressing IRF7, as shown in Figure 6.8C. Results show a high degree of conservation within the first few residues in the NES between all species investigated, but an increased variation within residues is observed towards the end of the NES.

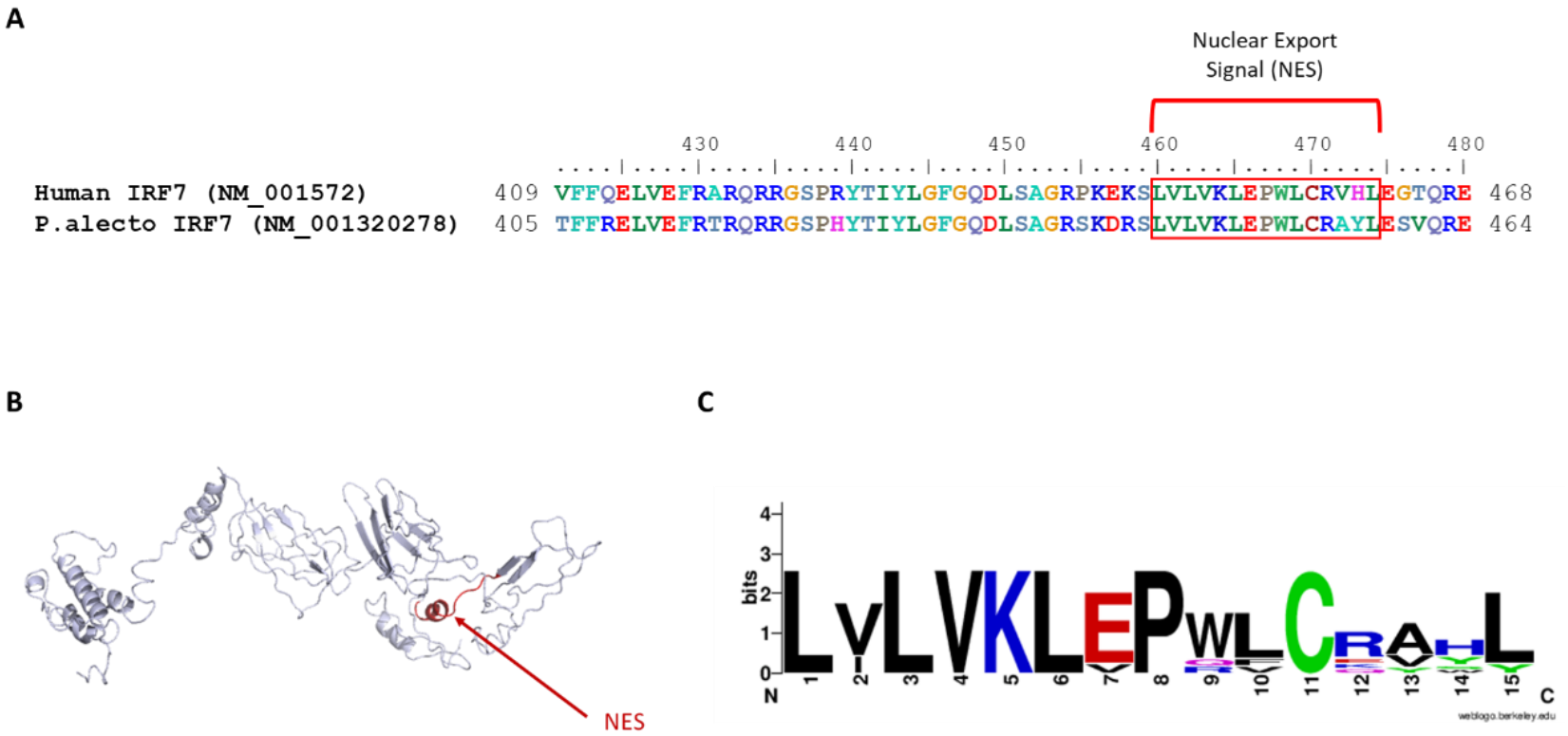

Figure 6.8 - Nuclear export sequence (NES) analysis. (A) *ClustalW multiple sequence alignment of P.alecto IRF7 with human IRF7, highlighting the NES conservation between the two species.* ***(B)*** *3D schematic representation of P.alecto IRF7 demonstrating the NES within its structure.* ***(C)*** *Conservation alignment of residues within the IRF7 NES of different species (Human IRF7 (NM_001572), P.alecto IRF7 (NM_001320278), M.davidii IRF7 (KU161112), Horse IRF7 (XM_023654749), Chimpanzee IRF7 (XM_016919997), Dog IRF7 (XM_038424039), Mouse IRF7 (NM_016850) and Chicken IRF7 (NM_205372)). Sequence conservation plot was generated using the WebLogo software. Residues are denoted by their one letter amino acid abbreviation. The number on the X-axis is representative of position within the specific NES sequence starting from 1(NES position 448) to 15 (NES residue 463). There is one stack for each position in the sequence where the overall height of the symbols in the stack represents the relative frequency of each amino acid at that position, indicative of residue conservation at that position.*

As IRF7 is pivotal for the induction of IFNs in response to viral stimulation, we aimed to utilise our generated paIRF7-mRFP constructs to observe the influence the absence of different protein domains within the IRF7 sequence has on its antiviral activity. The four paIRF7-mRFP constructs were expressed in VeroE6 cells alongside controls and infected with VSV-GFP at an MOI of 0.25. Supernatants from these cells were then quantified via plaque assay analysis to observe their influence on VSV replication (Figure 6.9A). Results indicate that although the VSV replication varies between the four paIRF7-mRFP constructs, they all exhibit a lower viral titre than the infected cells control, suggesting that despite the removal of different protein domains, *P.alecto* IRF7 remains somewhat active. Interestingly, the highest antiviral activity displayed against VSV replication was observed in constructs 2 and 3 which represent paIRF7-ΔID-mRFP and paIRF7-ΔID+VAD-mRFP respectively. The paIRF7-WT-mRFP, representing construct 1 which contains all the protein domains of the wildtype IRF7, displayed slightly less antiviral activity than constructs 2 and 3 and construct 4 demonstrated the least antiviral activity as represented by exhibiting the highest viral titre. Quantification of plaques was carried out by counting plaque formation at the 10^{-6} dilution to use for PFU/mL calculation, representative of VSV titre (Figure 6.9B). This investigation was only assessed once for each individual construct and therefore to achieve a true representation of antiviral activity for each paIRF7-mRFP construct against VSV-GFP infection in VeroE6 cells this study should be repeated for further confirmation. Additionally, an empty plasmid control should also be included to observe any influence of transfection on antiviral activity outcome.

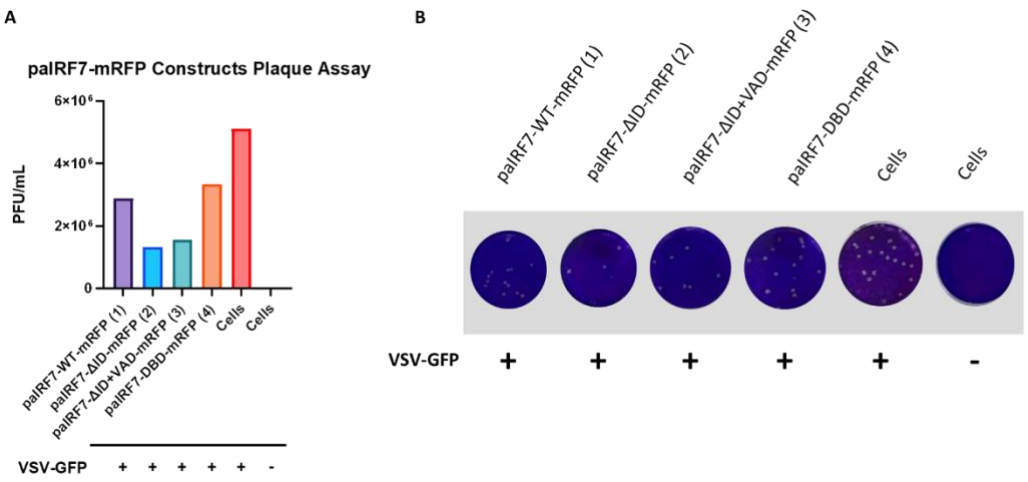

Figure 6.9 - The antiviral activity of palRF7-mRFP constructs measured against VSV-GFP replication. (A) *VeroE6 cells were transfected with 2µg of one of the IRF7-mRFP constructs (palRF7-WT-mRFP (1), palRF7-ΔID-mRFP (2), palRF7-ΔID+VAD-mRFP (3) or palRF7-DBD-mRFP (4)) or left non-transfected for 24 hours. Cells were subsequently infected with VSV-GFP at an MOI of 0.25 or left uninfected for 24 hours before quantification via plaque assay analysis using VeroE6 cells in a 12-well format. As this plaque assay was only carried out once, significance could not be determined. Figure was generated using Graphpad Prism 8 software.**(B)** Plaques were counted and used for PFU/mL calculation and quantification at the 10^{-6} dilution.*

6.2.2 IFI35

6.2.2.1 Bioinformatic Analysis of paIFI35

IFI35 has been identified in several mammalian species including human, monkey and cow, alongside a selection of non-mammalian animals such as chicken, zebrafish and frog (Jia et al., 2022, Li et al., 2021). IFI35 activity has been largely explored in humans, yet the characterisation of IFI35 in bats remains undetermined (Tan et al., 2008). Due to its pivotal role as an ISG in mammals, we aimed to investigate and characterise the IFI35 gene in the megabat species *P.alecto* (paIFI35). To evaluate the conservation of gene collinearity among IFI35 homologues at the chromosomal level, we compared IFI35 from *P.alecto* with selected species of interest for a broad analysis. IFI35 homologues in different species are located on different chromosomes, as shown in Figure 6.10A. For the megabat species *P.alecto* and the microbat *M.davidii*, the IFI35 gene is displayed on an uncharacterised gene scaffold, this is due to the lack of genomic annotation within these bat species.

Consequently, further annotation is required to determine the chromosomal location of these bat IFI35 genes. Overall, gene synteny remained largely conserved within the mammalian species investigated here and was also intriguingly similar to chicken IFI35. The IFI35 gene is flanked upstream by the genes G6PCR, AOC3 and PSME3 and downstream by RND2 in all respective species evaluated here.

Figure 6.10B demonstrates the direct comparison of protein domains of paIFI35 with human IFI35. IFI35 protein domains in both species were identified using the NCBI protein domain prediction software using the human IFI35 (NM_005533) and *P.alecto* IFI35 (XM_006924567) sequences also obtained from the NCBI database. Results indicate that IFI35 in both species are conserved in their domains, both possessing an N-terminus and two separate NID domains (NID1 and NID2). The N-terminus of IFI35 contains a leucine zipper motif in an alpha helical configuration and also includes NMI, which is a homologous IFN-induced protein. The two NID domains represent domains that are tandemly repeated within IFI35 proteins alongside NMI, which mediates protein interactions and subcellular localisation. Additionally, protein prediction software identified the presence of an RNA recognition motif superfamily, known as RBD in human IFI35. The RBD is an abundant domain present in eukaryotes which is recognised in proteins involved in post-transcriptional gene expression, such a mRNA and rRNA processing, RNA stability and export. This RBD consists of four stranded beta-sheets packed with two alpha-helices and usually interacts with ssRNA but has also been identified to interact with ssDNA and proteins. The RBD was not detected in paIFI35, but this may be due to lack of genomic annotation within bat species. Overall, however, it can be deduced that the protein domains in paIFI35 are highly conserved with those in human IFI35 and the two proteins share a similar sequence length. Figure 6.10C represents a schematic 3D demonstration of the N-terminus, NID1 and NID2 protein domains identified in paIFI35 within its protein confirmation.

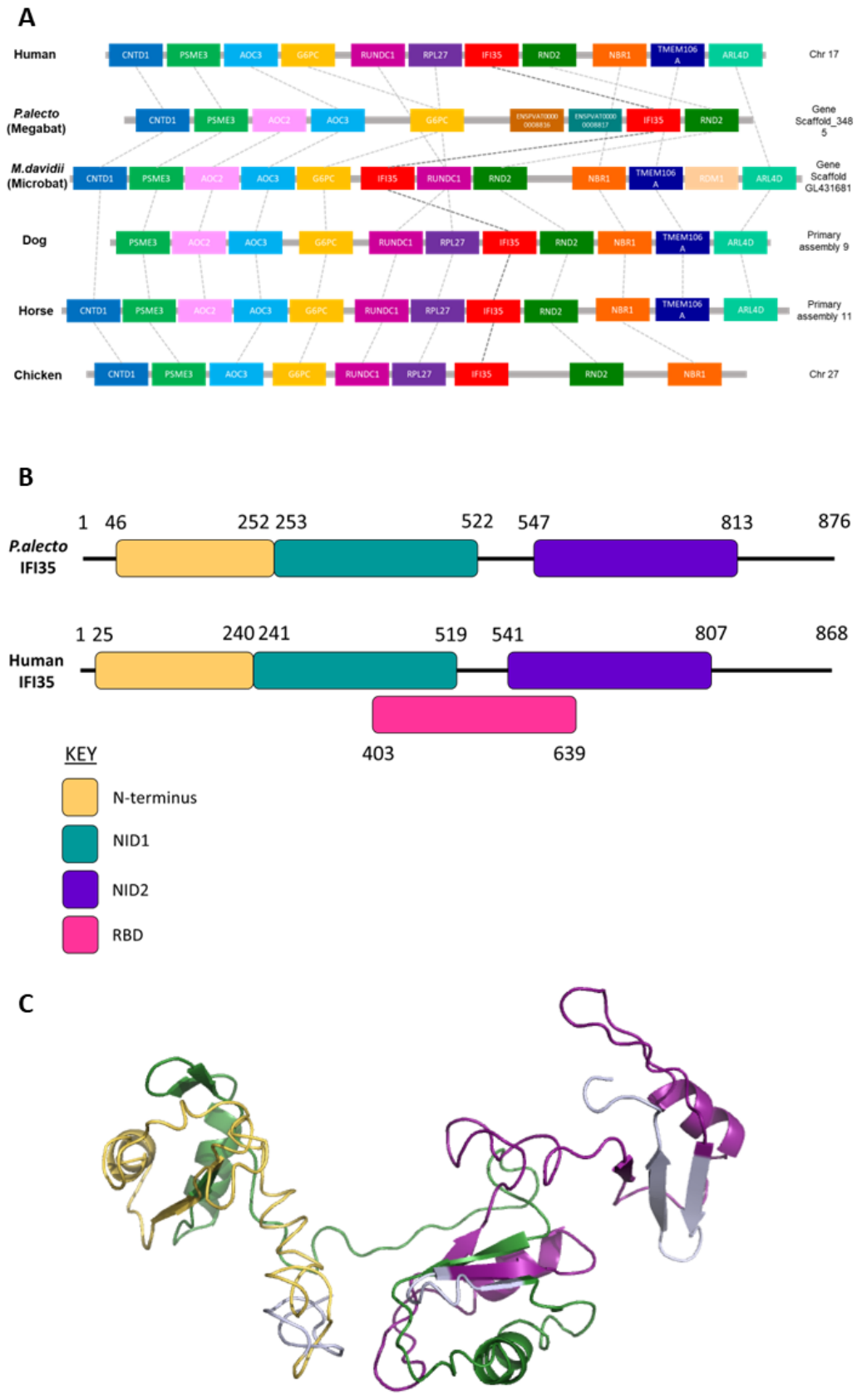
A
Human
CNTD1
PSME3
AOC3
G6PC
RUNDC1
RPL27
IFI35
RND2
NBR1
TMEM106A
ARL4D
Chr 17
P.alecto (Megabat)
CNTD1
PSME3
AOC2
AOC3
G6PC
IFI35
RND2
Gene Scaffold_3485
M.davidii (Microbat)
CNTD1
PSME3
AOC2
AOC3
G6PC
IFI35
RUNDC1
RND2
NBR1
TMEM106A
RDM1
ARL4D
Gene Scaffold GL431681
Dog
PSME3
AOC2
AOC3
G6PC
RUNDC1
RPL27
IFI35
RND2
NBR1
TMEM106A
ARL4D
Primary assembly 9
Horse
CNTD1
PSME3
AOC2
AOC3
G6PC
RUNDC1
RPL27
IFI35
RND2
NBR1
TMEM106A
ARL4D
Primary assembly 11
Chicken
CNTD1
PSME3
AOC3
G6PC
RUNDC1
RPL27
IFI35
RND2
NBR1
Chr 27
B
P.alecto IFI35
1
46
252
253
522
547
813
876
Human IFI35
1
25
240
241
519
541
807
868
403
639
KEY
N-terminus
NID1
NID2
RBD
C

Figure 6.10 - Bioinformatic analyses of P.alecto IFI35. (A) *Gene syntenic analysis showing the chromosomal location of the IFI35 locus in compared species, which is flanked upstream by G6PCR, AOC3 and PSME3 and downstream by RND2.* ***(B)*** *The conservation of protein domains in P.alecto IFI35 with human IFI35* ***(C)*** *3D schematic displaying P.alecto protein domains and structure.*

Due to the high degree of synteny between paIFI35 and IFI35 genes in other species, alongside the conservation of protein domains observed between paIFI35 and human paIFI35, we next sought to observe the amino acid sequence conservation between IFI35 from other mammalian species. Figure 6.11 shows the alignment of IFI35 sequences, including paIFI35, with human IFI35, generated using ClustalW multiple sequence alignment with a bootstrap of 1000 in BioEdit software. Amino acid conservation at each position is denoted by a dot, or the alternative residue if stated if varied at that position and gaps in the aligned amino acid sequence are represented by a dash. Overall, paIFI35 appears highly conserved with the amino acid sequence of human IFI35 but presents some alternative residue expression throughout the IFI35 sequence.

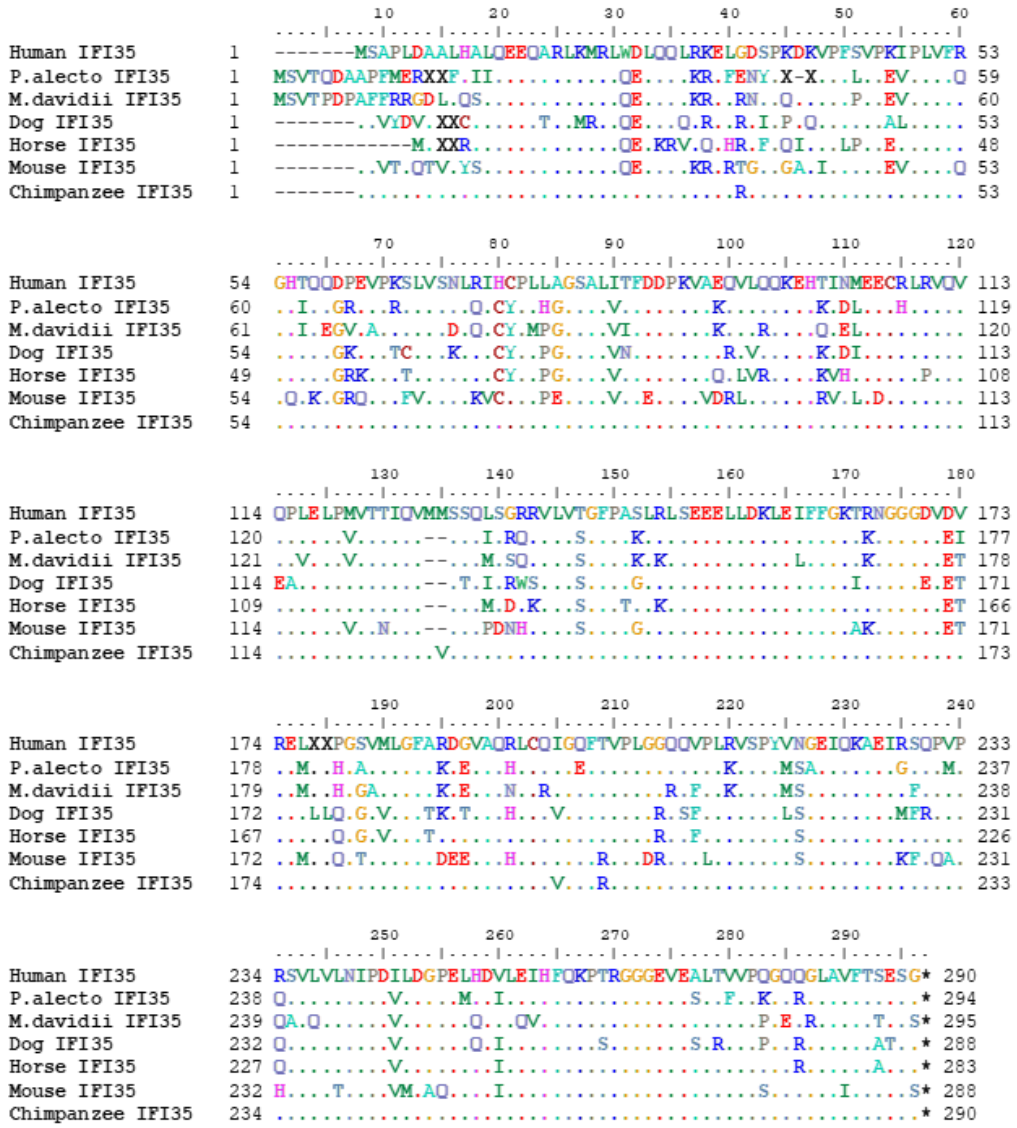

Figure 6.11 - Multiple sequence alignment (MSA) allowing sequence comparison of IFI35 in different mammalian species. *IFI35 sequences were retrieved from a selection of mammalian species including the megabat P.alecto and microbat M.davidii to align with human IFI35 for direct sequence comparison. Alignment was carried out in BioEdit software using the ClustalW multiple alignment tool with a bootstrap value of 1000. IFI35 sequences were retrieved from the NCBI database (Human IFI35 (NM_005533), P.alecto IFI35 (XM_006924567), M.davidii IFI35 (XM_015570566), Dog IFI35 (XM_038676367), Horse IFI35 (XM_001492387), Mouse IFI35 (NM_027320), Chimpanzee IFI35 (XM_001158983)).*

Phylogenetic analysis of paIFI35 displayed a close phylogenetic relationship to the microbat *M.davidii* and also to other mammals investigated (Figure 6.12A). IFI35 in bats appeared to cluster more closely with members of the Pegasoferae clade, containing dog and horse IFI35, than to human and chimpanzee IFI35 (Nishihara et al., 2006). However, human and chimpanzee IFI35 still exhibited a close mammalian phylogenetic relationship to paIFI35 of 73%. Chicken IFI35 appeared the most phylogenetically distant, however relation was still high at 73%. Pairwise identity analysis unveiled a similar relationship between paIFI35 and other mammals, whereby a high sequence conservation is observed between paIFI35 and other mammals sharing at least 82% pairwise identity (Figure 6.12B). A particularly high pairwise identity is observed between IFI35 in the bat species *P.alecto* and *M.davidii* with horse IFI35, with representative identity scores of around 90% and 93% respectively. Contrastingly, pairwise analysis identified the lowest conservation of paIFI35 is with chicken IFI35, with an identity score of less than 65% as expected for a non-mammalian IFI35 gene.

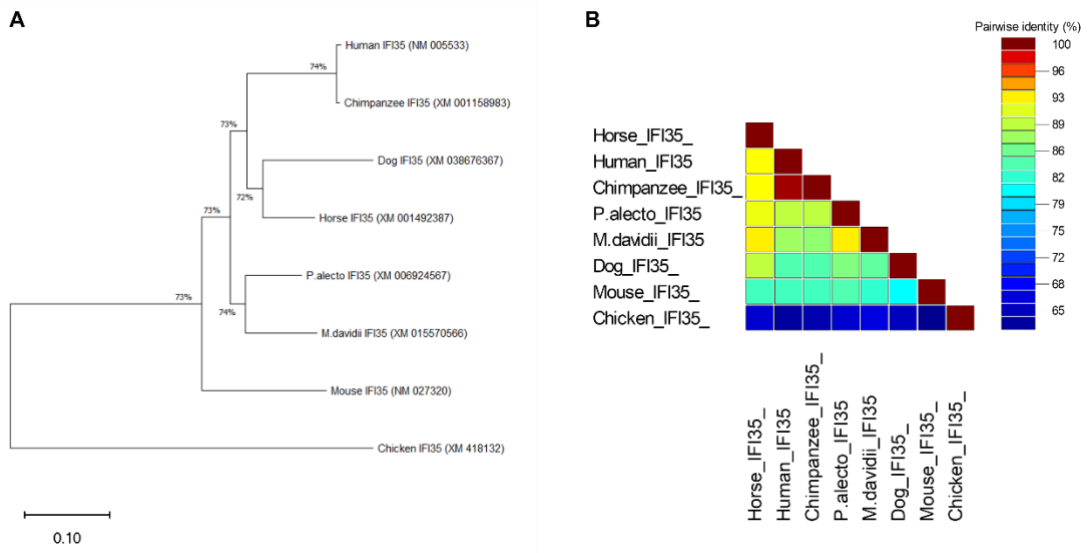

Figure 6.12 - Genomic analysis of IFI35 genes in selected species. (A) *Phylogenetic analysis of IFI35 genes in different species displays the close relationship of P.alecto IFI35 to other mammals. Bootstrap probabilities (%) are denoted at the node of each branch and scale bar represents the phylogenetic distance. Phylogenetic tree was generated using the maximum-likelihood method with a bootstrap value of 1000 in the MEGA11.0 software. IFI35 sequences were retrieved from the NCBI database, and their accession numbers are listed.* ***(B)*** *Pairwise % identity of IFI35 genes displays a high sequence similarity between P.alecto IFI35 and IFI35 genes in other mammalian species. Pairwise identity matrix was generated using the MUSCLE algorithm in SDT software. The IFI35 sequences used here were consistent with previous annotation.*

6.2.2.2 IFI35 Expression and Antiviral Activity

To our knowledge, the biological activity and role of IFI35 from the megabat *P.alecto* had not been previously explored *in vitro* and hence the cellular location and expression of paIFI35 is unknown. Therefore, we aimed to visualise the localisation of paIFI35 when expressed in mammalian cells via immunofluorescence analysis and staining against the FLAG-tag on the paIFI35-FLAG plasmid. HEK293T cells were transfected with paIFI35 and stained using immunofluorescent antibodies for confocal imaging (Figure 6.13A). Results show that paIFI35 expression is largely cytoplasmic but also appears partially within the cell nucleus. To confirm the successful expression of the paIFI35 plasmid used here, we also visualised IFI35 protein expression using different concentrations of paIFI35 expressed in HEK293T cells via Western blotting (Figure 6.13B). However, it should be noted that a loading control such as alpha tubulin should have been included here to ensure accuracy of band size.

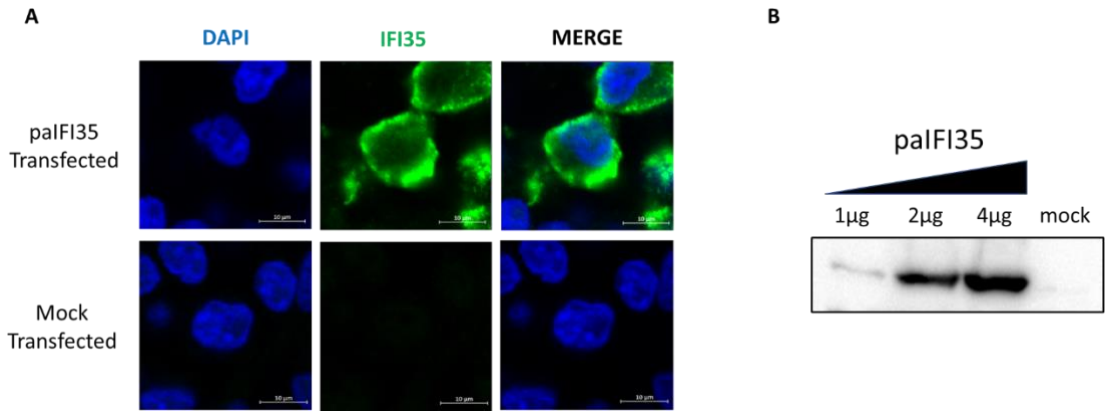

Figure 6.13 - Expression of P.alecto IFI35 (paIFI35) in HEK293T cells. (A) *HEK293T cells were transfected with 1µg of paIFI35-FLAG or mock-transfected. At 24 hours post-transfection cells were fixed and stained using anti-FLAG (rabbit) primary antibodies directed towards the FLAG tag on the paIFI35 plasmid and the secondary antibody Alexafluor anti-rabbit (mouse) 488. Nuclei were stained with DAPI before confocal visualisation. paIFI35 expression is exhibited throughout the cell cytoplasm and partially in the nucleus. Scale bars represent 10 µm.* ***(B)*** *HEK293T cells were transfected with different quantities (1 µg , 2 µg or 4 µg) of paIFI35 plasmid or mock-transfected with an empty pCAGG plasmid and analysed via Western blotting.*

As previous immunofluorescent results identified the cellular location of paIFI35 to exist largely in the cell cytoplasm, we aimed to further explore whether paIFI35 co-localised to any cytoplasmic organelles, which may also underlie its role within the bat host. To investigate this, HEK293T cells were transfected with paIFI35 as studied previously and were also co-transfected with plasmids targeted towards the ER, mitochondria, and peroxisome organelle structures (Figure 6.14). The co-transfected plasmids directed towards cellular organelles all expressed RFP, therefore staining of paIFI35 using immunofluorescent antibodies at a wavelength of 488, generating a green signal, permitted the co-observation of their expression patterns *in vitro*. Results indicated that paIFI35 did not co-localise with any of the organelles investigated here. However, it was evident that paIFI35 was present in small distinct clusters within the cytoplasm, suggesting a potential co-localisation to an alternative cytoplasmic structure which requires future investigation.

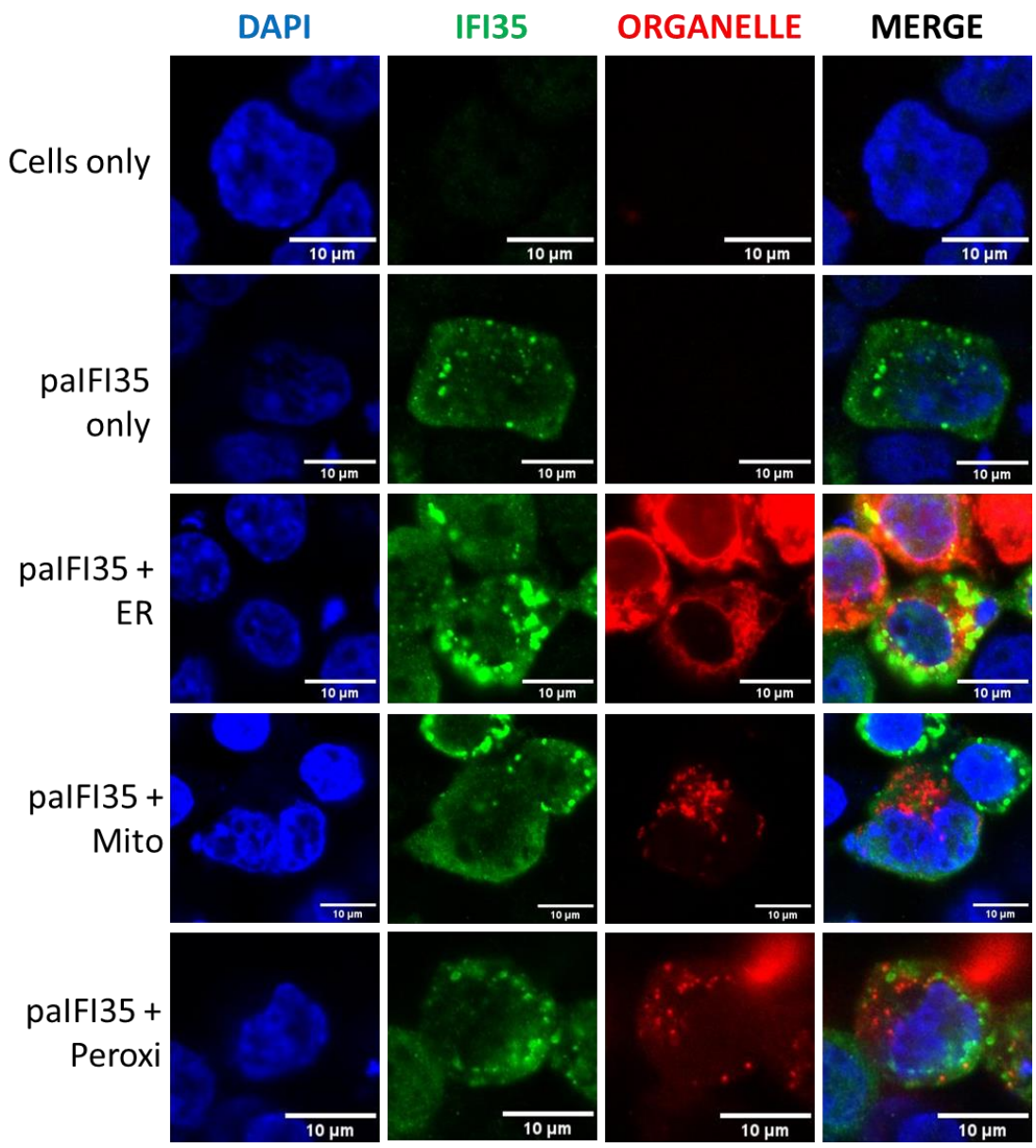

Figure 6.14 - Co-localisation analysis of paIFI35 and organelle expression in HEK293T cells. *HEK293T cells were transfected with 1µg of paIFI35-FLAG only, or were co-transfected using 1µg of paIFI35-FLAG alongside 1 µg of the following organelle plasmids; endoplasmic reticulum (ER) (Pmcherry-ER3), mitochondria (14.pHcRed1mito) or peroxisome (DsRedPeroxisome4) which all expressed RFP. At 24 hours post-transfection, cells were stained using anti-FLAG (rabbit) primary antibodies raised against FLAG tag in IFI35 and subsequently stained with Alexafluor anti-rabbit (goat) 488 secondary antibodies. Nuclei were stained with DAPI and cells were mounted for confocal imaging. paIFI35 does not appear to co-localise within any of the organelles investigated here but displays distinct localised expression patterns. Appropriate scale bars are included for each image and represent 10 µm.*

Due to previous contrasting evidence in the literature suggesting both a pro and antiviral function of IFI35 in human and other animals, we wanted to observe the influence of *P.alecto* IFI35 on the replication of VSV. This was quantified via a plaque assay whereby VeroE6 cells were transfected with paIFI35, paMx1, which is a known antiviral ISG, or alternatively left un-transfected. Cells were later infected with VSV-GFP at an MOI of 0.25 for 24 hours. Viral supernatant obtained from these cells was used for a plaque assay to quantify the viral replication of VSV in the presence of each expressed protein (Figure 6.15A). Results indicate that in the presence of the paMx1 control ISG, VSV replication was largely reduced at in comparison to the infected cells control, as represented by a reduced viral titre in PFU/mL. paIFI35, our protein of interest, also appeared to act in an antiviral manner here, reducing the replication of VSV-GFP in comparison to the infected cells control. However, it is worth noting that this investigation was only completed once due to time constraints and hence requires further repeats for statistical analysis of results to be undertaken. Plaques were counted and quantified at the 10^{-6} dilution to calculate PFU/mL to represent the amount of VSV replication taking place under each treatment (Figure 6.15B).

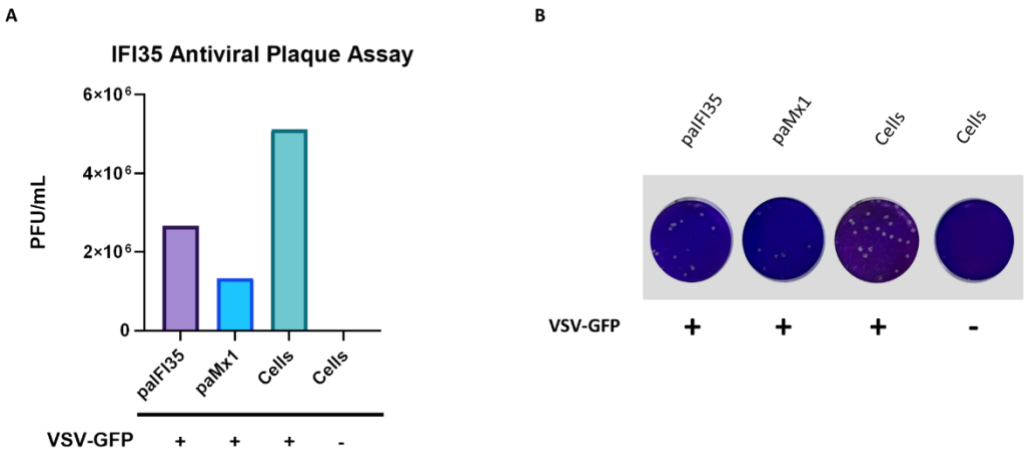

Figure 6.15 - The antiviral activity of paIFI35 measured against VSV-GFP replication. (A) *VeroE6 cells were transfected with 2µg of paIFI35, paMx1 or left non-transfected for 24 hours. Cells were subsequently infected with VSV-GFP at an MOI of 0.25 or left uninfected for 24 hours before quantification via plaque assay analysis using VeroE6 cells in a 12-well format. As this plaque assay was only carried out once, significance could not be determined. Figure was generated using Graphpad Prism 8 software.* ***(B)*** *Plaques were counted and used for PFU/mL calculation and quantification at the 10^{-6} dilution.*

6.3 Discussion

Despite the high degree of genetic conservation of the bat IFN system with the human IFN system as identified previously (La Cruz-Rivera et al., 2018), there remain limited studies investigating the functional characterisation of individual bat innate immune genes and how they regulate virus infection *in vitro*. This is largely attributed to the lack of availability of reagents existing within the field of bat antiviral immunology (Schountz, 2014). Two essential components of the innate immune system, IRF7 and IFI35, represent members of the IFN cascade in mammals and have been genetically annotated in the bat model species *P.alecto*. Due to prior transcriptomic evidence of their upregulation during viral infection in bats, as described in Chapter 3, we selected these two genes for further investigation. Furthermore, in alignment with the limited data within bat immunity, information regarding the genetic and functional annotation of these two genes in other species is widely available and thus provides valuable niches to investigate their roles in bats.

In order to understand the potential activities of the two innate immune genes, we first aimed to visualise the degree of conservation of paIRF7 and paIFI35 with their human counterparts and other mammals. Our investigations demonstrated a high degree of sequence conservation of both paIRF7 and paIFI35 genes with their human counterparts. The paIRF7 exhibited a conserved protein domain layout and possessed a similar sequence length to human IRF7, yet differed in its amino acid residues present within the VAD (Figure 6.1(A-C)). As the VAD has been previously identified as indispensable for IRF7 activation in humans (Lin et al., 2000), further studies investigating the impact that the alternative sequence length of paIRF7 VAD may infer on its antiviral potential and its critical role within the IFN cascade, requires further exploration. The paIFI35 also portrayed protein domain conservation with human IFI35, possessing both NMI and NID domains and sharing a similar sequence length (Figure 6.10B and Figure 6.11). However, the RBD identified in human IFI35 was not recognised when predicting paIFI35 domains, which may largely be due to the lack of annotation of the bat genome and thus warrants future consideration. Due to its high sequence and domain conservations, it is likely that paIFI35 does indeed possess this RBD but has not been detected via genomic annotation methods. Alignment of paIFI35 with human IFI35 and other mammals highlighted a high degree of sequence conservation (Figure 6.11). There were no distinct variations in amino acid sequence within the protein domains of IFI35 and hence it can be assumed that the high conservation of paIFI35 with human IFI35 confers a conserved functional role, which was later explored. Moreover, we explored the gene synteny of paIFI35 and identified that paIFI35 is flanked both upstream and downstream by the same genes as present in other mammalian and non-mammalian species (Figure 6.10A). However, we were unable to determine the chromosomal locations of the IFI35 gene in bats due to lack of annotation. Hopefully, future additional annotation of the *P.alecto* genome will allow for the identification of the chromosomal location of IFI35 which may be beneficial in comprehending its role in bats.

Using phylogenetic and pairwise identity-based bioinformatic analysis techniques, our research concluded the high degree of conservation of bat IRF7 and IFI35 with their human homologues and other mammalian species. A small cohort of species were selected here for analysis, the majority of which were mammalian in order to observe potential close relationships within the immune genes of bats. Further research exploring the IRF7 and IFI35 genes present in additional mammalian and non-mammalian species may provide a further insight into the relationship of these genes in bats with further species. Significantly, in our findings both IRF7 and IFI35 genes in bats appeared to group more closely with their homologues present in dog and horse than to human and other mammals (Figure 6.2A and Figure 6.12A). These findings align with previous studies exploring the close relationships of these animals encompassed within a superorder deemed Pegasoferae (Nishihara et al., 2006). Despite this closer grouping of bat IRF7 and IFI35 to dog and horse, the two genes still demonstrated a close phylogenetic relationship and high pairwise percentage identity with their human counterparts, which coincides with the previously observed high sequence and domain conservation of the innate immune genes in bats and humans (Figure 6.2(A-B) and Figure 6.12(A-B)).

In independent investigations, we expressed the paIRF7 and paIFI35 genes *in vitro* to characterise their subcellular localisation in mammalian cells and potentially determine if they behave in a similar manner to their established human counterparts. Upon transfection of paIRF7 in mammalian HEK293T cells, we found a conserved expression pattern with human IRF7 whereby the protein was expressed in its latent form solely within the cell cytoplasm and then proceeded to translocate to the cell nucleus upon IFN and viral stimulation (Figure 6.3). Due to the prior observation of high sequence similarity, we expected to see a similar expression pattern of the two mammalian IRF7 proteins *in vitro*. Subsequent studies into the influence of different protein domains within paIRF7 was then undertaken, whereby we identified that the

removal of the ID and C-terminus resulted in the expression of these paIRF7 constructs within the cell nucleus despite the absence of external stimuli (Figure 6.5). Subsequently construct 1 (paIRF7-mRFP) was the only construct that was solely expressed in the cell cytoplasm. However, in our first investigation, the expression of this construct remained restricted to the cytoplasm and didn't translocate to the nucleus like originally anticipated, despite possessing conserved domains of the wild type paIRF7 protein (Figure 6.5). Therefore, we repeated this experiment in order to identify if the prior findings were a true representation of the expression of the paIRF7-mRFP construct. New findings showed the parallel cytoplasmic expression of the construct in absence of viral stimulation, but upon infection with VSV-GFP, paIRF7-mRFP then successfully translocated to the cell nucleus (Figure 6.6). The difference in results between this repeat and previous findings are potentially due to the lack of activation of paIRF7 by VSV-GFP in the cell studied in the previous experiment, or alternatively, the activity of paIFR7 may have been masked by a high titre of virus with that cell. Additionally, it is worth noting that identifying cells within the population that expressed both paIRF7-mRFP was difficult, which was largely due to the fact that in most infected cells, the activity of the paIRF7-mRFP will have fought off the viral infection, resulting in a diminished VSV-GFP signal to detect by fluorescent microscopy. Further investigations may wish to repeat our approach to determine the true behaviour and expression of this construct in an array of cell lines, ideally in a bat cell line for a more representative outlook on paIRF7 *in vitro*.

The observed expression behaviour of the paIRF7 constructs, whereby the removal of the ID and C-terminus results in auto translocation to the cell nucleus has been previously reported by Lin et al. (2000), studying the expression of human IRF7 lacking different protein domains. This study determined that the altered localisation of the IRF7 genes lacking their C-terminus is due to the removal of a nuclear export sequence (NES) present within this region, hence the IRF7 remained in the nucleus

in this case. Therefore, we aligned this NES in paIRF7 with human IRF7 and found a high degree of conservation, suggesting the likelihood that paIRF7 also possesses this NES within its C-terminus region and subsequently its removal also results in nuclear expression (Figure 6.8A). Additional studies analysing the hypothetical NES and the influence of protein domain removal within paIRF7 may provide further comprehension into the roles of paIRF7 protein domains within bat immunity and antiviral defence.

In contrast to the well characterised cellular location of the human IRF7 gene, there is limited evidence of the location of IFI35 in humans and other species. Preliminary evidence suggests that human IFI35 is localised within the cytoplasm which appears similar to the pattern we observed for paIFI35 when expressed in VeroE6 cells. The paIFI35 was present in distinct clusters in the cytoplasm and was also identifiable in small amounts within the cell nucleus, which could potentially be due to its role as an ISG as this gene is transcribed within the cell nucleus and further exported to the cytoplasm (Figure 6.13A). Next, due to the distinct clusters of paIFI35 observed upon transfection of VeroE6 cells, we aimed to establish if paIFI35 localised to certain organelles within the cell cytoplasm as its location may also influence its role as an ISG. Prior findings found IFI35 in humans to negatively regulate RIG-I which is located close to the cell mitochondrion. Therefore, we theorised that the paIFI35 clusters we were observing may lie within the mitochondria of the cell. However, paIFI35 did not co-localise with the mitochondria nor the ER or peroxisome assessed here (Figure 6.14). Future research into the distribution of paIFI35 within the cell cytoplasm may prove fruitful in providing a basis for its role as an ISG. Furthermore, we originally aimed to assess the interaction of paIFI35 with RIG-I in bats to examine if paIFI35 negatively regulates RIG-I in the same manner as human IFI35 from previous studies to enable us to potentially determine the pro- or anti-viral activity of this ISG in bats. Due to the lack of time and resources we were unable to fulfil this

experiment but warrants subsequent investigation via co-immunoprecipitation studies to determine the interaction between paIFI35 and RIG-I in *P.alecto*.

For the expression studies of paIRF7 and paIFI35 undertaken in our work, it must be considered that this research used non-host mammalian cells as a close representation, but hence may not be completely illustrative of paIRF7 and paIFI35 expression within the original bat host. We originally aimed to undertake this investigation of innate immune gene expression and cellular localisation by overexpressing both genes in PaBr cells but had to redirect our research due to difficulties with this cell line including, but not limited to, cell growth, transfection and infection susceptibility. Therefore, our work undertaken here provides the foundation for further expression studies of bat IRF7 and IFI35 to hopefully be undertaken in host bat cell lines in the future for a more representative measure of bat immune gene cellular expression.

Lastly, due to the roles of both IRF7 and IFI35 in the innate immune cascade acting in response to viral infection in humans and other mammals, we aimed to verify if these genes in *P.alecto* behaved in an antiviral manner *in vitro*. Both immune genes were expressed in VeroE6 cells and infected with VSV-GFP before being assessed for antiviral activity via plaque assay quantification. For paIRF7 antiviral investigations, we assessed the influence of the four paIRF7-mRFP constructs which varied in their protein domains, on viral replication. We chose to further study these constructs to better understand the influence that the removal of protein domains had on the fundamental antiviral activity of IRF7 *in vitro*. As IRF7 is a central transcription factor in the innate immune cascade, we initially expected to observe antiviral activity against VSV-GFP replication in the presence of paIRF7. This was evident for all four paIRF7-mRFP constructs which showed antiviral activity in comparison with the infected cell control by exhibiting a lower viral titre (Figure 6.9 (A-B)). However, the variations in antiviral efficiency within the constructs themselves did not appear to

exhibit a strong trend with protein domain removal whereby the most antiviral were constructs paIRF7-ΔID-mRFP and paIRF7-ΔID+ VAD-mRFP with the wild type (paIRF7-WT-mRFP) displaying less antiviral activity. As this experiment was only completed once, repeats of this study may provide a more representative antiviral activity of these paIRF7 constructs against VSV-GFP replication. Furthermore, like expression studies, if investigated using bat host cells, results would be more representative of what happens in the natural host when challenged with viral infection. Additionally, research analysing the influence that protein domain removal may have on the induction of different ISGs in bats during viral infection is worth investigating in future studies.

Similarly, we only assessed the impact of paIFI35 on VSV-GFP replication in VeroE6 cells which was undertaken once and did not include an empty vector control, requiring repeating. However, our initial results demonstrated the potential antiviral activity of paIFI35 against VSV-GFP replication *in vitro*, identifiable by a reduced viral titre in the presence of paIFI35 in comparison to the infected cells control (Figure 6.15(A-B)).

Chapter 7. General Discussion

7.1 Summary of Results

Bats are key reservoirs for several high-impact zoonotic viruses known to result in significant disease in humans yet cause mild or no clinical disease in the bat host, as conventional for a reservoir species. However, despite their importance as zoonotic viral reservoirs, little is currently known about bat immunology and the host/virus relationships they exhibit. Existing studies, however, have identified that bats possess several comparable immunological genes and responses to humans and other mammals, whilst also demonstrating seemingly novel immunoregulatory mechanisms, often linked to their great longevity and powered flight, as reviewed by Banerjee et al. (2020). We endeavoured to examine and scrutinise central components of bat innate immunity to gain a better understanding of the immune mechanisms underlying the co-existence of bats with several pathogenic viruses. Utilising transcriptomic methods in addition to respective *in vitro* molecular biology and virology techniques, this work explored a plethora of key components of bat innate immunity, central to their IFN response, alongside examining their potential roles in bat antiviral defence.

7.2 Transcriptomic Analyses of Stimulated PaBr cells Provides a Valuable Insight into Host Gene Regulation in Bats

Transcriptomic analysis is an increasingly popular technique within the field of molecular biology as it possesses great advantages in studying the global response of cells under a certain condition or stimulus. In brief, the transcriptome encompasses a snapshot of all total transcripts (covering all types of coding and non-coding RNA) within a cell at any given time (Dong and Chen, 2013). Therefore, we aimed to utilise a transcriptomic approach to uncover the global response of bat cells (PaBr) to viral infection and IFN stimulation, to understand gene regulation in bats. Previous transcriptomic analyses have been successfully conducted in several bat species which also explored their global transcriptomic response to both viral infection and

IFN stimulation. However, prior studies are limited to a small collection of viruses including Ebola and NiV, but currently have not explored the response endured upon CedPV infection of bat cells. CedPV is a bat henipavirus that is very similar in its genomic structure to the highly pathogenic NiV and HeV. However, CedPV is non-pathogenic, which is largely attributed to the lack of RNA-editing within the P gene of CedPV, which in NiV and HeV results in the production of IFN antagonist proteins V and W (Shaw et al., 2004, Marsh et al., 2012). Additionally, CedPV has been shown to be non-pathogenic when used in experimental infections of animals commonly used for NiV/HeV infection such as hamsters, guinea pigs and ferrets (Marsh et al., 2012, Schountz et al., 2019). Therefore, CedPV can be used at a BSL-2 level, allowing for the ease of henipavirus-induced transcriptomics in our study as we do not possess the BSL-4 facilities required to assess or compare with NiV/HeV infection (Marsh et al., 2012). Furthermore, CedPV shares the same entry receptor (ephrin-B2) as HeV and NiV, which is an ubiquitous membrane protein that is conserved across mammalian species (Bonaparte et al., 2005, Negrete et al., 2005, Lisabeth et al., 2013). Thus, our observed CedPV-induced transcriptomics response of bat cells may potentially also reflect the response generated upon NiV or HeV infection.

Additionally, prior analyses investigating the bat transcriptomic response to IFN stimulation often used type I IFNs by stimulating with IFNα, which was also frequently undertaken using a universal IFNα that was hence non-unique to the bat host and thereby not as representative as stimulation with an IFN isolated from a bat host. Therefore, to provide a unique outlook and further contribute to the field of bat transcriptomic responses to IFN stimulation, we aimed to stimulate PaBr cells with a type III IFN using paIFNλ, which was expressed from the *P.alecto* model host. Type III IFNs have been identified in several bat species as functional effectors and exhibit seemingly analogous behaviour to their human counterparts (Zhou et al., 2011b). Significantly, type III IFNs are also stimulants of the IFN response and signal via the

JAK-STAT pathway (Mesev et al., 2019). We hence deemed it imperative to also explore the transcript level mechanisms taking place during type III IFN stimulation in the context of bat innate immunity. Overall, by studying transcriptomic events such as differential gene expression, gene ontology, alternative splicing and isoform switching within *P.alecto* during CedPV infection or paIFNλ stimulation, we were able to illustrate the diverse gene regulation mechanisms taking place in comparison to basal (uninfected or unstimulated) conditions of the bat cells, with an extensive focus directed towards the immune response of bats. Our transcriptomic studies enabled the observation of alternative patterns and trends within the transcriptomic response of PaBr cells to stimulation with CedPV (Chapter 3) and paIFNλ (Chapter 4) respectively.

Firstly, when examining differential gene expression, a technique which analyses gene transcript abundance within a transcriptome, we observed a high number (3,004) of significant DEGs in uninfected vs CedPV-infected PaBr cells (Figure 3.5A). Moreover, we detected the upregulation of several immune-related genes in the presence of CedPV infection, which we had initially hypothesised due to our understanding of the antiviral immune response in bats (Figure 3.5B). There was also a selection of downregulated genes identifiable in the presence of CedPV infection which possess various non-immune related roles, requiring future investigation. However, as this study is focusing on bat immunity, these genes were not further explored in this instance. In addition, because each transcript will exhibit its own pattern of variation between conditions, we also assessed variability in gene expression between the uninfected vs CedPV-infected bat cells, which again revealed the significance of several upregulated immune-related genes which displayed during infection (Figure 3.5C). However, it is worth noting here that two of these genes represent unannotated transcripts from *P.alecto*. Therefore, further annotation of the *P.alecto* genome in the future may enable the analysis of these

transcripts and determine the roles of these unknown genes. Moreover, we sought to classify the significant DEGs detected in uninfected vs CedPV infection via gene ontology analysis, as this permits the classification of transcripts into distinct biological processes, cellular components, and molecular functions, providing an essential perception of the roles of these transcripts. In alignment with previous DEG findings, GO demonstrated several immune and prospective antiviral-related functions in which genes displaying differential expression are clustered (Figure 3.7(A-C)). Most processes and functions annotated were in relation to immune and defence responses, alongside the response to stress and external stimuli. These findings were expected as the PaBr cells were challenged with viral infection, therefore the use of antiviral and innate immune pathways to counteract this infection was anticipated.

In contrast to our findings highlighting the existence and importance of antiviral immune mechanisms and the upregulation of immune-related genes during CedPV infection of PaBr cells, when stimulated with paIFNλ in a separate study, we observed a disparate story. Initially, as paIFNλ is a type III IFN and stimulator of the IFN cascade, we expected to perceive similar results to CedPV stimulation in recognising the upregulation of immune-related genes and pathways. However contrastingly, we did not observe a strong association of antiviral immune signalling within the PaBr cells when stimulated with paIFNλ. Primarily, only a small number of genes were detected as differentially expressed in unstimulated vs paIFNλ-treated PaBr cells (1,249) (Figure 4.5A). Alternatively, certain immune genes that were previously highlighted in CedPV infection (Figure 3.5B), were actually deemed non-significant in the presence of paIFNλ stimulation (Figure 4.5B). A few downregulated genes of interest were still detected in this study, but only at a lower significance level (Figure 4.5B). These downregulated genes were however previously detected as downregulated during CedPV infection also (Figure 3.5B) which included iMATN3,

TIMP3 and CALD1. Although these genes are non-immune related, future examination of why the expression of these genes is reduced during infection and IFN stimulation should be investigated. Additionally, gene variability was also assessed for paIFNλ stimulation, whereby despite a few genes showing somewhat distinct differences in expression between paIFNλ stimulation and unstimulated PaBr cells, overall, there was no obvious contrast and thus noteworthy variation of gene expression between the treatment groups. Similarly, despite the expected stimulation of the IFN system by paIFNλ, GO analysis failed to highlight significant processes and functions relating to innate immune responses of bats that we are interested in investigating (Figure 4.6 (A-C)). Instead, a limited cohort of molecular functions, often related to transcription, were annotated alongside diverse biological processes including biosynthetic processes and transcription regulation. The significance of these processes could be further explored in additional investigations studying molecular pathways involved in the type III IFN response in bats, to determine their role during paIFNλ stimulation, but as this was not directly related to our bat immune gene focus here it was not continued further.

In addition to the analysis of DEGs during CedPV and paIFNλ stimulation of PaBr cells, our transcriptomic studies also evaluated the presence and nature of alternative splicing events and isoform switching. Briefly, alternative splicing is a mechanism that enhances transcriptome diversity via the modification of pre-mRNA constructs, which allows for the subsequent production of a diverse range of mRNAs generated from an individual gene by alternative arrangements and combinations of exons from spliced RNA transcripts (Keren et al., 2010). Furthermore, as these modifications occur prior to translation, alternative splicing of transcripts often results in the production of alternative isoforms of a protein which, in turn, can result in functional consequences. Nearly 95% of all expressed human genes undergo alternative splicing, and whilst we do not know the number of genes belonging to bats, it is useful to investigate

alternative splicing events in our study of stimulated PaBr cells (Ab Hakim et al., 2017, Graveley, 2001, Consortium, 2012). This is because alternative splicing can give rise to proteins which differ in their structure, function, and localisation which consequently influence the outcome of the protein. Moreover, alternative splicing is recognised in a myriad of cellular processes including immune response regulation, pathogenic processes underlying disease such as cancer (Kim et al., 2018, Ren et al., 2021). Significantly for our investigations, viral infection has also been identified to influence alternative splicing events within a host (Chauhan et al., 2019).

Research has identified several viruses that are capable of manipulating host cell splicing machinery. Viruses that replicate within the cell nucleus of infected cells, such as influenza viruses and herpesviruses, can successfully gain access to host splicing machinery (Sciabica et al., 2003, Qiu et al., 1995). However, this capacity is not exclusive to nuclear viruses and has also been observed for cytoplasmic-replicating viruses such as flaviviruses (De Maio et al., 2016). The mechanisms underlying the hijacking of host splicing machinery is very complex and technically difficult to study (Ashraf et al., 2019). However, recent advantages in RNA sequencing techniques have revealed the altered splicing patterns of several hundreds of host genes, which occur either as a direct result of viral manipulation, or indirectly via virus-induced cellular damage or innate immune responses, as demonstrated in Figure 7.1. Thus, it is imperative that we gain a better understanding of the influence of viral infection on AS events within a variety of hosts in order to unearth the full transcriptomic potential during viral infection.

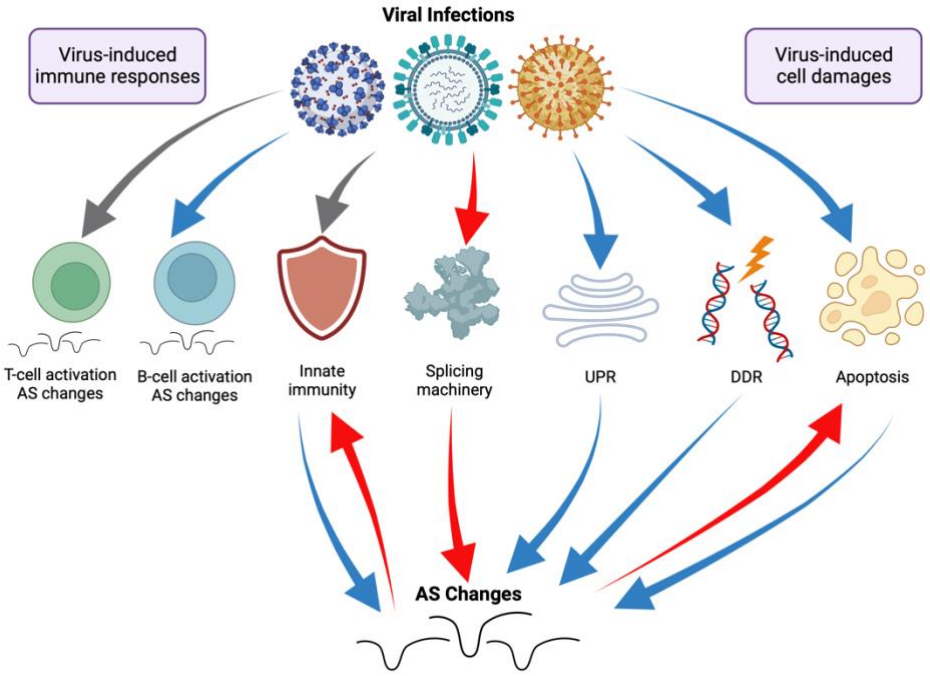

Figure 7.1 – Direct and indirect mechanisms for virus-induced splicing. *Direct viral manipulation of splicing machinery and resulting alternative splicing (AS) changes are represented by red arrows and also have the potential to modulate innate immunity. Blue arrows represent indirect, virus-induced cell damage and innate immune responses causing AS changes in infected cells. Grey arrows represent virus-induced B-cell and T-cell immune responses which can also undergo AS regulation. UPR (unfolded protein response), DDR (DNA damage response). Figure adapted from Ashraf et al. (2019) and made in Biorender.com.*

Within our transcriptomic study, a total of 3,004 DEGs were identified prior during CedPV-infection of PaBr cells. Of these DEGs, 470 were identified to undergo alternative splicing (Figure 3.8A). Using GO analysis for these specific genes, we were able to determine a selection of functions and processes which may be affected by these alternative splicing events, including RNA binding, mRNA processing and the regulation of intracellular signal transduction (Figure 3.8(C-E)). Whilst the roles of these processes in bats have not been explored here and without functional analyses, we cannot determine with certainty, if these pathways are influenced by alternative splicing, it is still worth considering that several of these processes are related to viral infections and immune responses. Therefore, the infection of PaBr cells by CedPV holds the potential to regulate these processes for the successful hijacking of mechanisms, such as cellular RNA processing machinery, for the benefit

of viral replication within the bat host. Functional studies investigating the highlighted functions in which genes undergoing alternative splicing belong to in bats, and how they are influenced by CedPV infection, warrant future investigation.

As formerly mentioned, the process of alternative splicing can result in isoform switching, in which alternative versions of the same protein are generated from the same initial transcript. During CedPV infection, we identified 195 genes to undergo a total of 246 alternative splicing events that resulted in 370 different isoforms (Figure 3.9(A-B)). There are several types of alternative splicing that can occur within a transcript, as previously described in Chapters 3 and 4. In uninfected vs CedPV-infected PaBr cells, we documented that the most significant forms of alternative splicing were MES, ES and ATSS (Figure 3.9C), the two latter occurring the most often in alternatively spliced genes resulting in functional consequences (Figure 3.9D). Lastly, we further explored the process of isoform switching in the context of functional consequence to determine if these genes possessed roles in antiviral and innate immunity. Overall, there were a wide spread of genes identified here with various biological roles and although we did not detect any key innate immune genes of interest to our investigations, there were still several immune-related genes evident. Thereby we selected four of these genes (DHX9, ILR1, IL23A and TRAF1) to investigate further and although the in-depth analysis of each individual gene within the 195 genes cohort resulting in isoform switching during CedPV infection would have proved insightful, we selected only representative immune-related genes relevant to our current investigations (Figure 3.10(A-D)). The examined immune genes were generally more highly expressed in the presence of CedPV infection, except for DHX9, which has roles in unwinding dsRNA and transcriptional regulation. Within the four immune genes studied here, each displayed an evident preference for certain isoforms in the presence and absence of CedPV infection which were evaluated in Chapter 3. Future studies should be undertaken to further elucidate the

influence that these alternative isoforms have on the activity of each immune gene in the presence of CedPV infection. Potential studies may aim to generate and express the alternative protein isoforms in the presence and absence of CedPV to determine their effect. Collectively, using the three direct approaches to transcriptomic analysis, we found a selection of 22 genes possessing various roles, which were recognised as significant in all three events (differential gene expression, alternative splicing and isoform switching) (Figure 3.12(A-B)). Future studies investigating the influence of CedPV infection in bats may wish to expand efforts directed towards this communal cohort of bat genes.

Alternative splicing and isoform switching was also studied in our parallel paIFNλ-stimulation transcriptomic study. Hereby, 338 significant genes were found to undergo a total of 448 alternative splicing events (Figure 4.7A). GO analysis was also performed on the differential splicing events of genes in unstimulated vs paIFNλ stimulation, which highlighted molecular functions and pathways potentially influenced by alternative splicing (Figure 4.7(C-E)). These included processes such as metabolic and cell cycle processes, RNA processing and binding amongst others. Although these processes may not seem directly related to innate immunity that we are interest in here, the potential effect of alternative splicing on these systems should be further studied. We also sought to identify the most significant alternative splicing events taking place in unstimulated vs paIFNλ-stimulated PaBr cells, but at our significance value of FDR<0.05, no alternative splicing events were deemed significant. However, it was obvious that the most common forms of splicing occurring were ES and ATSS, consistent with the splicing events previously observed for CedPV stimulation of the cells (Figure 3.9C). These results suggest a potentially favoured form of alternative splicing relating to exon skipping and the use of alternative transcription start sites in cells when faced with stimulation of the IFN system, or alternatively may just represent the most common alternative splicing

processes generally occurring, which hence warrants validation. Upon analysis of isoform switching with a functional consequence during paIFNλ stimulation, 23 genes were identified to undergo 33 alternative splicing events to produce a total of 27 separate isoforms with believed functional consequence (Figure 4.8A). Consistent with our CedPV study, we wanted to select four immune-related genes for further scrutiny to investigate the use of alternative isoforms during paIFNλ stimulation. However, there were no directly-immune-related genes from the 23 that result in a functional consequence, so we therefore decided to look at the top four most significant in this category (TCF4, CEP57L1, SSBP4 and TCEANC) (Figure 4.9) which possess diverse roles in the bat host. Results highlighted the preference for different isoforms in the presence and absence of stimulation, but as mentioned prior these require functional characterisation to determine the true isoform usage of these genes and to rule out potentially influencing factors that may be directing isoform usage.

To summarize, our two transcriptomic investigations successfully unveiled key areas of interest when investigating transcript level differentiations in bats. Our CedPV-infection study appeared fruitful in demonstrating the gene regulation of several non-immune and immune-related genes in response to viral infection in bat cells, whereas our paIFNλ transcriptomic study failed to demonstrate a strong connection of transcript activity within the immune pathway in bats. We also observed a higher number of significant genes induced during CedPV infection than during paIFNλ stimulation, which may potentially induce bias into our prior conclusion as many genes may have potentially gone undetected. Moreover, viral infection commonly activates both the type I IFN and type III IFN (and type II IFN) pathways, whereas paIFNλ as a type III IFN, is only targeting the type III IFN pathway itself, which does not come into effect as immediately as the type I IFN pathway. Therefore, the heightened number of genes and results we perceived during CedPV stimulation may

be largely resultant of the activation of the type I IFN pathway, alongside potentially type III IFN signalling. Whereas the paIFNλ stimulation of PaBr cells may not have been detected as efficiently due to the slower action of the type III IFN pathway, it may also be the case that paIFNλ stimulation generally induces fewer immune-related genes (Park and Iwasaki, 2020, Lazear et al., 2019). Ultimately, viral infection of mammalian cells elicits an alternative response to the direct stimulation of the type III IFN response, which largely accounts for the differences observed in our findings. Additional experiments to build on our preliminary findings of significant immune-genes, particularly those up-regulated during CedPV infection, could carry out RT-qPCR confirmation of these genes at the transcript level. Comparing the transcript expression of these immune-related genes in the presence or absence of CedPV infection in this manner, will allow for additional, more thorough determination of the true expression of these genes in bats.

Our transcriptomic studies used the well-established *P.alecto* cell line, which aligns with the common use of Pteropid bat cell lines as a model species within the literature. However, these cells (PaBr) are neuronal cells, therefore the RNA signatures and transcript behaviour we are observing in these studies may not be wholly representative of those expressed in other cells, such as epithelial for example present at the host-virus interface and first to respond to infection (Yang and Yan, 2021). Moreover, although this cell line is from a model species, we cannot generalise that these transcriptomic responses to viral infection and type III IFN stimulation are globally representative of all bats, as bats are extremely diverse and complex. Like in all *in vitro* conducted studies, our investigations of transcriptomes in cell culture models are likely not entirely representative of the transcriptomic responses occurring in actual bats when naturally challenged with viral infection and immune stimulation in the wild. In all, our results provide a respectable initial framework that have demonstrated the CedPV and paIFNλ-induced transcriptomic

responses in cells taken from the model species *P.alecto*. These studies may be built on in the future and utilised for further investigative studies into different bat genes and transcripts to understand bats and their roles as viral reservoirs.

7.3 Characterisation of Bat Innate Immune Genes Reveals a High Degree of Conservation with Human Homologues

Bats are important zoonotic viral reservoirs as they hold the potential to host a myriad of pathogenic viruses without exhibiting clinical signs of infection (Wynne and Wang, 2013). Researchers believe that this capacity to co-exist with viruses is largely linked to the ability of bat to control viral infection early on in the innate immune response via specific antiviral mechanisms within their IFN system (Schountz et al., 2017). The IFN system acts as the first line of defence against viral infection and ultimately works to establish an antiviral state in the host (Katze et al., 2002). Several aspects of bat innate immunity have been previously explored and identified as closely conserved with components of the human immune system, including PRRs, IFN expression, recognition and signalling and the induction of ISGs (Banerjee et al., 2020). However despite this, ultimately the immunological responses in bats remain largely unexplored (La Cruz-Rivera et al., 2018, Schountz, 2014). Therefore, we sought to characterise certain key components of the bat IFN system and assess their expression and activity whilst simultaneously evaluating conservation with their human counterparts. Although there are hundreds of genes involved in the IFN cascade in human, and seemingly bats, there remains limited tools to study each individual gene described (Wang et al., 2021). Therefore, using existing and accessible tools, we selected two genes, known to partake in alternative roles during the IFN cascade which have been identified within the genome of the *P.alecto* model species. The first gene, IRF7, is a master regulator of the IFN response and is central

to the production of IFNs in mammals in response to pathogenic infection. Secondly, IFI35 is an ISG identified in several species including human and bat, which has been recognised by the literature to hold potential conflicting pro- or anti-viral roles in humans. Thus, we selected IFI35 as an ISG produced during the IFN response for further analysis and characterisation in bats as to our knowledge, this gene had not been previously studied *in vitro*.

Initial bioinformatic analyses of IRF7 and IFI35 from *P.alecto*, referrable as paIRF7 and paIFI35 respectively, revealed a high degree of conservation in their amino acid sequences and protein domains to the described human homologues of these immune genes (Figure 6.1 (A-C), Figure 6.10(A-C) and Figure 6.11). Both genes appeared to exhibit similar sequence lengths to their human homologues whilst also largely possessing similar protein domains. A few disparities were evident however, including the variation in sequence within the VAD of paIRF7 in comparison to human IRF7 in addition to the differing RBD annotation within the IFI35 protein, which was identifiable in human IFI35 but absent in paIFI35. paIRF7 protein domains were subsequently explored in greater detail, however we believe that the lack of RBD present in paIFI35 is likely due to the lack of annotation for this bat gene and thus chose not to explore further in this instance. In addition to their high amino acid conservation with their human counterparts, both paIRF7 and paIFI35 displayed a strong phylogenetic and pairwise identity relationship to humans and other mammals (Figure 6.2 (A-B) and Figure 6.12(A-B). Both immune genes when examined in their respective independent studies, grouped more closely with IRF7 and IFI35 homologues present in dog and horse than to human. These close groupings of ostensibly different species align with the proposed clade of mammals branded Pegasoferae, which has been previously explored within the literature (Nishihara et al., 2006). Despite exhibiting a closer relationship to this clade, the two bat immune genes also demonstrated a close phylogenetic relationship with IRF7 and IFI35 in

humans, alongside exhibiting a high pairwise identity percentage, representative of close sequence conservation.

Following the investigation of these genes from a bioinformatic and genomic perspective, we sought to determine the expression and initial behaviour of paIRF7 and paIFI35 using *in vitro* studies. Although IRF7 in bats, including from *P.alecto*, has been previously explored, we were unable to establish any previous evidence of the cellular localisation of this protein when expressed in mammalian cells using molecular biology techniques (Zhou et al., 2014). Moreover, the exact cellular location of IFI35 in humans has not been examined in much detail, resulting in limited prior information for us to base our findings from. Nonetheless, we believed that the observation of the cellular location of paIF35 may enable us to predict its potential influence as an ISG within the bat host. Our work showed that when expressed in HEK293T cells and imaged via confocal analysis via immunofluorescence staining, paIRF7 behaved in an analogous manner to human IRF7, whereby it naturally resided in its latent form within the cell cytoplasm (Figure 6.3). Moreover, we subsequently stimulated paIRF7 with viral and IFN stimulating ligands to observe its behaviour as part of the IFN cascade, and successfully portrayed its translocation to the cell nucleus in the presence of these viral and IFN ligands. These findings are parallel to how IRF7 behaves in humans and other mammalian species (Ning et al., 2011). As previously mentioned, there was limited work in the literature suggesting the cellular location of IFI35 in mammalian species, but upon transfection of VeroE6 cells and imaging conducted as mentioned prior for paIRF7, we detected distinct clusters of paIFI35 residing largely in the cell cytoplasm whilst also observing the partial infiltration of paIFI35 into the cell nucleus (Figure 6.13A). It is somewhat unclear whether the nuclei signals are merely background in our imaging, but nonetheless, its cytoplasmic expression was evident. Additionally, we aimed to also assess the successful expression of our paIFI35 FLAG-tagged plasmid via the use of

Western blotting to stain against this marker when alternative amounts were transfected into cells for expression(Figure 6.13B). There appears to be a clear trend exhibiting a larger band size in the presence of a higher amount of transfected plasmid, however due to the lack of internal control required here, such as beta-actin for example, we cannot determine that the observable band variation is not due to loading bias and thus requires scrutiny. Irrespective of this, our transfection of paIFI35 and imaging via immunofluorescence staining was sufficient to continue our studies analysing paIFI35 expression patterns. Following the identification of largely cytoplasmic expression of paIFI35 *in vitro*, we sought to further explore its subcellular location patterns. As the paIFI35 protein appeared in distinct clusters, we believed that it could be localising to organelles within the cell. Accordingly, due to previous findings suggesting a direct interaction of IFI35 with RIG-I, which is often located in the cell cytoplasm, we hypothesised this too may be where paIFI35 would interact (Das et al., 2014, Yang et al., 2021). To assess paIFI35 expression, we co-transfected paIFI35 with different plasmids targeting a variety of cytoplasmic organelles including the ER, mitochondria and peroxisome (Figure 6.14). Unfortunately, immunofluorescence imaging revealed that paIFI35 did not successfully co-localise with any of these organelles. Future work studying the explicit subcellular co-location of paIFI35 may prove useful in understanding the role of paIFI35 in bats and other mammals.

Further to our prior observations of the different protein domains belonging to paIRF7, we wanted to determine their influence on the expression and function of this protein *in vitro*. To achieve this, we generated four different constructs of paIRF7 which varied in their protein domains (Figure 6.4(A-B)) and were cloned into mRFP vectors for ease of visualisation via confocal microscopy. Upon expression of the four separate paIRF7-mRFP constructs in VeroE6 cells and immunofluorescence imaging, we observed the predicted cytoplasmic location of the full-length paIRF7

construct, however contrastingly, all subsequent constructs lacking their C-terminus and ID also exhibited a nuclear expression (Figure 6.5). This expression pattern was unexpected because as previously discussed, paIRF7 naturally resides in the cell cytoplasm until stimulated, which was not applied here. Therefore, we believed there must be another influencing factor possibly lying within the C-terminus of paIRF7, causing the altered cellular localisation of constructs lacking this domain. To further ensure that stimulation was not influencing the altered expression pattern of paIRF7 constructs, we repeated our expression study in VeroE6 cells and this time infected using VSV-GFP for visualisation (Figure 6.6). Expression of all constructs in the presence of viral stimulation here remained the same as previously, which was also interesting for our full-length construct (paIRF7-WT-mRFP) which, in theory, should have translocated to the nucleus during infection as this construct possesses all the domains required of the wild-type protein. Upon consideration we thought that this may be due to bias in our cell selection during the imaging process, whereby we unintentionally selected a cell expressing VSV-GFP but in which paIRF7-WT-mRFP had not had sufficient time to translocate following stimulation. To deduce this theory, we repeated our stimulation of VeroE6 cells expressing this construct and indeed continued to find the successful expected translocation of the full-length paIRF7 construct to the cell nucleus (Figure 6.7). Redirecting our efforts back to the influence of the C-terminal domains on paIRF7-mRFP construct cellular localisation, we deduced from previous literature examining similar protein domain-influenced expression of human IRF7, that the observably altered expression may be due to the presence of a NES within the C-terminus of IRF7, Lin et al. (2000) annotated a leucine-rich region representative of a NES in the C-terminus of human IRF7. Subsequently, we aligned this human IRF7 NES amino acid sequence with the same region present in paIRF7 and identified a high conservation of residues, connoting the possession of NES within our paIRF7 constructs (Figure 6.8A). Moreover, we demonstrated that the amino acids within this NES region are highly conserved

across several different species, suggesting the potential for NES within IRF7 in a broad range of animals (Figure 6.8C). Future research exploring the influence that the addition or removal of NES poses on the cellular location and activity of paIRF7 *in vitro* is warranted and could potentially shed light into the functions of this key innate immune gene in bats and in other mammals.

Last of all, as both IRF7 and IFI35 are concerned in the IFN response to viral stimulation, we wished to determine if these genes in bats exhibited any antiviral activity, and additionally in the case of paIFI35, potential pro-viral activity. We measured the influence of paIRF7 and paIFI35 on the replication of VSV-GFP in VeroE6 cells and quantified via plaque assay analysis (Figure 6.9 and Figure 6.15). Our results displayed a clear antiviral trend for paIFI35 against VSV-GFP replication in comparison to the infected cells control. For our paIRF7-mRFP constructs, all four appeared initially antiviral, however they largely varied in the degree of antiviral activity they demonstrated. This variation did not appear to follow a distinct trend in relation to the protein domains present within each construct. However, we must note that these antiviral assays were only completed once and in order to assess the true influence of these innate immune genes on viral replication, we must repeat these investigations. Additionally, we could also assess the activity of the original wild type paIRF7 gene alongside the paIRF7-mRFP constructs to rule out any influencing factors that are not present within the wild-type, together with observing the influence of paIRF7 on the replication of several other viruses for a broader perspective.

Overall, our work exploring the genomic and cellular expression of paIRF7 and paIFI35, to our knowledge, provide the first descriptions of these individual bat innate immune genes *in vitro* and provide a framework for future studies to investigate their activity and roles within bat immunity. Additionally to our findings, we initially aimed to conduct a co-immunoprecipitation experiment to observe the interaction between paIFI35 and paRIG-I, as previous literature recognised the negative regulation of

RIG-I by IFI35 in humans and thus the function of paIFI35 in this context warrants future studies (Yang et al., 2021, Das et al., 2014). By generating paIRF7-mRFP constructs, we were able to provide initial findings demonstrating the influence of paIRF7 protein domains on its cellular location. Additional studies assessing these domains in detail could be undertaken such as their influence on downstream effectors, including ISG induction in the innate immune response. Other studies branching from our initial findings described here may wish to utilise bat host cell lines to repeat our expression and antiviral studies to determine a closer, slightly more representative action of these immune genes, although still *in vitro*, but in cells from the natural bat host reservoir.

7.4 paIFIT5 Displays Negative Regulation of 5'ppp-bearing RNA Viruses

The actions of ISGs induced during IFN induction represent major components in host antiviral defence (Hubel et al., 2019). Most mammals encode several IFIT genes, which act as ISGs and are responsible for a collection of cellular responses including sensing of nucleic acids alongside direct antiviral activity (Liu et al., 2013). We selected IFIT5 as a particular gene of interest due to its proven capacity to potentiate antiviral signalling combined with its further ability to sense several short cellular RNAs (Abbas et al., 2013, Fensterl and Sen, 2015, Santhakumar et al., 2018). IFIT5 can initiate downstream antiviral activity due to its ability to discriminate between viral and cellular mRNA by recognition of molecular signatures present at the 5'termini. Specifically, IFIT5 directly recognises the presence of a 5'ppp molecular signature carried by single-stranded RNA viruses (Abbas et al., 2013). This interaction permits the subsequent sequestering of viral RNA, inhibiting its replication and translation by host machinery and thereby acting in an antiviral manner. This interaction has been well studied for human IFIT5 and more recently chicken IFIT5,

yet the potential binding of IFIT5 to 5'ppp signatures currently remains undescribed in bats (Abbas et al., 2013, Santhakumar et al., 2018). Our work thus aimed to fill this gap in the literature by characterising the IFIT5 gene from *P.alecto* and determine its antiviral potential, principally against viruses bearing a 5'ppp signature.

We first studied the conservation of IFIT5 from *P.alecto* (paIFIT5) with IFIT5 present in humans and other animals in order to envision sequence similarities and phylogenetic relationships of the bat IFIT5 gene. Bioinformatic analyses showed a high sequence conservation of paIFIT5 with its human counterpart, differing by only a few nucleotides (Figure 5.2C). Furthermore, paIFIT5 shared the same pattern of TPR tandem repeats, which are conserved in all kingdoms of life and important in mediating protein-protein interactions, yet additionally possessed one more TPR that human IFIT5, deemed TPR3b (Figure 5.2(A-B)) (Vladimer et al., 2014). Within the human IFIT5 sequence there appears a large stretch of nucleotides after TPR3 and before TPR4, whereas alternatively for paIFIT5, protein domain prediction recognised an additional TPR (TPR3b) coded within this region. It is speculated whether the additional TPR repeat confers any advantage or disadvantage to the function of the paIFIT5 protein itself but could be studied in order to determine this potential influence on protein activity. Additionally, this work also examined gene synteny and phylogenetic relationships of paIFIT5 with other animals. IFIT5 was assessed from a selection of representative species and gene syntenic comparison showed that paIFIT5 is flanked up and downstream by similar genes to other species (Figure 5.1A). Moreover, phylogenetic analysis demonstrated that paIFIT5 grouped most closely with horse IFIT5, followed by human (Figure 5.1B). The conservation of paIFIT5 with horse and human, alongside other mammals, was also demonstrated during pairwise identity analysis (Figure 5.1C). Overall, we could conclude that paIFIT5 appeared highly conserved with its human counterpart, suggesting a potentially parallel role within the host that we successively investigated. We also

observed a parallel expression pattern of both paIFIT5 and human IFIT5 (huIFIT5) when expressed in VeroE6 cells, with both proteins localising to the cell cytoplasm and nucleus (Figure 5.3). Future studies confirming a more specific subcellular location of these proteins would be useful for future paIFIT5 investigations, as prior work had identified the partial co-localisation of human IFIT5 with the mitochondria and its associated interaction with RIG-I and MAVS at this interface (Zhang et al., 2013a).

Before studying the potential antiviral activity of paIFIT5, we first wanted to observe the inducibility of this gene by typical ligands. The induction of IFIT5 remains the least studied out of all IFIT proteins within the known literature, however , Zhang et al. (2013a) confirmed the inducibility of human IFIT5 at the protein and mRNA level by IFN stimulation and viral infection. Therefore, we hypothesised that due to their similarities, paIFIT5 would be successfully induced by this selection of ligands in the same manner as its human counterpart. Using RT-qPCR analysis, we observed the successful induction of paIFIT5 in the presence of NDV, poly(I:C) and paIFNb (Figure 5.4). These results confirm the induction of paIFIT5 by a variety of ligands, however further exploration using different virus types and IFNs could broaden this initial observation.

Following our confirmation of paIFIT5 *in vitro* expression and inducibility, we next aimed to examine its antiviral ability. As previously described, IFIT5 in humans displays antiviral activity by directly recognising and binding 5’ppp signatures present in negative-sense RNA viruses which permits enhanced immune signalling pathways via coordinating IRF3 and NF-kB-mediated gene expression (Zhang et al., 2013a). We firstly demonstrated the antiviral activity of paIFIFT5 against VSV, a negative-sense RNA viruses possessive of the 5’ppp RNA signature we are interested in (Figure 5.5). VeroE6 cells expressing paIFIT5 displayed antiviral activity against VSV replication, representative by over 2-fold reduction in viral titre compared to the

infected cells control. Our investigations assessing antiviral activity of paIFIT5 continued, as we wanted to study the antiviral action of paIFIT5 against other viral species bearing 5'ppp RNA that are understood to commonly infect bats. These viruses included the endogenous bat influenza virus (H17N10) and the highly pathogenic RVFV (Tong et al., 2012, Balkema-Buschmann et al., 2018). However, due to the insufficient isolation of the bat H17N10 virus and the high containment required to investigate RVFV infection, we adopted an altered approach to our previous VSV antiviral assay. Firstly, we confirmed the antiviral activity of paIFIT5 against H17N10 via utilising a VLP system to study viral replication (Figure 5.6A). In this investigation, we quantified the antiviral influence of paIFIT5 by measuring the luciferase signal generated from replication-deficient but transcriptionally active VLPs to measure the effect of paIFIT5 on the viral polymerase activity. Results showing a reduced reporter gene expression in the lysates of H17N10 VLP-producing HEK293T cells in the presence of paIFIT5 compared to the empty vector control advocated the antiviral activity of paIFIT5 targeted towards H17N10 polymerase activity. Similarly, we used a minireplicon system to determine paIFIT5 antiviral activity against RVFV replication (Figure 5.6B). However, in contrast to our findings for H17N10, our RVFV data were non-significant and thus we could not draw any conclusions on antiviral activity of paIFIT5 against RVFV in this case, warranting future study. Although our studies here were conducted using non-bat mammalian cells, these studies provide the initial framework for the antiviral potential of paIFIT5 against the negative-sense RNA-viruses assessed here and allow for future studies into paIFIT5 antiviral activity against a broader range of viruses. Future studies replicating our findings using paIFIT5 expressed in Pteropid cell lines should be considered as these may enable a more representative action of this protein against viruses within the natural bat host.

Ultimately, following our confirmative studies of paIFIT5 antiviral activity against negative-sense RNA viruses, we needed to mechanistically determine the direct

interaction of paIFIT5 with 5'ppp RNA. We adopted an RNA-immunoprecipitation method previously optimised by Santhakumar et al. (2018), which was successful in identifying the direct interaction of chicken IFIT5 with 5'ppp RNA and applied this to our paIFIT5 study. Two distinct RNA species simulating viral 5' RNA ends were generated to bear either the 5'ppp signature or alternatively possessed an OH group at their N-termini (Figure 6.7C). The interaction of these viral RNA species with paIFIT5 was assessed using biotinylation coupled with agarose beads and incubation with cells expressing paIFIT5, alongside human IFIT5 for comparison. Results showed that upon purification of ribonucleoproteins and staining against IFIT5, both paIFIT5 and human IFIT5 interacted with 5'ppp RNA only as anticipated (Figure 6.7B). These data are representative of the parallel discrimination of RNA species exhibited by both human and paIFIT5 and their ability to directly recognise and bind RNA possessing 5'ppp molecular signatures, present within the N-terminus of negative-sense RNA viruses. Limitations to these findings include the use of HEK293T cells to generate the paIFIT5 protein for immunoprecipitation, as despite being mammalian, this is a non-bat cell line and hence may not be as representative of paIFIT5 expression in bat cells. Future investigations could utilise our paIFIT5 foundation studies to investigate the potential interaction of this ISG with 5'ppp from a range of viruses and potentially exploring the recognition of additional viral RNA species. Furthermore, previous studies using human IFIT5 identified the enhancement of IRF3 and NF-kB gene expression induced by IFIT5 recognition of 5'ppp viral RNA and knock-down of IFIT5 also impaired the transcription of these genes (Zhang et al., 2013a). Thus, exploring the influence of gene transcription using similar knock-down experiments with paIFIT5 would prove interesting in clarifying the full antiviral mechanism of IFIT5 in bats.

7.5 Future Work

Although bat immunity remains comparatively understudied in comparison to other mammalian reservoirs, research directed towards understanding the role of bats as hosts of high-impact zoonotic viruses and their innate immunity is now continually expanding, having generated heightened attention interest following the recent COVID-19 pandemic. Irving et al. (2021) encapsulates how researchers a decade ago “would not have expected to see bat research gain the momentum it has now”. The data provided in this work focuses on largely unexplored or understudied components of bat innate immunity and provides a strong framework enabling significant opportunity for future investigations into bat antiviral immune responses based on our findings. In summary, our work investigating the transcriptomic response of the bat model species *P.alecto* to infection with Cedar virus and stimulation with a type III host IFN (paIFNl) are, to our knowledge, the first reported datasets of their kind and provide a substantial review of bat transcript expression and regulation during these challenges. Moreover, these data have highlighted key gene transcripts relevant to the antiviral immune response in bats and provide an initial foundation for future investigative studies examining the role of these genes within the bat immune response to viral infection. Infection of PaBr with CedPV proved successful in stimulating the immune response in *P.alecto*, represented by the upregulation and expression of immune-related genes during viral infection. Contrastingly, the stimulation of the type III IFN response in PaBr cells by paIFNλ failed to demonstrate a strong immune response and consequently warrants further examination to understand any potential immune or even non-immune-related mechanisms taking place in bats under these conditions. Combined, our transcriptomic investigations were generated with a focus on the innate immune response of bats and hence our results focus largely on this area, however, we also

observed and annotated several non-immune transcripts in PaBr cells which could be investigated in further studies to understand the role of these transcripts in bats.

Separate to our bat transcriptomic investigations, we selected three bat immune genes for further in-depth study (paIFIT5, paIRF7 and paIFI35). Although we desired to study a larger cohort of bat immune genes in the detail we demonstrated here, due to the restricted access and availability of reagents within bat research, alongside time constraints, we consequently adopted a directed approach aimed at investigating this selection of bat genes and their potential roles in bat antiviral immunity. Through this work, we successfully demonstrated the antiviral activity of paIFIT5 against a range of negative-sense RNA viruses and confirmed its ability to directly recognise and bind to 5'ppp molecular RNA signatures. Our studies further worked to characterise two bat genes central to the mammalian IFN response, IRF7 and a representative ISG, IFI35. We provided the first evidence of conserved gene expression of these genes between bats and humans in addition to establishing the influence of paIRF7 protein domains on its cellular location, alongside the potential antiviral roles of paIRF7 and paIFI35. Future studies building on our initial findings described here may seek to further investigate the three bat immune genes in more detail and their roles in antiviral immunity. Moreover, due to difficulties encountered using bat-derived cell lines in our work such as the lengthy process of optimisation and troubleshooting of transfection and infection within these cell lines, alongside the very slow growth of these cells, hindered our use of the PaBr cells, meaning we could not utilise these cells for all the experiments we had originally intended. Consequently, due to these difficulties and to make more efficient use of time, we had to opt for alternative mammalian cell lines for several of our expression analyses. Hence, these studies may warrant future study using bat cell lines for a more defined representation of these genes in the natural bat host. Alternatively, as stated previously, there are hundreds of conserved and novel bat immune genes that

remain undescribed and warrant an in-depth analysis as partaken in this study. Therefore, future research should also concentrate efforts towards previously undescribed bat immune genes which may hold substantial information on the virus-host equilibrium bats retain.

Lastly, this work focussed solely on the innate immune response of bats in the context of viral infection as an area of interest, but it is also worth considering the adaptive immune response elicited by bats to viruses. Despite currently limited studies investigating the adaptive immune response in bats, largely due to difficulties encountered with appropriate experimental models and reagents, recent developments have included the identification of bat cross-reactive antibodies and bat immune-cell populations (Baker et al., 2010, Wynne et al., 2013, Martínez Gómez et al., 2016, Periasamy et al., 2019, Banerjee et al., 2020). However, despite these recent advances to study bat immunology, experiments that endeavour to evaluate the adaptive immune response to infection require specialised facilities to house bats, which are either captive or those caught in the wild. The establishment of these colonies will hopefully open the door to for future advances in understanding the bat adaptive response, which could be exploited in the context of viral infection.

7.6 Concluding Remarks

In conclusion, this thesis has validated and characterised previously understudied genes and prosperous areas of bat research, with a focus driven towards bat antiviral immunity. Data presented here provides evidence of conserved immune mechanisms between bats and other mammals, whilst also demonstrating potentially novel findings and highlighting future areas of study. Our work provides significant contributions towards the field of bat immunology and the antiviral response of these zoonotic reservoirs and can expectantly be exploited to further comprehend the role

of bats as viral hosts and their host defence-immune tolerance mechanisms. As access to more bat reagents become available, future analyses of key genes central to bat immunoregulation and antiviral defence will hopefully provide a valuable perspective for the control of viral spillover and infection of bat-derived viruses into humans and other species. Furthermore, insights from these studies may permit the identification of future novel therapeutic targets in humans and other spillover species, essential in improving the global One Health status and prospectively preventing the future outbreak of 'Disease X'.

References

The Human Protein Atlas [Online]. Available: https://v16.proteinatlas.org/ENSG00000152778-IFIT5/cell#human [Accessed 2022].

IFIT5 gene [Online]. The Human Protein Atlas. Available: https://www.proteinatlas.org/ENSG00000152778-IFIT5/subcellular#human [Accessed 08/03/23].

AB HAKIM, N. H., MAJLIS, B. Y., SUZUKI, H. & TSUKAHARA, T. 2017. Neuron-specific splicing. *Bioscience trends,* 11**,** 16-22.

ABBAS, Y. M., PICHLMAIR, A., GÓRNA, M. W., SUPERTI-FURGA, G. & NAGAR, B. 2013. Structural basis for viral 5′-PPP-RNA recognition by human IFIT proteins. *Nature,* 494**,** 60-64.

AFELT, A., DEVAUX, C., SERRA-COBO, J. & FRUTOS, R. 2018. Bats, bat-borne viruses, and environmental changes. *Bats. IntechOpen, London***,** 113-132.

AFROUGH, B., DOWALL, S. & HEWSON, R. 2019. Emerging viruses and current strategies for vaccine intervention. *Clinical & Experimental Immunology,* 196**,** 157-166.

AGENCY, U. H. S. 2023. *UK Health Security Agency* [Online]. GOV.UK: UK Health Security Agency. Available: https://www.gov.uk/government/publications/emerging-infections-characteristics-epidemiology-and-global-distribution/emerging-infections-how-and-why-they-arise [Accessed 22nd March 2023].

AGUIRRE, A. A., CATHERINA, R., FRYE, H. & SHELLEY, L. 2020. Illicit wildlife trade, wet markets, and COVID-19: preventing future pandemics. *World Medical & Health Policy,* 12**,** 256-265.

AHN, M., ANDERSON, D. E., ZHANG, Q., TAN, C. W., LIM, B. L., LUKO, K., WEN, M., CHIA, W. N., MANI, S. & WANG, L. C. 2019. Dampened NLRP3-mediated inflammation in bats and implications for a special viral reservoir host. *Nature microbiology,* 4**,** 789-799.

AHN, M., CUI, J., IRVING, A. & WANG, L. 2016a. Unique loss of the PYHIN gene family in bats amongst mammals: implications for inflammasome sensing. Sci Rep 6: 21722.

AHN, M., CUI, J., IRVING, A. T. & WANG, L.-F. 2016b. Unique loss of the PYHIN gene family in bats amongst mammals: implications for inflammasome sensing. *Scientific reports,* 6**,** 1-7.

ALAMANCOS, G. P., PAGÈS, A., TRINCADO, J. L., BELLORA, N. & EYRAS, E. 2015. Leveraging transcript quantification for fast computation of alternative splicing profiles. *Rna,* 21**,** 1521-1531.

ALLEN, T., MURRAY, K. A., ZAMBRANA-TORRELIO, C., MORSE, S. S., RONDININI, C., DI MARCO, M., BREIT, N., OLIVAL, K. J. & DASZAK, P. 2017. Global hotspots and correlates of emerging zoonotic diseases. *Nature communications,* 8**,** 1124.

ALTIZER, S., BARTEL, R. & HAN, B. A. 2011. Animal migration and infectious disease risk. *science,* 331**,** 296-302.

ANDERS, S. & HUBER, W. 2012. Differential expression of RNA-Seq data at the gene level–the DESeq package. *Heidelberg, Germany: European Molecular Biology Laboratory (EMBL),* 10**,** f1000research.

ANDERS, S., REYES, A. & HUBER, W. 2012. Detecting differential usage of exons from RNA-seq data. *Nature Precedings***,** 1-1.

ANDERSON, S. C. & RUXTON, G. D. 2020. The evolution of flight in bats: a novel hypothesis. *Mammal Review,* 50**,** 426-439.

ANK, N. & PALUDAN, S. R. 2009. Type III IFNs: new layers of complexity in innate antiviral immunity. *Biofactors,* 35**,** 82-87.

ANK, N., WEST, H. & PALUDAN, S. R. 2006. IFN-λ: novel antiviral cytokines. *Journal of Interferon & Cytokine Research,* 26**,** 373-379.
ASHRAF, U., BENOIT-PILVEN, C., LACROIX, V., NAVRATIL, V. & NAFFAKH, N. 2019. Advances in analyzing virus-induced alterations of host cell splicing. *Trends in microbiology,* 27**,** 268-281.
AUSTAD, S. N. 2005. Diverse aging rates in metazoans: targets for functional genomics. *Mechanisms of ageing and development,* 126**,** 43-49.
AUSTAD, S. N. & FISCHER, K. E. 1991. Mammalian aging, metabolism, and ecology: evidence from the bats and marsupials. *Journal of gerontology,* 46**,** B47-B53.
AVOTA, E., BODEM, J., CHITHELEN, J., MANDASARI, P., BEYERSDORF, N. & SCHNEIDER-SCHAULIES, J. 2021. The manifold roles of sphingolipids in viral infections. *Frontiers in Physiology,* 12**,** 715527.
BADRANE, H. & TORDO, N. L. 2001. Host switching in Lyssavirus history from the Chiroptera to the Carnivora orders. *Journal of virology,* 75**,** 8096-8104.
BAKER, M., SCHOUNTZ, T. & WANG, L. F. 2013. Antiviral immune responses of bats: a review. *Zoonoses and public health,* 60**,** 104-116.
BAKER, M. L., TACHEDJIAN, M. & WANG, L.-F. 2010. Immunoglobulin heavy chain diversity in Pteropid bats: evidence for a diverse and highly specific antigen binding repertoire. *Immunogenetics,* 62**,** 173-184.
BAKER, M. L. & ZHOU, P. 2015. Bat immunology. *Bats and viruses: a new frontier of emerging infectious diseases***,** 327-348.
BAKER, R. J., LONGMIRE, J. L., MALTBIE, M., HAMILTON, M. J. & VAN DEN BUSSCHE, R. A. 1997. DNA synapomorphies for a variety of taxonomic levels from a cosmid library from the New World bat Macrotus waterhousii. *Systematic biology,* 46**,** 579-589.
BALKEMA-BUSCHMANN, A., RISSMANN, M., KLEY, N., ULRICH, R., EIDEN, M. & GROSCHUP, M. H. 2018. Productive propagation of rift valley fever phlebovirus vaccine strain MP-12 in Rousettus aegyptiacus fruit bats. *Viruses,* 10**,** 681.
BANERJEE, A., BAKER, M. L., KULCSAR, K., MISRA, V., PLOWRIGHT, R. & MOSSMAN, K. 2020. Novel insights into immune systems of bats. *Frontiers in immunology,* 11**,** 26.
BANERJEE, A., FALZARANO, D., RAPIN, N., LEW, J. & MISRA, V. 2019. Interferon regulatory factor 3-mediated signaling limits Middle-East respiratory syndrome (MERS) coronavirus propagation in cells from an insectivorous bat. *Viruses,* 11**,** 152.
BANERJEE, A., MISRA, V., SCHOUNTZ, T. & BAKER, M. L. 2018. Tools to study pathogen-host interactions in bats. *Virus research,* 248**,** 5-12.
BANERJEE, A., RAPIN, N., BOLLINGER, T. & MISRA, V. 2017. Lack of inflammatory gene expression in bats: a unique role for a transcription repressor. *Scientific reports,* 7**,** 2232.
BANERJEE, A., RAPIN, N., MILLER, M., GRIEBEL, P., ZHOU, Y., MUNSTER, V. & MISRA, V. 2016. Generation and Characterization of Eptesicus fuscus (Big brown bat) kidney cell lines immortalized using the Myotis polyomavirus large T-antigen. *Journal of virological methods,* 237**,** 166-173.
BANGE, F.-C., VOGEL, U., FLOHR, T., KIEKENBECK, M., DENECKE, B. & BÖTTGER, E. 1994. IFP 35 is an interferon-induced leucine zipper protein that undergoes interferon-regulated cellular redistribution. *Journal of Biological Chemistry,* 269**,** 1091-1098.
BARBER, G. N. 2015. STING: infection, inflammation and cancer. *Nature Reviews Immunology,* 15**,** 760-770.
BARZILAI, A., ROTMAN, G. & SHILOH, Y. 2002. ATM deficiency and oxidative stress: a new dimension of defective response to DNA damage. *DNA repair,* 1**,** 3-25.

BECKER, D. J., WASHBURNE, A. D., FAUST, C. L., PULLIAM, J. R., MORDECAI, E. A., LLOYD-SMITH, J. O. & PLOWRIGHT, R. K. 2019. Dynamic and integrative approaches to understanding pathogen spillover. The Royal Society.

BENTE, D. A., FORRESTER, N. L., WATTS, D. M., MCAULEY, A. J., WHITEHOUSE, C. A. & BRAY, M. 2013. Crimean-Congo hemorrhagic fever: history, epidemiology, pathogenesis, clinical syndrome and genetic diversity. *Antiviral research,* 100**,** 159-189.

BIRHAN, G., ALEBIE, A., ADMASSU, B., SHITE, A., MOHAMED, S. & DAGNAW, B. 2015. A Review on Emerging and re Emerging Viral Zoonotic Diseases.

BLATTEIS, C. M. 2003. Fever: pathological or physiological, injurious or beneficial? *Journal of thermal biology,* 28**,** 1-13.

BLEHERT, D. S., HICKS, A. C., BEHR, M., METEYER, C. U., BERLOWSKI-ZIER, B. M., BUCKLES, E. L., COLEMAN, J. T., DARLING, S. R., GARGAS, A. & NIVER, R. 2009. Bat white-nose syndrome: an emerging fungal pathogen? *Science,* 323**,** 227-227.

BONAPARTE, M. I., DIMITROV, A. S., BOSSART, K. N., CRAMERI, G., MUNGALL, B. A., BISHOP, K. A., CHOUDHRY, V., DIMITROV, D. S., WANG, L.-F. & EATON, B. T. 2005. Ephrin-B2 ligand is a functional receptor for Hendra virus and Nipah virus. *Proceedings of the National Academy of Sciences,* 102**,** 10652-10657.

BORREMANS, B., FAUST, C., MANLOVE, K. R., SOKOLOW, S. H. & LLOYD-SMITH, J. O. 2019. Cross-species pathogen spillover across ecosystem boundaries: mechanisms and theory. *Philosophical Transactions of the Royal Society B,* 374**,** 20180344.

BRIERLEY, L., VONHOF, M. J., OLIVAL, K. J., DASZAK, P. & JONES, K. E. 2016. Quantifying global drivers of zoonotic bat viruses: a process-based perspective. *The American Naturalist,* 187**,** E53-E64.

BRINKMANN, A., KOHL, C., RADONIĆ, A., DABROWSKI, P. W., MÜHLDORFER, K., NITSCHE, A., WIBBELT, G. & KURTH, A. 2020. First detection of bat-borne Issyk-Kul virus in Europe. *Scientific Reports,* 10**,** 1-7.

BROGGI, A., TAN, Y., GRANUCCI, F. & ZANONI, I. 2017. IFN-λ suppresses intestinal inflammation by non-translational regulation of neutrophil function. *Nature immunology,* 18**,** 1084-1093.

BROOK, C. E. & DOBSON, A. P. 2015. Bats as 'special'reservoirs for emerging zoonotic pathogens. *Trends in microbiology,* 23**,** 172-180.

BROWN, C. 2004. Emerging zoonoses and pathogens of public health significance--an overview. *Revue scientifique et technique-office international des epizooties,* 23**,** 435-442.

BRUNETTE, R. L., YOUNG, J. M., WHITLEY, D. G., BRODSKY, I. E., MALIK, H. S. & STETSON, D. B. 2012. Extensive evolutionary and functional diversity among mammalian AIM2-like receptors. *Journal of Experimental Medicine,* 209**,** 1969-1983.

BRZÓZKA, K., FINKE, S. & CONZELMANN, K.-K. 2006. Inhibition of interferon signaling by rabies virus phosphoprotein P: activation-dependent binding of STAT1 and STAT2. *Journal of virology,* 80**,** 2675-2683.

CAILLOUËT, K. A., MICHAELS, S. R., XIONG, X., FOPPA, I. & WESSON, D. M. 2008. Increase in West Nile neuroinvasive disease after hurricane Katrina. *Emerging infectious diseases,* 14**,** 804.

CALISHER, C. H., CHILDS, J. E., FIELD, H. E., HOLMES, K. V. & SCHOUNTZ, T. 2006. Bats: important reservoir hosts of emerging viruses. *Clinical microbiology reviews,* 19**,** 531-545.

CAPOBIANCHI, M. R., ULERI, E., CAGLIOTI, C. & DOLEI, A. 2015. Type I IFN family members: similarity, differences and interaction. *Cytokine & growth factor reviews,* 26**,** 103-111.

CHAKRABARTI, A., BANERJEE, S., FRANCHI, L., LOO, Y.-M., GALE JR, M., NÚÑEZ, G. & SILVERMAN, R. H. 2015. RNase L activates the NLRP3 inflammasome during viral infections. *Cell host & microbe,* 17**,** 466-477.
CHAN, M. & JOHANSSON, M. A. 2012. The incubation periods of dengue viruses. *PloS one,* 7**,** e50972.
CHAUHAN, K., KALAM, H., DUTT, R. & KUMAR, D. 2019. RNA splicing: a new paradigm in host–pathogen interactions. *Journal of molecular biology,* 431**,** 1565-1575.
CHEN, I.-Y., MORIYAMA, M., CHANG, M.-F. & ICHINOHE, T. 2019. Severe acute respiratory syndrome coronavirus viroporin 3a activates the NLRP3 inflammasome. *Frontiers in microbiology,* 10**,** 50.
CHEN, J., SHPALL, R. L., MEYERDIERKS, A., HAGEMEIER, M., BÖTTGER, E. C. & NAUMOVSKI, L. 2000. Interferon-inducible Myc/STAT-interacting protein Nmi associates with IFP 35 into a high molecular mass complex and inhibits proteasome-mediated degradation of IFP 35. *Journal of Biological Chemistry,* 275**,** 36278-36284.
CHEN, L., CHEN, K., HONG, Y., XING, L., ZHANG, J., ZHANG, K. & ZHANG, Z. 2022. The landscape of isoform switches in sepsis: a multicenter cohort study. *Scientific Reports,* 12**,** 10276.
CHEN, L., LIU, B., YANG, J. & JIN, Q. 2014. DBatVir: the database of bat-associated viruses. *Database,* 2014.
CHEN, L. H. & WILSON, M. E. 2008. The role of the traveler in emerging infections and magnitude of travel. *Medical Clinics of North America,* 92**,** 1409-1432.
CHEVALIER, V., PÉPIN, M., PLEE, L. & LANCELOT, R. 2010. Rift Valley fever-a threat for Europe? *Eurosurveillance,* 15.
CHUA, K., BELLINI, W., ROTA, P., HARCOURT, B., TAMIN, A., LAM, S., KSIAZEK, T., ROLLIN, P., ZAKI, S. & SHIEH, W.-J. 2000. Nipah virus: a recently emergent deadly paramyxovirus. *Science,* 288**,** 1432-1435.
CHUA, K. B., GOH, K. J., WONG, K. T., KAMARULZAMAN, A., TAN, P. S. K., KSIAZEK, T. G., ZAKI, S. R., PAUL, G., LAM, S. K. & TAN, C. T. 1999. Fatal encephalitis due to Nipah virus among pig-farmers in Malaysia. *The Lancet,* 354**,** 1257-1259.
CHUA, K. B., KOH, C. L., HOOI, P. S., WEE, K. F., KHONG, J. H., CHUA, B. H., CHAN, Y. P., LIM, M. E. & LAM, S. K. 2002. Isolation of Nipah virus from Malaysian Island flying-foxes. *Microbes and infection,* 4**,** 145-151.
CLAYTON, E. & MUNIR, M. 2020. Fundamental characteristics of bat interferon systems. *Frontiers in cellular and infection microbiology,* 10**,** 527921.
COCHET, M., VAIMAN, D. & LEFÈVRE, F. 2009. Novel interferon delta genes in mammals: cloning of one gene from the sheep, two genes expressed by the horse conceptus and discovery of related sequences in several taxa by genomic database screening. *Gene,* 433**,** 88-99.
COGSWELL-HAWKINSON, A., BOWEN, R., JAMES, S., GARDINER, D., CALISHER, C. H., ADAMS, R. & SCHOUNTZ, T. 2012. Tacaribe virus causes fatal infection of an ostensible reservoir host, the Jamaican fruit bat. *Journal of virology,* 86**,** 5791-5799.
COLLINS, S. E. & MOSSMAN, K. L. 2014. Danger, diversity and priming in innate antiviral immunity. *Cytokine & growth factor reviews,* 25**,** 525-531.
CONSORTIUM, E. P. 2012. An integrated encyclopedia of DNA elements in the human genome. *Nature,* 489**,** 57.
CONSTANTINE, D. G. 1967. *Activity patterns of the Mexican free-tailed bat*, University of New Mexico Press.
CONSTANTINE, D. G. 1968. *Rabies transmission by air in bat caves*, National Communicable Disease Center.
CONSTANTINE, D. G., EMMONS, R. W. & WOODIE, J. D. 1972. Rabies virus in nasal mucosa of naturally infected bats. *Science,* 175**,** 1255-1256.

CORRALES-AGUILAR, E. & SCHWEMMLE, M. 2020. *Bats and Viruses: Current Research and Future Trends*, United Kingdom.
COWLED, C., BAKER, M., TACHEDJIAN, M., ZHOU, P., BULACH, D. & WANG, L.-F. 2011. Molecular characterisation of Toll-like receptors in the black flying fox Pteropus alecto. *Developmental & Comparative Immunology,* 35**,** 7-18.
COWLED, C., BAKER, M. L., ZHOU, P., TACHEDJIAN, M. & WANG, L.-F. 2012. Molecular characterisation of RIG-I-like helicases in the black flying fox, Pteropus alecto. *Developmental & Comparative Immunology,* 36**,** 657-664.
CRAMERI, G., TODD, S., GRIMLEY, S., MCEACHERN, J. A., MARSH, G. A., SMITH, C., TACHEDJIAN, M., DE JONG, C., VIRTUE, E. R. & YU, M. 2009. Establishment, immortalisation and characterisation of pteropid bat cell lines. *PloS one,* 4**,** e8266.
CROOKS, G. E., HON, G., CHANDONIA, J.-M. & BRENNER, S. E. 2004. WebLogo: a sequence logo generator. *Genome research,* 14**,** 1188-1190.
D'ANDREA, L. D. & REGAN, L. 2003. TPR proteins: the versatile helix. *Trends in biochemical sciences,* 28**,** 655-662.
DAS, A., DINH, P. X., PANDA, D. & PATTNAIK, A. K. 2014. Interferon-inducible protein IFI35 negatively regulates RIG-I antiviral signaling and supports vesicular stomatitis virus replication. *Journal of virology,* 88**,** 3103-3113.
DASZAK, P., CUNNINGHAM, A. A. & HYATT, A. D. 2000. Emerging infectious diseases of wildlife--threats to biodiversity and human health. *science,* 287**,** 443-449.
DASZAK, P., CUNNINGHAM, A. A. & HYATT, A. D. 2001. Anthropogenic environmental change and the emergence of infectious diseases in wildlife. *Acta tropica,* 78**,** 103-116.
DASZAK, P., DAS NEVES, C., AMUASI, J., HAYMEN, D., KUIKEN, T., ROCHE, B., ZAMBRANA-TORRELIO, C., BUSS, P., DUNDAROVA, H. & FEFERHOLTZ, Y. 2020. Workshop report on biodiversity and pandemics of the Intergovernmental Platform on Biodiversity and Ecosystem Services. IPBES.
DE BENEDICTIS, P., MARCIANO, S., SCARAVELLI, D., PRIORI, P., ZECCHIN, B., CAPUA, I., MONNE, I. & CATTOLI, G. 2014. Alpha and lineage C betaCoV infections in Italian bats. *Virus genes,* 48**,** 366-371.
DE MAIO, F. A., RISSO, G., IGLESIAS, N. G., SHAH, P., POZZI, B., GEBHARD, L. G., MAMMI, P., MANCINI, E., YANOVSKY, M. J. & ANDINO, R. 2016. The dengue virus NS5 protein intrudes in the cellular spliceosome and modulates splicing. *PLoS pathogens,* 12**,** e1005841.
DE MASI, R. & ORLANDO, S. 2020. IFI35 as a biomolecular marker of neuroinflammation and treatment response in multiple sclerosis. *Life Sciences,* 259**,** 118233.
DE MASI, R., ORLANDO, S., BAGORDO, F. & GRASSI, T. 2021. IFP35 is a relevant factor in innate immunity, multiple sclerosis, and other chronic inflammatory diseases: a review. *Biology,* 10**,** 1325.
DE WEERD, N. A. & NGUYEN, T. 2012. The interferons and their receptors—distribution and regulation. *Immunology and cell biology,* 90**,** 483-491.
DIAMOND, M. S. & FARZAN, M. 2013. The broad-spectrum antiviral functions of IFIT and IFITM proteins. *Nature Reviews Immunology,* 13**,** 46-57.
DIAMOND, M. S. & KANNEGANTI, T.-D. 2022. Innate immunity: the first line of defense against SARS-CoV-2. *Nature immunology,* 23**,** 165-176.
DONG, Z. & CHEN, Y. 2013. Transcriptomics: advances and approaches. *Science China Life Sciences,* 56**,** 960-967.
DREDGE, B. K., POLYDORIDES, A. D. & DARNELL, R. B. 2001. The splice of life: alternative splicing and neurological disease. *Nature Reviews Neuroscience,* 2**,** 43-50.

DREXLER, J. F., CORMAN, V. M., GLOZA-RAUSCH, F., SEEBENS, A., ANNAN, A., IPSEN, A., KRUPPA, T., MÜLLER, M. A., KALKO, E. K. & ADU-SARKODIE, Y. 2009. Henipavirus RNA in African bats. *PloS one,* 4**,** e6367.

DREXLER, J. F., GEIPEL, A., KÖNIG, A., CORMAN, V. M., VAN RIEL, D., LEIJTEN, L. M., BREMER, C. M., RASCHE, A., COTTONTAIL, V. M. & MAGANGA, G. D. 2013. Bats carry pathogenic hepadnaviruses antigenically related to hepatitis B virus and capable of infecting human hepatocytes. *Proceedings of the National Academy of Sciences,* 110**,** 16151-16156.

EATON, B. T., BRODER, C. C., MIDDLETON, D. & WANG, L.-F. 2006. Hendra and Nipah viruses: different and dangerous. *Nature Reviews Microbiology,* 4**,** 23-35.

EDSON, D., FIELD, H., MCMICHAEL, L., VIDGEN, M., GOLDSPINK, L., BROOS, A., MELVILLE, D., KRISTOFFERSEN, J., DE JONG, C. & MCLAUGHLIN, A. 2015. Routes of Hendra virus excretion in naturally-infected flying-foxes: implications for viral transmission and spillover risk. *PloS one,* 10**,** e0140670.

EISENBERG, J. F. 1980. The density and biomass of tropical mammals. *Conservation biology***,** 35-55.

ELLWANGER, J. H. & CHIES, J. A. B. 2021. Zoonotic spillover: Understanding basic aspects for better prevention. *Genetics and Molecular Biology,* 44.

ELLWANGER, J. H., ZAMBRA, F. M. B., GUIMARÃES, R. L. & CHIES, J. A. B. 2018. MicroRNA-related polymorphisms in infectious diseases—tiny changes with a huge impact on viral infections and potential clinical applications. *Frontiers in immunology,* 9**,** 1316.

ESCALERA-ZAMUDIO, M., ZEPEDA-MENDOZA, M. L., LOZA-RUBIO, E., ROJAS-ANAYA, E., MÉNDEZ-OJEDA, M. L., ARIAS, C. F. & GREENWOOD, A. D. 2015. The evolution of bat nucleic acid-sensing Toll-like receptors. *Molecular ecology,* 24**,** 5899-5909.

FAGROUCH, Z., SARWARI, R., LAVERGNE, A., DELAVAL, M., DE THOISY, B., LACOSTE, V. & VERSCHOOR, E. J. 2012. Novel polyomaviruses in South American bats and their relationship to other members of the family Polyomaviridae. *Journal of general virology,* 93**,** 2652-2657.

FAUST, C. L., MCCALLUM, H. I., BLOOMFIELD, L. S., GOTTDENKER, N. L., GILLESPIE, T. R., TORNEY, C. J., DOBSON, A. P. & PLOWRIGHT, R. K. 2018. Pathogen spillover during land conversion. *Ecology letters,* 21**,** 471-483.

FELDMANN, H., CZUB, M., JONES, S., DICK, D., GARBUTT, M., GROLLA, A. & ARTSOB, H. 2002. Emerging and re-emerging infectious diseases. *Medical microbiology and immunology,* 191**,** 63-74.

FENG, F., YUAN, L., WANG, Y. E., CROWLEY, C., LV, Z., LI, J., LIU, Y., CHENG, G., ZENG, S. & LIANG, H. 2013. Crystal structure and nucleotide selectivity of human IFIT5/ISG58. *Cell research,* 23**,** 1055-1058.

FENG, H., SANDER, A.-L., MOREIRA-SOTO, A., YAMANE, D., DREXLER, J. F. & LEMON, S. M. 2019. Hepatovirus 3ABC proteases and evolution of mitochondrial antiviral signaling protein (MAVS). *Journal of hepatology,* 71**,** 25-34.

FENSTERL, V. & SEN, G. C. 2015. Interferon-induced Ifit proteins: their role in viral pathogenesis. *Journal of virology,* 89**,** 2462-2468.

FENTON, M. B. & SIMMONS, N. B. 2020. *Bats: a world of science and mystery*, University of Chicago Press.

FIELD, H. 2009. Bats and emerging zoonoses: henipaviruses and SARS. *Zoonoses and public health,* 56**,** 278-284.

FIELD, H., BARRATT, P., HUGHES, R., SHIELD, J. & SULLIVAN, N. 2000. Fatal case of Hendra virus infection in a horse in north Queensland: clinical and epidemiological features. *Australian veterinary journal 78*(4), pp.279-280.

FIELD, H., MACKENZIE, J. S. & DASZAK, P. 2007. Henipaviruses: emerging paramyxoviruses associated with fruit bats. *Wildlife and emerging zoonotic diseases: the biology, circumstances and consequences of cross-species transmission*, 133-159.
FIELD, H., MCCALL, B. & BARRETT, J. 1999. Australian bat lyssavirus infection in a captive juvenile black flying fox. *Emerging infectious diseases,* 5, 438.
FISHER, C. R., STREICKER, D. G. & SCHNELL, M. J. 2018. The spread and evolution of rabies virus: conquering new frontiers. *Nature Reviews Microbiology,* 16, 241-255.
FLEITH, R. C., MEARS, H. V., LEONG, X. Y., SANFORD, T. J., EMMOTT, E., GRAHAM, S. C., MANSUR, D. S. & SWEENEY, T. R. 2018. IFIT3 and IFIT2/3 promote IFIT1-mediated translation inhibition by enhancing binding to non-self RNA. *Nucleic acids research,* 46, 5269-5285.
FOLEY, N. M., HUGHES, G. M., HUANG, Z., CLARKE, M., JEBB, D., WHELAN, C. V., PETIT, E. J., TOUZALIN, F., FARCY, O. & JONES, G. 2018. Growing old, yet staying young: The role of telomeres in bats' exceptional longevity. *Science Advances,* 4, eaao0926.
FOX, B. A., SHEPPARD, P. O. & O'HARA, P. J. 2009. The role of genomic data in the discovery, annotation and evolutionary interpretation of the interferon-lambda family. *PloS one,* 4, e4933.
FUCHS, J., HÖLZER, M., SCHILLING, M., PATZINA, C., SCHOEN, A., HOENEN, T., ZIMMER, G., MARZ, M., WEBER, F. & MÜLLER, M. A. 2017. Evolution and antiviral specificities of interferon-induced Mx proteins of bats against Ebola, influenza, and other RNA viruses. *Journal of virology,* 91, e00361-17.
FUJII, H., WATANABE, S., YAMANE, D., UEDA, N., IHA, K., TANIGUCHI, S., KATO, K., TOHYA, Y., KYUWA, S. & YOSHIKAWA, Y. 2010. Functional analysis of Rousettus aegyptiacus "signal transducer and activator of transcription 1"(STAT1). *Developmental & Comparative Immunology,* 34, 598-602.
FUJII, R., OKAMOTO, M., ARATANI, S., OISHI, T., OHSHIMA, T., TAIRA, K., BABA, M., FUKAMIZU, A. & NAKAJIMA, T. 2001. A role of RNA helicase A in cis-acting transactivation response element-mediated transcriptional regulation of human immunodeficiency virus type 1. *Journal of Biological Chemistry,* 276, 5445-5451.
FUMAGALLI, M. R., ZAPPERI, S. & LA PORTA, C. A. 2021. Role of body temperature variations in bat immune response to viral infections. *Journal of the Royal Society Interface,* 18, 20210211.
GAD, H. H., DELLGREN, C., HAMMING, O. J., VENDS, S., PALUDAN, S. R. & HARTMANN, R. 2009. Interferon-λ is functionally an interferon but structurally related to the interleukin-10 family. *Journal of Biological Chemistry,* 284, 20869-20875.
GAMAGE, A. M., ZHU, F., AHN, M., FOO, R. J. H., HEY, Y. Y., LOW, D. H., MENDENHALL, I. H., DUTERTRE, C.-A. & WANG, L.-F. 2020. Immunophenotyping monocytes, macrophages and granulocytes in the Pteropodid bat Eonycteris spelaea. *Scientific reports,* 10, 1-16.
GARG, K. M., LAMBA, V., SANYAL, A., DOVIH, P. & CHATTOPADHYAY, B. 2023. Next Generation Sequencing Revolutionizes Organismal Biology Research in Bats. *Journal of Molecular Evolution*, 1-14.
GE, S. X., JUNG, D. & YAO, R. 2020. ShinyGO: a graphical gene-set enrichment tool for animals and plants. *Bioinformatics,* 36, 2628-2629.
GEISER, F. & KÖRTNER, G. 2010. Hibernation and daily torpor in Australian mammals. *Australian Zoologist,* 35, 204-215.
GEISER, F. & STAWSKI, C. 2011. Hibernation and torpor in tropical and subtropical bats in relation to energetics, extinctions, and the evolution of endothermy. *Integrative and comparative biology,* 51, 337-348.

GIBB, R., REDDING, D. W., CHIN, K. Q., DONNELLY, C. A., BLACKBURN, T. M., NEWBOLD, T. & JONES, K. E. 2020. Zoonotic host diversity increases in human-dominated ecosystems. *Nature,* 584**,** 398-402.
GIBBS, E. P. J. 2014. The evolution of One Health: a decade of progress and challenges for the future. *Veterinary Record,* 174**,** 85-91.
GLENNON, N. B., JABADO, O., LO, M. K. & SHAW, M. L. 2015. Transcriptome profiling of the virus-induced innate immune response in Pteropus vampyrus and its attenuation by Nipah virus interferon antagonist functions. *Journal of virology,* 89**,** 7550-7566.
GLORIA-SORIA, A., ARMSTRONG, P., POWELL, J. & TURNER, P. 2017. Infection rate of Aedes aegypti mosquitoes with dengue virus depends on the interaction between temperature and mosquito genotype. *Proceedings of the Royal Society B: Biological Sciences,* 284**,** 20171506.
GOODBOURN, S., DIDCOCK, L. & RANDALL, R. 2000. Interferons: cell signalling, immune modulation, antiviral response and virus countermeasures. *Journal of general virology,* 81**,** 2341-2364.
GRANDVAUX, N., SERVANT, M. J. & HISCOTT, J. 2002a. The interferon antiviral response: from viral invasion to evasion. *Current opinion in infectious diseases,* 15**,** 259-267.
GRANDVAUX, N., SERVANT, M. J., TENOEVER, B., SEN, G. C., BALACHANDRAN, S., BARBER, G. N., LIN, R. & HISCOTT, J. 2002b. Transcriptional profiling of interferon regulatory factor 3 target genes: direct involvement in the regulation of interferon-stimulated genes. *Journal of virology,* 76**,** 5532-5539.
GRAVELEY, B. R. 2001. Alternative splicing: increasing diversity in the proteomic world. *TRENDS in Genetics,* 17**,** 100-107.
GREENFELD, H., TAKASAKI, K., WALSH, M. J., ERSING, I., BERNHARDT, K., MA, Y., FU, B., ASHBAUGH, C. W., CABO, J. & MOLLO, S. B. 2015. TRAF1 coordinates polyubiquitin signaling to enhance Epstein-Barr virus LMP1-mediated growth and survival pathway activation. *PLoS pathogens,* 11**,** e1004890.
GRIfIIN, D. R. 2012. Migrations and homing of bats. *Biology of bats***,** 233.
GRUBAUGH, N. D., LADNER, J. T., KRAEMER, M. U., DUDAS, G., TAN, A. L., GANGAVARAPU, K., WILEY, M. R., WHITE, S., THÉZÉ, J. & MAGNANI, D. M. 2017. Genomic epidemiology reveals multiple introductions of Zika virus into the United States. *Nature,* 546**,** 401-405.
GUO, F., SUN, A., WANG, W., HE, J., HOU, J., ZHOU, P. & CHEN, Z. 2009. TRAF1 is involved in the classical NF-κB activation and CD30-induced alternative activity in Hodgkin's lymphoma cells. *Molecular immunology,* 46**,** 2441-2448.
GUO, W.-P., LIN, X.-D., WANG, W., TIAN, J.-H., CONG, M.-L., ZHANG, H.-L., WANG, M.-R., ZHOU, R.-H., WANG, J.-B. & LI, M.-H. 2013. Phylogeny and origins of hantaviruses harbored by bats, insectivores, and rodents. *PLoS pathogens,* 9**,** e1003159.
GUPTA, P., SINGH, M. P., GOYAL, K., TRIPTI, P., ANSARI, M. I., OBLI RAJENDRAN, V., DHAMA, K. & MALIK, Y. S. 2021. Bats and viruses: a death-defying friendship. *Virusdisease***,** 1-13.
HABJAN, M., HUBEL, P., LACERDA, L., BENDA, C., HOLZE, C., EBERL, C. H., MANN, A., KINDLER, E., GIL-CRUZ, C. & ZIEBUHR, J. 2013. Sequestration by IFIT1 impairs translation of 2′ O-unmethylated capped RNA. *PLoS pathogens,* 9**,** e1003663.
HABJAN, M., PENSKI, N., WAGNER, V., SPIEGEL, M., ÖVERBY, A. K., KOCHS, G., HUISKONEN, J. T. & WEBER, F. 2009. Efficient production of Rift Valley fever virus-like particles: the antiviral protein MxA can inhibit primary transcription of bunyaviruses. *Virology,* 385**,** 400-408.

HAHN, B. H., SHAW, G. M., DE, K. M., COCK & SHARP, P. M. 2000. AIDS as a zoonosis: scientific and public health implications. *Science,* 287**,** 607-614.
HAIDER, N., ROTHMAN-OSTROW, P., OSMAN, A. Y., ARRUDA, L. B., MACFARLANE-BERRY, L., ELTON, L., THOMASON, M. J., YEBOAH-MANU, D., ANSUMANA, R. & KAPATA, N. 2020. COVID-19—zoonosis or emerging infectious disease? *Frontiers in Public Health,* 8**,** 763.
HALL, T. A. BioEdit: a user-friendly biological sequence alignment editor and analysis program for Windows 95/98/NT. Nucleic acids symposium series, 1999. [London]: Information Retrieval Ltd., c1979-c2000., 95-98.
HALLORAN, M. E. 1998. Concepts of Infectious Diseases Epidemiology. *Modern epidemiology*.
HALPIN, K., HYATT, A. D., FOGARTY, R., MIDDLETON, D., BINGHAM, J., EPSTEIN, J. H., RAHMAN, S. A., HUGHES, T., SMITH, C. & FIELD, H. E. 2011. Pteropid bats are confirmed as the reservoir hosts of henipaviruses: a comprehensive experimental study of virus transmission. *The American journal of tropical medicine and hygiene,* 85**,** 946.
HALPIN, K., YOUNG, P. L., FIELD, H. & MACKENZIE, J. 2000. Isolation of Hendra virus from pteropid bats: a natural reservoir of Hendra virus. *Journal of General Virology,* 81**,** 1927-1932.
HAWKINS, J. A., KACZMAREK, M. E., MÜLLER, M. A., DROSTEN, C., PRESS, W. H. & SAWYER, S. L. 2019. A metaanalysis of bat phylogenetics and positive selection based on genomes and transcriptomes from 18 species. *Proceedings of the National Academy of Sciences,* 116**,** 11351-11360.
HAYMAN, D., BOWEN, R., CRYAN, P., MCCRACKEN, G., O'SHEA, T., PEEL, A., GILBERT, A., WEBB, C. & WOOD, J. 2013. Ecology of zoonotic infectious diseases in bats: current knowledge and future directions. *Zoonoses and public health,* 60**,** 2-21.
HAYMAN, D. T. 2016. Bats as viral reservoirs. *Annual review of virology,* 3**,** 77-99.
HAYMAN, D. T. 2019. Bat tolerance to viral infections. *Nature microbiology,* 4**,** 728-729.
HAYMAN, D. T., SUU-IRE, R., BREED, A. C., MCEACHERN, J. A., WANG, L., WOOD, J. L. & CUNNINGHAM, A. A. 2008. Evidence of henipavirus infection in West African fruit bats. *PloS one,* 3**,** e2739.
HE, G., HE, B., RACEY, P. A. & CUI, J. 2010. Positive selection of the bat interferon alpha gene family. *Biochemical genetics,* 48**,** 840-846.
HESS, I. M., MASSEY, P. D., WALKER, B., MIDDLETON, D. J. & WRIGHT, T. M. 2011. Hendra virus: what do we know? *New South Wales Public Health Bulletin,* 22**,** 118-122.
HILL, J. E. & SMITH, J. D. 1984. Bats: a natural history.
HOLLAND, R. A. 2007. Orientation and navigation in bats: known unknowns or unknown unknowns? *Behavioral Ecology and Sociobiology,* 61**,** 653-660.
HOLLAND, R. A., WATERS, D. A. & RAYNER, J. M. 2004. Echolocation signal structure in the Megachiropteran bat Rousettus aegyptiacus Geoffroy 1810. *Journal of experimental biology,* 207**,** 4361-4369.
HÖLZER, M., KRÄHLING, V., AMMAN, F., BARTH, E., BERNHART, S. H., CARMELO, V. A., COLLATZ, M., DOOSE, G., EGGENHOFER, F. & EWALD, J. 2016. Differential transcriptional responses to Ebola and Marburg virus infection in bat and human cells. *Scientific reports,* 6**,** 34589.
HÖLZER, M., SCHOEN, A., WULLE, J., MÜLLER, M. A., DROSTEN, C., MARZ, M. & WEBER, F. 2019. Virus-and interferon alpha-induced transcriptomes of cells from the microbat Myotis daubentonii. *Iscience,* 19**,** 647-661.
HONDA, K., TAKAOKA, A. & TANIGUCHI, T. 2006. Type I inteferon gene induction by the interferon regulatory factor family of transcription factors. *Immunity,* 25**,** 349-360.

HONDA, K., YANAI, H., MIZUTANI, T., NEGISHI, H., SHIMADA, N., SUZUKI, N., OHBA, Y., TAKAOKA, A., YEH, W.-C. & TANIGUCHI, T. 2004. Role of a transductional-transcriptional processor complex involving MyD88 and IRF-7 in Toll-like receptor signaling. *Proceedings of the National Academy of Sciences,* 101**,** 15416-15421.

HONDA, K., YANAI, H., NEGISHI, H., ASAGIRI, M., SATO, M., MIZUTANI, T., SHIMADA, N., OHBA, Y., TAKAOKA, A. & YOSHIDA, N. 2005. IRF-7 is the master regulator of type-I interferon-dependent immune responses. *Nature,* 434**,** 772-777.

HOOPER, P., GOULD, A., RUSSELL, G., KATTENBELT, J. & MITCHELL, G. 1996. The retrospective diagnosis of a second outbreak of equine morbillivirus infection. *Australian veterinary journal,* 74**,** 244-245.

HOST, K. M. & DAMANIA, B. 2016. Discovery of a novel bat gammaherpesvirus. *Msphere,* 1**,** e00016-16.

HOWARD, C. R. & FLETCHER, N. F. 2012. Emerging virus diseases: can we ever expect the unexpected? *Emerging microbes & infections,* 1**,** 1-9.

HU, B., HUO, Y., YANG, L., CHEN, G., LUO, M., YANG, J. & ZHOU, J. 2017. ZIKV infection effects changes in gene splicing, isoform composition and lncRNA expression in human neural progenitor cells. *Virology journal,* 14**,** 1-11.

HUBEL, P., URBAN, C., BERGANT, V., SCHNEIDER, W. M., KNAUER, B., STUKALOV, A., SCATURRO, P., MANN, A., BRUNOTTE, L. & HOFFMANN, H. H. 2019. A protein-interaction network of interferon-stimulated genes extends the innate immune system landscape. *Nature immunology,* 20**,** 493-502.

HUMPHRIES, M. M., THOMAS, D. W. & SPEAKMAN, J. R. 2002. Climate-mediated energetic constraints on the distribution of hibernating mammals. *Nature,* 418**,** 313-316.

HUONG, N. Q., NGA, N. T. T., LONG, N. V., LUU, B. D., LATINNE, A., PRUVOT, M., PHUONG, N. T., QUANG, L. T. V., HUNG, V. V. & LAN, N. T. 2020. Coronavirus testing indicates transmission risk increases along wildlife supply chains for human consumption in Viet Nam, 2013-2014. *PLoS One,* 15**,** e0237129.

HUTCHEON, J. M., KIRSCH, J. A. & PETTIGREW, J. D. 1998. Base–compositional biases and the bat problem. III. The question of microchiropteran monophyly. *Philosophical Transactions of the Royal Society of London. Series B: Biological Sciences,* 353**,** 607-617.

IHA, K., OMATSU, T., WATANABE, S., UEDA, N., TANIGUCHI, S., FUJII, H., ISHII, Y., KYUWA, S., AKASHI, H. & YOSHIKAWA, Y. 2010. Molecular cloning and expression analysis of bat toll-like receptors 3, 7 and 9. *Journal of Veterinary Medical Science,* 72**,** 217-220.

IKEDA, F., HECKER, C. M., ROZENKNOP, A., NORDMEIER, R. D., ROGOV, V., HOFMANN, K., AKIRA, S., DÖTSCH, V. & DIKIC, I. 2007. Involvement of the ubiquitin-like domain of TBK1/IKK-i kinases in regulation of IFN-inducible genes. *The EMBO journal,* 26**,** 3451-3462.

IRVING, A. T., AHN, M., GOH, G., ANDERSON, D. E. & WANG, L.-F. 2021. Lessons from the host defences of bats, a unique viral reservoir. *Nature,* 589**,** 363-370.

IRVING, A. T., ZHANG, Q., KONG, P.-S., LUKO, K., ROZARIO, P., WEN, M., ZHU, F., ZHOU, P., NG, J. H. & SOBOTA, R. M. 2020. Interferon regulatory factors IRF1 and IRF7 directly regulate gene expression in bats in response to viral infection. *Cell reports,* 33**,** 108345.

IWASAKI, A. 2012. A virological view of innate immune recognition. *Annual review of microbiology,* 66**,** 177-196.

IYER, S. S., HE, Q., JANCZY, J. R., ELLIOTT, E. I., ZHONG, Z., OLIVIER, A. K., SADLER, J. J., KNEPPER-ADRIAN, V., HAN, R. & QIAO, L. 2013.

Mitochondrial cardiolipin is required for Nlrp3 inflammasome activation. *Immunity,* 39**,** 311-323.
JAIN, A., BACOLLA, A., CHAKRABORTY, P., GROSSE, F. & VASQUEZ, K. M. 2010. Human DHX9 helicase unwinds triple-helical DNA structures. *Biochemistry,* 49**,** 6992-6999.
JAIN, A., BACOLLA, A., DEL MUNDO, I. M., ZHAO, J., WANG, G. & VASQUEZ, K. M. 2013. DHX9 helicase is involved in preventing genomic instability induced by alternatively structured DNA in human cells. *Nucleic acids research,* 41**,** 10345-10357.
JANEWAY JR, C. A. & MEDZHITOV, R. 2002. Innate immune recognition. *Annual review of immunology,* 20**,** 197-216.
JEBB, D., FOLEY, N. M., WHELAN, C. V., TOUZALIN, F., PUECHMAILLE, S. J. & TEELING, E. C. 2018. Population level mitogenomics of long-lived bats reveals dynamic heteroplasmy and challenges the free radical theory of ageing. *Scientific reports,* 8**,** 13634.
JEBB, D., HUANG, Z., PIPPEL, M., HUGHES, G. M., LAVRICHENKO, K., DEVANNA, P., WINKLER, S., JERMIIN, L. S., SKIRMUNTT, E. C. & KATZOURAKIS, A. 2019. Six new reference-quality bat genomes illuminate the molecular basis and evolution of bat adaptations. *BioRxiv***,** 836874.
JIA, Y. Q., WANG, X. W., CHEN, X., QIU, X. X., WANG, X. L. & YANG, Z. Q. 2022. Characterization of chicken IFI35 and its antiviral activity against Newcastle disease virus. *Journal of Veterinary Medical Science,* 84**,** 473-483.
JILG, N., LIN, W., HONG, J., SCHAEFER, E. A., WOLSKI, D., MEIXONG, J., GOTO, K., BRISAC, C., CHUSRI, P. & FUSCO, D. N. 2014. Kinetic differences in the induction of interferon stimulated genes by interferon-α and interleukin 28B are altered by infection with hepatitis C virus. *Hepatology,* 59**,** 1250-1261.
JOHNSON, C. K., HITCHENS, P. L., PANDIT, P. S., RUSHMORE, J., EVANS, T. S., YOUNG, C. C. & DOYLE, M. M. 2020. Global shifts in mammalian population trends reveal key predictors of virus spillover risk. *Proceedings of the Royal Society B,* 287**,** 20192736.
JOHNSON, G., NOUR, A. A., NOLAN, T., HUGGETT, J. & BUSTIN, S. 2014. Minimum information necessary for quantitative real-time PCR experiments. *Quantitative Real-Time PCR: Methods and Protocols***,** 5-17.
JOHNSON, N., VOS, A., FREULING, C., TORDO, N., FOOKS, A. & MÜLLER, T. 2010. Human rabies due to lyssavirus infection of bat origin. *Veterinary microbiology,* 142**,** 151-159.
JONES, G. & HOLDERIED, M. W. 2007. Bat echolocation calls: adaptation and convergent evolution. *Proceedings of the Royal Society B: Biological Sciences,* 274**,** 905-912.
JONES, K. E., PATEL, N. G., LEVY, M. A., STOREYGARD, A., BALK, D., GITTLEMAN, J. L. & DASZAK, P. 2008. Global trends in emerging infectious diseases. *Nature,* 451**,** 990-993.
KANG, Y.-J., YANG, D.-C., KONG, L., HOU, M., MENG, Y.-Q., WEI, L. & GAO, G. 2017. CPC2: a fast and accurate coding potential calculator based on sequence intrinsic features. *Nucleic acids research,* 45**,** W12-W16.
KASSAMBARA, A. 2017. Principal Component Methods in R: Practical Guide. *Principal Component Methods in R: Practical Guide. STHDA*.
KATIBAH, G. E., LEE, H. J., HUIZAR, J. P., VOGAN, J. M., ALBER, T. & COLLINS, K. 2013. tRNA binding, structure, and localization of the human interferon-induced protein IFIT5. *Molecular cell,* 49**,** 743-750.
KATIBAH, G. E., QIN, Y., SIDOTE, D. J., YAO, J., LAMBOWITZ, A. M. & COLLINS, K. 2014. Broad and adaptable RNA structure recognition by the human interferon-induced tetratricopeptide repeat protein IFIT5. *Proceedings of the National Academy of Sciences,* 111**,** 12025-12030.

KATO, H., TAKEUCHI, O., MIKAMO-SATOH, E., HIRAI, R., KAWAI, T., MATSUSHITA, K., HIIRAGI, A., DERMODY, T. S., FUJITA, T. & AKIRA, S. 2008. Length-dependent recognition of double-stranded ribonucleic acids by retinoic acid–inducible gene-I and melanoma differentiation–associated gene 5. *The Journal of experimental medicine,* 205**,** 1601-1610.
KATZE, M. G., HE, Y. & GALE, M. 2002. Viruses and interferon: a fight for supremacy. *Nature Reviews Immunology,* 2**,** 675-687.
KAWAI, T. & AKIRA, S. 2006. Innate immune recognition of viral infection. *Nature immunology,* 7**,** 131-137.
KAWAI, T., SATO, S., ISHII, K. J., COBAN, C., HEMMI, H., YAMAMOTO, M., TERAI, K., MATSUDA, M., INOUE, J.-I. & UEMATSU, S. 2004. Interferon-α induction through Toll-like receptors involves a direct interaction of IRF7 with MyD88 and TRAF6. *Nature immunology,* 5**,** 1061-1068.
KAWASAKI, T. & KAWAI, T. 2014. Toll-like receptor signaling pathways. *Frontiers in immunology,* 5**,** 461.
KEATTS, L. O., ROBARDS, M., OLSON, S. H., HUEFFER, K., INSLEY, S. J., JOLY, D. O., KUTZ, S., LEE, D. S., CHETKIEWICZ, C.-L. B. & LAIR, S. 2021. Implications of zoonoses from hunting and use of wildlife in North American arctic and boreal biomes: Pandemic potential, monitoring, and mitigation. *Frontiers in Public Health***,** 451.
KELLEY, J., DE BONO, B. & TROWSDALE, J. 2005. IRIS: a database surveying known human immune system genes. *Genomics,* 85**,** 503-511.
KEPLER, T. B., SAMPLE, C., HUDAK, K., ROACH, J., HAINES, A., WALSH, A. & RAMSBURG, E. A. 2010. Chiropteran types I and II interferon genes inferred from genome sequencing traces by a statistical gene-family assembler. *BMC genomics,* 11**,** 1-12.
KEREN, H., LEV-MAOR, G. & AST, G. 2010. Alternative splicing and evolution: diversification, exon definition and function. *Nature Reviews Genetics,* 11**,** 345-355.
KILLIP, M. J., FODOR, E. & RANDALL, R. E. 2015. Influenza virus activation of the interferon system. *Virus research,* 209**,** 11-22.
KIM, H. K., PHAM, M. H. C., KO, K. S., RHEE, B. D. & HAN, J. 2018. Alternative splicing isoforms in health and disease. *Pflügers Archiv-European Journal of Physiology,* 470**,** 995-1016.
KIM, T., PAZHOOR, S., BAO, M., ZHANG, Z., HANABUCHI, S., FACCHINETTI, V., BOVER, L., PLUMAS, J., CHAPEROT, L. & QIN, J. 2010. Aspartate-glutamate-alanine-histidine box motif (DEAH)/RNA helicase A helicases sense microbial DNA in human plasmacytoid dendritic cells. *Proceedings of the National Academy of Sciences,* 107**,** 15181-15186.
KINGSLEY, D. H. 2018. Emerging foodborne and agriculture-related viruses. *Preharvest Food Safety***,** 205-225.
KLAUSEN, M. S., JESPERSEN, M. C., NIELSEN, H., JENSEN, K. K., JURTZ, V. I., SOENDERBY, C. K., SOMMER, M. O. A., WINTHER, O., NIELSEN, M. & PETERSEN, B. 2019. NetSurfP-2.0: Improved prediction of protein structural features by integrated deep learning. *Proteins: Structure, Function, and Bioinformatics,* 87**,** 520-527.
KOCH, L. K., CUNZE, S., KOCHMANN, J. & KLIMPEL, S. 2020. Bats as putative Zaire ebolavirus reservoir hosts and their habitat suitability in Africa. *Scientific reports,* 10**,** 1-9.
KOTENKO, S. V., GALLAGHER, G., BAURIN, V. V., LEWIS-ANTES, A., SHEN, M., SHAH, N. K., LANGER, J. A., SHEIKH, F., DICKENSHEETS, H. & DONNELLY, R. P. 2003. IFN-λs mediate antiviral protection through a distinct class II cytokine receptor complex. *Nature immunology,* 4**,** 69-77.
KOUADIO, L., NOWAK, K., AKOUA-KOFFI, C., WEISS, S., ALLALI, B. K., WITKOWSKI, P. T., KRÜGER, D. H., COUACY-HYMANN, E., CALVIGNAC-

SPENCER, S. & LEENDERTZ, F. H. 2015. Lassa virus in multimammate rats, Côte d'Ivoire, 2013. *Emerging infectious diseases,* 21**,** 1481.
KOYAMA, S., ISHII, K. J., COBAN, C. & AKIRA, S. 2008. Innate immune response to viral infection. *Cytokine,* 43**,** 336-341.
KRUEGER, F. 2015. Trim Galore!: A wrapper around Cutadapt and FastQC to consistently apply adapter and quality trimming to FastQ files, with extra functionality for RRBS data. *Babraham Institute*.
KUMAR, P., SWEENEY, T. R., SKABKIN, M. A., SKABKINA, O. V., HELLEN, C. U. & PESTOVA, T. V. 2014. Inhibition of translation by IFIT family members is determined by their ability to interact selectively with the 5′-terminal regions of cap0-, cap1-and 5′ ppp-mRNAs. *Nucleic acids research,* 42**,** 3228-3245.
KUNO, G. 2001. Persistence of arboviruses and antiviral antibodies in vertebrate hosts: its occurrence and impacts. *Reviews in medical virology,* 11**,** 165-190.
KURIAKOSE, T. & KANNEGANTI, T.-D. 2017. Regulation and functions of NLRP3 inflammasome during influenza virus infection. *Molecular immunology,* 86**,** 56-64.
KURPIERS, L. A., SCHULTE-HERBRÜGGEN, B., EJOTRE, I. & REEDER, D. M. 2016. Bushmeat and emerging infectious diseases: lessons from Africa. *Problematic wildlife: a cross-disciplinary approach***,** 507-551.
KUZMIN, I. V., SCHWARZ, T. M., ILINYKH, P. A., JORDAN, I., KSIAZEK, T. G., SACHIDANANDAM, R., BASLER, C. F. & BUKREYEV, A. 2017. Innate immune responses of bat and human cells to filoviruses: commonalities and distinctions. *Journal of virology,* 91**,** e02471-16.
LA CRUZ-RIVERA, D., PAMELA, C., KANCHWALA, M., LIANG, H., KUMAR, A., WANG, L.-F., XING, C. & SCHOGGINS, J. W. 2018. The IFN response in bats displays distinctive IFN-stimulated gene expression kinetics with atypical RNASEL induction. *The Journal of Immunology,* 200**,** 209-217.
LAING, E. D., STERLING, S. L., WEIR, D. L., BEAUREGARD, C. R., SMITH, I. L., LARSEN, S. E., WANG, L.-F., SNOW, A. L., SCHAEFER, B. C. & BRODER, C. C. 2019. Enhanced autophagy contributes to reduced viral infection in black flying fox cells. *Viruses,* 11**,** 260.
LAU, S. K., WOO, P. C., LI, K. S., HUANG, Y., TSOI, H.-W., WONG, B. H., WONG, S. S., LEUNG, S.-Y., CHAN, K.-H. & YUEN, K.-Y. 2005. Severe acute respiratory syndrome coronavirus-like virus in Chinese horseshoe bats. *Proceedings of the National Academy of Sciences,* 102**,** 14040-14045.
LAUDENBACH, B. T., KREY, K., EMSLANDER, Q., ANDERSEN, L. L., REIM, A., SCATURRO, P., MUNDIGL, S., DÄCHERT, C., MANSKE, K. & MOSER, M. 2021. NUDT2 initiates viral RNA degradation by removal of 5′-phosphates. *Nature Communications,* 12**,** 6918.
LAVORGNA, A., DE FILIPPI, R., FORMISANO, S. & LEONARDI, A. 2009. TNF receptor-associated factor 1 is a positive regulator of the NF-κB alternative pathway. *Molecular Immunology,* 46**,** 3278-3282.
LAWRENCE, T. M., HUDACEK, A. W., DE ZOETE, M. R., FLAVELL, R. A. & SCHNELL, M. J. 2013. Rabies virus is recognized by the NLRP3 inflammasome and activates interleukin-1β release in murine dendritic cells. *Journal of virology,* 87**,** 5848-5857.
LAZEAR, H. M., SCHOGGINS, J. W. & DIAMOND, M. S. 2019. Shared and distinct functions of type I and type III interferons. *Immunity,* 50**,** 907-923.
LEE, A. K., KULCSAR, K. A., ELLIOTT, O., KHIABANIAN, H., NAGLE, E. R., JONES, M. E., AMMAN, B. R., SANCHEZ-LOCKHART, M., TOWNER, J. S. & PALACIOS, G. 2015. De novo transcriptome reconstruction and annotation of the Egyptian rousette bat. *BMC genomics,* 16**,** 1-11.
LEE, H.-C., CHATHURANGA, K. & LEE, J.-S. 2019. Intracellular sensing of viral genomes and viral evasion. *Experimental & molecular medicine,* 51**,** 1-13.

LEE, M.-K., KIM, H.-E., PARK, E.-B., LEE, J., KIM, K.-H., LIM, K., YUM, S., LEE, Y.-H., KANG, S.-J. & LEE, J.-H. 2016. Structural features of influenza A virus panhandle RNA enabling the activation of RIG-I independently of 5′-triphosphate. *Nucleic acids research,* 44**,** 8407-8416.
LEI, M. & DONG, D. 2016. Phylogenomic analyses of bat subordinal relationships based on transcriptome data. *Scientific Reports,* 6**,** 1-8.
LEI, M., DONG, D., MU, S., PAN, Y.-H. & ZHANG, S. 2014. Comparison of brain transcriptome of the greater horseshoe bats (Rhinolophus ferrumequinum) in active and torpid episodes. *PLoS One,* 9**,** e107746.
LEMEY, P., PYBUS, O. G., WANG, B., SAKSENA, N. K., SALEMI, M. & VANDAMME, A.-M. 2003. Tracing the origin and history of the HIV-2 epidemic. *Proceedings of the National Academy of Sciences,* 100**,** 6588-6592.
LEROY, E. M., EPELBOIN, A., MONDONGE, V., POURRUT, X., GONZALEZ, J.-P., MUYEMBE-TAMFUM, J.-J. & FORMENTY, P. 2009. Human Ebola outbreak resulting from direct exposure to fruit bats in Luebo, Democratic Republic of Congo, 2007. *Vector-borne and zoonotic diseases,* 9**,** 723-728.
LEROY, E. M., KUMULUNGUI, B., POURRUT, X., ROUQUET, P., HASSANIN, A., YABA, P., DÉLICAT, A., PAWESKA, J. T., GONZALEZ, J.-P. & SWANEPOEL, R. 2005. Fruit bats as reservoirs of Ebola virus. *Nature,* 438**,** 575-576.
LETKO, M., SEIFERT, S. N., OLIVAL, K. J., PLOWRIGHT, R. K. & MUNSTER, V. J. 2020. Bat-borne virus diversity, spillover and emergence. *Nature Reviews Microbiology,* 18**,** 461-471.
LEUNG, D. W. & AMARASINGHE, G. K. 2016. When your cap matters: structural insights into self vs non-self recognition of 5′ RNA by immunomodulatory host proteins. *Current opinion in structural biology,* 36**,** 133-141.
LI, D. & WU, M. 2021. Pattern recognition receptors in health and diseases. *Signal transduction and targeted therapy,* 6**,** 291.
LI, J., ZHANG, G., CHENG, D., REN, H., QIAN, M. & DU, B. 2015a. Molecular characterization of RIG-I, STAT-1 and IFN-beta in the horseshoe bat. *Gene,* 561**,** 115-123.
LI, L., CHEN, S. N., LI, N. & NIE, P. 2021. Transcriptional and subcellular characterization of interferon induced protein-35 (IFP35) in mandarin fish, Siniperca chuatsi. *Developmental & Comparative Immunology,* 115**,** 103877.
LI, N., PARRISH, M., CHAN, T. K., YIN, L., RAI, P., YOSHIYUKI, Y., ABOLHASSANI, N., TAN, K. B., KIRALY, O. & CHOW, V. T. 2015b. Influenza infection induces host DNA damage and dynamic DNA damage responses during tissue regeneration. *Cellular and molecular life sciences,* 72**,** 2973-2988.
LI, S.-F., ZHAO, F.-R., SHAO, J.-J., XIE, Y.-L., CHANG, H.-Y. & ZHANG, Y.-G. 2017. Interferon-omega: Current status in clinical applications. *International immunopharmacology,* 52**,** 253-260.
LI, W., SHI, Z., YU, M., REN, W., SMITH, C., EPSTEIN, J. H., WANG, H., CRAMERI, G., HU, Z. & ZHANG, H. 2005. Bats are natural reservoirs of SARS-like coronaviruses. *Science,* 310**,** 676-679.
LI, X., SHU, C., YI, G., CHATON, C. T., SHELTON, C. L., DIAO, J., ZUO, X., KAO, C. C., HERR, A. B. & LI, P. 2013. Cyclic GMP-AMP synthase is activated by double-stranded DNA-induced oligomerization. *Immunity,* 39**,** 1019-1031.
LI, Y., WANG, J., HICKEY, A. C., ZHANG, Y., LI, Y., WU, Y., ZHANG, H., YUAN, J., HAN, Z. & MCEACHERN, J. 2008. Antibodies to Nipah or Nipah-like viruses in bats, China. *Emerging infectious diseases,* 14**,** 1974-1976.
LIANG, Y.-Z., WU, L.-J., ZHANG, Q., ZHOU, P., WANG, M.-N., YANG, X.-L., GE, X.-Y., WANG, L.-F. & SHI, Z.-L. 2015. Cloning, expression, and antiviral activity of interferon β from the Chinese microbat, Myotis davidii. *Virologica Sinica,* 30**,** 425-432.

LIAO, K.-C. & GARCIA-BLANCO, M. A. 2021. Role of alternative splicing in regulating host response to viral infection. *Cells,* 10**,** 1720.
LIFSON, A. 1996. Mosquitoes, models, and dengue. *The Lancet,* 347**,** 1201-1202.
LIN, R., MAMANE, Y. & HISCOTT, J. 2000. Multiple regulatory domains control IRF-7 activity in response to virus infection. *Journal of Biological Chemistry,* 275**,** 34320-34327.
LISABETH, E. M., FALIVELLI, G. & PASQUALE, E. B. 2013. Eph receptor signaling and ephrins. *Cold Spring Harbor perspectives in biology,* 5**,** a009159.
LIU, S., CAI, X., WU, J., CONG, Q., CHEN, X., LI, T., DU, F., REN, J., WU, Y.-T. & GRISHIN, N. V. 2015. Phosphorylation of innate immune adaptor proteins MAVS, STING, and TRIF induces IRF3 activation. *Science,* 347**,** aaa2630.
LIU, Y., ZHANG, Y.-B., LIU, T.-K. & GUI, J.-F. 2013. Lineage-specific expansion of IFIT gene family: an insight into coevolution with IFN gene family. *PLoS One,* 8**,** e66859.
LIVAK, K. J. & SCHMITTGEN, T. D. 2001. Analysis of relative gene expression data using real-time quantitative PCR and the 2− ΔΔCT method. *methods,* 25**,** 402-408.
LO, M. Y., NGAN, W. Y., TSUN, S. M., HSING, H.-L., LAU, K. T., HUNG, H. P., CHAN, S. L., LAI, Y. Y., YAO, Y. & PU, Y. 2019. A field study into Hong Kong's wet markets: raised questions into the hygienic maintenance of meat contact surfaces and the dissemination of microorganisms associated with nosocomial infections. *Frontiers in Microbiology,* 10**,** 2618.
LONG, J. S., MISTRY, B., HASLAM, S. M. & BARCLAY, W. S. 2019. Host and viral determinants of influenza A virus species specificity. *Nature Reviews Microbiology,* 17**,** 67-81.
LOVE, M. I., HUBER, W. & ANDERS, S. 2014. Moderated estimation of fold change and dispersion for RNA-seq data with DESeq2. *Genome biology,* 15**,** 1-21.
LUIS, A. D., HAYMAN, D. T., O'SHEA, T. J., CRYAN, P. M., GILBERT, A. T., PULLIAM, J. R., MILLS, J. N., TIMONIN, M. E., WILLIS, C. K. & CUNNINGHAM, A. A. 2013. A comparison of bats and rodents as reservoirs of zoonotic viruses: are bats special? *Proceedings of the Royal Society B: Biological Sciences,* 280**,** 20122753.
LUPFER, C., MALIK, A. & KANNEGANTI, T.-D. 2015. Inflammasome control of viral infection. *Current opinion in virology,* 12**,** 38-46.
LYMAN, C. P. 1970. Thermoregulation and metabolism in bats. *Biology of bats,* 1**,** 301-330.
MA, Z., NI, G. & DAMANIA, B. 2018. Innate sensing of DNA virus genomes. *Annual review of virology,* 5**,** 341-362.
MACHIELS, B., STEVENSON, P. G., VANDERPLASSCHEN, A. & GILLET, L. 2013. A gammaherpesvirus uses alternative splicing to regulate its tropism and its sensitivity to neutralization. *PLoS pathogens,* 9**,** e1003753.
MAIN, E. R., XIONG, Y., COCCO, M. J., D'ANDREA, L. & REGAN, L. 2003. Design of stable α-helical arrays from an idealized TPR motif. *Structure,* 11**,** 497-508.
MANIVASAGAM, S. & KLEIN, R. S. 2021. Type III Interferons: Emerging Roles in Autoimmunity. *Frontiers in immunology,* 12**,** 764062.
MARCELLO, T., GRAKOUI, A., BARBA–SPAETH, G., MACHLIN, E. S., KOTENKO, S. V., MACDONALD, M. R. & RICE, C. M. 2006. Interferons α and λ inhibit hepatitis C virus replication with distinct signal transduction and gene regulation kinetics. *Gastroenterology,* 131**,** 1887-1898.
MARIATHASAN, S., WEISS, D. S., NEWTON, K., MCBRIDE, J., O'ROURKE, K., ROOSE-GIRMA, M., LEE, W. P., WEINRAUCH, Y., MONACK, D. M. & DIXIT, V. M. 2006. Cryopyrin activates the inflammasome in response to toxins and ATP. *Nature,* 440**,** 228-232.

MARSH, G. A., DE JONG, C., BARR, J. A., TACHEDJIAN, M., SMITH, C., MIDDLETON, D., YU, M., TODD, S., FOORD, A. J. & HARING, V. 2012. Cedar virus: a novel Henipavirus isolated from Australian bats.
MARTÍNEZ GÓMEZ, J. M., PERIASAMY, P., DUTERTRE, C.-A., IRVING, A. T., NG, J. H. J., CRAMERI, G., BAKER, M. L., GINHOUX, F., WANG, L.-F. & ALONSO, S. 2016. Phenotypic and functional characterization of the major lymphocyte populations in the fruit-eating bat Pteropus alecto. *Scientific reports,* 6**,** 37796.
MATHEWS, F. 2009. Zoonoses in wildlife: integrating ecology into management. *Advances in parasitology,* 68**,** 185-209.
MCCOLL, K., CHAMBERLAIN, T., LUNT, R., NEWBERRY, K., MIDDLETON, D. & WESTBURY, H. 2002. Pathogenesis studies with Australian bat lyssavirus in grey-headed flying foxes (Pteropus poliocephalus). *Australian Veterinary Journal,* 80**,** 636-641.
MEMISH, Z. A., MISHRA, N., OLIVAL, K. J., FAGBO, S. F., KAPOOR, V., EPSTEIN, J. H., ALHAKEEM, R., DUROSINLOUN, A., AL ASMARI, M. & ISLAM, A. 2013. Middle East respiratory syndrome coronavirus in bats, Saudi Arabia. *Emerging infectious diseases,* 19**,** 1819.
MENDENHALL, I. H., WEN, D. L. H., JAYAKUMAR, J., GUNALAN, V., WANG, L., MAUER-STROH, S., SU, Y. C. & SMITH, G. J. 2019. Diversity and evolution of viral pathogen community in cave nectar bats (Eonycteris spelaea). *Viruses,* 11**,** 250.
MENDOZA, H., RUBIO, A. V., GARCÍA-PEÑA, G. E., SUZÁN, G. & SIMONETTI, J. A. 2020. Does land-use change increase the abundance of zoonotic reservoirs? Rodents say yes. *European Journal of Wildlife Research,* 66**,** 6.
MESEV, E. V., LEDESMA, R. A. & PLOSS, A. 2019. Decoding type I and III interferon signalling during viral infection. *Nature microbiology,* 4**,** 914-924.
METEYER, C. U., BARBER, D. & MANDL, J. N. 2012. Pathology in euthermic bats with white nose syndrome suggests a natural manifestation of immune reconstitution inflammatory syndrome. *Virulence,* 3**,** 583-588.
MIDDLETON, D. J., MORRISSY, C., VAN DER HEIDE, B., RUSSELL, G., BRAUN, M., WESTBURY, H., HALPIN, K. & DANIELS, P. 2007. Experimental Nipah virus infection in pteropid bats (Pteropus poliocephalus). *Journal of comparative pathology,* 136**,** 266-272.
MIKNIS, Z. J., MAGRACHEVA, E., LI, W., ZDANOV, A., KOTENKO, S. V. & WLODAWER, A. 2010. Crystal structure of human interferon-λ1 in complex with its high-affinity receptor interferon-λR1. *Journal of molecular biology,* 404**,** 650-664.
MILBANK, C. & VIRA, B. 2022. Wildmeat consumption and zoonotic spillover: contextualising disease emergence and policy responses. *The Lancet Planetary Health,* 6**,** e439-e448.
MILLER, M. R., MCMINN, R. J., MISRA, V., SCHOUNTZ, T., MÜLLER, M. A., KURTH, A. & MUNSTER, V. J. 2016. Broad and temperature independent replication potential of filoviruses on cells derived from old and new world bat species. *The Journal of Infectious Diseases,* 214**,** S297-S302.
MILWARD, E., SHAHANDEH, A., HEIDARI, M., JOHNSTONE, D., DANESHI, N. & HONDERMARCK, H. 2016. Transcriptomics.
MISRA, V., DUMONCEAUX, T., DUBOIS, J., WILLIS, C., NADIN-DAVIS, S., SEVERINI, A., WANDELER, A., LINDSAY, R. & ARTSOB, H. 2009. Detection of polyoma and corona viruses in bats of Canada. *Journal of general virology,* 90**,** 2015-2022.
MOGENSEN, T. H. 2009. Pathogen recognition and inflammatory signaling in innate immune defenses. *Clinical microbiology reviews,* 22**,** 240-273.

MONDUL, A. M., KREBS, J. W. & CHILDS, J. E. 2003. Trends in national surveillance for rabies among bats in the United States (1993–2000). *Journal of the American Veterinary Medical Association,* 222**,** 633-639.
MORATELLI, R. & CALISHER, C. H. 2015. Bats and zoonotic viruses: can we confidently link bats with emerging deadly viruses? *Memórias do Instituto Oswaldo Cruz,* 110**,** 1-22.
MORENO-SANTILLÁN, D. D., MACHAIN-WILLIAMS, C., HERNÁNDEZ-MONTES, G. & ORTEGA, J. 2019. De novo transcriptome assembly and functional annotation in five species of bats. *Scientific Reports,* 9**,** 1-12.
MORSE, S. 2004. Factors and determinants of disease emergence. *Revue scientifique et technique-Office international des épizooties,* 23**,** 443-452.
MOSLEY, B., URDAL, D., PRICKETT, K., LARSEN, A., COSMAN, D., CONLON, P., GILLIS, S. & DOWER, S. 1987. The interleukin-1 receptor binds the human interleukin-1 alpha precursor but not the interleukin-1 beta precursor. *Journal of biological chemistry,* 262**,** 2941-2944.
MUHIRE, B. M., VARSANI, A. & MARTIN, D. P. 2014. SDT: a virus classification tool based on pairwise sequence alignment and identity calculation. *PloS one,* 9**,** e108277.
MÜLLER, M. A., DEVIGNOT, S., LATTWEIN, E., CORMAN, V. M., MAGANGA, G. D., GLOZA-RAUSCH, F., BINGER, T., VALLO, P., EMMERICH, P. & COTTONTAIL, V. M. 2016. Evidence for widespread infection of African bats with Crimean-Congo hemorrhagic fever-like viruses. *Scientific reports,* 6**,** 26637.
MUNSTER, V. J., ADNEY, D. R., VAN DOREMALEN, N., BROWN, V. R., MIAZGOWICZ, K. L., MILNE-PRICE, S., BUSHMAKER, T., ROSENKE, R., SCOTT, D. & HAWKINSON, A. 2016. Replication and shedding of MERS-CoV in Jamaican fruit bats (Artibeus jamaicensis). *Scientific Reports,* 6**,** 21878.
MURRAY, K., SELLECK, P., HOOPER, P., HYATT, A., GOULD, A., GLEESON, L., WESTBURY, H., HILEY, L., SELVEY, L. & RODWELL, B. 1995. A morbillivirus that caused fatal fisease in horses and humans. *Science,* 268**,** 94-97.
MURRAY, K. A., ALLEN, T., LOH, E., MACHALABA, C. & DASZAK, P. 2016. Emerging viral zoonoses from wildlife associated with animal-based food systems: risks and opportunities. *Food Safety Risks from Wildlife: Challenges in Agriculture, Conservation, and Public Health***,** 31-57.
NADIMPALLI, M. L. & PICKERING, A. J. 2020. A call for global monitoring of WASH in wet markets. *The Lancet Planetary Health,* 4**,** e439-e440.
NEGREDO, A., PALACIOS, G., VÁZQUEZ-MORÓN, S., GONZÁLEZ, F., DOPAZO, H., MOLERO, F., JUSTE, J., QUETGLAS, J., SAVJI, N. & DE LA CRUZ MARTÍNEZ, M. 2011. Discovery of an ebolavirus-like filovirus in europe. *PLoS pathogens,* 7**,** e1002304.
NEGRETE, O. A., LEVRONEY, E. L., AGUILAR, H. C., BERTOLOTTI-CIARLET, A., NAZARIAN, R., TAJYAR, S. & LEE, B. 2005. EphrinB2 is the entry receptor for Nipah virus, an emergent deadly paramyxovirus. *Nature,* 436**,** 401-405.
NEUWEILER, G. 2000. *The biology of bats*, Oxford University Press on Demand.
NG, J. H., TACHEDJIAN, M., DEAKIN, J., WYNNE, J. W., CUI, J., HARING, V., BROZ, I., CHEN, H., BELOV, K. & WANG, L.-F. 2016. Evolution and comparative analysis of the bat MHC-I region. *Scientific reports,* 6**,** 1-18.
NI, G., MA, Z. & DAMANIA, B. 2018. cGAS and STING: At the intersection of DNA and RNA virus-sensing networks. *PLoS pathogens,* 14**,** e1007148.
NIETO-TORRES, J. L., VERDIÁ-BÁGUENA, C., JIMENEZ-GUARDEÑO, J. M., REGLA-NAVA, J. A., CASTAÑO-RODRIGUEZ, C., FERNANDEZ-DELGADO, R., TORRES, J., AGUILELLA, V. M. & ENJUANES, L. 2015. Severe acute

respiratory syndrome coronavirus E protein transports calcium ions and activates the NLRP3 inflammasome. *Virology,* 485**,** 330-339.
NING, S., PAGANO, J. & BARBER, G. 2011. IRF7: activation, regulation, modification and function. *Genes & Immunity,* 12**,** 399-414.
NISHIHARA, H., HASEGAWA, M. & OKADA, N. 2006. Pegasoferae, an unexpected mammalian clade revealed by tracking ancient retroposon insertions. *Proceedings of the National Academy of Sciences,* 103**,** 9929-9934.
NISHIHARA, H., MARUYAMA, S. & OKADA, N. 2009. Retroposon analysis and recent geological data suggest near-simultaneous divergence of the three superorders of mammals. *Proceedings of the National Academy of Sciences,* 106**,** 5235-5240.
O'LEARY, D. R., HAYES, E. B., VORNDAM, A. V., CLARK, G. G. & GUBLER, D. J. 2002. Assessment of dengue risk in relief workers in Puerto Rico after Hurricane Georges, 1998. *The American journal of tropical medicine and hygiene,* 66**,** 35-39.
O'MARA, M. T., WIKELSKI, M., VOIGT, C. C., TER MAAT, A., POLLOCK, H. S., BURNESS, G., DESANTIS, L. M. & DECHMANN, D. K. 2017. Cyclic bouts of extreme bradycardia counteract the high metabolism of frugivorous bats. *elife,* 6**,** e26686.
O'SULLIVAN, J., ALLWORTH, A., PATERSON, D., SNOW, T., BOOTS, R., GLEESON, L., GOULD, A., HYATT, A. & BRADFIELD, J. 1997. Fatal encephalitis due to novel paramyxovirus transmitted from horses. *The Lancet,* 349**,** 93-95.
O'DEA, M. A., TU, S.-L., PANG, S., DE RIDDER, T., JACKSON, B. & UPTON, C. 2016. Genomic characterization of a novel poxvirus from a flying fox: evidence for a new genus? *Journal of General Virology,* 97**,** 2363-2375.
O'SHEA, T. J., CRYAN, P. M., CUNNINGHAM, A. A., FOOKS, A. R., HAYMAN, D. T., LUIS, A. D., PEEL, A. J., PLOWRIGHT, R. K. & WOOD, J. L. 2014. Bat flight and zoonotic viruses. *Emerging infectious diseases,* 20**,** 741.
OELOFSEN, M. & VAN DER RYST, E. 1999. Could bats act as reservoir hosts for Rift Valley fever virus?
OLIVAL, K. J. & HAYMAN, D. T. 2014. Filoviruses in bats: current knowledge and future directions. *Viruses,* 6**,** 1759-1788.
OLIVAL, K. J., HOSSEINI, P. R., ZAMBRANA-TORRELIO, C., ROSS, N., BOGICH, T. L. & DASZAK, P. 2017. Host and viral traits predict zoonotic spillover from mammals. *Nature,* 546**,** 646-650.
OLSON, M. V. 1999. When less is more: gene loss as an engine of evolutionary change. *The American Journal of Human Genetics,* 64**,** 18-23.
OMATSU, T., BAK, E.-J., ISHII, Y., KYUWA, S., TOHYA, Y., AKASHI, H. & YOSHIKAWA, Y. 2008. Induction and sequencing of Rousette bat interferon α and β genes. *Veterinary immunology and immunopathology,* 124**,** 169-176.
OPPMANN, B., LESLEY, R., BLOM, B., TIMANS, J. C., XU, Y., HUNTE, B., VEGA, F., YU, N., WANG, J. & SINGH, K. 2000. Novel p19 protein engages IL-12p40 to form a cytokine, IL-23, with biological activities similar as well as distinct from IL-12. *Immunity,* 13**,** 715-725.
ÖSTERLUND, P. I., PIETILÄ, T. E., VECKMAN, V., KOTENKO, S. V. & JULKUNEN, I. 2007. IFN regulatory factor family members differentially regulate the expression of type III IFN (IFN-λ) genes. *The Journal of Immunology,* 179**,** 3434-3442.
ØVSTEBØ, R., OLSTAD, O. K., BRUSLETTO, B., MØLLER, A. S., AASE, A., HAUG, K. B. F., BRANDTZAEG, P. & KIERULF, P. 2008. Identification of genes particularly sensitive to lipopolysaccharide (LPS) in human monocytes induced by wild-type versus LPS-deficient Neisseria meningitidis strains. *Infection and immunity,* 76**,** 2685-2695.

PAMELA, C., KANCHWALA, M., LIANG, H., KUMAR, A., WANG, L.-F., XING, C. & SCHOGGINS, J. W. 2018. The IFN response in bats displays distinctive IFN-stimulated gene expression kinetics with atypical RNASEL induction. *The Journal of Immunology,* 200**,** 209-217.

PANDA, D., DAS, A., DINH, P. X., SUBRAMANIAM, S., NAYAK, D., BARROWS, N. J., PEARSON, J. L., THOMPSON, J., KELLY, D. L. & LADUNGA, I. 2011. RNAi screening reveals requirement for host cell secretory pathway in infection by diverse families of negative-strand RNA viruses. *Proceedings of the National Academy of Sciences,* 108**,** 19036-19041.

PAPENFUSS, A. T., BAKER, M. L., FENG, Z.-P., TACHEDJIAN, M., CRAMERI, G., COWLED, C., NG, J., JANARDHANA, V., FIELD, H. E. & WANG, L.-F. 2012. The immune gene repertoire of an important viral reservoir, the Australian black flying fox. *BMC genomics,* 13**,** 1-17.

PARHAM, C., CHIRICA, M., TIMANS, J., VAISBERG, E., TRAVIS, M., CHEUNG, J., PFLANZ, S., ZHANG, R., SINGH, K. P. & VEGA, F. 2002. A receptor for the heterodimeric cytokine IL-23 is composed of IL-12Rβ1 and a novel cytokine receptor subunit, IL-23R. *The Journal of Immunology,* 168**,** 5699-5708.

PARK, A. & IWASAKI, A. 2020. Type I and type III interferons–induction, signaling, evasion, and application to combat COVID-19. *Cell host & microbe,* 27**,** 870-878.

PATON, N. I., LEO, Y. S., ZAKI, S. R., AUCHUS, A. P., LEE, K. E., LING, A. E., CHEW, S. K., ANG, B., ROLLIN, P. E. & UMAPATHI, T. 1999. Outbreak of Nipah-virus infection among abattoir workers in Singapore. *The Lancet,* 354**,** 1253-1256.

PATRICOLA, C. M. & WEHNER, M. F. 2018. Anthropogenic influences on major tropical cyclone events. *Nature,* 563**,** 339-346.

PATRO, R., DUGGAL, G., LOVE, M., IRIZARRY, R. & KINGSFORD, C. Salmon: fast and bias-aware quantification of transcript expression using dual-phase inference. *Salmon: fast and bias-aware quantification of transcript expression using dual-phase inference*.

PATZ, J. A., DASZAK, P., TABOR, G. M., AGUIRRE, A. A., PEARL, M., EPSTEIN, J., WOLFE, N. D., KILPATRICK, A. M., FOUFOPOULOS, J. & MOLYNEUX, D. 2004. Unhealthy landscapes: policy recommendations on land use change and infectious disease emergence. *Environmental health perspectives,* 112**,** 1092-1098.

PAUN, A. & PITHA, P. 2007. The IRF family, revisited. *Biochimie,* 89**,** 744-753.

PAVLOVICH, S. S., LOVETT, S. P., KOROLEVA, G., GUITO, J. C., ARNOLD, C. E., NAGLE, E. R., KULCSAR, K., LEE, A., THIBAUD-NISSEN, F. & HUME, A. J. 2018. The Egyptian rousette genome reveals unexpected features of bat antiviral immunity. *Cell,* 173**,** 1098-1110. e18.

PAWESKA, J. T., STORM, N., GROBBELAAR, A. A., MARKOTTER, W., KEMP, A. & JANSEN VAN VUREN, P. 2016. Experimental inoculation of Egyptian fruit bats (Rousettus aegyptiacus) with Ebola virus. *Viruses,* 8**,** 29.

PECKHAM, D., SCAMBLER, T., SAVIC, S. & MCDERMOTT, M. F. 2017. The burgeoning field of innate immune-mediated disease and autoinflammation. *The Journal of pathology,* 241**,** 123-139.

PEEL, A. J., YINDA, C. K., ANNAND, E. J., DALE, A. S., EBY, P., EDEN, J.-S., JONES, D. N., KESSLER, M. K., LUNN, T. J. & PEARSON, T. 2022. Novel Hendra Virus Variant Circulating in Black Flying Foxes and Grey-Headed Flying Foxes, Australia. *Emerging Infectious Diseases,* 28**,** 1043.

PERIASAMY, P., HUTCHINSON, P. E., CHEN, J., BONNE, I., SHAHUL HAMEED, S. S., SELVAM, P., HEY, Y. Y., FINK, K., IRVING, A. T. & DUTERTRE, C.-A. 2019. Studies on B cells in the fruit-eating black flying fox (Pteropus alecto). *Frontiers in immunology,* 10**,** 489.

PERVOLARAKI, K., RASTGOU TALEMI, S., ALBRECHT, D., BORMANN, F., BAMFORD, C., MENDOZA, J. L., GARCIA, K. C., MCLAUCHLAN, J., HÖFER, T. & STANIFER, M. L. 2018. Differential induction of interferon stimulated genes between type I and type III interferons is independent of interferon receptor abundance. *PLoS pathogens,* 14**,** e1007420.
PESTKA, S., KRAUSE, C. D. & WALTER, M. R. 2004. Interferons, interferon-like cytokines, and their receptors. *Immunological reviews,* 202**,** 8-32.
PHILBEY, A. W., KIRKLAND, P. D., ROSS, A. D., DAVIS, R. J., GLEESON, A. B., LOVE, R. J., DANIELS, P. W., GOULD, A. R. & HYATT, A. D. 1998. An apparently new virus (family Paramyxoviridae) infectious for pigs, humans, and fruit bats. *Emerging infectious diseases,* 4**,** 269.
PICHLMAIR, A., LASSNIG, C., EBERLE, C.-A., GÓRNA, M. W., BAUMANN, C. L., BURKARD, T. R., BÜRCKSTÜMMER, T., STEFANOVIC, A., KRIEGER, S. & BENNETT, K. L. 2011. IFIT1 is an antiviral protein that recognizes 5′-triphosphate RNA. *Nature immunology,* 12**,** 624-630.
PLOWRIGHT, R. K., FOLEY, P., FIELD, H. E., DOBSON, A. P., FOLEY, J. E., EBY, P. & DASZAK, P. 2011. Urban habituation, ecological connectivity and epidemic dampening: the emergence of Hendra virus from flying foxes (Pteropus spp.). *Proceedings of the Royal Society B: Biological Sciences,* 278**,** 3703-3712.
PLOWRIGHT, R. K., PARRISH, C. R., MCCALLUM, H., HUDSON, P. J., KO, A. I., GRAHAM, A. L. & LLOYD-SMITH, J. O. 2017. Pathways to zoonotic spillover. *Nature Reviews Microbiology,* 15**,** 502-510.
PLOWRIGHT, R. K., REASER, J. K., LOCKE, H., WOODLEY, S. J., PATZ, J. A., BECKER, D. J., OPPLER, G., HUDSON, P. J. & TABOR, G. M. 2021. Land use-induced spillover: a call to action to safeguard environmental, animal, and human health. *The Lancet Planetary Health,* 5**,** e237-e245.
POWER, A. G. & MITCHELL, C. E. 2004. Pathogen spillover in disease epidemics. *the american naturalist,* 164**,** S79-S89.
PREVENTION, C. F. D. C. A. 2023. *Zoonotic Diseases* [Online]. Centres for Disease Control and Prevention. Available: https://www.cdc.gov/onehealth/basics/zoonotic-diseases.html#:~:text=Direct%20contact%3A%20Coming%20into%20contact%20with%20the%20saliva%2C,or%20surfaces%20that%20have%20been%20contaminated%20with%20germs. [Accessed 27-03-23 2023].
QIU, Y., NEMEROFF, M. & KRUG, R. M. 1995. The influenza virus NS1 protein binds to a specific region in human U6 snRNA and inhibits U6-U2 and U6-U4 snRNA interactions during splicing. *Rna,* 1**,** 304-316.
RAHMAN, S. A., HASSAN, S. S., OLIVAL, K. J., MOHAMED, M., CHANG, L.-Y., HASSAN, L., SAAD, N. M., SHOHAIMI, S. A., MAMAT, Z. C. & NAIM, M. 2010. Characterization of Nipah virus from naturally infected Pteropus vampyrus bats, Malaysia. *Emerging infectious diseases,* 16**,** 1990.
RAJ, B. & BLENCOWE, B. J. 2015. Alternative splicing in the mammalian nervous system: recent insights into mechanisms and functional roles. *Neuron,* 87**,** 14-27.
RANDALL, R. E. & GOODBOURN, S. 2008. Interferons and viruses: an interplay between induction, signalling, antiviral responses and virus countermeasures. *Journal of general virology,* 89**,** 1-47.
READ, S. A., WIJAYA, R., RAMEZANI-MOGHADAM, M., TAY, E., SCHIBECI, S., LIDDLE, C., LAM, V. W., YUEN, L., DOUGLAS, M. W. & BOOTH, D. 2019. Macrophage coordination of the interferon lambda immune response. *Frontiers in Immunology,* 10**,** 2674.
REN, P., LU, L., CAI, S., CHEN, J., LIN, W. & HAN, F. 2021. Alternative splicing: a new cause and potential therapeutic target in autoimmune disease. *Frontiers in Immunology,* 12**,** 713540.

ROGERS, R., DOUGLAS, I., BALDOCK, F., GLAVILLE, R., SEPPANEN, K., GLEESON, L., SELLECK, P. & DUNN, K. 1996. Investigation of a second focus of equine morbillivirus infection in coastal Queensland. *Australian veterinary journal,* 74**,** 243-244.
ROHDE, R. E., MAYES, B. C., SMITH, J. S. & NEILL, S. U. 2004. Bat rabies, Texas, 1996–2000. *Emerging infectious diseases,* 10**,** 948.
RUIZ-ARAVENA, M., MCKEE, C., GAMBLE, A., LUNN, T., MORRIS, A., SNEDDEN, C. E., YINDA, C. K., PORT, J. R., BUCHHOLZ, D. W. & YEO, Y. Y. 2022. Ecology, evolution and spillover of coronaviruses from bats. *Nature Reviews Microbiology,* 20**,** 299-314.
RULLI, M. C., D'ODORICO, P., GALLI, N. & HAYMAN, D. T. 2021. Land-use change and the livestock revolution increase the risk of zoonotic coronavirus transmission from rhinolophid bats. *Nature Food,* 2**,** 409-416.
SADLER, A. J. & WILLIAMS, B. R. 2008. Interferon-inducible antiviral effectors. *Nature reviews immunology,* 8**,** 559-568.
SAEED, O. S., EL-DEEB, A. H., GADALLA, M. R., EL-SOALLY, S. A. G. & AHMED, H. A. H. 2021. Genetic Characterization of Rift Valley Fever Virus in Insectivorous Bats, Egypt. *Vector-Borne and Zoonotic Diseases,* 21**,** 1003-1006.
SAJID, M., ULLAH, H., YAN, K., HE, M., FENG, J., SHEREEN, M. A., HAO, R., LI, Q., GUO, D. & CHEN, Y. 2021. The functional and antiviral activity of interferon alpha-inducible IFI6 against hepatitis B virus replication and gene expression. *Frontiers in Immunology,* 12**,** 634937.
SAMUEL, C. E. 2001. Antiviral actions of interferons. *Clinical microbiology reviews,* 14**,** 778-809.
SANTHAKUMAR, D., IQBAL, M., NAIR, V. & MUNIR, M. 2017. Chicken IFN kappa: a novel cytokine with antiviral activities. *Scientific Reports,* 7**,** 2719.
SANTHAKUMAR, D., ROHAIM, M. A. M. S., HUSSEIN, H. A., HAWES, P., FERREIRA, H. L., BEHBOUDI, S., IQBAL, M., NAIR, V., ARNS, C. W. & MUNIR, M. 2018. Chicken interferon-induced protein with tetratricopeptide repeats 5 antagonizes replication of RNA viruses. *Scientific reports,* 8**,** 6794.
SARKAR, S. N. & SEN, G. C. 2004. Novel functions of proteins encoded by viral stress-inducible genes. *Pharmacology & therapeutics,* 103**,** 245-259.
SATO, M., HATA, N., ASAGIRI, M., NAKAYA, T., TANIGUCHI, T. & TANAKA, N. 1998. Positive feedback regulation of type I IFN genes by the IFN-inducible transcription factor IRF-7. *FEBS letters,* 441**,** 106-110.
SCHAD, J. & VOIGT, C. C. 2016. Adaptive evolution of virus-sensing toll-like receptor 8 in bats. *Immunogenetics,* 68**,** 783-795.
SCHAFER, S., MIAO, K., BENSON, C. C., HEINIG, M., COOK, S. A. & HUBNER, N. 2015. Alternative splicing signatures in RNA-seq data: percent spliced in (PSI). *Current protocols in human genetics,* 87**,** 11.16. 1-11.16. 14.
SCHATTGEN, S. A. & FITZGERALD, K. A. 2011. The PYHIN protein family as mediators of host defenses. *Immunological reviews,* 243**,** 109-118.
SCHLEE, M. & HARTMANN, G. 2016. Discriminating self from non-self in nucleic acid sensing. *Nature Reviews Immunology,* 16**,** 566-580.
SCHOGGINS, J. W. & RICE, C. M. 2011. Interferon-stimulated genes and their antiviral effector functions. *Current opinion in virology,* 1**,** 519-525.
SCHOGGINS, J. W., WILSON, S. J., PANIS, M., MURPHY, M. Y., JONES, C. T., BIENIASZ, P. & RICE, C. M. 2011. A diverse range of gene products are effectors of the type I interferon antiviral response. *Nature,* 472**,** 481-485.
SCHOUNTZ, T. 2014. Immunology of bats and their viruses: challenges and opportunities. *Viruses,* 6**,** 4880-4901.
SCHOUNTZ, T., BAKER, M. L., BUTLER, J. & MUNSTER, V. 2017. Immunological control of viral infections in bats and the emergence of viruses highly pathogenic to humans. *Frontiers in immunology,* 8**,** 1098.

SCHOUNTZ, T., CAMPBELL, C., WAGNER, K., ROVNAK, J., MARTELLARO, C., DEBUYSSCHER, B. L., FELDMANN, H. & PRESCOTT, J. 2019. Differential innate immune responses elicited by Nipah virus and Cedar virus correlate with disparate in vivo pathogenesis in hamsters. *Viruses,* 11**,** 291.
SCHRODER, K., HERTZOG, P. J., RAVASI, T. & HUME, D. A. 2004. Interferon-γ: an overview of signals, mechanisms and functions. *Journal of leukocyte biology,* 75**,** 163-189.
SCHRODINGER, LLC 2015. The AxPyMOL Molecular Graphics Plugin for Microsoft PowerPoint, Version 1.8.
SCHWARTZ, D. A. 2021. Prioritizing the continuing global challenges to emerging and reemerging viral infections. Frontiers Media SA.
SCIABICA, K. S., DAI, Q. J. & SANDRI-GOLDIN, R. M. 2003. ICP27 interacts with SRPK1 to mediate HSV splicing inhibition by altering SR protein phosphorylation. *The EMBO journal,* 22**,** 1608-1619.
SELVEY, L. A., WELLS, R. M., MCCORMACK, J. G., ANSFORD, A. J., MURRAY, K., ROGERS, R. J., LAVERCOMBE, P. S., SELLECK, P. & SHERIDAN, J. W. 1995. Infection of humans and horses by a newly described morbillivirus. *Medical Journal of Australia,* 162**,** 642-644.
SEMENZA, J. C., SUDRE, B., MINIOTA, J., ROSSI, M., HU, W., KOSSOWSKY, D., SUK, J. E., VAN BORTEL, W. & KHAN, K. 2014. International dispersal of dengue through air travel: importation risk for Europe. *PLoS neglected tropical diseases,* 8**,** e3278.
SETH, R. B., SUN, L., EA, C.-K. & CHEN, Z. J. 2005. Identification and characterization of MAVS, a mitochondrial antiviral signaling protein that activates NF-κB and IRF3. *Cell,* 122**,** 669-682.
SHA, W., MITOMA, H., HANABUCHI, S., BAO, M., WENG, L., SUGIMOTO, N., LIU, Y., ZHANG, Z., ZHONG, J. & SUN, B. 2014. Human NLRP3 inflammasome senses multiple types of bacterial RNAs. *Proceedings of the National Academy of Sciences,* 111**,** 16059-16064.
SHABMAN, R. S., SHRIVASTAVA, S., TSIBANE, T., ATTIE, O., JAYAPRAKASH, A., MIRE, C. E., DILLEY, K. E., PURI, V., STOCKWELL, T. B. & GEISBERT, T. W. 2016. Isolation and characterization of a novel gammaherpesvirus from a microbat cell line. *MSphere,* 1**,** e00070-15.
SHARP, P. M. & HAHN, B. H. 2010. The evolution of HIV-1 and the origin of AIDS. *Philosophical Transactions of the Royal Society B: Biological Sciences,* 365**,** 2487-2494.
SHATKIN, A. 1976. Capping of eucaryotic mRNAs. *Cell,* 9**,** 645-653.
SHAW, A. E., HUGHES, J., GU, Q., BEHDENNA, A., SINGER, J. B., DENNIS, T., ORTON, R. J., VARELA, M., GIFFORD, R. J. & WILSON, S. J. 2017. Fundamental properties of the mammalian innate immune system revealed by multispecies comparison of type I interferon responses. *PLoS biology,* 15**,** e2004086.
SHAW, M. L., GARCÍA-SASTRE, A., PALESE, P. & BASLER, C. F. 2004. Nipah virus V and W proteins have a common STAT1-binding domain yet inhibit STAT1 activation from the cytoplasmic and nuclear compartments, respectively. *Journal of virology,* 78**,** 5633-5641.
SHAW, T. I., SRIVASTAVA, A., CHOU, W.-C., LIU, L., HAWKINSON, A., GLENN, T. C., ADAMS, R. & SCHOUNTZ, T. 2012. Transcriptome sequencing and annotation for the Jamaican fruit bat (Artibeus jamaicensis). *PloS one,* 7**,** e48472.
SHEN, Y.-Y., LIANG, L., ZHU, Z.-H., ZHOU, W.-P., IRWIN, D. M. & ZHANG, Y.-P. 2010. Adaptive evolution of energy metabolism genes and the origin of flight in bats. *Proceedings of the National Academy of Sciences,* 107**,** 8666-8671.
SHEPPARD, P., KINDSVOGEL, W., XU, W., HENDERSON, K., SCHLUTSMEYER, S., WHITMORE, T. E., KUESTNER, R., GARRIGUES, U., BIRKS, C. &

RORABACK, J. 2003. IL-28, IL-29 and their class II cytokine receptor IL-28R. *Nature immunology,* 4**,** 63-68.
SHI, Z. & HU, Z. 2008. A review of studies on animal reservoirs of the SARS coronavirus. *Virus research,* 133**,** 74-87.
SHIMADA, K., CROTHER, T. R., KARLIN, J., DAGVADORJ, J., CHIBA, N., CHEN, S., RAMANUJAN, V. K., WOLF, A. J., VERGNES, L. & OJCIUS, D. M. 2012. Oxidized mitochondrial DNA activates the NLRP3 inflammasome during apoptosis. *Immunity,* 36**,** 401-414.
SIEGLER, G., KREMMER, E., GONNELLA, R. & NIEDOBITEK, G. 2003. Epstein-Barr virus encoded latent membrane protein 1 (LMP1) and TNF receptor associated factors (TRAF): colocalisation of LMP1 and TRAF1 in primary EBV infection and in EBV associated Hodgkin lymphoma. *Molecular Pathology,* 56**,** 156.
SIGNORINO, G., MOHAMMADI, N., PATANÈ, F., BUSCETTA, M., VENZA, M., VENZA, I., MANCUSO, G., MIDIRI, A., ALEXOPOULOU, L. & TETI, G. 2014. Role of Toll-like receptor 13 in innate immune recognition of group B streptococci. *Infection and immunity,* 82**,** 5013-5022.
SINGH, R. K., DHAMA, K., CHAKRABORTY, S., TIWARI, R., NATESAN, S., KHANDIA, R., MUNJAL, A., VORA, K. S., LATHEEF, S. K. & KARTHIK, K. 2019. Nipah virus: epidemiology, pathology, immunobiology and advances in diagnosis, vaccine designing and control strategies–a comprehensive review. *Veterinary Quarterly,* 39**,** 26-55.
SMITH, I. & WANG, L.-F. 2013. Bats and their virome: an important source of emerging viruses capable of infecting humans. *Current opinion in virology,* 3**,** 84-91.
SOMMEREYNS, C., PAUL, S., STAEHELI, P. & MICHIELS, T. 2008. IFN-lambda (IFN-λ) is expressed in a tissue-dependent fashion and primarily acts on epithelial cells in vivo. *PLoS pathogens,* 4**,** e1000017.
SONNHAMMER, E. L., EDDY, S. R. & DURBIN, R. 1997. Pfam: a comprehensive database of protein domain families based on seed alignments. *Proteins: Structure, Function, and Bioinformatics,* 28**,** 405-420.
SPEAKMAN, J. R., THOMAS, D. W., KUNZ, T. & FENTON, M. B. 2003. Physiological ecology and energetics of bats. *Bat ecology***,** 430-490.
SPRINGER, M. S., TEELING, E. C., MADSEN, O., STANHOPE, M. J. & DE JONG, W. W. 2001. Integrated fossil and molecular data reconstruct bat echolocation. *Proceedings of the National Academy of Sciences,* 98**,** 6241-6246.
STANIFER, M. L., PERVOLARAKI, K. & BOULANT, S. 2019. Differential regulation of type I and type III interferon signaling. *International journal of molecular sciences,* 20**,** 1445.
STEWART, W., ALLEN, R. & SULKIN, S. Persistent infection in bats and bat cell cultures with Japanese encephalitis virus. Bacteriol. Proc, 1969.
STREICKER, D. G., RECUENCO, S., VALDERRAMA, W., GOMEZ BENAVIDES, J., VARGAS, I., PACHECO, V., CONDORI CONDORI, R. E., MONTGOMERY, J., RUPPRECHT, C. E. & ROHANI, P. 2012. Ecological and anthropogenic drivers of rabies exposure in vampire bats: implications for transmission and control. *Proceedings of the Royal Society B: Biological Sciences,* 279**,** 3384-3392.
SUBUDHI, S., RAPIN, N., DORVILLE, N., HILL, J. E., TOWN, J., WILLIS, C. K., BOLLINGER, T. K. & MISRA, V. 2018. Isolation, characterization and prevalence of a novel Gammaherpesvirus in Eptesicus fuscus, the North American big brown bat. *Virology,* 516**,** 227-238.
SUBUDHI, S., RAPIN, N. & MISRA, V. 2019. Immune system modulation and viral persistence in bats: understanding viral spillover. *Viruses,* 11**,** 192.

SUK, J. E., VAUGHAN, E. C., COOK, R. G. & SEMENZA, J. C. 2020. Natural disasters and infectious disease in Europe: a literature review to identify cascading risk pathways. *European journal of public health,* 30**,** 928-935.
SULKIN, S. E. & ALLEN, R. 1974. *Virus infections in bats*.
SULKIN, S. E., ALLEN, R., MIURA, T. & TOYOKAWA, K. 1970. Studies of arthropod-borne virus infections in chiroptera. VI. Isolation of Japanese B encephalitis virus from naturally infected bats. *American Journal of Tropical Medicine and Hygiene,* 19**,** 77-87.
SWANEPOEL, R., LEMAN, P. A., BURT, F. J., ZACHARIADES, N. A., BRAACK, L., KSIAZEK, T. G., ROLLIN, P. E., ZAKI, S. R. & PETERS, C. J. 1996. Experimental inoculation of plants and animals with Ebola virus. *Emerging infectious diseases,* 2**,** 321.
TAN, J., QIAO, W., WANG, J., XU, F., LI, Y., ZHOU, J., CHEN, Q. & GENG, Y. 2008. IFP35 is involved in the antiviral function of interferon by association with the viral tas transactivator of bovine foamy virus. *Journal of virology,* 82**,** 4275-4283.
TANAKA, Y. & CHEN, Z. J. 2012. STING specifies IRF3 phosphorylation by TBK1 in the cytosolic DNA signaling pathway. *Science signaling,* 5**,** ra20-ra20.
TAYLOR, L. H., LATHAM, S. M. & WOOLHOUSE, M. E. 2001. Risk factors for human disease emergence. *Philosophical Transactions of the Royal Society of London. Series B: Biological Sciences,* 356**,** 983-989.
TEELING, E. C., MADSEN, O., MURPHY, W. J., SPRINGER, M. S. & O'BRIEN, S. J. 2003. Nuclear gene sequences confirm an ancient link between New Zealand's short-tailed bat and South American noctilionoid bats. *Molecular Phylogenetics and Evolution,* 28**,** 308-319.
TEELING, E. C., SCALLY, M., KAO, D. J., ROMAGNOLI, M. L., SPRINGER, M. S. & STANHOPE, M. J. 2000. Molecular evidence regarding the origin of echolocation and flight in bats. *Nature,* 403**,** 188-192.
TEELING, E. C., SPRINGER, M. S., MADSEN, O., BATES, P., O'BRIEN, S. J. & MURPHY, W. J. 2005. A molecular phylogeny for bats illuminates biogeography and the fossil record. *Science,* 307**,** 580-584.
TERENZI, F., HUI, D. J., MERRICK, W. C. & SEN, G. C. 2006. Distinct induction patterns and functions of two closely related interferon-inducible human genes, ISG54 and ISG56. *Journal of Biological Chemistry,* 281**,** 34064-34071.
TEUFEL, F., ALMAGRO ARMENTEROS, J. J., JOHANSEN, A. R., GÍSLASON, M. H., PIHL, S. I., TSIRIGOS, K. D., WINTHER, O., BRUNAK, S., VON HEIJNE, G. & NIELSEN, H. 2022. SignalP 6.0 predicts all five types of signal peptides using protein language models. *Nature biotechnology,* 40**,** 1023-1025.
THEHUMANPROTEINATLAS. 2023. *IFIT5 Gene* [Online]. Human Protein Atlas, available from www.proteinatlas.org: Human Protein Atlas. Available: https://v15.proteinatlas.org/ENSG00000152778-IFIT5/tissue [Accessed 24-03-23 2023].
TONG, S., LI, Y., RIVAILLER, P., CONRARDY, C., CASTILLO, D. A. A., CHEN, L.-M., RECUENCO, S., ELLISON, J. A., DAVIS, C. T. & YORK, I. A. 2012. A distinct lineage of influenza A virus from bats. *Proceedings of the National Academy of Sciences,* 109**,** 4269-4274.
TONG, S., ZHU, X., LI, Y., SHI, M., ZHANG, J., BOURGEOIS, M., YANG, H., CHEN, X., RECUENCO, S. & GOMEZ, J. 2013. New world bats harbor diverse influenza A viruses. *PLoS pathogens,* 9**,** e1003657.
TOWNER, J. S., AMMAN, B. R., SEALY, T. K., CARROLL, S. A. R., COMER, J. A., KEMP, A., SWANEPOEL, R., PADDOCK, C. D., BALINANDI, S. & KHRISTOVA, M. L. 2009. Isolation of genetically diverse Marburg viruses from Egyptian fruit bats. *PLoS pathogens,* 5**,** e1000536.
TOWNER, J. S., POURRUT, X., ALBARIÑO, C. G., NKOGUE, C. N., BIRD, B. H., GRARD, G., KSIAZEK, T. G., GONZALEZ, J.-P., NICHOL, S. T. & LEROY, E.

M. 2007. Marburg virus infection detected in a common African bat. *PloS one,* 2**,** e764.
TSAGKOGEORGA, G., PARKER, J., STUPKA, E., COTTON, J. A. & ROSSITER, S. J. 2013. Phylogenomic analyses elucidate the evolutionary relationships of bats. *Current Biology,* 2**3,** 2262-2267.
TSUCHIDA, T., ZOU, J., SAITOH, T., KUMAR, H., ABE, T., MATSUURA, Y., KAWAI, T. & AKIRA, S. 2010. The ubiquitin ligase TRIM56 regulates innate immune responses to intracellular double-stranded DNA. *Immunity,* 33**,** 765-776.
UHLÉN, M., FAGERBERG, L., HALLSTRÖM, B. M., LINDSKOG, C., OKSVOLD, P., MARDINOGLU, A., SIVERTSSON, Å., KAMPF, C., SJÖSTEDT, E. & ASPLUND, A. 2015. Tissue-based map of the human proteome. *Science,* 347**,** 1260419.
UZÉ, G. & MONNERON, D. 2007. IL-28 and IL-29: newcomers to the interferon family. *Biochimie,* 89**,** 729-734.
VAN PESCH, V., LANAYA, H., RENAULD, J.-C. & MICHIELS, T. 2004. Characterization of the murine alpha interferon gene family. *Journal of virology,* 78**,** 8219-8228.
VELEBIT, B., RADIN, D. & TEODOROVIC, V. 2015. Transmission of common foodborne viruses by meat products. *Procedia Food Science,* 5**,** 304-307.
VERHELST, J., HULPIAU, P. & SAELENS, X. 2013. Mx proteins: antiviral gatekeepers that restrain the uninvited. *Microbiology and Molecular Biology Reviews,* 77**,** 551-566.
VILLA, B. R. & COCKRUM, E. L. 1962. Migration in the guano bat Tadarida brasiliensis mexicana (Saussure). *Journal of Mammalogy,* 43**,** 43-64.
VIRTUE, E. R., MARSH, G. A., BAKER, M. L. & WANG, L.-F. 2011. Interferon production and signaling pathways are antagonized during henipavirus infection of fruit bat cell lines. *PLoS One,* 6**,** e22488.
VITTING-SEERUP, K. & SANDELIN, A. 2019. IsoformSwitchAnalyzeR: analysis of changes in genome-wide patterns of alternative splicing and its functional consequences. *Bioinformatics,* 35**,** 4469-4471.
VLADIMER, G. I., GÓRNA, M. W. & SUPERTI-FURGA, G. 2014. IFITs: emerging roles as key anti-viral proteins. *Frontiers in immunology,* 5**,** 94.
VOIGT, C. C. & KINGSTON, T. 2016. *Bats in the Anthropocene: conservation of bats in a changing world*, Springer Nature.
WACHARAPLUESADEE, S., SINTUNAWA, C., KAEWPOM, T., KHONGNOMNAN, K., OLIVAL, K. J., EPSTEIN, J. H., RODPAN, A., SANGSRI, P., INTARUT, N. & CHINDAMPORN, A. 2013. Group C betacoronavirus in bat guano fertilizer, Thailand. *Emerging infectious diseases,* 19**,** 1349.
WACHER, C., MÜLLER, M., HOFER, M. J., GETTS, D. R., ZABARAS, R., OUSMAN, S. S., TERENZI, F., SEN, G. C., KING, N. J. & CAMPBELL, I. L. 2007. Coordinated regulation and widespread cellular expression of interferon-stimulated genes (ISG) ISG-49, ISG-54, and ISG-56 in the central nervous system after infection with distinct viruses. *Journal of virology,* 81**,** 860-871.
WANG, E. T., SANDBERG, R., LUO, S., KHREBTUKOVA, I., ZHANG, L., MAYR, C., KINGSMORE, S. F., SCHROTH, G. P. & BURGE, C. B. 2008. Alternative isoform regulation in human tissue transcriptomes. *Nature,* 456**,** 470-476.
WANG, J., YANG, B., HU, Y., ZHENG, Y., ZHOU, H., WANG, Y., MA, Y., MAO, K., YANG, L. & LIN, G. 2013. Negative regulation of Nmi on virus-triggered type I IFN production by targeting IRF7. *The Journal of Immunology,* 191**,** 3393-3399.
WANG, L.-F. & ANDERSON, D. E. 2019. Viruses in bats and potential spillover to animals and humans. *Current opinion in virology,* 34**,** 79-89.
WANG, L.-F., GAMAGE, A. M., CHAN, W. O., HILLER, M. & TEELING, E. C. 2021. Decoding bat immunity: the need for a coordinated research approach. *Nature Reviews Immunology,* 21**,** 269-271.

WANG, X., JOHANSEN, L. M., TAE, H.-J. & TAPAROWSKY, E. J. 1996. IFP 35 forms complexes with B-ATF, a member of the AP1 family of transcription factors. *Biochemical and biophysical research communications,* 229**,** 316-322.
WANG, Y., PAN, Y., PARSONS, S., WALKER, M. & ZHANG, S. 2007. Bats respond to polarity of a magnetic field. *Proceedings of the Royal Society B: Biological Sciences,* 274**,** 2901-2905.
WANG, Z., ZHU, T., XUE, H., FANG, N., ZHANG, J., ZHANG, L., PANG, J., TEELING, E. C. & ZHANG, S. 2017. Prenatal development supports a single origin of laryngeal echolocation in bats. *Nature ecology & evolution,* 1**,** 0021.
WASSENAAR, T. M. & ZOU, Y. 2020. 2019_nCoV/SARS-CoV-2: rapid classification of betacoronaviruses and identification of Traditional Chinese Medicine as potential origin of zoonotic coronaviruses. *Letters in Applied Microbiology,* 70**,** 342-348.
WATANABE, S., MASANGKAY, J. S., NAGATA, N., MORIKAWA, S., MIZUTANI, T., FUKUSHI, S., ALVIOLA, P., OMATSU, T., UEDA, N. & IHA, K. 2010. Bat coronaviruses and experimental infection of bats, the Philippines. *Emerging infectious diseases,* 16**,** 1217.
WATHELET, M. G., LIN, C. H., PAREKH, B. S., RONCO, L. V., HOWLEY, P. M. & MANIATIS, T. 1998. Virus infection induces the assembly of coordinately activated transcription factors on the IFN-β enhancer in vivo. *Molecular cell,* 1**,** 507-518.
WATSON, J. T., GAYER, M. & CONNOLLY, M. A. 2007. Epidemics after natural disasters. *Emerging infectious diseases,* 13**,** 1.
WEATHERMAN, S., FELDMANN, H. & DE WIT, E. 2018. Transmission of henipaviruses. *Current opinion in virology,* 28**,** 7-11.
WEISS, S., WITKOWSKI, P. T., AUSTE, B., NOWAK, K., WEBER, N., FAHR, J., MOMBOULI, J.-V., WOLFE, N. D., DREXLER, J. F. & DROSTEN, C. 2012. Hantavirus in bat, sierra leone. *Emerging infectious diseases,* 18**,** 159.
WELLS, A. I. & COYNE, C. B. 2018. Type III interferons in antiviral defenses at barrier surfaces. *Trends in immunology,* 39**,** 848-858.
WHO. 2023. *Zoonoses* [Online]. World Health Organisation: WHO. Available: https://www.who.int/news-room/fact-sheets/detail/zoonoses [Accessed 14-03-23 2023].
WILKE, A. B., BEIER, J. C. & BENELLI, G. 2019. Complexity of the relationship between global warming and urbanization–an obscure future for predicting increases in vector-borne infectious diseases. *Current opinion in insect science,* 35**,** 1-9.
WILKINSON, G. S. & SOUTH, J. M. 2002. Life history, ecology and longevity in bats. *Aging cell,* 1**,** 124-131.
WILLIAMSON, M., HOOPER, P., SELLECK, P., GLEESON, L., DANIELS, P., WESTBURY, H. & MURRAY, P. 1998. Transmission studies of Hendra virus (equine morbilli-virus) in fruit bats, horses and cats. *Australian veterinary journal,* 76**,** 813-818.
WILLIAMSON, M., HOOPER, P., SELLECK, P., WESTBURY, H. & SLOCOMBE, R. 2000. Experimental hendra virus infectionin pregnant guinea-pigs and fruit Bats (Pteropus poliocephalus). *Journal of comparative pathology,* 122**,** 201-207.
WINKLER, W. 1968. Airborne rabies virus isolation. *Bulletin of the Wildlife Disease Association,* 4**,** 37-40.
WITTE, K., WITTE, E., SABAT, R. & WOLK, K. 2010. IL-28A, IL-28B, and IL-29: promising cytokines with type I interferon-like properties. *Cytokine & growth factor reviews,* 21**,** 237-251.
WOLFE, N. D., DASZAK, P., KILPATRICK, A. M. & BURKE, D. S. 2005. Bushmeat hunting, deforestation, and prediction of zoonotic disease. *Emerging infectious diseases,* 11**,** 1822.

WOLFE, N. D., DUNAVAN, C. P. & DIAMOND, J. 2007. Origins of major human infectious diseases. *Nature,* 447**,** 279-283.
WONG, S., LAU, S., WOO, P. & YUEN, K. Y. 2007. Bats as a continuing source of emerging infections in humans. *Reviews in medical virology,* 17**,** 67-91.
WOOD, J. L., LEACH, M., WALDMAN, L., MACGREGOR, H., FOOKS, A. R., JONES, K. E., RESTIF, O., DECHMANN, D., HAYMAN, D. T. & BAKER, K. S. 2012. A framework for the study of zoonotic disease emergence and its drivers: spillover of bat pathogens as a case study. *Philosophical Transactions of the Royal Society B: Biological Sciences,* 367**,** 2881-2892.
WOOLHOUSE, M. E. & GOWTAGE-SEQUERIA, S. 2005. Host range and emerging and reemerging pathogens. *Emerging infectious diseases,* 11**,** 1842.
WU, Z., YANG, L., YANG, F., REN, X., JIANG, J., DONG, J., SUN, L., ZHU, Y., ZHOU, H. & JIN, Q. 2014. Novel henipa-like virus, Mojiang paramyxovirus, in rats, China, 2012. *Emerging infectious diseases,* 20**,** 1064.
WYNNE, J. W., DI RUBBO, A., SHIELL, B. J., BEDDOME, G., COWLED, C., PECK, G. R., HUANG, J., GRIMLEY, S. L., BAKER, M. L. & MICHALSKI, W. P. 2013. Purification and characterisation of immunoglobulins from the Australian black flying fox (Pteropus alecto) using anti-fab affinity chromatography reveals the low abundance of IgA. *PloS one,* 8**,** e52930.
WYNNE, J. W., SHIELL, B. J., MARSH, G. A., BOYD, V., HARPER, J. A., HEESOM, K., MONAGHAN, P., ZHOU, P., PAYNE, J. & KLEIN, R. 2014. Proteomics informed by transcriptomics reveals Hendra virus sensitizes bat cells to TRAIL-mediated apoptosis. *Genome biology,* 15**,** 1-21.
WYNNE, J. W. & WANG, L.-F. 2013. Bats and viruses: friend or foe? *PLoS Pathogens,* 9**,** e1003651.
XIAHOU, Z., WANG, X., SHEN, J., ZHU, X., XU, F., HU, R., GUO, D., LI, H., TIAN, Y. & LIU, Y. 2017. NMI and IFP35 serve as proinflammatory DAMPs during cellular infection and injury. *Nature Communications,* 8**,** 950.
XIE, J., LI, Y., SHEN, X., GOH, G., ZHU, Y., CUI, J., WANG, L.-F., SHI, Z.-L. & ZHOU, P. 2018. Dampened STING-dependent interferon activation in bats. *Cell host & microbe,* 23**,** 297-301. e4.
XING, L., NIU, M. & KLEIMAN, L. 2014. Role of the OB-fold of RNA helicase A in the synthesis of HIV-1 RNA. *Biochimica et Biophysica Acta (BBA)-Gene Regulatory Mechanisms,* 1839**,** 1069-1078.
YANG, H., LIN, C. H., MA, G., BAFFI, M. O. & WATHELET, M. G. 2003. Interferon regulatory factor-7 synergizes with other transcription factors through multiple interactions with p300/CBP coactivators. *Journal of Biological Chemistry,* 278**,** 15495-15504.
YANG, H., WINKLER, W. & WU, X. 2021. Interferon Inducer IFI35 Regulates RIG-I-Mediated Innate Antiviral Response through Mutual Antagonism with Influenza Virus Protein NS1. *Journal of virology,* 95**,** e00283-21.
YANG, J. & YAN, H. 2021. Mucosal epithelial cells: the initial sentinels and responders controlling and regulating immune responses to viral infections. *Cellular & Molecular Immunology,* 18**,** 1628-1630.
YANG, J. & ZHANG, Y. 2015. I-TASSER server: new development for protein structure and function predictions. *Nucleic acids research,* 43**,** W174-W181.
YOB, J. M., FIELD, H., RASHDI, A. M., MORRISSY, C., VAN DER HEIDE, B., ROTA, P., BIN ADZHAR, A., WHITE, J., DANIELS, P. & JAMALUDDIN, A. 2001. Nipah virus infection in bats (order Chiroptera) in peninsular Malaysia. *Emerging infectious diseases,* 7**,** 439.
YOUNG, P. L., HALPIN, K., SELLECK, P. W., FIELD, H., GRAVEL, J. L., KELLY, M. A. & MACKENZIE, J. S. 1996. Serologic evidence for the presence in Pteropus bats of a paramyxovirus related to equine morbillivirus. *Emerging infectious diseases,* 2**,** 239.

ZHANG, B., LIU, X., CHEN, W. & CHEN, L. 2013a. IFIT5 potentiates anti-viral response through enhancing innate immune signaling pathways. *Acta Biochim Biophys Sin,* 45**,** 867-874.
ZHANG, G., COWLED, C., SHI, Z., HUANG, Z., BISHOP-LILLY, K. A., FANG, X., WYNNE, J. W., XIONG, Z., BAKER, M. L. & ZHAO, W. 2013b. Comparative analysis of bat genomes provides insight into the evolution of flight and immunity. *Science,* 339**,** 456-460.
ZHANG, L. & PAGANO, J. S. 1997. IRF-7, a new interferon regulatory factor associated with Epstein-Barr virus latency. *Molecular and cellular biology,* 17**,** 5748-5757.
ZHANG, Q., ZENG, L.-P., ZHOU, P., IRVING, A. T., LI, S., SHI, Z.-L. & WANG, L.-F. 2017. IFNAR2-dependent gene expression profile induced by IFN-α in Pteropus alecto bat cells and impact of IFNAR2 knockout on virus infection. *PloS one,* 12**,** e0182866.
ZHANG, S. & GROSSE, F. 1997. Domain structure of human nuclear DNA helicase II (RNA helicase A). *Journal of Biological Chemistry,* 272**,** 11487-11494.
ZHANG, S., HERRMANN, C. & GROSSE, F. 1999. Pre-mRNA and mRNA binding of human nuclear DNA helicase II (RNA helicase A). *Journal of cell science,* 112**,** 1055-1064.
ZHANG, Y.-Z. & HOLMES, E. C. 2020. A genomic perspective on the origin and emergence of SARS-CoV-2. *Cell,* 181**,** 223-227.
ZHANG, Z., YUAN, B., LU, N., FACCHINETTI, V. & LIU, Y.-J. 2011. DHX9 pairs with IPS-1 to sense double-stranded RNA in myeloid dendritic cells. *The Journal of Immunology,* 187**,** 4501-4508.
ZHOU, J., LI, C., LIU, X., CHIU, M. C., ZHAO, X., WANG, D., WEI, Y., LEE, A., ZHANG, A. J. & CHU, H. 2020. Infection of bat and human intestinal organoids by SARS-CoV-2. *Nature medicine,* 26**,** 1077-1083.
ZHOU, P., COWLED, C., MANSELL, A., MONAGHAN, P., GREEN, D., WU, L., SHI, Z., WANG, L.-F. & BAKER, M. L. 2014. IRF7 in the Australian black flying fox, Pteropus alecto: evidence for a unique expression pattern and functional conservation. *PloS one,* 9**,** e103875.
ZHOU, P., COWLED, C., MARSH, G. A., SHI, Z., WANG, L.-F. & BAKER, M. L. 2011a. Type III IFN receptor expression and functional characterisation in the pteropid bat, Pteropus alecto. *PLoS One,* 6**,** e25385.
ZHOU, P., COWLED, C., TODD, S., CRAMERI, G., VIRTUE, E. R., MARSH, G. A., KLEIN, R., SHI, Z., WANG, L.-F. & BAKER, M. L. 2011b. Type III IFNs in pteropid bats: differential expression patterns provide evidence for distinct roles in antiviral immunity. *The Journal of Immunology,* 186**,** 3138-3147.
ZHOU, P., COWLED, C., WANG, L.-F. & BAKER, M. L. 2013a. Bat Mx1 and Oas1, but not Pkr are highly induced by bat interferon and viral infection. *Developmental & Comparative Immunology,* 40**,** 240-247.
ZHOU, P., FAN, H., LAN, T., YANG, X.-L., SHI, W.-F., ZHANG, W., ZHU, Y., ZHANG, Y.-W., XIE, Q.-M. & MANI, S. 2018. Fatal swine acute diarrhoea syndrome caused by an HKU2-related coronavirus of bat origin. *Nature,* 556**,** 255-258.
ZHOU, P., TACHEDJIAN, M., WYNNE, J. W., BOYD, V., CUI, J., SMITH, I., COWLED, C., NG, J. H., MOK, L. & MICHALSKI, W. P. 2016. Contraction of the type I IFN locus and unusual constitutive expression of IFN-α in bats. *Proceedings of the National Academy of Sciences,* 113**,** 2696-2701.
ZHOU, X., LIAO, J., MEYERDIERKS, A., FENG, L., NAUMOVSKI, L., BÖTTGER, E. C. & OMARY, M. B. 2000. Interferon-α induces Nmi-IFP35 heterodimeric complex formation that is affected by the phosphorylation of IFP35. *Journal of Biological Chemistry,* 275**,** 21364-21371.

ZHOU, X., MICHAL, J. J., ZHANG, L., DING, B., LUNNEY, J. K., LIU, B. & JIANG, Z. 2013b. Interferon induced IFIT family genes in host antiviral defense. *International journal of biological sciences,* 9**,** 200.

ZHOU, X., XU, S., XU, J., CHEN, B., ZHOU, K. & YANG, G. 2012. Phylogenomic analysis resolves the interordinal relationships and rapid diversification of the Laurasiatherian mammals. *Systematic biology,* 61**,** 150.

ZHU, S., DING, S., WANG, P., WEI, Z., PAN, W., PALM, N. W., YANG, Y., YU, H., LI, H.-B. & WANG, G. 2017. Nlrp9b inflammasome restricts rotavirus infection in intestinal epithelial cells. *Nature,* 546**,** 667-670.

Appendix: List of Publications

Publications arising from work undertaken during the course of this PhD:

Clayton, E. and Munir, M., 2020. Fundamental characteristics of bat interferon systems. *Frontiers in cellular and infection microbiology*, *10*, p.527921.

Clayton, E., Rohaim, M.A., Bayoumi, M. and Munir, M., 2022. The molecular virology of coronaviruses with special reference to SARS-CoV-2. *Coronavirus Therapeutics–Volume I: Basic Science and Therapy Development*, pp.15-31.

Clayton, E., Ackerley, J., Aelmans, M., Ali, N., Ashcroft, Z., Ashton, C., Barker, R., Budryte, V., Burrows, C., Cai, S. and Callaghan, A., 2022. Structural Bases of Zoonotic and Zooanthroponotic Transmission of SARS-CoV-2. *Viruses*, *14*(2), p.418.

Rohaim, M.A., **Clayton, E**., Sahin, I., Vilela, J., Khalifa, M.E., Al-Natour, M.Q., Bayoumi, M., Poirier, A.C., Branavan, M., Tharmakulasingam, M. and Chaudhry, N.S., 2020. Artificial intelligence-assisted loop mediated isothermal amplification (AI-LAMP) for rapid detection of SARS-CoV-2. *Viruses*, *12*(9), p.972.

Rohaim, M.A., El Naggar, R.F., **Clayton, E**. and Munir, M., 2021. Structural and functional insights into non-structural proteins of coronaviruses. *Microbial pathogenesis*, *150*, p.104641.